# Appendix A: Data Matrix

The data matrix is an Excel spreadsheet with a width greater than can be reproduced legibly on a standard 8"×11" page. For this reason a hard copy of the matrix does not appear here. Additionally, the spreadsheet contains hyperlinks to almost seventy supporting documents, including QAPPs, reports emails, and memos. These hyperlinks rely on maintenance of a fixed file directory structure. Due to the large number of linked files and overall size, this appendix is provided electronically on CD.

# Appendix B: Tributaries and Loading

## Appendix B-1. 2017-18 Tributary Grab Sample Time series

Time series of grab samples and calculated constituents required by the water quality model for Owasco Lake tributaries during 2017 and 2018 Triangles represent outliers removed from data prior to load estimation. Data are presented here as daily averages when multiple grab samples were taken on the same date.

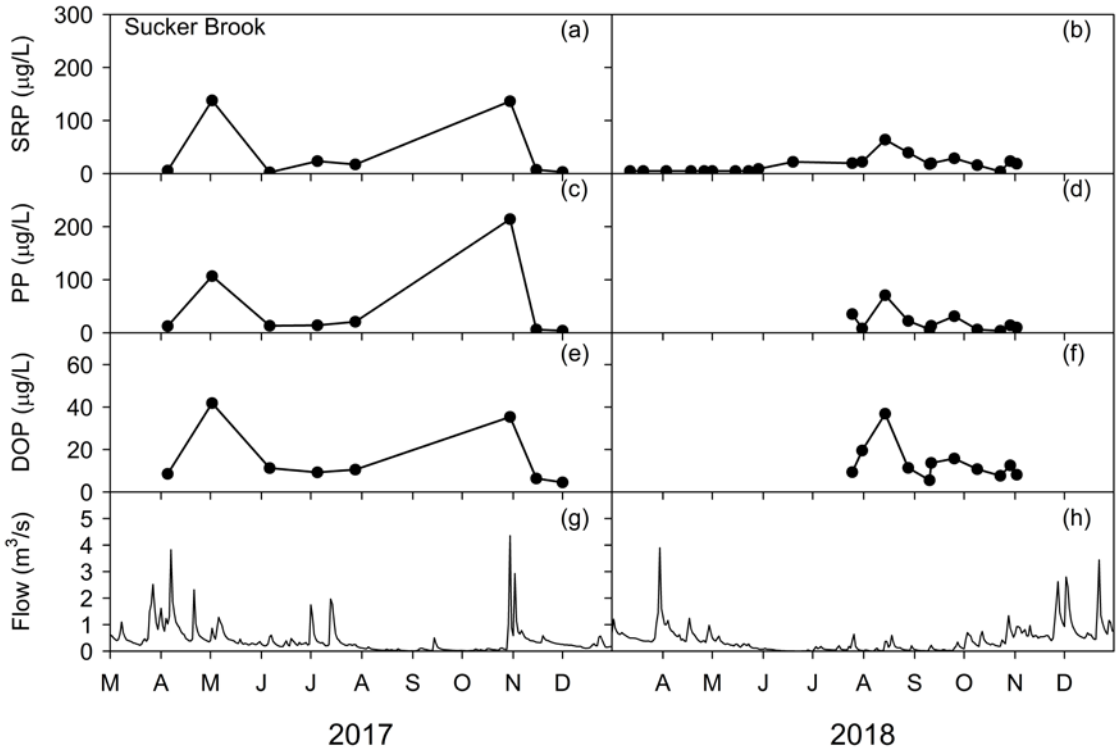

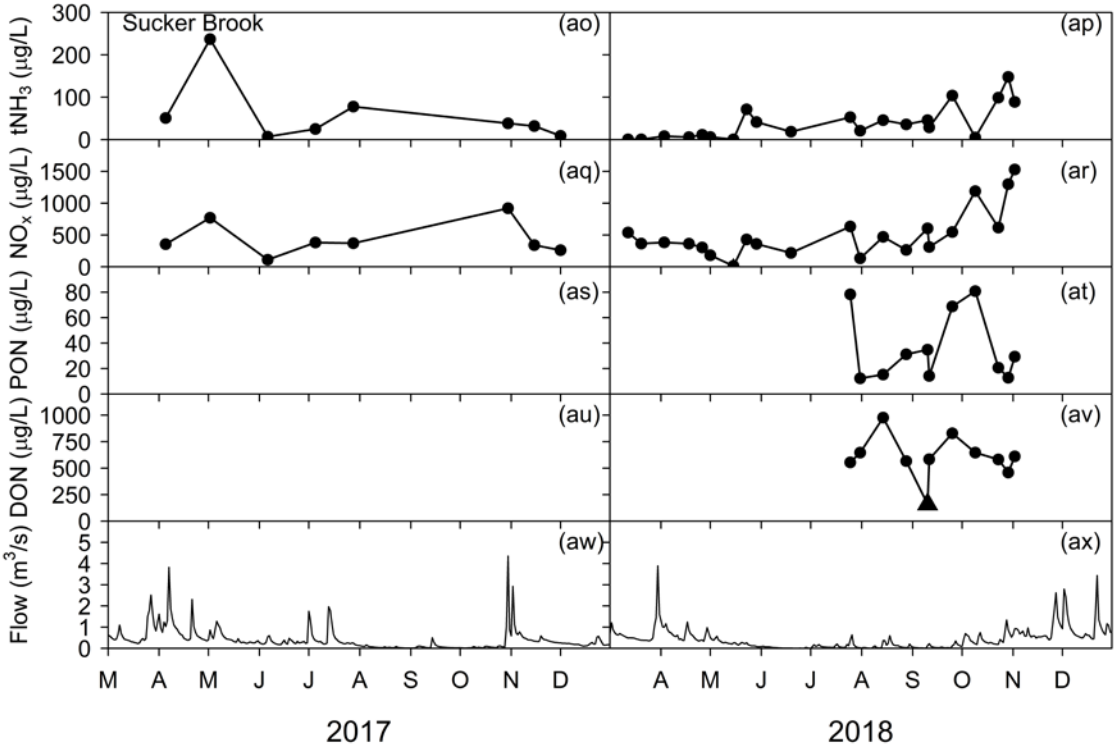
Sucker Brook
(ao)
(ap)
(aq)
(ar)
(as)
(at)
(au)
(av)
(aw)
(ax)
tNH3 (µg/L)
NOx (µg/L)
PON (µg/L)
DON (µg/L)
Flow (m3/s)
M A M J J A S O N D
A M J J A S O N D
2017
2018

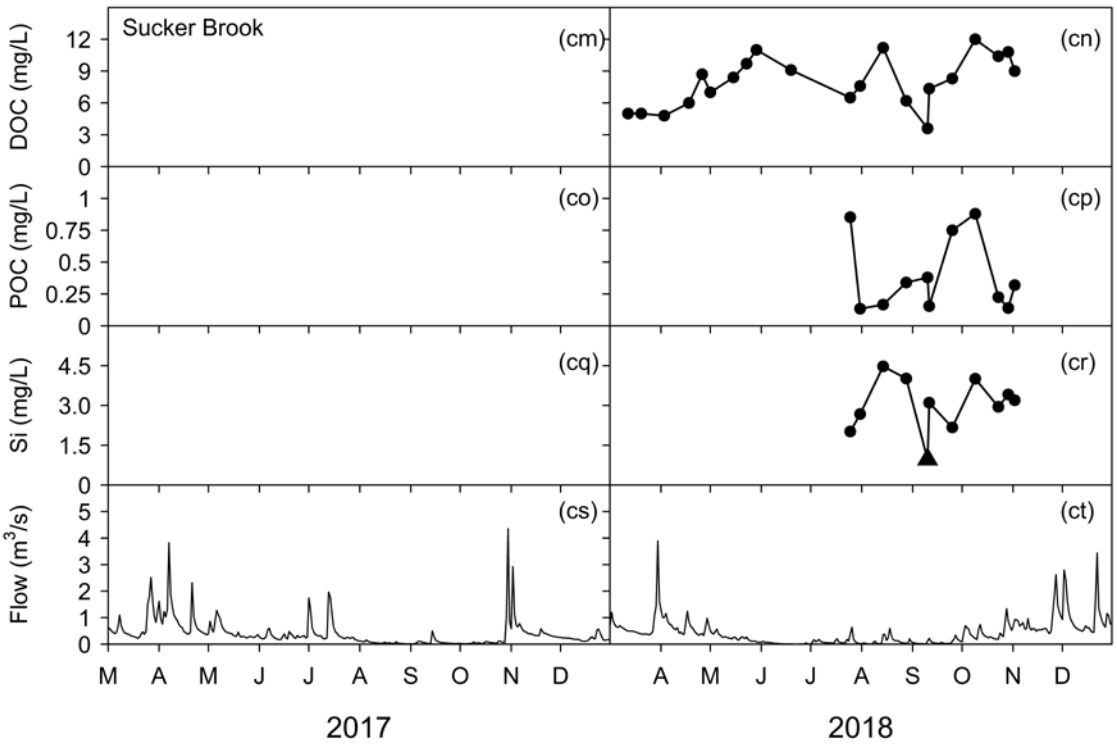
Sucker Brook
(cm)
(cn)
(co)
(cp)
(cq)
(cr)
(cs)
(ct)
DOC (mg/L)
POC (mg/L)
Si (mg/L)
Flow (m3/s)
M A M J J A S O N D
A M J J A S O N D
2017
2018

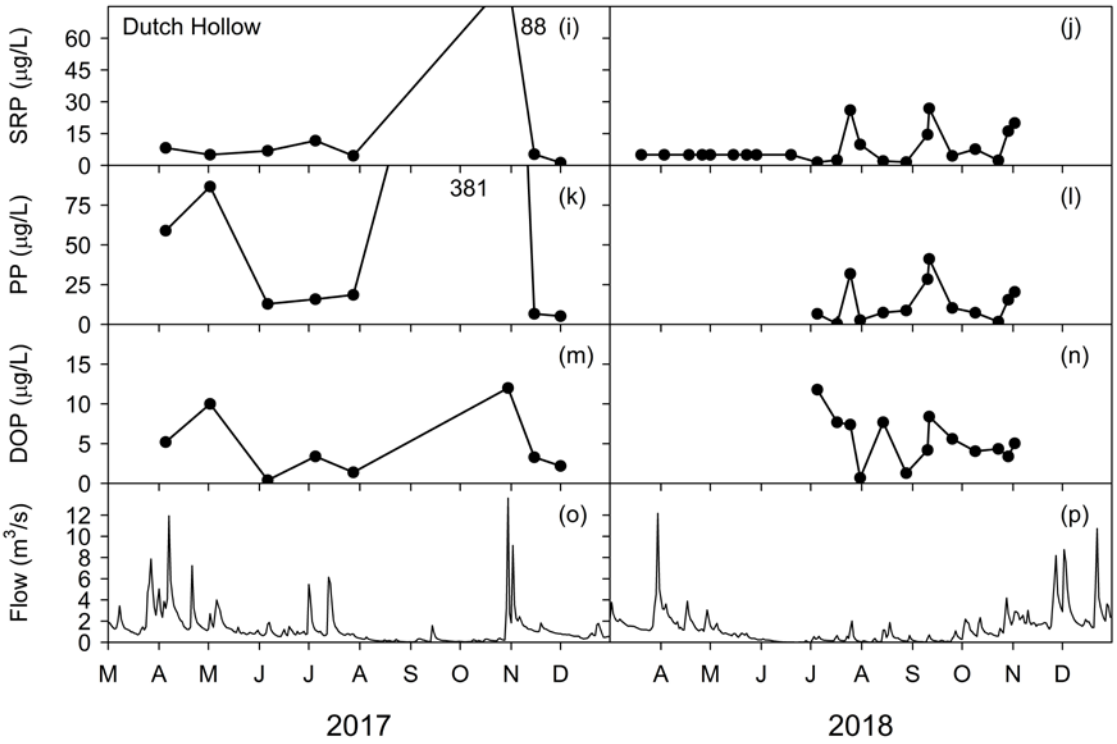
Dutch Hollow
88
381
(i)
(j)
(k)
(l)
(m)
(n)
(o)
(p)
SRP (µg/L)
PP (µg/L)
DOP (µg/L)
Flow (m3/s)
M A M J J A S O N D
A M J J A S O N D
2017
2018

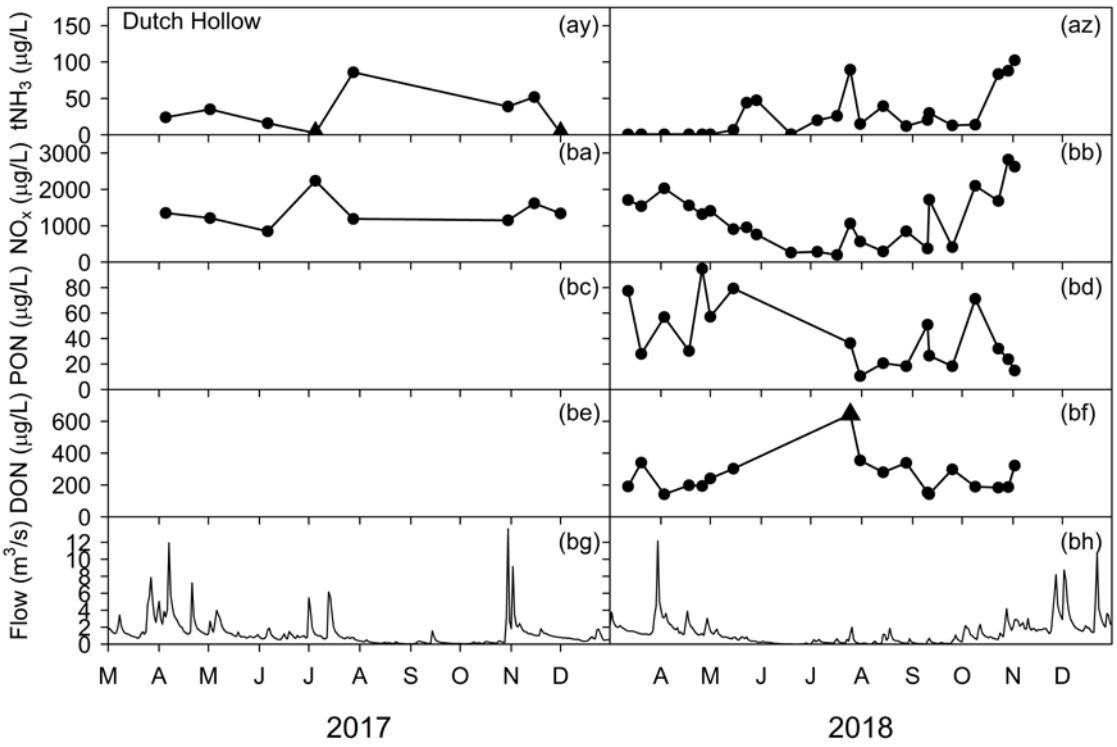
Dutch Hollow
(ay)
(az)
(ba)
(bb)
(bc)
(bd)
(be)
(bf)
(bg)
(bh)
tNH3 (µg/L)
NOx (µg/L)
PON (µg/L)
DON (µg/L)
Flow (m3/s)
M A M J J A S O N D
A M J J A S O N D
2017
2018

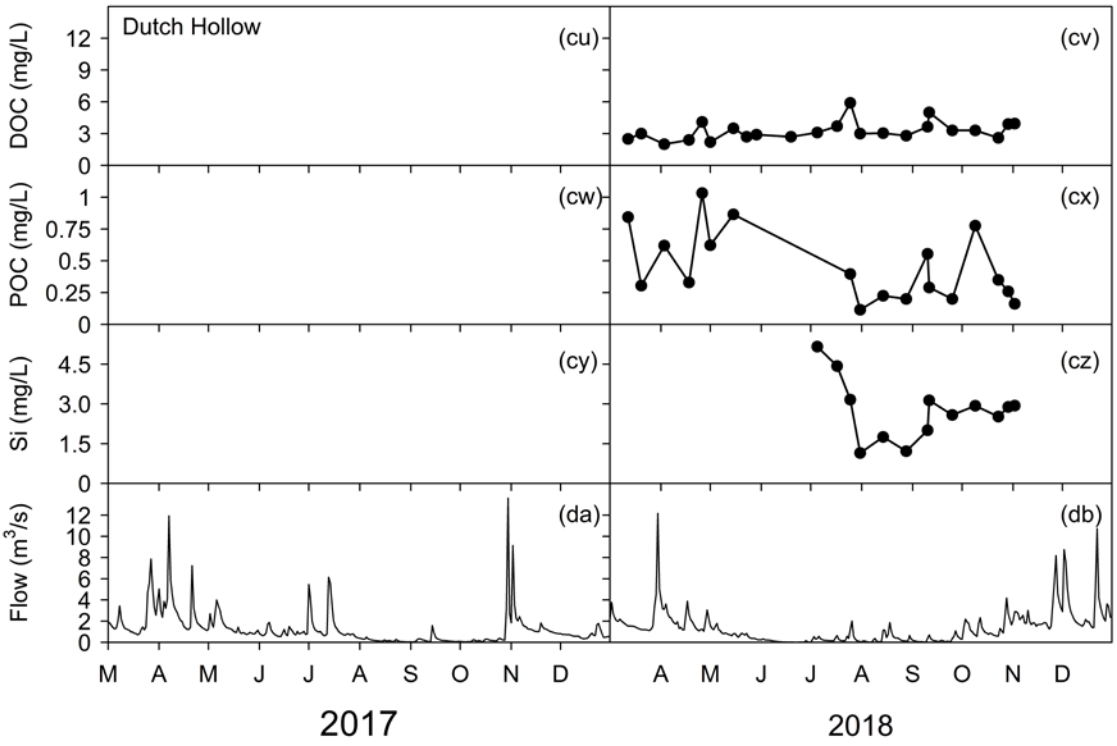
Dutch Hollow
(cu)
(cv)
(cw)
(cx)
(cy)
(cz)
(da)
(db)
DOC (mg/L)
POC (mg/L)
Si (mg/L)
Flow (m3/s)
M A M J J A S O N D
A M J J A S O N D
2017
2018

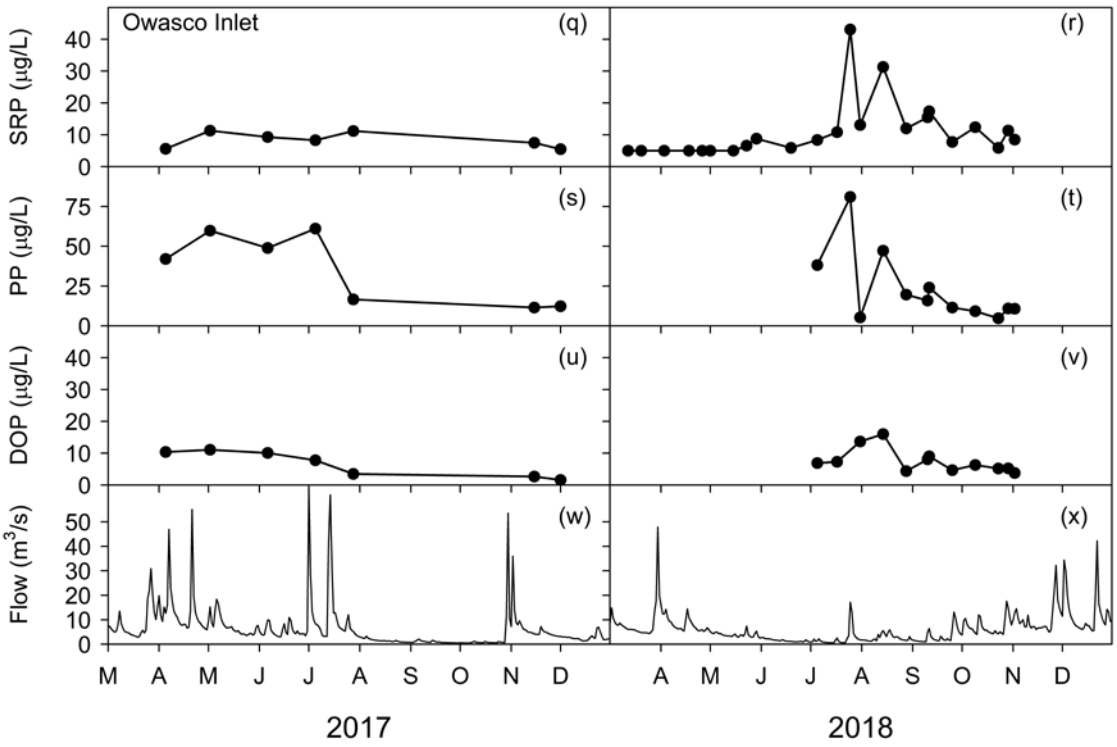
Owasco Inlet
(q)
(r)
(s)
(t)
(u)
(v)
(w)
(x)
SRP (µg/L)
PP (µg/L)
DOP (µg/L)
Flow (m3/s)
M A M J J A S O N D
A M J J A S O N D
2017
2018

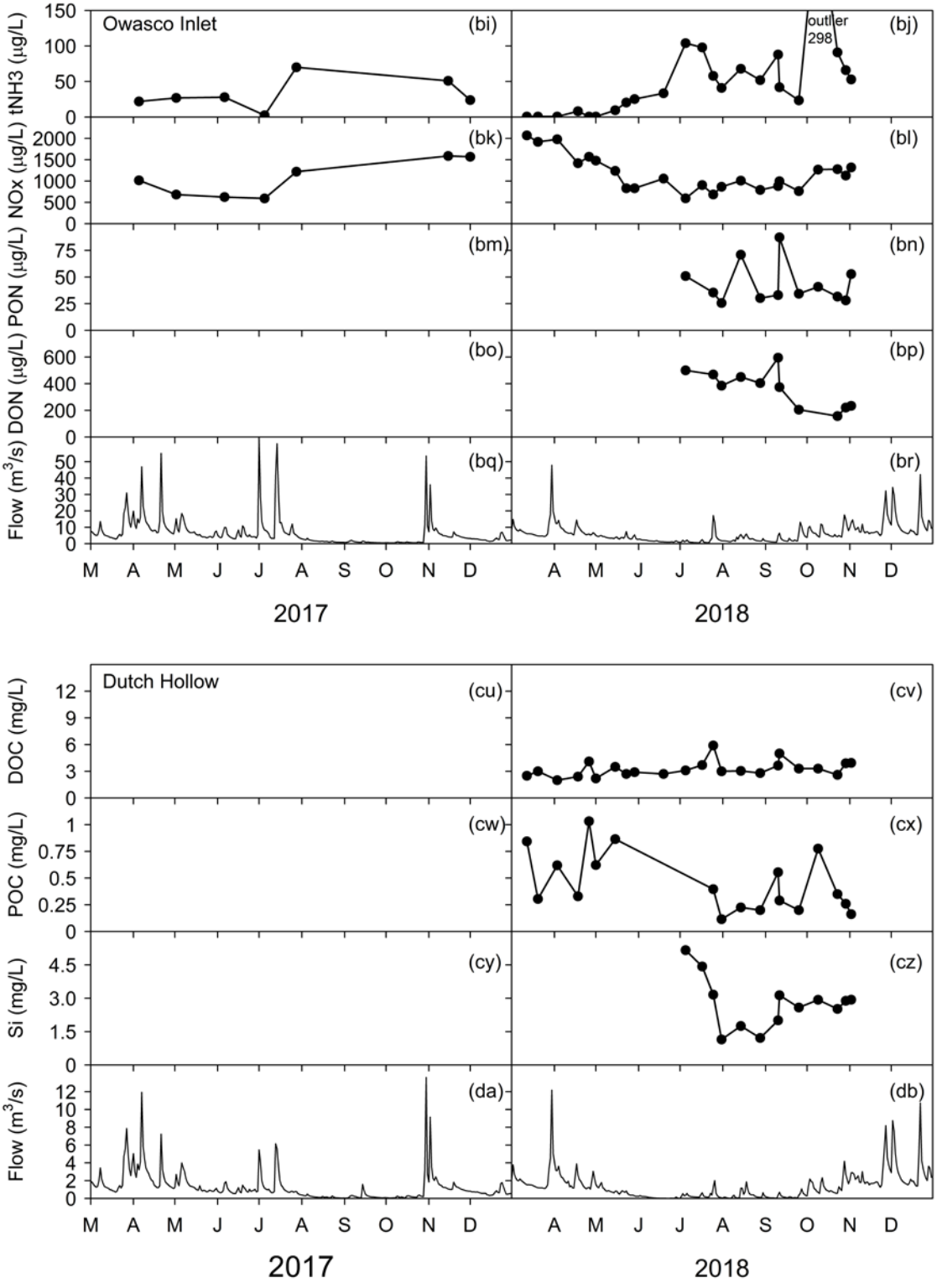
Owasco Inlet
(bi)
outlier
298
(bj)
(bk)
(bl)
(bm)
(bn)
(bo)
(bp)
(bq)
(br)
tNH3 (µg/L)
NOx (µg/L)
PON (µg/L)
DON (µg/L)
Flow (m3/s)
M A M J J A S O N D
A M J J A S O N D
2017
2018
Dutch Hollow
(cu)
(cv)
(cw)
(cx)
(cy)
(cz)
(da)
(db)
DOC (mg/L)
POC (mg/L)
Si (mg/L)
Flow (m3/s)
M A M J J A S O N D
A M J J A S O N D
2017
2018

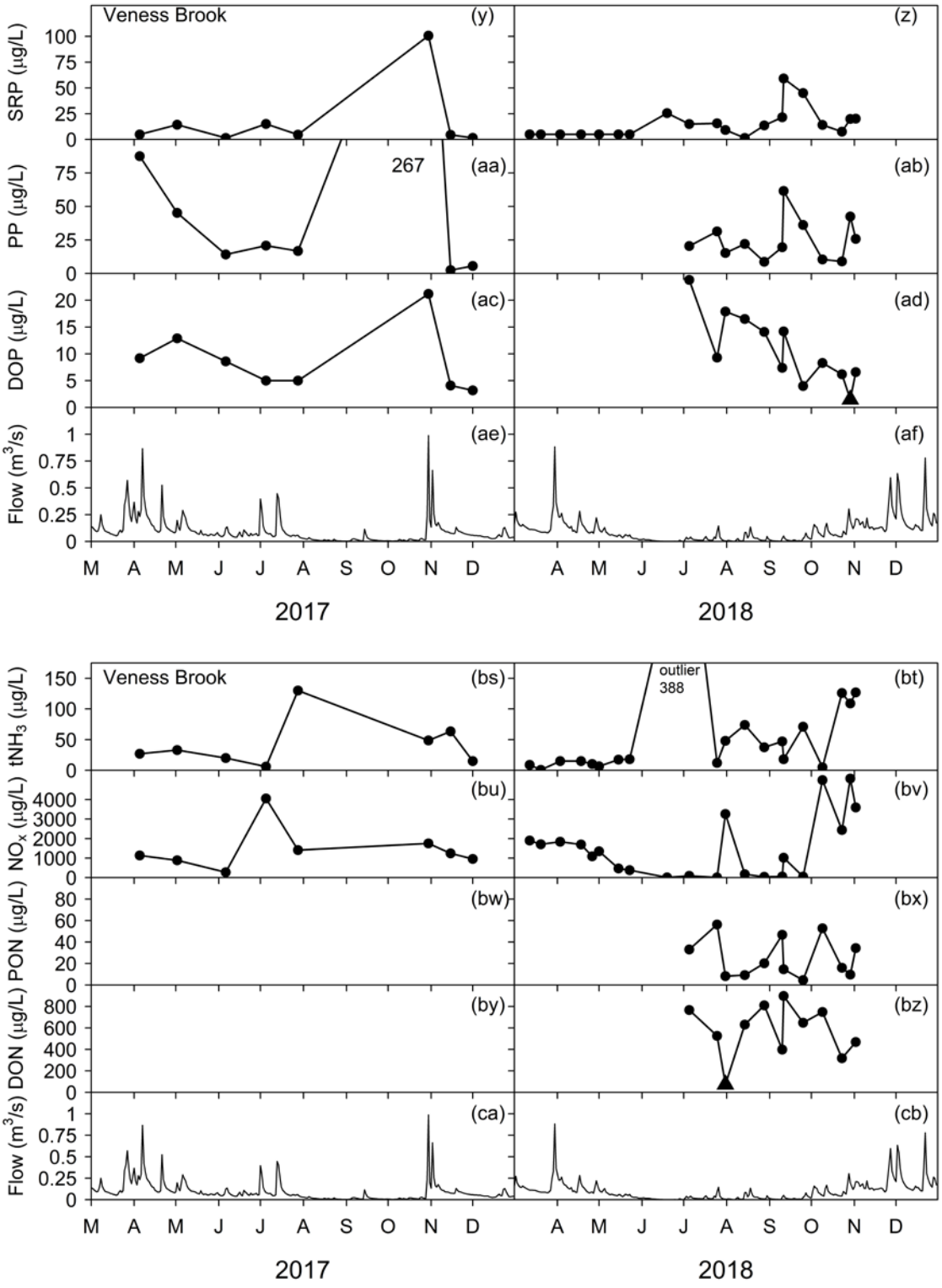
Veness Brook
(y)
(z)
SRP (µg/L)
267
(aa)
(ab)
PP (µg/L)
(ac)
(ad)
DOP (µg/L)
(ae)
(af)
Flow (m3/s)
M A M J J A S O N D
A M J J A S O N D
2017
2018
Veness Brook
outlier
388
(bs)
(bt)
tNH3 (µg/L)
(bu)
(bv)
NOx (µg/L)
(bw)
(bx)
PON (µg/L)
(by)
(bz)
DON (µg/L)
(ca)
(cb)
Flow (m3/s)
M A M J J A S O N D
A M J J A S O N D
2017
2018

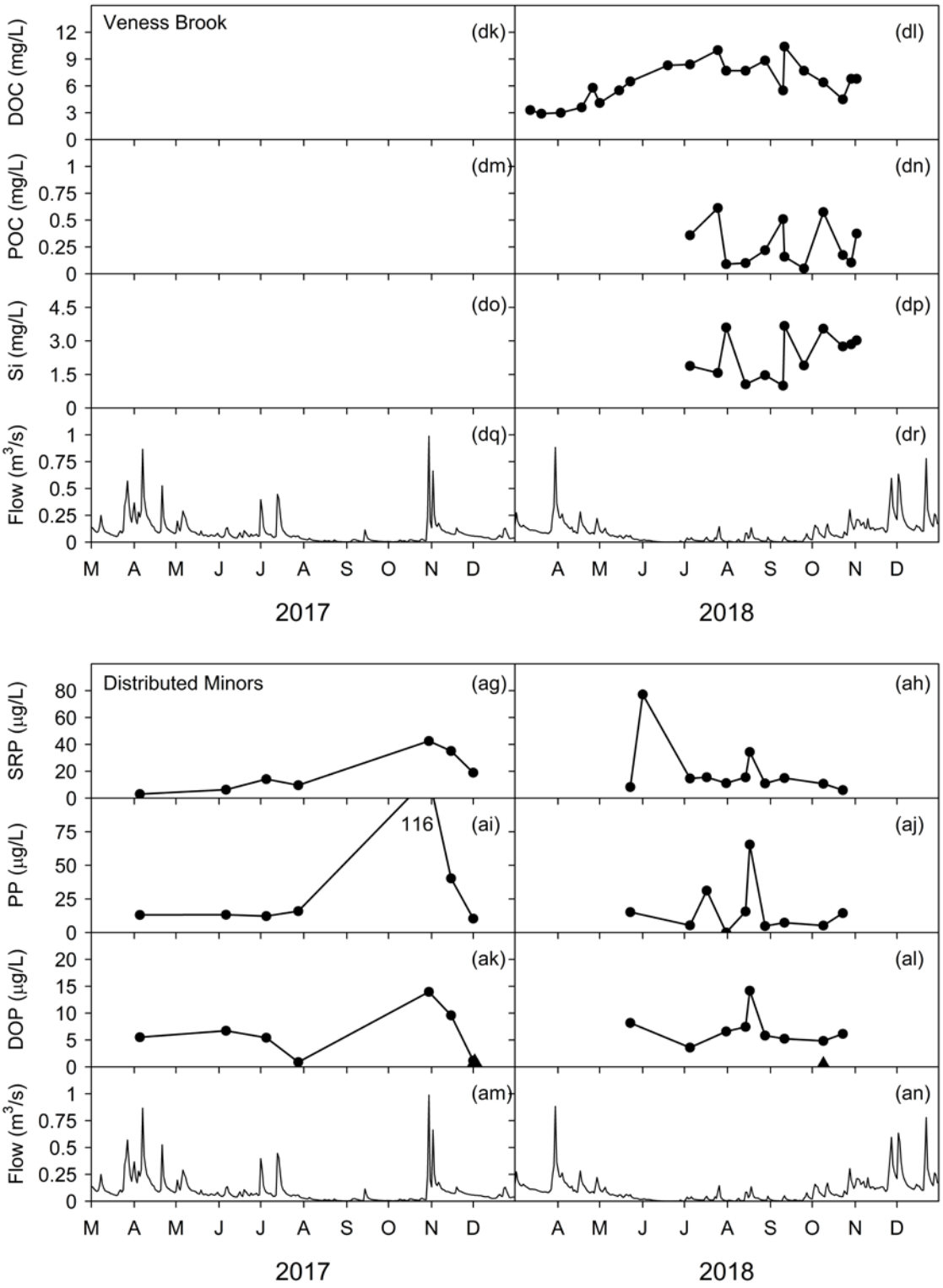


*NOTE: The "floating" outlier is the result of data averaging.

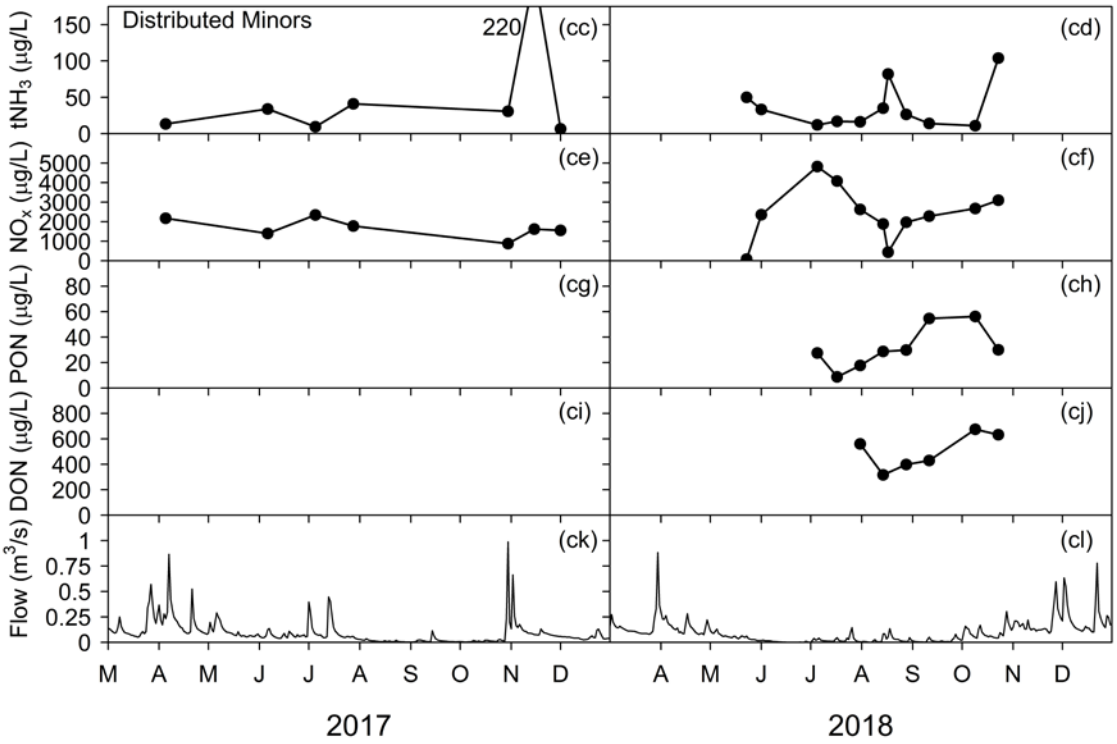
Distributed Minors
220
(cc)
(cd)
(ce)
(cf)
(cg)
(ch)
(ci)
(cj)
(ck)
(cl)
tNH3 (µg/L)
NOx (µg/L)
PON (µg/L)
DON (µg/L)
Flow (m3/s)
M A M J J A S O N D
A M J J A S O N D
2017
2018

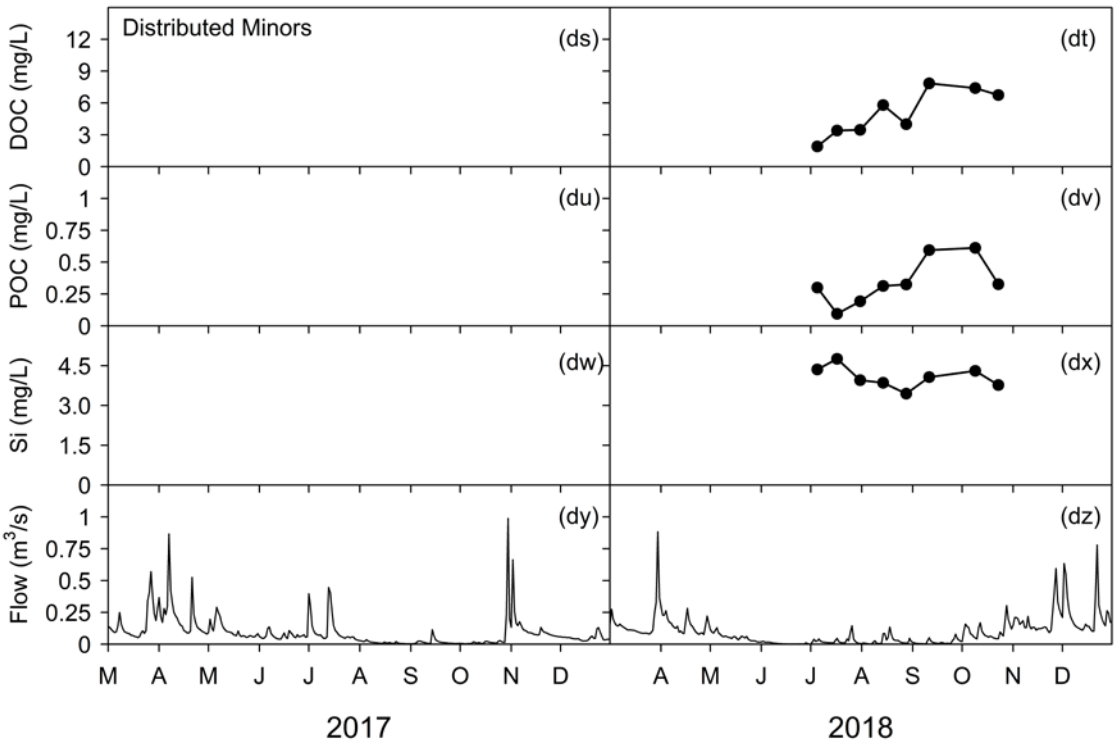
Distributed Minors
(ds)
(dt)
(du)
(dv)
(dw)
(dx)
(dy)
(dz)
DOC (mg/L)
POC (mg/L)
Si (mg/L)
Flow (m3/s)
M A M J J A S O N D
A M J J A S O N D
2017
2018

## Appendix B-2. Outliers Removed Prior to Load Estimation

**Table B-1.** Outliers excluded from C-Q regressions used for load estimation in FLUX32.

| Tributary | Constituent | Date | Flow ($m^3/s$) | Observed Concentration (µg/L) | Leverage (%)[a] | Reason(s) for exclusion |
|---|---|---|---|---|---|---|
| Sucker Brook | Silica | 9/10/18 | 0.128 | 967.60 | -0.05 | below data trend, causes underestimation of concentration at low flow, identified as outlier by FLUX |
| Sucker Brook | $NO_x$ | 5/15/18 | 0.261 | 13.30 | -9.24 | identified as unexpectedly low but verified result from lab, identified as outlier by FLUX w/ large impact on load |
| Sucker Brook | DON | 9/10/18 | 0.128 | 160.11 | -1.76 | calculated constituent, low sample relative to rest of trend, also identified by FLUX |
| Dutch Hollow Brook | $tNH_3$ | 7/5/17<br>12/1/17 | 1.147<br>0.828 | 2.50<br>2.50 | 2.52<br>-0.17 | samples below LOD, identified as outliers by FLUX, both fall below the data trend |
| Dutch Hollow Brook | PP | 7/17/18 | 0.654 | 0.40 | -15.78 | falls below the data trend, identified as outlier by FLUX |
| Dutch Hollow Brook | DON | 7/25/18 | 1.243 | 644.07 | -9.81 | calculated constituent, high relative to rest of trend, identified as outlier by FLUX |
| Inlet | $tNH_3$ | 10/9/18 | 4.600 | 298.00 | -15.09 | falls above data trend, associated with failed duplicate in lab, identified by FLUX as outlier |
| Veness | $tNH_3$ | 7/5/18 | 0.027 | 388 | -14.28 | Identified as outlier by FLUX, large |

| Tributary | Constituent | Date | Flow ($m^3/s$) | Observed Concentration (µg/L) | Leverage (%)[a] | Reason(s) for exclusion |
|---|---|---|---|---|---|---|
| Brook | | | | | | influence on loads, increased CV |
| Veness Brook | DOP | 10/29/18 | 0.195 | 1.50 | 8.20 | high flow with low concentration outside of data trend, causes underestimation of concentration at high flows, identified as outlier by FLUX |
| Veness Brook | DON | 7/31/18 | 0.006 | 73.74 | -37.17 | very low compared to data trend, causes underestimation at low flow and overestimation at high flows, calculated constituent identified as outlier by FLUX |
| distributed minors | DOP | 12/1/17<br>10/9/18 | 0.909<br>0.762 | 0.30<br>0.10 | -1.99<br>-12.49 | falls outside of data trend, calculated constituent, both identified as outliers by FLUX |

[a] Determined using jackknife routine in FLUX32; represents change in load when specified data point is excluded

# Appendix B-3. Concentration Flow Relationships for Constituent Grab Samples

All relationships are presented as a single regression line after the removal of any data deemed outliers, which are plotted as open circles. If multiple regression lines were used to estimate loads, such as stratification based on flow, those relationships are presented in Section 2 and denoted with a (*) below.

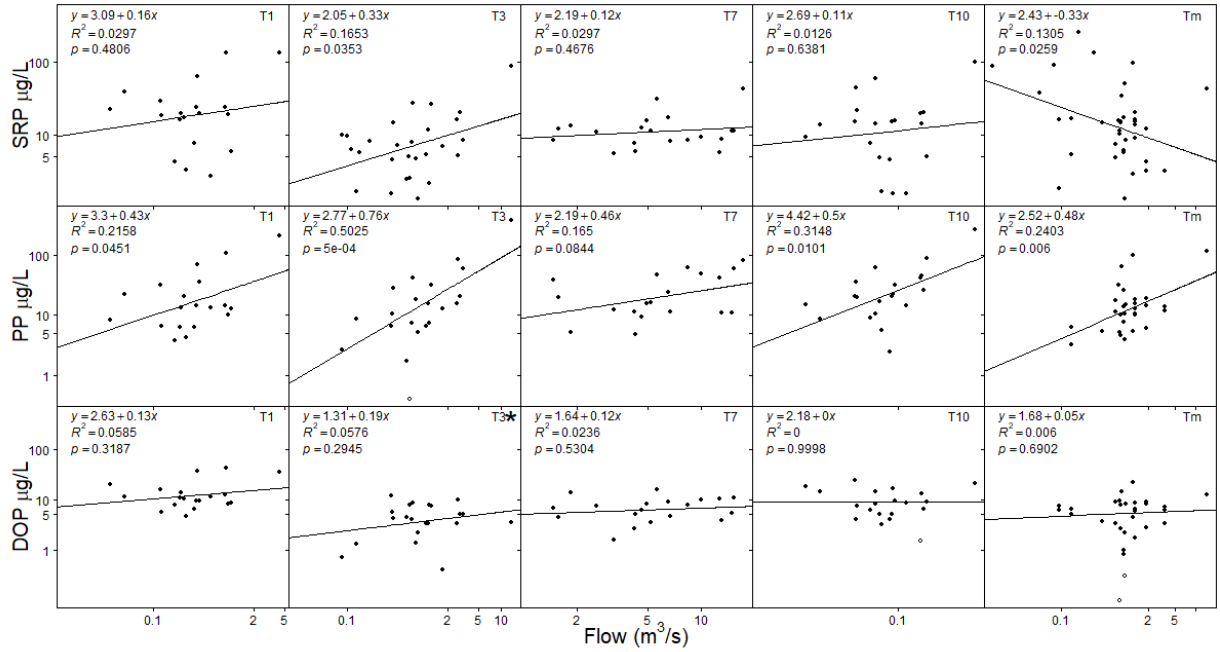


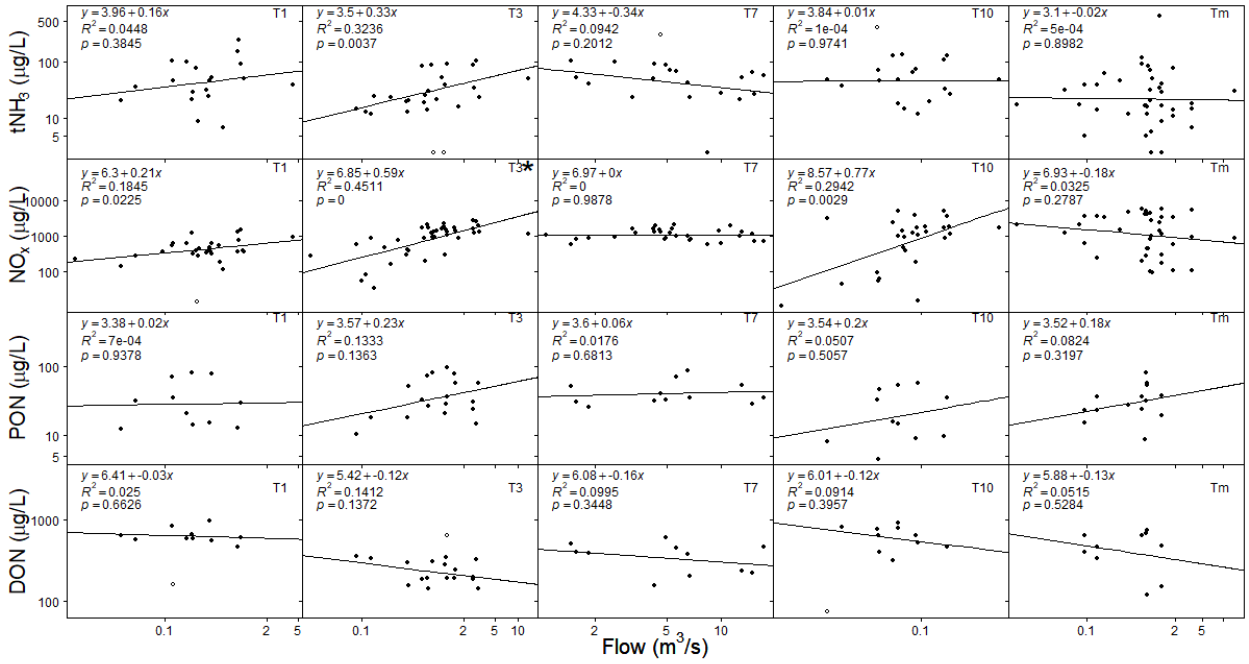

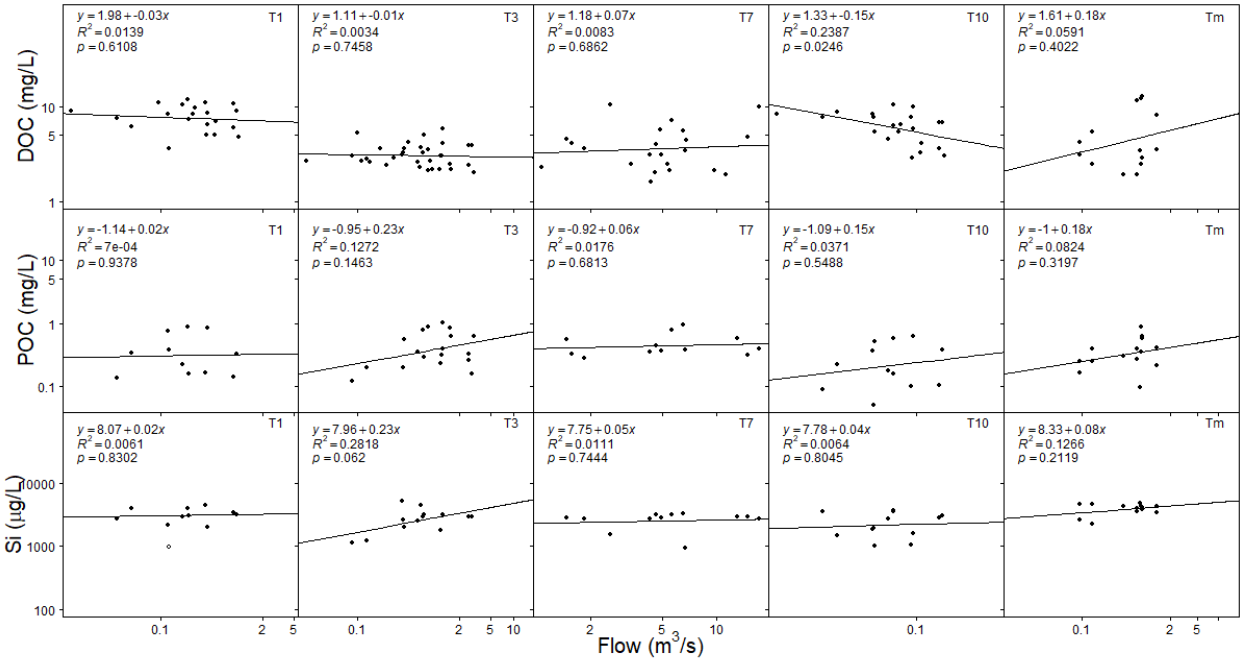
y = 1.98 + -0.03x
R² = 0.0139
p = 0.6108
T1
y = 1.11 + -0.01x
R² = 0.0034
p = 0.7458
T3
y = 1.18 + 0.07x
R² = 0.0083
p = 0.6862
T7
y = 1.33 + -0.15x
R² = 0.2387
p = 0.0246
T10
y = 1.61 + 0.18x
R² = 0.0591
p = 0.4022
Tm
DOC (mg/L)
y = -1.14 + 0.02x
R² = 7e-04
p = 0.9378
T1
y = -0.95 + 0.23x
R² = 0.1272
p = 0.1463
T3
y = -0.92 + 0.06x
R² = 0.0176
p = 0.6813
T7
y = -1.09 + 0.15x
R² = 0.0371
p = 0.5488
T10
y = -1 + 0.18x
R² = 0.0824
p = 0.3197
Tm
POC (mg/L)
y = 8.07 + 0.02x
R² = 0.0061
p = 0.8302
T1
y = 7.96 + 0.23x
R² = 0.2818
p = 0.062
T3
y = 7.75 + 0.05x
R² = 0.0111
p = 0.7444
T7
y = 7.78 + 0.04x
R² = 0.0064
p = 0.8045
T10
y = 8.33 + 0.08x
R² = 0.1266
p = 0.2119
Tm
Si (µg/L)
Flow (m³/s)

# Appendix B-4. Daily Constituent Concentration Inputs to the Water Quality Model for 2017 and 2018

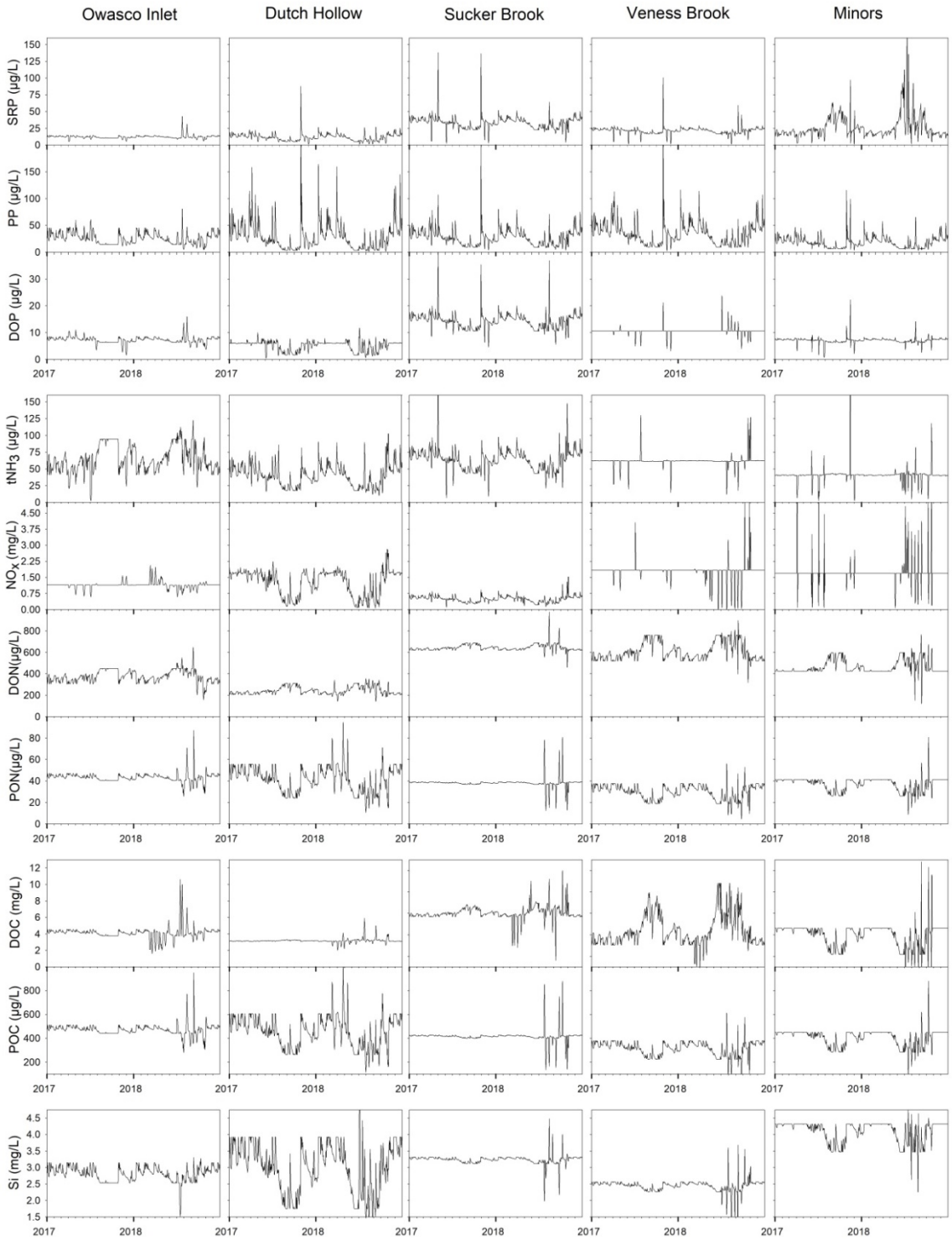

## Appendix B-5. Full GWLF-E Watershed Modeling Report

Use of data from multiple projects, each with a unique goal, can introduce variability into load estimation using observed samples. Sample size for some constituent load and concentration estimates was quite low for Owasco Lake Tributaries, especially calculated constituents. Although the use of actual observed samples is the most desirable, watershed modeling can also provide estimates of constituent loading. For this project, estimates were available through the use of the Enhanced Generalized Watershed Loading Functions (GWLF-E) model. GWLF-E is a combined distributed/lumped parameter watershed model, allowing for multiple land use/land cover scenarios. The most recent version utilizes data from the National Land Cover Database 2011.

As of the writing of this report, GWLF-E is integrated with an open source online application maintained by the Stroud Water Research Center (Model My Watershed, www.modelmywatershed.org) that allows users to define an area of interest and model water quality and hydrology. The online tool uses available geospatial information system (GIS) layers to derive inputs for the area of interest and local meteorological data for 1961 through 1990 to model water quality. The model input file was exported from the online platform and calibration of the GWLF-E completed using updated meteorological data for the period of interest.

CE-QUAL-W2 uses hour meteorological data as a driver. The temperature and precipitation data was daily average for the years of interest (1999-2018) and were used to drive GWLF-E using a custom built data manipulation program for correct formatting. Other changes to model inputs were completed using the GWLF-E desktop program which provides six model driver categories with coefficients that can be edited manually.

Initial hydrology calibration was completed in smaller tributary watersheds with active stream gages, including the Owasco Inlet to the USGS gage in Moravia, and Dutch Hollow Brook. These efforts demonstrated good agreement between modeled and observed monthly flows after minor calibration of model inputs. Hydrology of the entire Owasco Lake watershed was calibrated using this projects flow budget and lessons learned from the smaller watersheds with stream gages. Modeled hydrology agreed well with the flow budget derived as part of the water quality modeling effort when monthly mean flows were compared (Figures B-1, B-2). Slight underestimation of modeled flows at the high end of the observed flow range was present throughout all testing and final model runs, and exists in other studies utilizing GWLF-E (i.e. Tetra Tech, 2007).

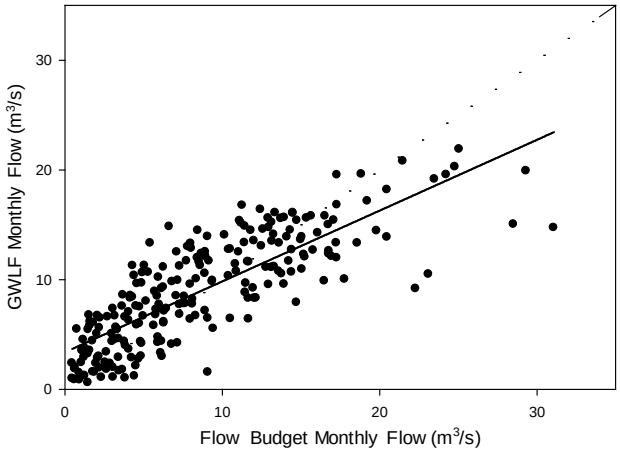


**Figure B-1**. Mean monthly flow ($m^3/s$) from the Owasco Lake flow budget developed as part of this project, compared to monthly mean modeled flow from the GWLF-E model for 1999-2018 ($R^2$ = 0.675, NSE = 0.760).

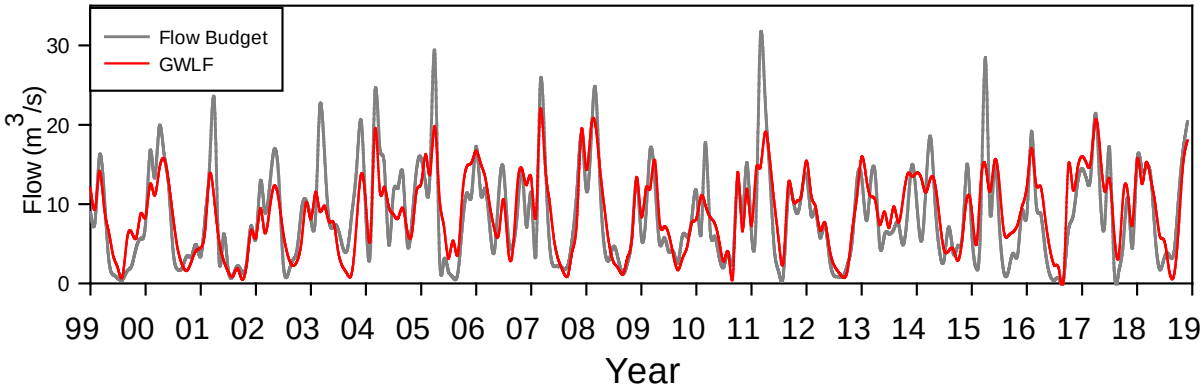


**Figure B-2**. Timeseries of mean monthly flow ($m^3/s$) from the Owasco Lake flow budget and modeled flows from GWLF-E from 1999-2018.

The GWLF-E model provides estimated loads of total and dissolved phosphorus and nitrogen as well as total suspended solids. A summary of the sources from which the model derives these estimated loads is available as well. Although these constituents aren't drivers for the water quality model, comparing load estimates derived using FLUX32 to a watershed model provided an approximation of variability in load estimation using different methodologies. Load estimates for comparison to GWLF-E that were derived using FLUX32 were the annual sum of constituent parts. Total phosphorus was the sum of daily mass (kg) of SRP, PP, and DOP; dissolved phosphorus was the sum of SRP and DOP. Total nitrogen was the sum of $tNH_3$, $NO_x$, DON, and PON; dissolved nitrogen was the sum of $tNH_3$, $NO_x$, and DON. The relative contribution of the dissolved portion of phosphorus and nitrogen varied between methodologies (Table B-2). This disparity likely is the result of how GWLF-E characterizes solid state nutrients as associated with sediment erosion and point source inputs without consideration for

compounds dissolving once they are in an aqueous environment (Haith, 1992). For this reason only loads of total phosphorus and nitrogen were compared as part of this project.

Table B-2. Percent of TP and TN made up of dissolved constituents as determined by FLUX32 software and the GWLF-E watershed model.

| Method | FLUX32 | | GWLF-E | |
|---|---|---|---|---|
| Constituent | TDP (%) | TDN (%) | TDP (%) | TDN (%) |
| Mean | 40 | 97 | 31 | 35 |
| Minimum | 37 | 97 | 25 | 33 |
| Maximum | 44 | 98 | 38 | 36 |

Constituent loading is dependent upon concentration and is a function of flow, with increases in flow resulting in an increased load if concentration remains the same. Assumptions made when setting up the GWLF-E driver file can significantly alter modeled constituent loading for a given flow regime due to the impacts of soil erodibility, attenuation, alteration of nutrient values from various land cover types, as well as the use of rural and urban best management practices which can alter either side of the concentration flow relationship. In the Owasco Lake watershed, initial model runs demonstrated a significant deficit of nitrogen loading compared to estimates using FLUX32 software. The agricultural land around Owasco Lake, and much of the Finger Lakes Region of New York State, contains tile drainage; a system of perforated piping to improve growing conditions for crops. Nitrogen constituents, especially nitrate, are labile in soil, and tile drainage contributes a significant amount of nitrogen loads downstream. After discussion with local Soil and Water Conservation Districts, a coefficient was included in the GWLF-E driver file that allotted 10% of all agricultural area with tile drainage. This addition resulted in similar loading estimates for total nitrogen between GWLF-E and FLUX32.

After hydrology and nitrogen calibration, the annual average total phosphorus loads using GWLF-E were nearly three times higher than those derived using FLUX32 software. Multiple reasons were identified that could impact the model estimates of phosphorus loading to be higher than observed values. First, the large wetland area at the mouth of the Owasco Inlet might alter the character of constituents as they move through. Particulate matter is deposited and dissolved constituents can be taken up within wetlands during the growing season. To account for these processes the “percent drainage” coefficient was adjusted within GWLF-E. The Owasco Inlet tributary watershed makes up approximately 57% of the total Owasco Lake watershed area, so a coefficient of 0.57 was applied. Second, a lot of effort has been placed in developing and implementing best management practices (BMP’s) within the Owasco Lake watershed. BMP’s linked with improved water quality from the watershed can play an important role in nutrient load reductions. An agricultural census for Cayuga County by the United Stated Department of Agriculture lists the use of no till agriculture (20%), reduced till agriculture (22%), and cover crops (21%) (USDA, 2019). In GWLF-E coefficients were applied under the BMP category to

include these inputs as well as some assumed values based off of reports of streambank stabilization efforts in the watershed (Ecologic, 2015). Finally, sediment loading (TSS) was compared between FLUX32 and GWLF-E, demonstrating a similar disparity to that observed for phosphorus. This suggests that much of the difference is due to high particulate loads derived through GWLF-E. To adjust this, under the "Transport" tab, an adjustment was made to decrease the amount of erosion along streambanks. This change was suggested in a report on the use of GWLF-E in the northeastern United States as a result of lower erodibility of glaciated soils, compared to the default value which is set for highly erodible soils. All changes to model inputs are listed in Table B-3.

**Table B-3**. Driver calibration for GWLF-E model for the entire Owasco Lake watershed.

| Category | Driver | Downloaded value from MMW | Calibrated value | Justification |
|---|---|---|---|---|
| Transport | % tile drainage | 0.0 | 0.1* | Conversations with local SWCD |
| Transport | Sed A Adjustment | 1.5 | 0.3 | {Penn State, 2007} |
| Nutrient | Dissolved runoff coefficient for Hay/Pasture | 0.52 | 0.2 | {Haith, 1992} Table B-15 |
| Nutrient | Dissolved runoff coefficient for Crops | 0.52 | 0.3 | {Haith, 1992} Table B-15 |
| Animal | Dairy Cows Grazing | Yes | No | Conversations with local dairy farmers |
| Delivery | Percent Drainage | 0.00 | 0.57* | This study |
| BMP | Cover Crop | 0.0 | 0.2* | {USDA, 2019} |
| BMP | Conservation Tillage | 0.0 | 0.3* | {USDA, 2019} |
| BMP | Conservation Plan | 0.0 | 0.3* | {Cayuga County, 2015} Table 5-2 |
| BMP | Nutrient Management | 0.0 | 0.3* | {Cayuga County, 2015} Table 5-2 |
| BMP | Grazing land management/Ag-land retirement | 0.0 | 0.1* | Assumption based on {Cayuga County, 2015} Table 5-2 |
| BMP | Animal waste management system | 0.0 | 0.1* | Assumption based on {Cayuga County, 2015} Table 5-2 |
| BMP | Runoff Control | 0.0 | 0.1* | Assumption based on {Cayuga County, 2015} Table 5-2 |

| | | | | |
|---|---|---|---|---|
| BMP | Phytase in Feed | 0.0 | 0.1* | Assumption based on {Cayuga County, 2015} Table 5-2 |
| BMP | Stream length w/ vegetated buffer (km) | 0.0 | 25.0 | Assumed length based on {Cayuga County, 2015} Table 5-2 |
| BMP | Stream length w/ fencing (km) | 0.0 | 10.0 | Assumed length based on {Cayuga County, 2015} Table 5-2 |
| BMP | Stream length w/ bank stabilization (km) | 0.0 | 25.0 | Assumed length based on {Cayuga County, 2015} Table 5-2 |

*Represents a percentage as a decimal number

Watershed modeling of a large, complex system such as the entire Owasco Lake watershed proved challenging, however, lessons learned throughout the process are useful to understand what drives estimates of loads from a watershed model and how it compares to those estimated using FLUX32 software. Further fine tuning of the model might result in even better agreement between the two methods, but there is need for published data to back up any further calibration of model inputs. Annual total phosphorus load estimates were consistently higher from GWLF-E even after calibration of model inputs. Total nitrogen and sediment load estimates compared more closely but with a high amount of variability from year to year (Table B-4).

The year 2003 represents the worst comparison for TN and TSS (corresponding to the only year where TP estimates were higher using FLUX32) which lined up with the worst hydrograph fit. During this period the modeled flow were consistently low with respect to this projects flow budget highlighting the importance of hydrology in driving the GWLF-E model. Even though four meteorological stations were used to create the weather inputs used in GWLF-E, localized storms might have played a role in the disparity in flow during some years.

Table B-4. Comparison of annual load estimates from the Owasco Lake watershed (kg) using the GWLF-E model and FLUX32 software

| Year | TP GWLF | TP FLUX | TN GWLF | TN FLUX | TSS GWLF | TSS FLUX |
|---|---|---|---|---|---|---|
| 1999 | 21,173 | 9,378 | 357,373 | 293,222 | 3,780,300 | 3,033,917 |
| 2000 | 21,669 | 16,990 | 390,745 | 485,445 | 4,256,280 | 5,597,652 |
| 2001 | 16,969 | 12,018 | 254,079 | 345,644 | 3,103,740 | 3,848,485 |
| 2002 | 19,677 | 15,142 | 337,832 | 462,224 | 4,098,350 | 5,049,930 |
| 2003 | 19,110 | 21,504 | 336,242 | 601,766 | 3,652,460 | 7,151,953 |
| 2004 | 28,817 | 23,039 | 489,556 | 644,832 | 5,938,130 | 7,637,964 |
| 2005 | 32,805 | 19,141 | 567,918 | 513,511 | 5,825,580 | 6,062,978 |
| 2006 | 29,926 | 18,588 | 513,145 | 548,148 | 5,844,870 | 6,186,096 |
| 2007 | 26,428 | 17,953 | 476,660 | 497,745 | 4,268,610 | 5,848,442 |
| 2008 | 26,149 | 17,027 | 471,824 | 484,696 | 4,174,900 | 5,572,335 |
| 2009 | 21,714 | 12,192 | 365,081 | 397,286 | 4,369,970 | 4,023,776 |
| 2010 | 26,804 | 15,026 | 405,495 | 453,783 | 4,984,500 | 4,920,819 |
| 2011 | 32,869 | 22,292 | 558,181 | 613,881 | 6,934,740 | 7,412,168 |
| 2012 | 19,450 | 10,156 | 323,412 | 336,240 | 3,643,010 | 3,391,223 |
| 2013 | 29,681 | 16,092 | 519,664 | 501,924 | 5,924,250 | 5,381,310 |
| 2014 | 24,049 | 14,910 | 424,668 | 467,691 | 4,521,750 | 4,958,936 |
| 2015 | 27,376 | 15,800 | 474,724 | 444,020 | 5,624,690 | 5,149,478 |
| 2016 | 26,600 | 12,521 | 478,387 | 375,725 | 4,401,960 | 4,163,866 |
| 2017 | 32,072 | 20,047 | 603,876 | 550,001 | 5,606,700 | 6,962,387 |
| 2018 | 29,874 | 19,554 | 513,437 | 575,942 | 4,778,950 | 6,449,809 |
| Mean | 25,661 | 16,469 | 443,115 | 479,686 | 4,786,687 | 5,440,176 |
| Min | 16,969 | 9,378 | 254,079 | 293,222 | 3,103,740 | 3,033,917 |
| Max | 32,869 | 23,039 | 603,876 | 644,832 | 6,934,740 | 7,637,964 |
| Range | 15,899 | 13,661 | 349,796 | 351,610 | 3,831,000 | 4,604,047 |

References:

Ecologic LLC. 2015. Owasco Lake Watershed Management and Waterfront Revitilization Plan; Watershed and Waterbody Inventory Report.

Haith, D., Mandel, R., Shyan Wu, R. 1992. Generalized Watershed Loading Functions User's Manual Version 2.0. Cornell University Department of Agricultural & Biological Engineering.

Tetra Tech Inc. 2007. Limberlost Creek Watershed Sediment and Nutrient TMDL Development; Draft for U.S. EPA Approval. Accessed at: https://www.in.gov/idem/nps/files/tmdl_limberlost_draftreport.pdf

United States Department of Agriculture (USDA). 2019. 2017 Census of Agriculture County Profile Cayuga County New York. Accessed at: https://www.nass.usda.gov/Publications/AgCensus/2012/Online_Resources/County_Profiles/New_York/cp36011.pdf

# Appendix C: Limnology

**Owasco Lake In-Lake Model**

**Biological Components Final Report**
**Dreissenid Mussel, Plankton, and Mussel Bed Nutrient Survey Components Final Report**

**Kimberly L. Schulz, Ph.D.**

**Department of Environmental and Forest Biology**

**SUNY College of Environmental Science and Forestry**

**200 Bray Hall (grant office), 456 Illick Hall (faculty office), 1 Forestry Drive, Syracuse, NY 13210**

**Telephone: (315) 470-6808; email: kschulz@esf.edu or kschulz@syr.edu**

**Table of Contents**

# Contents

# 1 I. Overview of Biological Component – Project Justification and Objectives:

## *1.1 **Overview***

Owasco Lake, NY, is one of a number of lakes in the Northern Temperate Zone that has shown increases in algal blooms and harmful algal blooms (HABs). A number of factors may contribute to these blooms, including nutrient loading (e.g., nitrogen and phosphorus), changes in climate that alter runoff timing and frequency, reduce ice cover duration and may increase surface water temperatures and the invasion of non-native species (e.g., Jöhnk at al. 2008, Pendergrass, A.G. and R. Knutti. 2018. Rantala et al. 2017, Sinha et al 2017).

Zooplankton, especially large species in the genus *Daphnia*, as well as invasive dreissenid mussels, both are efficient grazers of phytoplankton; both plankton and mussels have the ability to reduce algal concentrations at any given nutrient level (e.g., Sarnelle et al. 2005). However, zooplankton and mussels can exhibit selective feeding and may avoid consuming cyanobacteria, and they also excrete nutrients that may stimulate algal growth, including growth of HAB-producing species(e.g., Sarnelle 2005).

The invasions of predatory zooplankton such as *Cercopagis*, the fish-hook waterflea, and the two species of benthic Mollusca, zebra and quagga mussels (*Dreissena polymorpha* and *Dreissena rostriformis bugensis*) to many lakes in New York State may be altering nutrient recycling and the grazing of phytoplankton, potentially contributing to increases in HABs.

Upstate Freshwater Institute has developed an in-lake model that has been applied in other systems, such as Cayuga Lake, and the overall goal of this project is to parameterize a similar model for Owasco Lake, which has experienced a number of HABs in recent years (https://www.dec.ny.gov/chemical/83332.html).

The primary tasks of this biological component of the project were to assist Upstate Freshwater Institute with collection of data to allow parameterization of these biological components for an in-lake model for Owasco Lake that includes biological parameters.

**Specifically, data on the spatial/depth distributions of: (1) dreissenid populations, and characterization of the (2) phytoplankton and (3) zooplankton assemblages were collected and analyzed for input to the UFI in-lake model. In addition, nutrient samples from above mussel beds were collected and provided to UFI for analysis to inform estimates of nutrient recycling by mussels**.

To support the application of a dreissenid module to the Owasco Lake In-lake Model, a dreissenid mussel survey in Owasco Lake therefore was required. The most recent benthic survey was completed in 2007 (Watkins et al. 2007). During that survey it was determined that zebra mussels had invaded the lake, primarily in shallow regions (<20 m), but quagga mussels had not yet invaded Owasco Lake. Quagga mussels were reported as having invaded Owasco Lake subsequently, but the extent of that invasion had not been quantified. Assessing the distribution of mussels at different depths of Owasco Lake was needed to parameterize UFI's 2-D nutrient modeling effort.

To that end, we collected both images of the benthos (sediment-water interface) and mussel samples from sites around the lake using a rig that was constructed to allow sampling of a standardized area of sediment that was also sampled for mussels, which were identified and counted in the laboratory. The goals of this dreissenid

task were to estimate the current dreissenid mussel composition (zebra and quagga mussels) in different depths and regions of the lake as well as to test the efficacy of using images to monitor benthic mussels.

In addition, a number of nutrient samples were collected by divers above mussel beds at differing depths, substrate types and mussel densities for analysis by Upstate Freshwater Institute (UFI) to estimate and validate model predictions for nutrient release from the mussel beds.

To parametrize the plankton components of the model, phytoplankton grab samples and zooplankton tows also were collected by UFI during their regular nutrient monitoring, and provided to SUNY ESF for analysis. These samples were enumerated and the taxonomic composition was quantified. The phytoplankton and zooplankton data were converted to summary parameters, including number and mass of zooplankton grazers, omnivores and predators over the summer season, and the biovolume of specific taxonomic groups of phytoplankton, that then could be input directly into the UFI water quality model.

This report summarizes the methods and results for the biological components of the Owasco In-Lake Model Project.

As listed in the initial project outline, the specific responsibilities for biological components were as follows:

1. Coordinate biological and nutrient sampling with Upstate Freshwater Institute.
2. Determine site locations; review parameter selection, and sampling frequency needs with UFI.
3. Work with the State University of New York's Dive Safety Officer to establish dive safety procedures and ensure adequate training of divers.
4. Oversee, train, and supervise field sampling and field assistants.
5. Oversee and supervise transfer of field nutrient samples to Upstate Freshwater Institute and receipt of plankton samples from Upstate Freshwater Institute.
6. Oversee training and supervision of mussel samplers and undergraduate student counters.
7. Organize, enter, and validate field data, images, and mussel survey counts.
8. Count plankton and zooplankton in samples received from Upstate Freshwater Institute.
9. Organize and analyze mussel and plankton data and deliver data and report to Upstate Freshwater Institute.

These objectives have been accomplished, although we were unsuccessful in finding a method that enabled quantification of mussels using image analysis.

### *1.2 Summary of delays in start and effect on completion of project, as well as additional delays*

Although all of these components have been completed, because the contractual start of the project was delayed until June 2018, we were unable to recruit the graduate student to the project, and the biological components relied on summer undergraduate employees and the biological component PI (Schulz) as field hands and analysts, along with undergraduate volunteers in Fall 2018 and Spring 2019.

In addition, a delay in purchase of dive equipment at SUNY ESF's Purchasing office due to difficulty in obtaining alternate vendor bids pushed the dive plan approval back even further. Nonetheless, submission of dive protocols to the divemaster for approval was completed by the mid-June 2018. The necessary equipment

for divers was ordered and received in late June/early July, and training of personnel for diving on this project was co-ordinated by the SUNY ESF dive master from June through August. Preliminary dives and method testing for this project were approved by August 2018 and completed in August and September 2018. However, the delay prevented the dive master from being able to complete the three deep dives he had been planning to perform with another trained dive master (deep dives require special certifications and safety protocols), so we were unable to collect voucher mussel samples from deeper than the ~25 meter depth that our protocols permitted for the faculty and student divers.

Upstate Freshwater Institute also began their sampling for biological parameters later than expected, and our first plankton samples were received in July 2018. Plankton samples were collected by UFI from July through September 2018 and delivered to SUNY ESF for processing.

In addition, the PI was hindered in completing laboratory work due to a serious family injury that resulted in hospitalization, surgery, and rehabilitation, which made overtime work impossible from January-April 2019. Health issues in mid-2019 through early 2020 and then the extra work associated with the COVID-19 pandemic's effect teaching in March-May 2020 (moving to remote instruction and redesigning a large course with five lab sections) greatly interfered with progress as the project analysis was being completed. Nonetheless, despite these many setbacks, the required analyses and are now completed and a summary of the data collection, analyses and results are included in this project.

Due to delay in receiving all the required components from Schulz, UFI is still completing the modeling effort. All components of the originally conceived project have been analyzed and the Owasco Lake Model can be parameterized with the needed mussel, phytoplankton and zooplankton components to inform the consideration of factors contributing to HABs in Owasco Lake.

### *1.3 **Summary of Personnel Involved in the Biological Component***

**Primary Investigator for the Biological Components**: Kimberly L. Schulz, Associate Professor
Department of Environmental and Forest Biology,
State University of New York, College of Environmental Science and Forestry, Syracuse, NY 13215
(315) 470-6808 kschulz@esf.edu

**Dive Safety Officer**

Jason Meany, Deep Stop SCUBA, 150 Township Blvd, Suite 20, Camillus, NY 13031; 315-378-7175, jmeany@deepstopscuba.com

Responsibilities:

1. Approved all gear for use in the underwater imaging and scuba dive surveys.
2. Worked with PM Schulz and the research divers to certify that the dive methods are appropriate and train all dive personnel on the protocols and safety training.
3. Was contracted to collect 3-5 deep (>80-100+ feet) calibration samples

**Research Divers – late summer 2018**

Alexander Romer (alexromer2@gmail.com) and Robert Pedian (bob.pedian@gmail.com)

Responsibilities:

1. Learn dive protocols and be tested and cleared for project protocols by Dive Safety Officer, Jason Meany.
2. Assist with constructing field gear; checking and cleaning gear daily.
3. Along with PM Schulz, serve as surface tender or two-person dive crew for each sample collection site.

**Volunteer Student Assistants and Researchers**

In the field: Tyler Duby, Matthew Cowen, Lydia Pleasants, Alexandra Cormack

In the lab: Lydia Pleasants, Alexandra Cormack, Carrick Palmer, Kyla Watson, Jack Zeng

Volunteer responsibilities in the field included:

1. Cowen, a former U.S. Navy sonar operator, was responsible for initial sonar setup and calibration with PM Schulz.
2. Student volunteers assisted as surface tenders during field sampling under supervision of PM Schulz (Duby and Cowen).
3. Cowen also assisted PM Schulz with sonar data collection.

Volunteer responsibilities in the laboratory included:

1. Students were trained by PM Schulz to identify dreissenid mussels and to distinguish zebra and quagga mussels (Duby and Pleasants)
2. Students assisted PM Schulz in counting frozen mussel samples, previously collected in the field, by separating into empty mussel shells versus live mussels (Cormack, Duby, Palmer, Pleasants, Watson, Zeng).
3. Students assisted PM Schulz in identifying collected mussels as zebra or quagga (Duby and Pleasants).
4. Cowen assisted PM Schulz with sonar data and plotting data.

# II. Methods and Results

## 1.4 Part A: Mussel Objectives

The main objectives of the mussel component of the project were:

1. To survey mussel distribution and investigate patterns of mussel distribution with depth.

2. To provide nutrient samples collected above mussel beds where mussels would be quantified

A decade-old survey of Owasco Lake in 2007 (Watkins et al. 2010), approximately a decade after zebra mussels had invaded the lake, used an Ekman dredge to sample the organisms living on the surficial sediment in a transect on a centerline from the north to the south end of the lake. This survey indicated that zebra mussels,

(*Dreissena polymorpha*), but not quagga mussels (*Dreissena rostriformis bugensis*) were present in the lake at that time, reaching densities of 3,000-4,000 mussels per $m^2$ and reaching maximum abundances in the 10 m depth samples. They expressed concern that invasion quagga mussels would pose a risk to endemic benthic invertebrates that were persisting in a deeper water refuge in the lake at the time of that survey.

However, reports on iMap invasives and qualitative observations by Finger Lakes Institute and others indicated that quagga mussels have since invaded Owasco Lake. While zebra mussels tend to be most abundant on hard substrates and shallower regions of lakes, quagga mussels are able to thrive on soft sediments and are able to survive in deep waters, having been found to dominate the benthos in profundal areas of deep lakes (Karatayev et al. 2015).

Therefore the first objective was to resurvey the lake to quantify the presence and current distribution of invasive mussels in Owasco Lake, so that UFI could parameterize that portion of their 2D lake model.

### 1.4.1 A. 1. Survey of Mussel Distribution and Nutrients Above Mussel Beds – Field Sampling

After several test dives, UFI and ESF personnel agreed on a sampling strategy of sampling six transects, two each on the north and south end of the lake (Table 1; Figures 1A-D), one on the west shore on a rocky steep area about 1/3 of the way up the lake, and one near frequent HAB blooms on the sediment-rich and shallower-sloped east side of the lake, about 2/3 up the east shore (Figure 2).

In consultation with UFI, we established 6 transects from shallow (~2 m) to deep (~23 m) water to quantify mussel distribution in the lake, with the goals of determining the patterns of zebra and quagga mussel distributions with depth around the lake (Table 1; Figures 1A-D). These are the same sites for which nutrient samples were provided to UFI for analysis (see Part A.2).

Depth and site locations were geo-referenced using a high-end commercial side-scan sonar (Hummingbird Helix 5; SI.GPS).

We used underwater photography to take images of the mussels at the bottom of Owasco Lake and sampled known areas of the benthos with SCUBA for laboratory analysis (identification and quantification) to determine how many and what types of these dreissenid mussels are currently found at different locations in the lake, and how extensively these mussels cover the lake bottom. We imaged, collected water from above these mussel beds, and sampled the mussels at geo-referenced locations along the transects.

Quantification of zebra and quagga mussel distributions on the bottom of Owasco Lake was performed by use of a combination of direct sample collection by divers at known locations determined with sonar (and depth confirmed with dive computers) in conjunction with imaging of these reference sites. The hope was that images could be used to survey mussels on additional sites around the lake bottom quickly, as taking images and having an automated method for analyzing the images potentially would be less laborious than direct collect and counting, and would allow greater resolution for estimating coverage of the lake bottom with mussels if many photos could be collected from around the lake and analyzed quickly with imaging software.

**Table 1.** Site numbers, depths, GPS locations, and whether a nutrient sample was collected (nutrient samples were not collected in conditions such as high plant density or the sediments being disturbed). The site locations are indicated with purple dots on Figures 1 A-D.

| Mussel Site Number | Waypoint | Latitude (sonar) | Longitude (sonar) | Depth in meters (sonar or dive watch) | Nutrient Sample Provided to UFI |
|---|---|---|---|---|---|
| OW11A* | 47 | 42 45.517 | 76 28.163 | 3.0 | Yes |
| OW11B* | 47 | 42 45.517 | 76 28.163 | 1.8 | Yes |
| OW12A* | 48 | 42 45.535 | 76 28.226 | 5.9 | Yes |
| OW12B* | 48 | 42 45.535 | 76 28.226 | 4.1 | Yes |
| OW12C* | 48 | 42 45.535 | 76 28.226 | 7.1 | Yes |
| OW13** | between 48-49 | N/A | N/A | 10.9 | No |
| OW14** | 49 | 42 45.540 | 76 28.225 | 16.8 | Yes |
| OW15** | 50 | 42 45.540 | 76 28.225 | 11.8 | Yes |
| OW16 | 53 | 42 53.913 | 76 32.413 | 1 | Yes |
| OW17 | 54 | 42 53.819 | 76 32.415 | 4.9 | Yes |
| OW18 | 55 | 42 53.583 | 76 32.424 | 9.9 | Yes |
| OW19 | 56 | 42 53.315 | 76 32.346 | 13.8 | Yes |
| OW20 | 57 | 42 53.070 | 76 32.160 | 21.6 | Yes |
| OW21 | 58 | 42 45.560 | 76 27.759 | 1 | Yes |
| OW22 | 59 | 42 45.705 | 76 27.881 | 6.0 | Yes |
| OW24 | 62 | 42 45.920 | 76 28.078 | 21.9 | Yes |
| OW25 | 63 | 42 45.773 | 76 27.944 | 14.1 | Yes |
| OW26 | 64 | 42 45.740 | 76 27.966 | 11.2 | Yes |
| OW27 | 66 | 42 51.907 | 76 30.946 | 1 | Yes |
| OW28 | 67 | 42 51.946 | 76 31.020 | 4.8 | Yes |
| OW29 | 69 | 42 52.008 | 76 31.038 | 16.4 | Yes |
| OW30 | 70 | 42 52.014 | 76 31.014 | 8.2 | Yes |
| OW31 | 71 | 42 52.018 | 76 31.053 | 22.9 | Yes |
| OW32 | 72 | 42 48.410 | 76 30.782 | 1.0 | Yes |
| OW33 | 73 | 42 48.413 | 76 30.748 | 11.9 | Yes |
| OW34 | 74 | 42 48.416 | 76 30.761 | 4.5 | Yes |
| OW35 | 75 | 42 48.439 | 76 30.770 | 17.9 | Yes |
| OW36 | 76 | 42 48.446 | 76 30.783 | 20.6 | Yes |

*Sites marked with an asterisk were collected while the boat was moored at the same sample site as another sample collection location. These sites were in close proximity (<5m) to each other, and given the wind conditions, movement of the boat, and/or the slight angle of the line on the camera rig (due to wind) their location could not be resolved to greater precision. The depth at these sites was determined with the dive watch depth reading. Note: at all sites, not just these, the sonar depth reading also was confirmed with the dive watch reading.

**Three sites at which 'deep' mussel samples were collected in a smaller quadrat after the standard sampling of surface mussels was completed

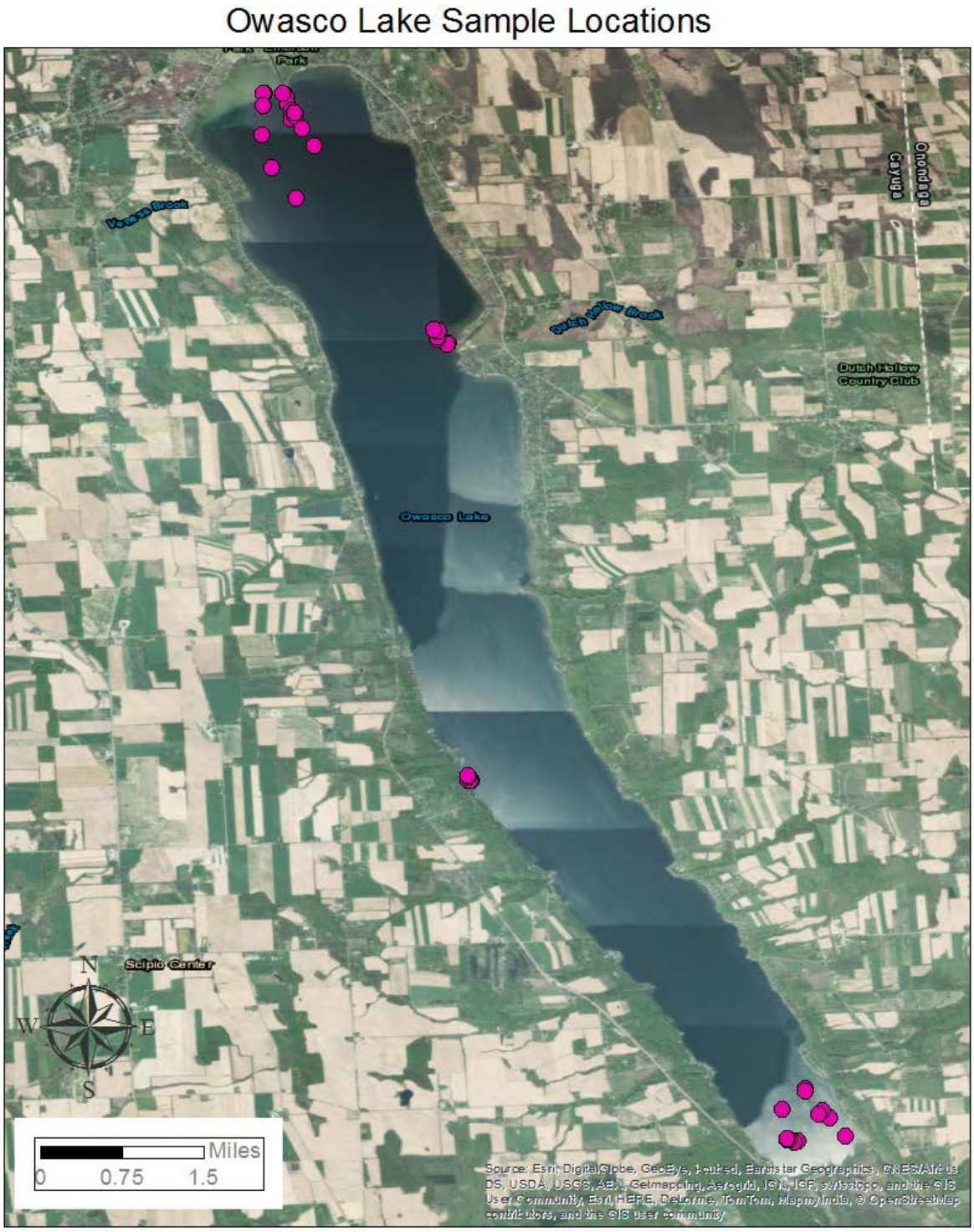


**Figures 1A.** Sampling transects and quadrat locations selected for this survey of Owasco Lake. Two shallow to deep transects were performed at both the North and South ends of the lake, one on the Northeast side, near the site of many HAB reports, and one on the southwest side. Note: the points on the Southwest side survey are close together due to the steep topography at this transect. See Table 1 for the coordinates and other site information.


**Figure 1B.** Locations of the one eastern and two northern and transects and sites. See Table 1 for the coordinates and other site information.

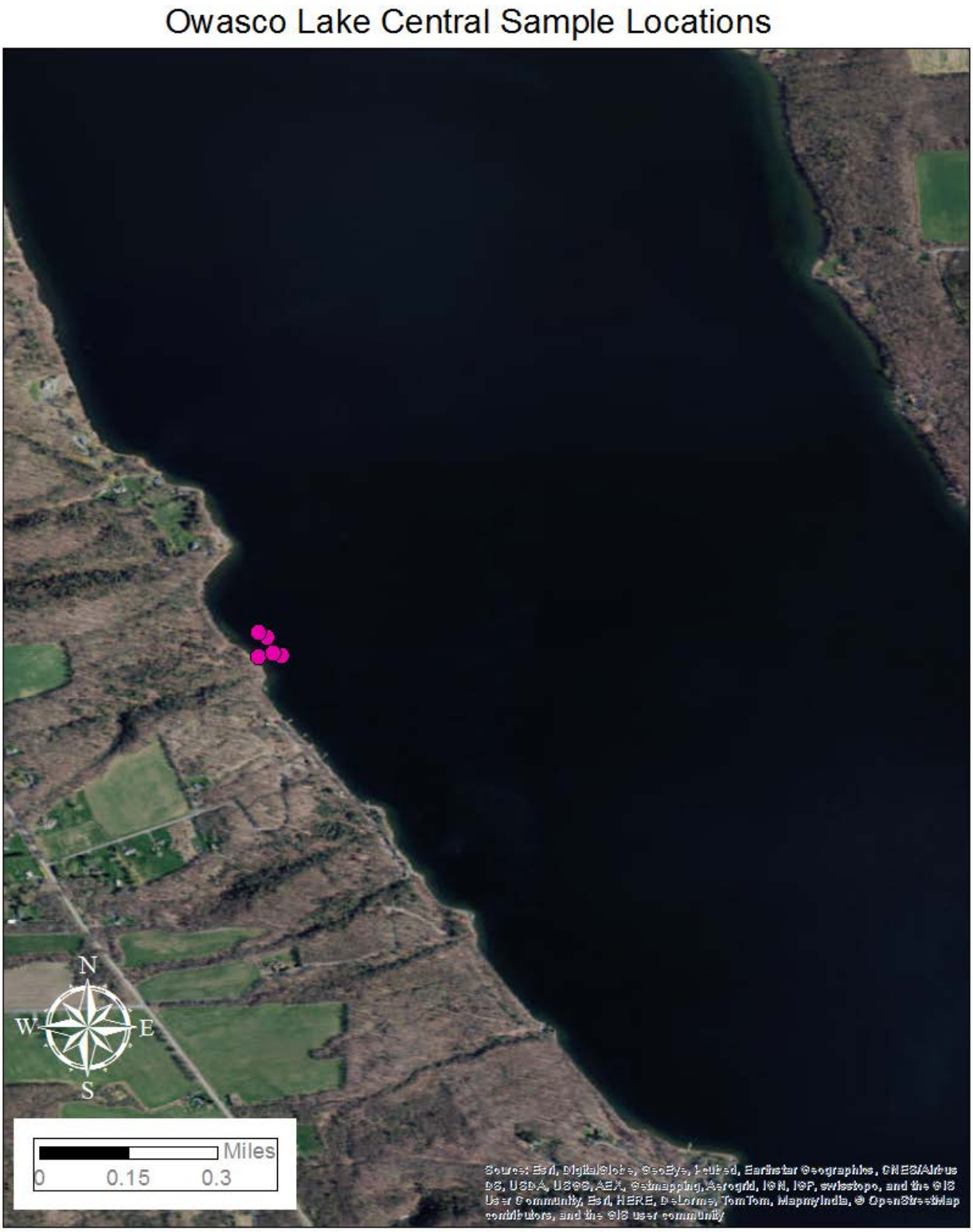


**Figure 1C.** Locations of Central/Western Owasco Lake transects and sites. See Table 1 for the coordinates and other site information.


**Figure 1D.** Locations of Southern Owasco Lake transects and sites. See Table 1 for the coordinates and other site information.

Lewis MacCaffrey (DEC) has demonstrated that mounting an underwater camera to a milk crate could allow imaging of lake sediments and dreissenid mussels. Because a milk crate has a closed top and so cannot be sampled by divers, we constructed a different version of a mussel camera rig to allow for imaging and collection of the imaged sample for laboratory analysis.(Figure 2a). This rig was constructed by Schulz and the undergraduate research divers with help from the machine shop at SUNY ESF. The frame was made from PVC and consisted of a standard 0.5 x 0.5 meters PVC dive sampling quadrat (a sampling square of known area) as the bottom of a PVC cube, with a GoPro attached to a crossbar at the top end of the cube, and lines connecting the corners of the top piece to a line for lowering the rig from the boat. The machine shop constructed attachments for two high-intensity dive lights so they could be attached to side struts to illuminate the entire bottom quadrat. The dive lights provided excellent illumination, but also were limited in battery life (~2 hours run time on a charge).

The GoPro was enclosed in a deep dive waterproof case and was set to record pulsed images, so the least disturbed image could be used for analysis. In cases where the GoPro image was slightly askew due to currents or bending of the frame, the dimensions of the quadrat in a partial image could be calibrated with the length of known PVC pieces in the image (e.g., Figure 2b). The open top and sides allowed for divers to access the imaged site.

(a) (b)

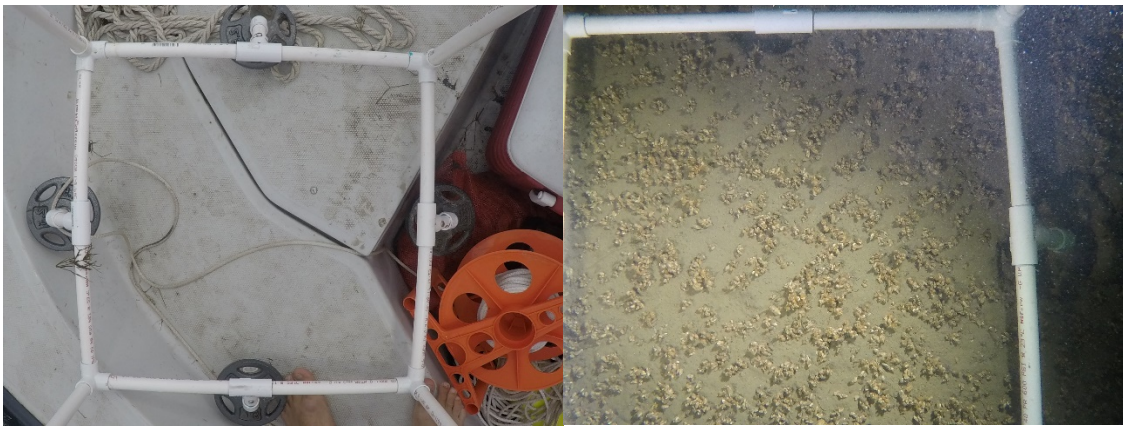

**Figure 2**. (a) View from the GoPro of the sample quadrat while still on the boat. The camera is mounted with dive lights above the rig. (b) Typical view of the quadrat at the bottom of the lake with soft sediments and visible mussels covering much of the sediment surface.

The dive plan for sampling was approved by the Dive Safety Officer, Jason Meany, and he trained all of the divers on the protocol using blackout masks in a pool, until the sampling could be carried out in the zero visibility conditions that were present once sampling of mussels began, due to the stirring of the sediments.

According to the plan, at each station, an electronic dive slate with the site number was first be displayed under the camera before lowering over the side, so that the series of images that followed could be matched with the site/quadrat number. Then the rig was lowered slowly to the bottom and allowed to sit until any plume suspended by the quadrat was seen to dissipate on the sonar image. In calm conditions, sediment disturbance was minimal, but in windy conditions, if the tender vessel was pulling on the anchor, sampling the quadrat, and

interpretation of images was not always possible, as the sampling rig was dragged along this bottom. This necessitated limiting mussel and nutrient sample collection to calm days.

Dive lights were generally left off during the descent of the dive rig to the bottom of the lake, so those images are often greenish or dark in hue depending on the depth.

As mentioned, at times, such as in Figure 2 above, the camera would become slightly skewed due to movement on the trip down, but the known length of the PVC pieces could then be used to determine the image sizes for potential calibration. All images were uploaded to a Google Drive and images and movie clips from the GoPro can be accessed at a folder containing all raw images collected during the dive surveys: https://drive.google.com/drive/folders/1l9AwPQoICqr_jAZFkTtmXb-4Ri4X4wql?usp=sharing.

Lowering the rig to the sediments stirred up sediment if the area was covered in soft mud (most of the Owasco Lake bottom). We could visualize any sediment disturbance on the sonar after the rig was deployed and reached the bottom. The divers waited at least 5 minutes to descend slowly down the line to the sample site. The two divers had distinct tasks. Diver 1 carried an acid-washed re-sealable plastic bag labeled with the site number. Diver 2 carried a double plastic mesh sampling bag, gloves and trowel, Before either diver touched the bottom and disturbed sediments, the nutrient sample was collected by Diver 1 from 0.5-1 m above the quadrat in an acid-rinsed bag.

Upon Diver 1's completion of that task, Diver 2 descended to the bottom of the lake and knelt at the edge of the quadrat. Diver 2 turned off the dive lights to save batteries and because once sampling commenced, suspended sediments reduced visibility to 0 meters even with the light on. Diver 1 remained about 1 meter above the quadrat, watching the progress of Diver 1 and monitoring air bubble release to ensure safety of Diver 2. If any concern about safety had been observed, Diver 1 would have signaled the tender on the vessel by a pre-arranged number of pulls on the line and proceeded to assist Diver 2 and follow safety protocols to abort the dive if necessary.

Diver 2, provisioned with a doubled plastic mesh collecting bag, trowel and gloves, was responsible for collecting all surface mussels for identification and counting after Diver 1 had finished collecting the nutrients and had then become established in the safety observer position.

Once collection of mussels began, the sediment was disturbed by the movements of Diver 2, resulting in zero visibility, so all collection was done by hand/feel. This was one of the tasks practiced in a pool in advance, with the dive master giving the divers blackout masks and requiring them to collect small objects and verifying that they were able to collect *all* the small objects from within a quadrat with zero visibility.

Collection at the site continued until all mussels were removed from the surface of the site. The mussel-collecting diver (Diver 2) then signaled completion, and joined the tending diver (Diver 1) who was hovering and observing ~one meter above the collector, and the two surfaced in accordance with safe diving protocols. On the deeper dives, dive logs and dive watches were monitored closely to ensure dive safety and perform any required decompression.

As soon as the diver surfaced, the boat tender labeled the mussel bag with the site number, made sure it was drained, and immediately put it on ice in a cooler. The boat tender also collected the nutrient bag from Diver 1 and carefully used some of the water to rinse the acid-washed nutrient sample bottles provided by UFI, and then filled the bottle with the rest of the sample and immediately placed it in a separate cooler.

Fortunately, there were no safety issues on any of the dives.

The test dives and five sampling survey transects from shallow (1 m) to deeper water (~25 m) were completed around the lake (including transects on south, east, west and north shores) in August and September 2019. At several sites, the nutrient sample bags did not contain enough water to rinse and fill the bottles, or were spilled accidentally by the tender, accounting for the sites with mussel samples, but lacking corresponding water chemistry values (Table 2).

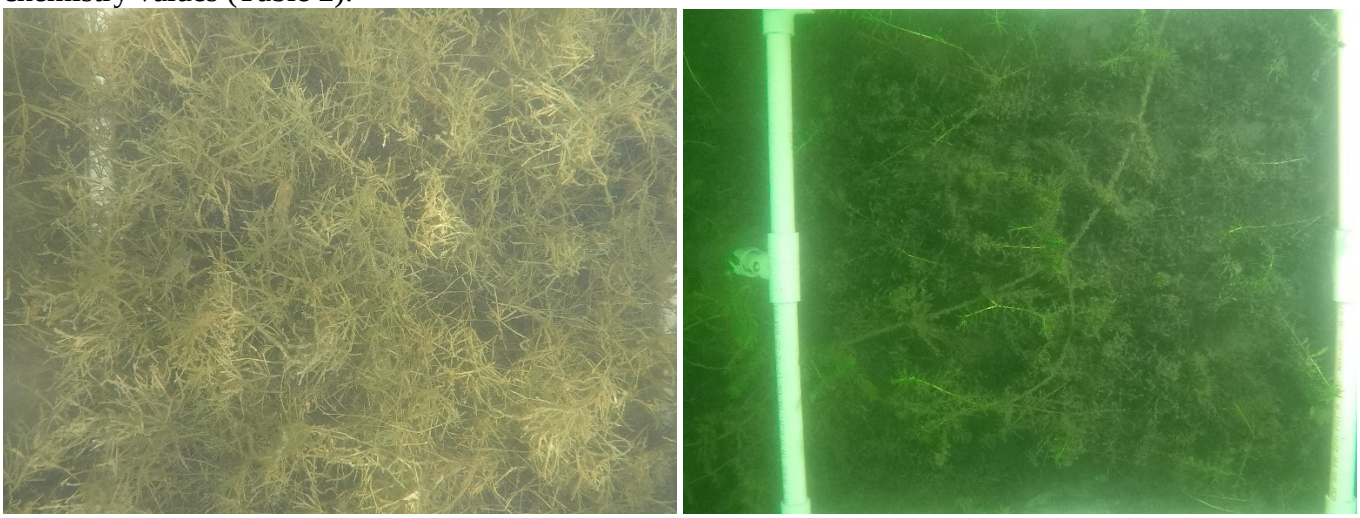

**Figure 3A and 3B.** Examples of images of sites with plants (3A - Site OW21; 3B – Site OW22)

At sites with macrophytes, the images just showed plants, and mussels were not visible. Note the tendency of the GoPro to become uncentered during some descents. Different camera rig attachments were tested to reduce this tendency, but none of the tested standard attachments was completely stable in all conditions, again requiring reliance on the known size PVC connectors to calibrate image sizes (e.g., Figure 3). Although we realized that images would not be useful in macrophyte beds, we still collected some samples in these shallow regions so we could characterize the mussel populations and nutrients in these areas.

We collected mussel samples at the bottom of the lake from shallow (~1-3 m) to deep (~20 m) sites along the five transects and collected water as described above from above these mussel beds. Upon return to shore after a day of diving, nutrient samples were delivered to UFI, or UFI personnel picked them up within 12 hours of sampling completion. Sample days often extended past normal business hours, in which case samples were stored in a portable cooler in the field and in a walk-in cooler (0-2$^{o}$C) at SUNY ESF upon return to the laboratory, until UFI could receive the samples the next morning.

We anticipated that deep dives by the ESF divemaster would be completed in Spring/Early Summer of 2018, but the lack of funding and approval for these dives in early summer when the dive master was available (before the commercial dive shop he runs was operating at full-capacity for the season) made this impossible. The delay in project start prevented him from being able to collect those samples.

Upon return to the lab, mussel samples were frozen until counting.

### 1.4.2 A.2. Observation and Preliminary Estimation of Live Mussels Below the Surficial Sediments

During collection of mussels from the first sites at approximately 10 m depth, we (Schulz and Pedian) made the surprising observation that the sediments were very unconsolidated in composition, and it was possible without

much effort for a diver to extend his or her arm into the sediments past the elbow and to the shoulder. The best analogy we could make about the consistency of the sediments was that they were equivalent to the thickness of a milkshake or smoothie. In addition, it was observed (tactilely, since visibility is zero after sediments have been disturbed) that there seemed to be intact (closed) and possibly live mussels present beneath the surface sediments.

The presence of these mussels was intriguing, but beyond the scope of this study. We didn't want to include these deeper mussels in the counts of the mussels at the site, since that would be a change in sampling protocol. In addition, these deeper mussels, even if alive, would obviously not be visible from images of surface sediments and would complicate comparison of counts with image analysis. Therefore, we continued to collect surficial mussels according to standard protocol at these sites and all other sites.
However we realized that if there were mussels alive deep in the sediments, their potential movements and respiration might have an influence on sediment mixing and the release of nutrients from deep sediments to the sediment surface. After convening onboard the vessel, we decided to take pilot samples of deeper mussels after collection of the standard surface mussel samples.

Accordingly, after the standard nutrient and surface mussel sampling at sites 13, 14 and 15, we collected deeper mussels from a smaller quadrat (0.25 m X 0.25 m) placed within the sample grid after the surficial mussels had been removed according to the standard protocols. We attempted to keep the depth of sampling for these separate collections somewhat consistent, by marking a spot on each of our arms at approximately 50 cm depth and collecting mussels to that depth, and only sampled these deep mussels at these three sites. These deeper mussels were also returned to the lab and frozen until analysis.

Counts revealed that there were substantial numbers of live mussels deep in the sediments of these sites (Figure 4). About 75% of the intact mussels deep in the sediments were quagga mussels. It is unclear if these mussels are metabolically active or if they can move up and down in the sediments. Their presence deep in the sediments is intriguing and perhaps warrants further investigation, especially related to the potential for sediment movement and oxygen consumption or effects on redox potential in the sediments, which also may affect nutrient release from sediments.

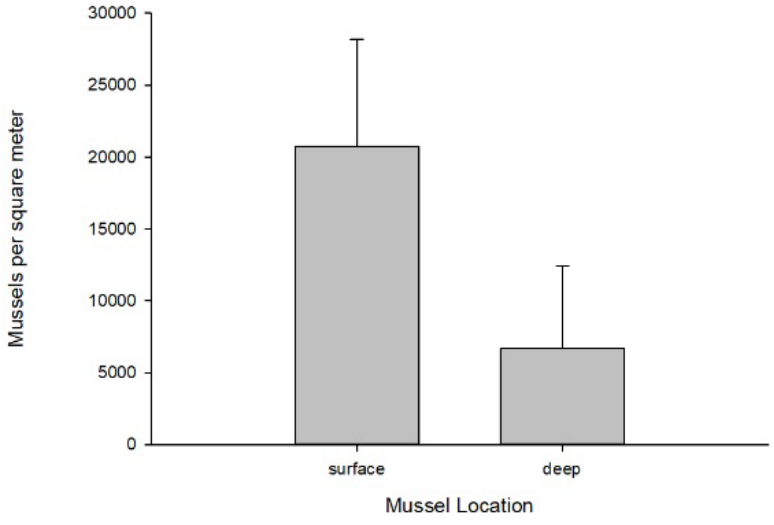

**Figure 4.** Number of live mussels per square meter at the surface and below the surface to ~50 cm depth at 3 test sites.

### 1.4.3 A.3. Survey of Mussel Distribution and Nutrients Above Mussel Beds - Nutrient composition above mussel beds

Upstate Freshwater Institute analyzed the water samples collected above the sediment water interface at the sampling quadrats parameterized the in-lake model (Table 2).

Not every site with mussel counts had nutrient concentration data, and many sites with nutrient concentrations did not have mussel counts (see mussel-counting section for more details). Higher concentrations above mussel beds might suggest nutrients are being released from the beds to the overlying water. The data from 13 sites with mussel counts and nutrient data (Table 3) did not show any simple significant linear regression relationships between mussel density and any of the nutrient concentrations. Benthic nutrient concentrations are influenced by numerous factors including water depth, water oxygen concentrations, sediment composition, as well as the possible relationship with mussel concentrations.

**Table 2.** Results of water chemistry analysis from water samples collected ~0.5 m above the sediment surface by the SUNY ESF scientific divers and analyzed within 24 hours of collection by Upstate Freshwater Institute.

| Sampling Date | Depth (m) dive watch | tNH3 (µgN/L) | TP (µgP/L) | TDP (µgP/L) | SRP (µgP/L) |
|---|---|---|---|---|---|
| 08/20/2018 | 16.8 | 48 | 14.9 | 8.6 | 5.8 |
| 08/20/2018 | 11.8 | 86 | 12.6 | 5.8 | 0.8 |
| 08/20/2018 | 3 | 43 | 39.3 | 8 | 0.3 |
| 08/20/2018 | 1.8 | 38 | 72.1 | 7.4 | 0.3 |
| 08/20/2018 | 5.9 | 74 | 57.2 | 15.2 | 5 |
| 08/20/2018 | 4.1 | 54 | 25.1 | 8.2 | 1 |
| 08/20/2018 | 7.1 | 93 | 62.6 | 10.2 | 5.3 |
| 09/01/2018 | 0.93 | 43 | 14.5 | 5.7 | 0.7 |
| 09/15/2018 | 5.1 | 19 | 11.7 | 2.1 | 0.3 |
| 09/15/2018 | 10.14 | 27 | 12.2 | 0.5 | 0.3 |
| 09/15/2018 | 13.8 | 40 | 35.7 | 5.3 | 3.7 |
| 09/15/2018 | 21.5 | 5 | 10 | 3.5 | 1 |
| 09/15/2018 | 1 | 22 | 14.6 | 3.2 | 0.3 |
| 09/15/2018 | 6 | 36 | 39.8 | 0.5 | 0.6 |
| 09/15/2018 | No sample | | | | |
| 09/15/2018 | 21.9 | 24 | 14.8 | 3.6 | 0.6 |
| 09/15/2018 | 14.1 | 99 | 19.5 | 0.5 | 4.9 |
| 09/15/2018 | 11.2 | 37 | 13.1 | 2.3 | 0.3 |
| 09/16/2018 | 1 | 31 | 11.3 | 6.3 | 0.9 |
| 09/16/2018 | 4.8 | 35 | 10.1 | 2.4 | 0.3 |
| 09/16/2018 | 16.4 | 19 | 17.7 | 0.5 | 0.3 |
| 09/16/2018 | 8.2 | 35 | 10.4 | 2.5 | 0.3 |
| 09/16/2018 | 22.9 | 17 | 12.1 | 1.4 | 0.3 |
| 09/16/2018 | 1 | 22 | 13.9 | 2.2 | 1 |
| 09/16/2018 | 11.9 | 34 | 13.5 | 1.1 | 0.3 |
| 09/16/2018 | 4.5 | 18 | 18.8 | 0.5 | 0.3 |
| 09/16/2018 | 17.9 | 11 | 15.8 | 2 | 0.3 |
| 09/16/2018 | 20.6 | 5 | 16.1 | 3.9 | 0.7 |

**Table 3**. Inorganic nutrient chemistry data for sites with both mussel counts and nutrient chemistry

| Site | Depth (m) | tNH3 (µgN/L) | TP | TDP | SRP | Mussels per $m^2$ |
|---|---|---|---|---|---|---|
| OW11 A | 3 | 43 | 39.3 | 8 | 0.3 | 812 |
| OW11 B | 1.8 | 38 | 72.1 | 7.4 | 0.3 | 392 |
| OW12 A | 5.9 | 74 | 57.2 | 15.2 | 5 | 6484 |
| OW12 B | 4.1 | 54 | 25.1 | 8.2 | 1 | 7032 |
| OW 14 | 16.8 | 48 | 14.9 | 8.6 | 5.8 | 16148 |
| OW 15 B | 11.8 | 86 | 12.6 | 5.8 | 0.8 | 29336 |
| OW19 | 13.8 | 40 | 35.7 | 5.3 | 3.7 | 8980 |
| OW26 | 11.2 | 37 | 13.1 | 2.3 | 0.3 | 6472 |
| OW29 | 16.4 | 19 | 17.7 | 0.5 | 0.3 | 21500 |
| OW30 | 8.2 | 35 | 10.4 | 2.5 | 0.3 | 19628 |
| OW31 | 22.9 | 17 | 12.1 | 1.4 | 0.3 | 3644 |
| OW33 | 11.9 | 34 | 13.5 | 1.1 | 0.3 | 5440 |
| OW36 | 20.6 | 5 | 16.1 | 3.9 | 0.7 | 9364 |

### 1.4.4 A. 4. Counting of mussel samples and image analysis

We counted the frozen mussels that were collected at each site to estimate the number of mussels in the lake. Samples were kept frozen and small subsamples removed for processing each day. Because the delay in funding prevented recruitment of a graduate student to the project, and funds were not available for a student in 2019, counting was performed by the PI and a group of undergraduate volunteers who were trained to identify zebra and quagga mussels. This small army of volunteers was dedicated and reliable, but only able to work 4-8 hours per week for credit. Much of the counting was therefore performed by Schulz.

For each sample, mussels were each identified as zebra or quagga mussels, and dead shells were separated from the mussels that had been alive (were intact) at the time of sampling. Because there were so many shells on the sediment surface, the process of separation of mussels that had been alive at the time of sampling from the loose shells was laborious and time consuming.

We spent some time (several weeks) trying to develop a protocol for subsampling the mussels, but were unable to achieve subsamples that had similar species composition and body masses by various types of mixing/homogenization, and did not find a protocol in our literature survey. So we proceeded with counting the entire sample. Some of the larger samples required many tens of hours of labor to identify to species and count. We would recommend that future surveys use smaller quadrats to reduce the large time commitment of sample identification and processing.

In total, surface mussel samples from 14 sites were completely processed and sorted to species of mussel (Table 4). Shells of the zebra and quagga mussels that had been collected alive were placed in separate bags for each sample and re-frozen. Later these samples were used to measure the lengths of each type of mussel at each site to help parameterize the filtration rates. At each site a subset of 25 mussels of each species (when present) was measured with a digital micrometer to estimate the size composition of mussels at each site for parameterization of mussel filtration rates for the UFI model (Appendix 1).

We used images from five of the sites during Spring and early Summer 2019 in the open source ImageJ software package and attempted various methods for automating counting from images, with the goal mentioned previously of being able to increase resolution of mussel density estimates through image analysis.

Schulz uses ImageJ to automatically count microscope images of DAPI stained bacteria taken using epifluorescence microscopy on a compound microscope, and we have found this method agree with 99% accuracy to manual user counts of bacteria, so we were optimistic about the potential efficacy of this approach.

Despite concerted attempts to adjust contrast and other parameters to increase the ability of the software to identify and count mussels, we did not succeed in getting the program to identify the mussels automatically. In fact, even with manual counting of mussels in the images, it was often hard to identify mussels because they are not a 2-dimensional surface (unlike the bacteria), but are packed in clumps. In addition, the mussels are found in different orientations and it is hard or impossible to distinguish live from dead mussels. We concluded that our image analysis would not provide an accurate indication of mussel abundance. However, we know Lewis McCaffrey (DEC) is attempting a similar analysis, and perhaps he will have more success. In that event, or if someone wants to investigate other software or machine learning for estimation, the images are available at the link provided earlier in this document. In our investigations, it seemed potentially possible to determine a relative abundance of the mussels with image analysis, but we were discouraged about the likelihood of obtaining quantitative mussel estimates from this method. Unfortunately, that means that rapid surveying of exact numbers of mussels from additional photographic imaging may not be successful. However, such a survey might allow a *qualitative* estimation of the mussel density over the lake bottom.

Based on our manual counted samples, we determined that at many locations in Owasco Lake, there are now thousands of mussels per unit of $m^2$ of sediment area (Table 4; Figure 5). We also found that compared with the previous 2007 survey (Watkins et al. 2010), quagga mussels in the lake now extend down to the deepest sites we sampled (~25 m). It is unfortunate the dive master was unable to sample deeper sites in 2019 as that would have been informative for determining mussel extent. Perhaps Lewis McCaffrey's sampling can help inform that distribution. Since oxygen concentrations in the hypolimnion of Owasco Lake in summer are low, it is likely that the metalimnetic sediment samples we collected may represent the maximal extent of the mussel distribution, but it is possible that mussels persist in deeper water. The deepest sites we sampled were below the thermocline and still contained substantial numbers of mussels.

We determined that in many locations there are thousands to tens of thousands of mussels per square meter of benthic surface area. We also found that there are now quagga mussels in the lake that extend down to at least 25 m, while zebra mussels remain in the lake, but are mostly on hard bottom, steep areas on the west shore. Many mussels are also present on the aquatic plants in the lake, and their feeding may also influence nutrients in the water or HAB formation, but this has not been investigated extensively previously. We also found that in the soft sediment areas, live mussels extend deep in to the sediments, which is surprising as this has not been reported previously; we are uncertain the role that these mussels may play in resuspending nutrients from deep sediments.

While zebra mussels remain in the lake, they are more common on hard bottom, steep areas on the western shore, and on shallow sites with plants (Table 4; Figure 4). Similar observations of zebra mussels dominating in shallow areas and quagga mussels in deep areas have been made in other systems (e.g., Karatayev et al. 2010). The depth at which quagga mussels begin to dominate the mussel assemblage appears to occur at around 7 meters (Figure 4).

Many mussels were present on the aquatic plants in the lake (Table 4). These are likely not counted during sampling with Ekman or other dredges. Although macrophyte samples are also laborious to process -- as the mussels need to be separated from the plant material, many small mussels recruit to plants. The high proportion of juvenile mussels on the plants also makes it harder to identify species and to measure lengths. The role of these mussels in the water column may be more substantial than appreciated, and the synergistic effect of mussel filtration increasing light penetration, which may increase macrophyte growth, likely promotes both plant growth and recruitment of zebra mussels nearshore.

However, the presence of these mussels on plants and their feeding – not just in the sediments, but also in the water column while attached to plants – may also influence nutrients in the water or HAB formation. Further investigation of the water column feeding selectivity and processes on the nearshore phytoplankton might be informative.
We also found that in the soft sediment areas, live mussels extend deep into the sediments, which is surprising as this has not been reported previously and we are uncertain the role that these mussels may play in resuspending nutrients from deep sediments.

**Table 4**. Total zebra and quagga mussels in the **0.25 $m^2$** samples collected from Otisco Lake in summer 2018 that were alive when sampled

| SITE | Total per $m^2$ | Depth (m) | Total Mussels Alive (# per 0.25 m^2) | Total Quagga Mussels Alive (# per 0.25 m^2) | Total Zebra Mussels Alive (# per 0.25 m^2) | Habitat notes |
|---|---|---|---|---|---|---|
| OW11 A | 812 | 3 | 203 | 99 | 104 | in macrophyte bed |
| OW11 B | 392 | 1.8 | 98 | 60 | 38 | in macrophyte bed |
| OW12 A | 6484 | 5.9 | 1621 | 510 | 1111 | |
| OW12 B | 7032 | 4.1 | 1758 | 127 | 1631 | in macrophyte bed |
| OW13 | 3316 | 10.9 | 829 | 829 | 0 | |
| OW 14 | 16148 | 16.8 | 4037 | 4033 | 4 | |
| OW 15 B | 29336 | 11.8 | 7334 | 7332 | 2 | |
| OW19 | 8980 | 13.8 | 2245 | 1956 | 289 | |
| OW26 | 6472 | 11.2 | 1618 | 1615 | 3 | |
| OW29 | 21500 | 16.4 | 5375 | 5154 | 221 | |
| OW30 | 19628 | 8.2 | 4907 | 3983 | 924 | |
| OW31 | 3644 | 22.9 | 911 | 749 | 162 | |
| OW33 | 5440 | 11.9 | 1360 | 1108 | 251 | |
| OW36 | 9364 | 20.6 | 2341 | 2308 | 33 | |

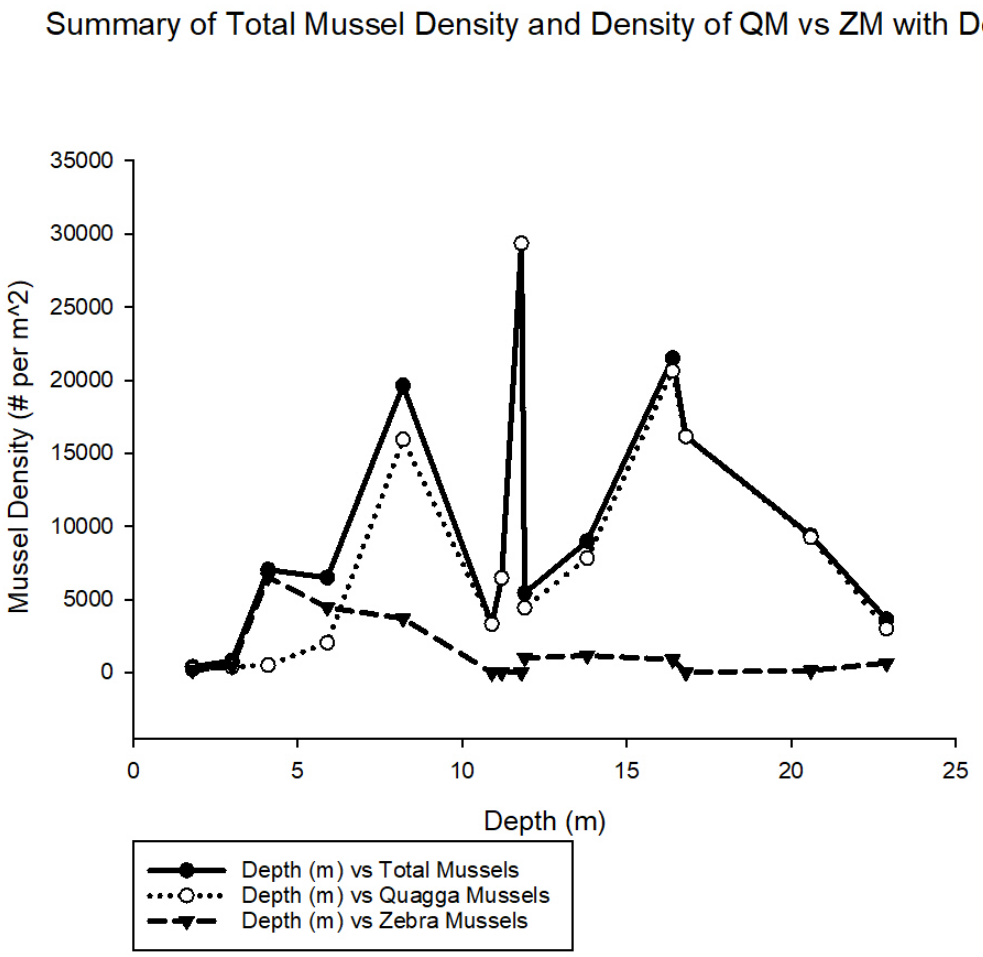


**Figure 5**. Distribution of mussels with depth for all quadrats sampled

## 1.5 **Part B: Phytoplankton Objectives**

The primary objectives of the phytoplankton component of this project were to parameterize the seasonal phytoplankton distribution component of the model. Specifically, these were to:

B1. Identify and count phytoplankton in samples collected by UFI from their monitoring station during the 2018 season

B2. Convert the phytoplankton densities to biovolumes using species-specific conversion factors

B3. Create a summary table for each of the major groupings of phytoplankton used in UFI's in-lake model, ready for input to the model

B4. Summarize results of phytoplankton counts from samples collected from nearshore stations in Owasco Lake in 2016, where UFI did not sample with fluoroprobes (and so biovolume and taxonomic group summaries were not compiled). Not surprisingly, the nearshore phytoplankton and zooplankton compositions vary significantly from those of the offshore 2018 sampling sites. Because the goal of this analysis was not for model input per se, but to fully characterize the phytoplankton assemblage, more subsamples (10 per sample) were enumerated for these samples than for the 2018 samples. The methods for sample processing also varied slightly. The 2016 summary and methodological differences are elaborated briefly in section B1/B2. The biomass summaries for 2016 phytoplankton are provided in Appendix 6.

### 1.5.1 B.1/B.2. Identification and Counting Methods and Conversion to Biovolumes

Phytoplankton samples were collected by UFI according to their standard protocols, and preserved with Lugol's solution. UFI collected samples with a Kemmerer bottle from 0.5 m depth at their monitoring site. Samples were provided to SUNY ESF after collection.

Methods were standard for phytoplankton analysis and generally paralleled those of the Cayuga Lake modelling project performed by Cornell University. Upon receipt of the phytoplankton samples at ESF, they were stored at 4$^{o}$C in the dark until counting. Every 1-2 months, samples were checked for color and additional Lugol's solution was added if necessary (only one sample required addition of more Lugol's solution, on one date). One sample was observed on the first check-in date to have had a cracked lid, resulting in sample loss and loss of color, so this sample was not processed due to sample volume loss and likelihood of inconsistent preservation.

In order to count the phytoplankton sample, it was first concentrated using the Utermöhl method, which allows phytoplankton to settle out of a larger volume and be concentrated on a coverslip for counting on an inverted microscope. In this process, the sample bottles were inverted 10X to homogenate, and then concentrated by settling for at least 2 hours in a 1 cm (10 mL) Utermöhl chamber constructed by Aquatic Research Instruments.

Counting was performed using a Leica DMB IRB inverted microscope, generally using a 10X objective, with a 1.5 x side magnifier and a 10X HG Plan ocular. For one sample in 2018, when there was a humungous 😊 bloom of small *Microcystis*-like cells, the subsamples were counted with the higher magnification ocular, so a different concentration factor was applied to calculate biovolume, as described next.

The field of view dimensions for each ocular were confirmed with a stage micrometer. For the 10X objective the diameter of a complete field of view was 1.368 mm, so given the 1 cm height of the settling chamber each complete field of view counted the cells in 0.0137 mL For the few samples counted at higher power, the diameter of the field of view was 0.32 mm, so the complete sample enumerated was 0.0008 mL.

All the phytoplankton in replicate complete fields of view were enumerated, using a method in which random fields along a diagonal transect from upper right to lower left of the counting chamber were fully enumerated, with every cell within the field or touching a set half of the field identified and counted as being within the field.

Phytoplankton were identified to Genus when possible, or to the lowest taxonomic group possible with the limitations of the Utermöhl method, but always at least to Phylum. (Note: formerly 'Division' was standard for phytoplankton, as in the Cayuga Lake report. The current convention is to use 'Phylum' rather than 'Division' for phytoplankton, to be consistent with other organisms).

Cell numbers were converted to biomass using biovolume conversion factors for the same taxa at similar seasons from the Cayuga Lake study or literature values, and reported as $\mu m^3$ cell volume per mL of water. Biovolumes from major taxonomic groups were summed for input by UFI into their in-lake model. The conversion factors and their sources are given in Appendix 2.

This process was repeated for each sample, and seasonal patterns in biomass for the major taxonomic groups used in the modeling effort were provided to UFI, along with the count data from the microscopic analysis.

In 2016, when the goal was taxonomic enumeration of the sample, 10 fields were enumerated and the entire chamber was searched for rare taxa.

In 2018, when the goal was to parameterize the in-lake model, three or 4 fields were enumerated, making sure sample size was at least 200 identified individuals. On one sampling date in 2018, there was a massive bloom of single-celled cyanobacteria that were categorized as *Microcystis* based on shape, but obviously it would have required genetic analysis to determine the actual strain of cyanobacteria. For purposes of biovolume correction, this distinction is unimportant. The bloom was so dense that the microscope field was packed with cells and very difficult/impossible to enumerate at the normal objective/power. Therefore, for these samples, magnification was switched to a higher power objective to make counting feasible. These counts were than adjusted for the smaller volume of sample counted, and the cells were highlighted in yellow to make the distinction clear, and a comment entered into the spreadsheet. All other phytoplankton samples for both 2016 and 2018 were enumerated at the magnification listed as standard.

Because of the current state of flux of phytoplankton taxonomy, taxonomic names were checked after counting in February and March, but before sample data analysis, for Phylum and Family accuracy on the taxonomy browser function in AlgaeBase.com (accessed in June 2020).

Detailed summary tables of the taxonomic composition and biovolume conversions for samples from each field collection date in 2018 are provided in Appendices 2 and 3.

### 1.5.2 B.3. Summary tables for model input

After identification and enumeration were complete, the densities and biovolumes of species for the taxonomic group's use in the in-lake model were pooled for each date, and provided to UFI in a tabular form for input into the lake model (Tables 5 and 6 below).

**Table 5**. Phytoplankton density (#/mL) summarized for major taxonomic groups (Cynanophyta, Chlorophyta [including taxa currently reclassified as Charophyta], Bacillariophyta, Chrysophyta, Cryptophyta, Euglenophyta, and Dinoflagellates) in 2018 for input to the Owasco Lake model

| Date | Cyano. | Chlorop. | Bacill. | Chryso. | Crypto. | Eugleno. | Dino |
|---|---|---|---|---|---|---|---|
| 5-Jul-18 | 6065 | 1754 | 913 | 73 | 37 | 0 | 0 |
| 18-Jul-18 | 25089 | 4238 | 3946 | 0 | 49 | 0 | 0 |
| 2-Aug-18 | 408116 | 4238 | 3946 | 0 | 49 | 0 | 0 |
| 31-Aug-18 | 8477 | 2972 | 1364 | 0 | 0 | 0 | 49 |
| 12-Sep-18 | 30301 | 3215 | 4287 | 0 | 49 | 0 | 0 |
| 27-Sep-18 | 5213 | 974 | 633 | 1705 | 49 | 0 | 244 |

**Table 6.** Phytoplankton biovolumes ($\mu m^3 mL^{-1}$) summarized for major taxonomic groups (Cynanophyta, Chlorophyta [including taxa currently reclassified as Charophyta], Bacillariophyta, Chrysophyta, Cryptophyta, Euglenophyta, and Dinoflagellates) in 2018 for input to the Owaco Lake model.

| Date | Cyano. | Chloro. | Bacill. | Chryso. | Crypto. | Eugleno. | Dino. |
|---|---|---|---|---|---|---|---|
| 5-Jul-18 | 2.48E+05 | 1.39E+05 | 7.99E+05 | 6.85E+03 | 1.30E+04 | 0.00E+00 | 0.00E+00 |
| 18-Jul-18 | 2.30E+05 | 8.40E+05 | 1.48E+06 | 0.00E+00 | 1.74E+04 | 0.00E+00 | 0.00E+00 |
| 2-Aug-18 | 5.01E+06 | 8.40E+05 | 1.48E+06 | 0.00E+00 | 1.74E+04 | 0.00E+00 | 0.00E+00 |
| 31-Aug-18 | 1.92E+05 | 2.01E+05 | 1.23E+06 | 0.00E+00 | 0.00E+00 | 0.00E+00 | 2.05E+05 |
| 12-Sep-18 | 1.33E+05 | 9.26E+04 | 3.92E+06 | 0.00E+00 | 1.74E+04 | 0.00E+00 | 0.00E+00 |
| 27-Sep-18 | 3.51E+04 | 2.79E+04 | 5.49E+05 | 1.60E+05 | 1.74E+04 | 0.00E+00 | 1.03E+06 |

### 1.5.3 **B.4. Summary tables for taxonomic enumeration of 2016 phytoplankton assemblage on each sampling date and from each sampling location**

Summary tables of the composition of the phytoplankton assemblage and cell counts on each sampling date were made from the count data and compiled in Appendix 6.

## 1.6 Part C: Zooplankton Objectives

The primary objectives of the zooplankton component of this project were to parameterize the seasonal zooplankton distribution component of the model. Specifically, these were to:

C.1. Identify and count zooplankton in samples collected by UFI from their monitoring station during the 2018 season

C2. Estimate the size and biomass of the zooplankton in the samples and convert the zooplankton densities to biomass

C3. Create two summary tables, with values for each sampling date for the zooplankton to be used in UFI's in-lake model, ready for input into the model. The first table needed was the estimated biomass (μg/L) for the major taxonomic groups on each sample date. The second table pooled individual species or genera in terms of functional group (predator, omnivore, herbivore) and provided summed biomass for each of these functional groups on each date.

### 1.6.1 C.1. Identify and count zooplankton in samples collected by UFI from their monitoring station during the 2018 season

Samples were collected by Upstate Freshwater Institute using a 0.5 m diameter zooplankton net and a tow depth from 15 meters to the surface at their primary sampling site. These zooplankton samples were preserved in ethanol, delivered to Schulz, and stored in cool, dark conditions until enumeration.

Before processing, samples were poured through a 20 □m m sample into a known volume. The zooplankton samples were rinsed gently with filtered tap water and suspended in a measured 100 mL total volume for counting. Using a calibrated wide-bore pipette, the samples were homogenized with a star-shaped mixing pattern to avoid a centrifugation effect, and a subsample was rapidly removed and placed in a zooplankton counting tray. Each subsample was completely enumerated under a Leica MZ 12.5 dissecting scope. Complete subsamples were enumerated until over 200 animals from a known volume of sample were counted and identified.

The invasive predatory cladoceran, *Cercopagis pengoi*, commonly known as the fish-hook flea, forms clumps and cannot be subsampled accurately. In samples where *C. pengoi* was present (based on a scan of the sample at low power), the entire sample was scanned for Cp and the entire population in the sample was enumerated. This is, unfortunately, the only way to assess this organism's abundance accurately. *C. pengoi* was

one of the few predatory zooplankton in this zooplankton assemblage, so its accurate assessment was necessary to quantify composition of trophic functional groups.

Generally we found a small-bodied zooplankton assemblage with low abundances of large bodied zooplankton such as *Daphnia*. Rotifers and smaller Cladocera, such as *Chydorus* were more abundant, and these taxa have low grazing impact on the phytoplankton and are unlikely to promote clear water phases in the lake.

**Table 7**. Genera of zooplankton found in Owasco Lake samples from summer 2018, along with their functional feeding groups.

| **Genus/species** | **Taxonomic group** | **Herbivore/Predator/Omnivore** |
|---|---|---|
| *Collotheca* | Rotifer | herbivore |
| *Lecane* | Rotifer | herbivore |
| *Pompholyx* | Rotifer | herbivore |
| *Asplanchna* | Rotifer | predator |
| *Trichocerca* | Rotifer | herbivore |
| *Synchaeta* | Rotifer | herbivore |
| *Polyarthra* | Rotifer | herbivore |
| *Keratella* | Rotifer | herbivore |
| *Brachionus* | Rotifer | herbivore |
| *Ascomorpha* | Rotifer | herbivore |
| *Testudinella* | Rotifer | herbivore |
| *Kellicottia* | Rotifer | herbivore |
| *Ploesoma* | Rotifer | herbivore |
| *Conochilis* | Rotifer | herbivore |
| *Ceriodaphnia* | Cladoceran | herbivore |
| *Bosmina longirostris* | Cladoceran | herbivore |
| *Eubosmina* | Cladoceran | herbivore |
| *Daphnia retrocurva* | Cladoceran | herbivore |
| *Cercopagis pengoi* | Cladoceran | predator |
| *Leptodora kindtii* | Cladoceran | predator |
| *Alona* | Cladoceran | herbivore |
| *Chydorus* | Cladoceran | herbivore |
| *Daphnia galeata mendotae* | Cladoceran | herbivore |
| *Diacyclops thomasi female* | Copepod | omnivore |
| *Diacyclops thomasi male* | Copepod | omnivore |
| *Diacyclops thomasi copepodid* | Copepod | herbivore |
| *Diacyclops thomasi nauplii* | Copepod | herbivore |
| *Difflugia* | Arcellinida | herbivore |
| Veliger | Mollusca | herbivore |

### 1.6.2 C2. Estimate the size and biomass of the zooplankton in the samples and convert the zooplankton densities to biomass values

Methods for zooplankton analysis were modelled on the zooplankton methods used by Cornell to analyze Cayuga Lake zooplankton samples for use by UFI for the Cayuga Lake model. The sources of the zooplankton biomass conversion factors are provided in Appendix 7. Sizes of common taxa were determined using a calibrated ocular micrometer at known magnifications, and biomass was estimated with standard length-weight regressions taken from these measurements, or from the literature for rarer taxa (where finding sufficient individuals for measurement would have been impractical or impossible). When literature values were needed for length estimations, values from Finger Lakes or standard Great Lakes regressions were used. In other cases, such as for rare or small rotifers, general literature values were used, if available.

### 1.6.3 C3. Create two summary tables, with values for each sampling date for the zooplankton to be used in UFI's in-lake model, ready for input to the model.

After identification and enumeration were complete, the densities and biovolumes of species for the taxonomic group's use in the in-lake model were pooled for each date, and provided to UFI in a tabular form for input into the lake model (Tables 8 and 9 below).

One interesting observation is that not a single calanoid copepod was observed in any sample. In addition, while *Cercopagis pengoi*, an invasive predator to the region (commonly known as the fish-hook flea), was at times abundant in the lake, a related invader, *Bythotrophes*, the spiny water flea, was not found in any sample and apparently has still not invaded the Finger Lakes from Lake Ontario.

**Table 8.** Biomass of zooplankton in each taxonomic group at each sampling date during summer 2018. Units are mass (μg/L)

| Date | *Daphnia* | Non-daphnid Cladocera | Copepods | Rotifers | Other |
|---|---|---|---|---|---|
| 5-Jul-18 | 0.08 | 1.32 | 5.54 | 1.64 | 0.38 |
| 18-Jul-18 | 0.00 | 1.78 | 0.39 | 1.33 | 0.38 |
| 2-Aug-18 | 0.20 | 11.56 | 0.72 | 1.63 | 0.04 |
| 15-Aug-18 | 2.35 | 40.37 | 1.86 | 1.49 | 0.19 |
| 31-Aug-18 | 2.10 | 16.13 | 1.05 | 1.81 | 0.11 |
| 12-Sep-18 | 1.55 | 8.58 | 0.72 | 0.73 | 0.04 |
| 27-Sep-18 | 2.63 | 10.01 | 1.49 | 0.06 | 0.04 |

**Table 9.** Biomass of zooplankton in functional feeding groups during summer 2018. Units are mass (μg/L).

| Date | Predator | Omnivore | Herbivore |
|---|---|---|---|
| 5-Jul-18 | 1.54 | 5.06 | 2.36 |
| 18-Jul-18 | 1.69 | 0.10 | 2.09 |
| 2-Aug-18 | 4.58 | 0.21 | 9.35 |
| 15-Aug-18 | 10.13 | 0.44 | 35.70 |
| 31-Aug-18 | 4.12 | 0.31 | 16.77 |
| 12-Sep-18 | 2.96 | 0.31 | 8.35 |
| 27-Sep-18 | 0.90 | 1.39 | 11.94 |

References Cited

Jöhnk at al. 2008. Summer heatwaves promote blooms of harmful cyanobacteria. Global Change Biol. 14:412-495. https://doi.org/10.1111/j.1365-2486.2007.01510.

Karatayev, A.Y., L.E. Burlakova and D.K. Padilla. 2015. Zebra versus quagga mussels: a review of their spread, population dynamics and ecosystem impacts. Hydrobiologia 74: 97-112.

Pendergrass, A.G. and R. Knutti. 2018. The uneven nature of daily precipitation and climate change. Geophysical Research Letters.doi 10.1029/2018GLO80298.

Rantala, M.V., T.P. Luoto, J. Weckstrom, M. Rautio, and L. Nevalalinen. 2017. Climate drivers of diatom distribution in shallow subarctic lakes. Freshwater Biology DOI: 10.1111/fwb.13042

Sarnelle, O., A.E. Wilson, S.K. Hamilton, L.B. Kroll and D.F. Raikow. 2005. Complex interactions between the zebra mussel, *Dreissena polymorpha* and the harmful phytoplankter, *Microcystis aeruginosa*. Limnology and Oceanography

Sarnelle, O. *Daphnia* as keystone grazers: effects on phytoplankton diversity and grazing resistance.

Sinha, E et al. 2017. Eutrophication will increase during the 21st century as a result of precipitation changes. Science 357, 405–408. https://doi.org/10.4319/lo.2005.50.3.0896

Watkins,J., L. Rudstam, E. Mills and M. Leopold. 2007. The benthic community of Owasco Lake as an indicator of lake ecosystem health.

# Appendix 1. Size distribution of zebra and quagga mussels at different sites in Owasco Lake in 2018

| *All values in mm; digital caliper micrometer - 0.01mm* | | | | | | | | *no ZM in the sample from this site | | *only 1 ZM in the sam | | *only 4 ZM in the sample from this site | | | | *only 2 ZM in the sample from this site | | | | | | *only 3 ZM in the sample from this site | | | | | | | | | |
|---|---|---|---|---|---|---|---|---|---|---|---|---|---|---|---|---|---|---|---|---|---|---|---|---|---|---|---|---|---|---|---|
| **Site 11A** | | **Site 11B** | | **Site 12A** | | **Site 12B** | | **Site 13 A** | | **Site 13 Deep Mussels (subsurface, but alive)** | | **Site 14 A** | | **Site 14 Deep Mussels (subsurface, but alive)** | | **Site15 A** | | **Site 15 Deep Mussels (subsurface, but alive)** | | **Site 19** | | **Site 26** | | **Site 29** | | **Site 30** | | **Site 31** | | **Site 33** | | **Site 36** | |
| **Quagga** | **Zebra** | **Quagga** | **Zebra** | **Quagga** | **Zebra** | **Quagga** | **Zebra** | **Quagga** | **Zebra** | **Quagga** | **Zebra** | **Quagga** | **Zebra** | **Quagga** | **Zebra** | **Quagga** | **Zebra** | **Quagga** | **Zebra** | **Quagga** | **Zebra** | **Quagga** | **Zebra** | **Quagga** | **Zebra** | **Quagga** | **Zebra** | **Quagga** | **Zebra** | **Quagga** | **Zebra** | **Quagga** | **Zebra** |
| 10.32 | 11.48 | 12.91 | 5.67 | 5.87 | 7.79 | 9.09 | 13.45 | 25.93 | none | 9.20 | 10.22 | 19.31 | 12.17 | 8.78 | 12.43 | 10.76 | 16.78 | 9.56 | 14.51 | 22.68 | 22.46 | 11.60 | 17.01 | 18.61 | 13.01 | 7.57 | 8.80 | 19.06 | 12.24 | 15.94 | 14.43 | 5.54 | 10.84 |
| 8.07 | 8.60 | 11.30 | 11.52 | 6.79 | 10.28 | 10.76 | 13.29 | 13.00 | | 19.99 | | 9.21 | 5.74 | 6.77 | 14.54 | 6.78 | 18.41 | 20.17 | 17.73 | 7.75 | 13.95 | 13.49 | 7.95 | 10.62 | 10.32 | 17.60 | 7.74 | 9.06 | 19.49 | 15.03 | 17.17 | 17.28 | 14.83 |
| 6.86 | 11.17 | 11.47 | 8.99 | 9.41 | 5.74 | 6.40 | 11.20 | 21.32 | | 11.16 | | 18.12 | 11.96 | 15.57 | 11.93 | 7.11 | | 10.81 | 15.54 | 9.19 | 16.15 | 10.82 | 10.80 | 15.31 | 9.46 | 14.71 | 10.78 | 11.93 | 10.58 | 9.22 | 14.62 | 11.00 | 8.94 |
| 6.85 | 12.80 | 11.56 | 7.81 | 8.25 | 9.45 | 9.95 | 7.65 | 11.25 | | 13.76 | | 6.79 | 6.98 | 19.66 | 19.21 | 9.93 | | 11.74 | 13.69 | 12.12 | 13.43 | 6.61 | | 5.93 | 5.34 | 16.58 | 8.01 | 5.84 | 5.97 | 11.08 | 9.06 | 11.70 | 10.02 |
| 6.98 | 11.93 | 9.94 | 13.46 | 10.38 | 8.08 | 6.73 | 12.10 | 7.85 | | 11.69 | | 1.33 | | 8.75 | 15.49 | 6.79 | | 8.94 | 9.06 | 26.93 | 18.47 | 17.78 | | 12.91 | 7.51 | 7.48 | 8.06 | 7.60 | 10.24 | 12.74 | 13.89 | 7.55 | 7.57 |
| 7.93 | 9.83 | 7.10 | 11.41 | 7.20 | 5.00 | 8.90 | 10.03 | 7.32 | | 11.45 | | 5.06 | | 7.85 | 12.26 | 10.53 | | 21.90 | 22.99 | 14.03 | 16.42 | 18.70 | | 19.53 | 9.37 | 9.70 | 10.10 | 14.51 | 10.88 | 10.09 | 10.95 | 10.07 | 12.18 |
| 11.93 | 11.61 | 6.42 | 13.97 | 11.96 | 9.14 | 9.94 | 11.59 | 11.19 | | 10.00 | | 10.26 | | 8.39 | 14.72 | 22.44 | | 13.52 | 10.71 | 20.00 | 16.94 | 10.02 | | 14.67 | 12.80 | 10.12 | 6.25 | 7.41 | 10.60 | 14.76 | 10.38 | 16.81 | 6.84 |
| 6.68 | 11.63 | 8.97 | 10.01 | 7.10 | 8.84 | 7.32 | 9.00 | 19.89 | | 8.72 | | 7.41 | | 12.43 | 12.51 | 12.63 | | 17.74 | 16.98 | 11.95 | 13.91 | 13.34 | | 14.10 | 11.84 | 9.45 | 6.60 | 12.29 | 13.48 | 14.84 | 9.16 | 13.78 | 8.54 |
| 8.62 | 10.06 | 9.25 | 11.15 | 10.19 | 7.04 | 12.36 | 10.97 | 19.65 | | 22.52 | | 11.22 | | 9.89 | 13.01 | 11.12 | | 6.76 | 14.20 | 9.40 | 15.71 | 22.50 | | 17.19 | 8.03 | 18.41 | 10.38 | 5.71 | 15.57 | 8.96 | 18.52 | 21.67 | 9.33 |
| 6.92 | 8.66 | 5.82 | 13.20 | 6.68 | 6.68 | 7.12 | 14.41 | 7.14 | | 13.91 | | 7.69 | | 10.14 | 15.75 | 8.19 | | 8.49 | 14.35 | 21.83 | 15.95 | 10.04 | | 16.71 | 11.13 | 12.00 | 7.55 | 15.77 | 11.01 | 16.12 | 10.94 | 12.59 | 16.81 |
| 9.15 | 10.82 | 10.19 | 5.64 | 8.89 | 7.78 | 8.65 | 10.40 | 12.61 | | 9.85 | | 6.71 | | 6.67 | 14.44 | 5.68 | | 21.79 | 16.02 | 17.48 | 16.60 | 10.01 | | 9.70 | 11.01 | 5.24 | 9.29 | 10.27 | 18.56 | 15.27 | 9.40 | 21.58 | 7.92 |
| 8.01 | 8.54 | 11.80 | 9.64 | 5.09 | 9.28 | 7.59 | 12.96 | 10.74 | | 11.95 | | 4.38 | | 8.71 | 19.46 | 7.75 | | 7.97 | 14.66 | 19.43 | 15.79 | 11.22 | | 12.90 | 9.56 | 13.14 | 9.61 | 8.89 | 16.61 | 9.44 | 15.14 | 23.71 | 6.65 |
| 10.84 | 12.53 | 7.58 | 12.31 | 7.50 | 11.45 | 8.46 | 7.88 | 14.83 | | 11.93 | | 20.35 | | 13.25 | 11.61 | 8.37 | | 17.83 | 16.27 | 9.34 | 16.79 | 10.85 | | 13.64 | 6.96 | 7.75 | 6.83 | 15.52 | 16.48 | 11.68 | 11.95 | 23.06 | 14.07 |
| 7.85 | 10.27 | 7.32 | 10.51 | 6.30 | 7.66 | 7.99 | 10.65 | 21.31 | | 19.80 | | 6.27 | | 8.37 | 14.05 | 15.70 | | 12.27 | 9.95 | 17.11 | 17.50 | 15.67 | | 10.45 | 5.71 | 14.99 | 8.46 | 22.26 | 10.52 | 15.64 | 9.15 | 16.68 | 17.26 |
| 6.69 | 9.90 | 11.79 | 8.82 | 6.42 | 7.52 | 8.10 | 16.35 | 15.10 | | 11.49 | | 8.11 | | 10.00 | 13.31 | 11.52 | | 7.23 | 14.54 | 17.91 | 15.25 | 7.75 | | 9.78 | 11.73 | 9.76 | 7.35 | 9.86 | 9.12 | 15.83 | 7.51 | 6.75 | 6.76 |
| 9.19 | 10.09 | 10.12 | 11.57 | 10.85 | 11.75 | 6.33 | 12.50 | 10.71 | | 11.51 | | 5.87 | | 8.12 | 11.35 | 6.74 | | 19.54 | 9.51 | 5.36 | 15.22 | 11.93 | | 14.84 | 8.36 | 13.82 | 8.26 | 9.78 | 13.99 | 10.00 | 9.08 | 20.15 | 17.46 |
| 6.68 | 8.77 | 4.19 | 12.19 | 7.19 | 10.57 | 14.56 | 9.59 | 24.42 | | 12.14 | | 22.25 | | 19.46 | 17.94 | 8.08 | | 10.53 | 16.71 | 11.92 | 15.44 | 9.83 | | 14.46 | 7.82 | 7.13 | 6.76 | 8.76 | 15.86 | 14.00 | 11.34 | 14.35 | 14.11 |
| 8.38 | 10.68 | 6.66 | 8.80 | 8.39 | 5.97 | 9.93 | 12.54 | 16.61 | | 20.42 | | 9.46 | | 10.94 | 16.29 | 6.80 | | 18.55 | 14.79 | 10.39 | 21.62 | 12.59 | | 13.88 | 10.36 | 12.24 | 11.39 | 9.12 | 14.10 | 16.32 | 10.54 | 11.96 | 17.97 |
| 6.78 | 7.75 | 12.44 | 11.63 | 5.96 | 7.75 | 4.75 | 13.31 | 10.89 | | 6.84 | | 10.91 | | 8.33 | 20.56 | 9.62 | | 19.30 | 14.07 | 18.98 | 13.88 | 16.07 | | 14.46 | 9.03 | 7.76 | 9.31 | 11.73 | 11.83 | 8.44 | 12.99 | 10.91 | 14.75 |
| 10.18 | 9.13 | 10.96 | 10.13 | 6.72 | 9.32 | 9.08 | 11.88 | 13.29 | | 10.79 | | 12.40 | | 9.10 | 14.62 | 12.72 | | 20.42 | 11.75 | 18.89 | 15.86 | 11.54 | | 19.02 | 12.44 | 16.15 | 11.95 | 8.10 | 6.92 | 8.45 | 9.07 | 9.14 | 9.25 |
| 7.44 | 10.07 | 8.99 | 12.12 | 6.28 | 9.93 | 6.39 | 6.78 | 13.38 | | 8.57 | | 6.88 | | 9.64 | 18.43 | 22.92 | | 13.32 | 13.62 | 9.64 | 15.03 | 10.95 | | 11.96 | 11.39 | 14.03 | 10.35 | 7.51 | 9.94 | 13.45 | 12.58 | 7.40 | 12.35 |
| 5.76 | 9.18 | 11.16 | 12.31 | 12.23 | 6.15 | 6.07 | 12.28 | 6.21 | | 9.85 | | 11.60 | | 9.81 | 14.43 | 7.14 | | 6.03 | 17.09 | 12.39 | 18.07 | 11.86 | | 14.62 | 7.76 | 11.54 | 6.69 | 12.73 | 17.61 | 18.76 | 11.74 | 6.32 | 9.65 |
| 13.93 | 7.69 | 8.60 | 13.24 | 5.45 | 9.39 | 6.25 | 10.23 | 10.70 | | 13.38 | | 12.09 | | 7.88 | 20.69 | 3.79 | | 12.92 | 14.70 | 20.62 | 16.32 | 7.37 | | 12.84 | 7.10 | 9.77 | 6.53 | 8.62 | 12.76 | 9.87 | 14.61 | 16.44 | 14.88 |
| 8.82 | 8.32 | 7.07 | 10.76 | 6.36 | 7.56 | 8.52 | 8.73 | 8.17 | | 13.73 | | 5.60 | | 9.39 | 14.18 | 7.72 | | 9.53 | 13.16 | 12.95 | 12.63 | 13.17 | | 14.94 | 10.31 | 11.54 | 8.53 | 10.20 | 12.81 | 8.63 | 6.74 | 7.40 | 16.12 |
| 7.40 | 7.74 | 7.81 | 12.32 | 7.00 | 9.30 | 9.99 | 12.44 | 12.71 | | 18.92 | | 8.62 | | 11.38 | 18.62 | 8.24 | | 19.52 | 18.25 | 6.74 | 15.03 | 10.56 | | 13.01 | 10.25 | 12.23 | 9.20 | 8.80 | 14.86 | 13.46 | 10.43 | 17.41 | 7.14 |

# 2 Appendix 2. Biovolume conversions used to calculate biovolumes of Owasco Lake phytoplankton, with data source

| Finger Lakes Biovolume Estimates | | | | | | | | | | | | | | | |
|---|---|---|---|---|---|---|---|---|---|---|---|---|---|---|---|
| Biovolume densities are estimated based on Schaffner and Abbott's measurements of phytoplankton from derived from June to September measurements in Cayuga Lake unless noted otherwise | | | | | | | | | | | | | | | |
| | | | | | | | Cell Biovolume Estimate Used | | | | | | | | |
| **Genus or Lowest Taxonomic Unit** | **Phylum/Larger taxonomic g** | **Class** | **Estimate 1** | **Estimate 2** | **Estimate 3** | **Estimate 4** | **um^3** | | **Source** | | | | | | |
| Asterionella (per cell) | Bacillariophyta | Bacillariophyceae | 506 | 422 | 1430 | 864 | 134 | | Schaffner | | | | | | |
| Asterionella (colonies) | Bacillariophyta | Bacillariophyceae | 506 | 422 | 1430 | 864 | 806 | | Schaffner | | | | | | |
| Aulacoseira | Bacillariophyta | Coscinodiscophyceae | 600 | 750 | 480 | | 610 | | Schaffner | | | | | | |
| Cyclotella | Bacillariophyta | Mediophyceae | 393 | | | | 393 | | Schaffner | Note: from centric record | | | | | |
| Cocconeis | Bacillariophyta | Bacillariophyceae | 85 | 135 | | | 110 | | Schaffner | Note: also from generic record | | | | | |
| Cymbella | Bacillariophyta | Bacillariophyceae | 59 | | | | 59 | | Schaffner | | | | | | |
| Diatoma | Bacillariophyta | Bacillariophyceae | 65 | | | | 65 | | Schaffner | Note: from generic record | | | | | |
| Fragilaria (cells) | Bacillariophyta | Bacillariophyceae | 155 | | | | 155 | | Schaffner | | | | | | |
| Fragilaria (filaments) | Bacillariophyta | Bacillariophyceae | 1296 | 1500 | 1080 | 1875 | 1438 | | Schaffner | | | | | | |
| Gyrosigma | Bacillariophyta | Bacillariophyceae | 2492 | 2860 | | | 2676 | | diatom.ansp.org | (not just diatom values) | | | | | |
| Navicula | Bacillariophyta | Bacillariophyceae | 1104 | | | | 1104 | | Schaffner | Note: also from generic record in Cayuga | | | | | |
| Nitzschia | Bacillariophyta | Bacillariophyceae | 625 | | | | 625 | | Schaffner | Note: also from generic record in Cayuga | | | | | |
| Surirella | Bacillariophyta | Bacillariophyceae | 227 | | | | 227 | | Schaffner | Note: also from generic record in Cayuga | | | | | |
| Synedra | Bacillariophyta | Bacillariophyceae | 942 | 880 | 980 | | 934 | | Schaffner | | | | | | |
| Tabellaria | Bacillariophyta | Bacillariophyceae | 1913 | 1875 | | | 1894 | | Schaffner | | | | | | |
| Urosolenia | Bacillariophyta | Bacillariophyceae | 4379 | 4625 | | | 4502 | | diatom.ansp.org NYS records | (not just diatom values) | | | | | |
| Cosmarium | Charophyta | Zygnematophyceae | 681 | | | | 681 | | Schaffner | | | | | | |
| eukaryotic oval cell non-flagellate* | Chlorophyta | * | 33 | 16 | | | 25 | | Schaffner | | | | | | |
| eukaryotic round cell non-flagellate | Chlorophyta | * | 3 | 24 | 48 | 14 | 22 | | Schaffner | | | | | | |
| eukaryotic round flagellate | Chlorophyta | * | 65 | 21 | 180 | | 89 | | Schaffner | | | | | | |
| Pediastrum | Chlorophyta | Chlorophyceae | 350770 | | | | 350770 | | Schaffner | | | | | | |
| Scenedesmus (cells) | Chlorophyta | Chlorophyceae | 33 | 13 | 28 | | 25 | | Schaffner | | | | | | |
| Scenedesmus (filaments) | Chlorophyta | Chlorophyceae | 64 | 67 | | | 66 | | Schaffner | | | | | | |
| Sphaerocystis | Chlorophyta | Chlorophyceae | 302 | 65 | | | 184 | | Schaffner | | | | | | |
| Selenastrum | Chlorophyta | Chlorophyceae | 67 | | | | 67 | | Schaffner | | | | | | |
| Tetraspora | Chlorophyta | Chlorophyceae | 357 | | | | 357 | | diatom.ansp.org NYS | (not just diatom values) | | | | | |
| Cryptomonas-like flagellate | Cryptophyta | Cryptomonas | 134 | 317 | 619 | | 356 | | Schaffner | | | | | | |
| Anabaena | Cyanobacteria | Cyanophycea | 113 | 151 | 87 | | 117 | per cell | Schaffner | single cell | | | | | |
| Anabaena (filaments) | Cyanobacteria | Cyanophycea | use cell numbers | | | | 117 | per cell | Schaffner | | | | | | |
| Anabaena flosaquae morph (oval cells) | Cyanobacteria | Cyanophycea | use Anabaena | | | | 117 | per cell | Schaffner | | | | | | |
| Aphanizomenon | Cyanobacteria | Cyanophycea | use Anabaena | | | | 196 | | https://diatom.ansp.org/taxaservice/ShowBiovols.aspx?naded_id=806008 | | | | | | |
| Calothrix | Cyanobacteria | Cyanophycea | | | | | 85 | | https://diatom.ansp.org/taxa/taxon814010.html | | | | | (not just diatom value | |
| Chroococcus | Cyanobacteria | Cyanophycea | | | | | 170 | | Schaffner | | | | | | |
| Coelosphaerium | Cyanobacteria | Cyanophycea | | | | | 7 | per cell | Wehr and Sheath 2003 | | | | | | |
| Gleocapsa | Cyanobacteria | Cyanophycea | | | | 0.7-6 | 7 | per cell | Wehr and Sheath 2003 | | | | | | |
| Merismopedia | Cyanobacteria | Cyanophycea | | | | 1.2-6.5 | 5.94 | per cell | Wehr and Sheath 2003 | | | | | | |
| Microcystis | Cyanobacteria | Microcystaceae | | | | 0.8-6 | 3.4 | per cell | Wehr and Sheath 2003 | | | | | | |
| Oscillatoria | Cyanobacteria | Cyanophycea | 25.13 | 18.85 | 84.83 | | 43 | per cell | Schaffner | | | | | | |
| Synechococcus | Cyanobacteria | Cyanophycea | | | | | 5.94 | | from dimensions in Wehr and Sheath 2003 | | | | | | |
| Synecocystis | Cyanobacteria | Cyanophycea | | | | | 31.81 | per cell | Wehr and Sheath 2003 | | | | | | |
| Euglenoid | Euglenozoa | Euglenophyceae | 1539 | 1288 | 2356 | | 1728 | | Schaffner | | | | | | |
| Peridinium | Miozoa | Dinophyceae | 1288 | 8181 | 3163 | | 4211 | | Schaffner | | | | | | |
| Dinobryon | Ochrophyta | Chrysophyceae | 95 | 42 | 144 | | 94 | | Schaffner | | | | | | |
| Mallomonas | Ochrophyta | Synurophyceae | 733 | 785 | | | 759 | | Schaffner | | | | | | |

**Appendix 3A.** Detailed taxonomic composition of phytoplankton and biovolume calculations for Owasco Lake Phytoplankton, 5 July 2018

| Sample 1 | 5-Jul-18 | | | | | Cyanob. | Chlorop. | Bacill. | Chrysop. | Cryptop. | Euglenop. | Dino/Pyrrop. | |
|---|---|---|---|---|---|---|---|---|---|---|---|---|---|
| Site: UFI Owasco Site 2 | | Depth on bottle | none (but should be 0.5m | density | (#/mL) | 6065 | 1754 | 913 | 73 | 37 | 0 | 0 | |
| UFI ID: OW SITE 2 | site 2 | units are # of cells unless listed as filament | | biovolume | um^3/mL | 2.48E+05 | 1.39E+05 | 7.99E+05 | 6.85E+03 | 1.30E+04 | 0.00E+00 | 0.00E+00 | |
| | | | | | | | | | Volume Cou | Cell Density | Cell biovol | Total biovolume | |
| Genus or Lowest Taxonomic Unit | Phylum/Larger taxonomic group | Class | Additional Information | Field 1 | Field 2 | Field 3 | Field 4 | # Cells | mL sample | #/mL | um^3 | um^3/mL | Notes |
| Asterionella (cells total) | Bacillariophyta | Bacillariophyceae | | 0 | 0 | 0 | 0 | 0 | 0.055 | 0 | 134 | 0.00E+00 | |
| Asterionella (colonies) | Bacillariophyta | Bacillariophyceae | | 0 | 0 | 0 | 0 | 0 | 0.055 | 0 | 806 | 0.00E+00 | |
| Aulacoseira | Bacillariophyta | Coscinodiscophyceae | | 0 | 0 | 0 | 0 | 0 | 0.055 | 0 | 610 | 0.00E+00 | |
| Cyclotella | Bacillariophyta | Mediophyceae | | 0 | 0 | 0 | 0 | 0 | 0.055 | 0 | 393 | 0.00E+00 | |
| Cocconeis | Bacillariophyta | Bacillariophyceae | | 1 | 0 | 0 | 0 | 1 | 0.055 | 37 | 110 | 4.01E+03 | |
| Cymbella | Bacillariophyta | Bacillariophyceae | | 0 | 1 | 0 | 0 | 1 | 0.055 | 37 | 59 | 2.15E+03 | |
| Diatoma | Bacillariophyta | Bacillariophyceae | | 0 | 0 | 0 | 1 | 1 | 0.055 | 37 | 65 | 2.39E+03 | |
| Fragilaria (cells) | Bacillariophyta | Bacillariophyceae | | 0 | 0 | 0 | 0 | 0 | 0.055 | 0 | 155 | 0.00E+00 | |
| Fragilaria (filaments) | Bacillariophyta | Bacillariophyceae | | 0 | 0 | 0 | 0 | 0 | 0.055 | 0 | 1438 | 0.00E+00 | |
| Gyrosigma | Bacillariophyta | Bacillariophyceae | | 0 | 0 | 0 | 0 | 0 | 0.055 | 0 | 2676 | 0.00E+00 | |
| Navicula | Bacillariophyta | Bacillariophyceae | | 0 | 0 | 0 | 0 | 0 | 0.055 | 0 | 1104 | 0.00E+00 | |
| Nitzschia | Bacillariophyta | Bacillariophyceae | | 4 | 2 | 0 | 2 | 8 | 0.055 | 292 | 625 | 1.83E+05 | |
| Surirella | Bacillariophyta | Bacillariophyceae | | 0 | 0 | 0 | 0 | 0 | 0.055 | 0 | 227 | 0.00E+00 | |
| Synedra | Bacillariophyta | Bacillariophyceae | | 3 | 4 | 3 | 3 | 13 | 0.055 | 475 | 934 | 4.44E+05 | |
| Tabellaria | Bacillariophyta | Bacillariophyceae | | 0 | 0 | 0 | 0 | 0 | 0.055 | 0 | 1894 | 0.00E+00 | |
| Urosolenia | Bacillariophyta | Bacillariophyceae | | 0 | 0 | 0 | 1 | 1 | 0.055 | 37 | 4502 | 1.64E+05 | |
| Cosmarium | Charophyta | Zygnematophyceae | | 0 | 0 | 0 | 0 | 0 | 0.055 | 0 | 681 | 0.00E+00 | |
| eukaryotic oval cell non-flagellate* | Chlorophyta | * | Most are likely in Chlorophy | 1 | 0 | 0 | 3 | 4 | 0.055 | 146 | 25 | 3.59E+03 | |
| eukaryotic round cell non-flagellate | Chlorophyta | * | Most are likely in Chlorophy | 4 | 11 | 1 | 15 | 31 | 0.055 | 1133 | 22 | 2.52E+04 | |
| eukaryotic round flagellate | Chlorophyta | * | Most are likely in Chlorophy | 0 | 0 | 0 | 0 | 0 | 0.055 | 0 | 89 | 0.00E+00 | |
| Pediastrum | Chlorophyta | Chlorophyceae | | 0 | 0 | 0 | 0 | 0 | 0.055 | 0 | 350770 | 0.00E+00 | |
| Scenedesmus (cells) | Chlorophyta | Chlorophyceae | | 4 | 0 | 0 | 0 | 4 | 0.055 | 146 | 25 | 3.58E+03 | |
| Scenedesmus (filaments) | Chlorophyta | Chlorophyceae | | 1 | 0 | 0 | 0 | 1 | 0.055 | 37 | 66 | 2.40E+03 | |
| Sphaerocystis | Chlorophyta | Chlorophyceae | | 0 | 0 | 0 | 0 | 0 | 0.055 | 0 | 184 | 0.00E+00 | |
| Selenastrum | Chlorophyta | Chlorophyceae | | 0 | 0 | 0 | 0 | 0 | 0.055 | 0 | 67 | 0.00E+00 | |
| Tetraspora | Chlorophyta | Chlorophyceae | | 4 | 2 | 0 | 2 | 8 | 0.055 | 292 | 357 | 1.04E+05 | |
| Cryptomonas-like flagellate | Cryptophyta | Cryptomonas | | 0 | 1 | 0 | 0 | 1 | 0.055 | 37 | 356 | 1.30E+04 | |
| Anabaena | Cyanobacteria | Cyanophycea | | 0 | 0 | 0 | 0 | 0 | 0.055 | 0 | 117 | 0.00E+00 | |
| Anabaena (filaments) | Cyanobacteria | Cyanophycea | | 0 | 0 | 0 | 0 | 0 | 0.055 | 0 | 117 | 0.00E+00 | |
| Anabaena flosaquae morph (oval cells | Cyanobacteria | Cyanophycea | | 0 | 0 | 0 | 0 | 0 | 0.055 | 0 | 117 | 0.00E+00 | |
| Aphanizomenon | Cyanobacteria | Cyanophycea | | 0 | 0 | 0 | 0 | 0 | 0.055 | 0 | 196 | 0.00E+00 | |
| Calothrix | Cyanobacteria | Cyanophycea | | 0 | 0 | 0 | 0 | 0 | 0.055 | 0 | 85 | 0.00E+00 | |
| Chroococcus | Cyanobacteria | Cyanophycea | | 18 | 5 | 8 | 6 | 37 | 0.055 | 1352 | 170 | 2.29E+05 | |
| Coelosphaerium | Cyanobacteria | Cyanophycea | | 0 | 0 | 0 | 0 | 0 | 0.055 | 0 | 7 | 0.00E+00 | |
| Gleocapsa | Cyanobacteria | Cyanophycea | | 0 | 0 | 0 | 0 | 0 | 0.055 | 0 | 7 | 0.00E+00 | |
| Merismopedia | Cyanobacteria | Cyanophycea | | 0 | 0 | 0 | 0 | 0 | 0.055 | 0 | 6 | 0.00E+00 | |
| Microcystis | Cyanobacteria | Microcystaceae | cells | 16 | 51 | 15 | 17 | 99 | 0.055 | 3617 | 3 | 1.23E+04 | |
| Oscillatoria | Cyanobacteria | Cyanophycea | filaments | 0 | 0 | 0 | 0 | 0 | 0.055 | 0 | 43 | 0.00E+00 | |
| Synechococcus | Cyanobacteria | Cyanophycea | | 9 | 6 | 11 | 4 | 30 | 0.055 | 1096 | 6 | 6.52E+03 | |
| Synecocystis | Cyanobacteria | Cyanophycea | | 0 | 0 | 0 | 0 | 0 | 0.055 | 0 | 32 | 0.00E+00 | |
| Euglenoid | Euglenozoa | Euglenophyceae | | 0 | 0 | 0 | 0 | 0 | 0.055 | 0 | 1728 | 0.00E+00 | |
| Peridinium | Miozoa | Dinophyceae | | 0 | 0 | 0 | 0 | 0 | 0.055 | 0 | 4211 | 0.00E+00 | |
| Dinobryon | Ochrophyta | Chrysophyceae | | 0 | 2 | 0 | 0 | 2 | 0.055 | 73 | 94 | 6.85E+03 | |
| Mallomonas | Ochrophyta | Synurophyceae | | 0 | 0 | 0 | 0 | 0 | 0.055 | 0 | 759 | 0.00E+00 | |

# Appendix 3B . Detailed taxonomic composition of phytoplankton and biovolume calculations for Owasco Lake Phytoplankton, 18 July 2018

| | | | | | | Cyanob. | Chlorop. | Bacill. | Chrysop. | Cryptop. | Euglenop. | Dino/Pyrrop. |
|---|---|---|---|---|---|---|---|---|---|---|---|---|
| Sample 2 | 18-Jul-18 | | | density | (#/mL) | 25089 | 4238 | 3946 | 0 | 49 | 0 | 0 |
| Site: UFI Owasco Site 2 | | | | biovolume | um^3/mL | 2.30E+05 | 8.40E+06 | 1.48E+06 | 0.00E+00 | 1.74E+04 | 0.00E+00 | 0.00E+00 |
| UFI ID: OW SITE 2 | site 2 | Depth on bottle | 0.5 m | | | | | | | | | |
| | | units are # of cells unless listed as filament | | | | | | | | | | |
| Genus or Lowest Taxonomic Unit | Phylum/Larger taxonomic group | Class | Additional Information | Field 1 | Field 2 | Field 3 | | # Cells | Volume Cou mL sample | Cell Density #/mL | Cell biovol um^3 | Total biovolume um^3/mL |
| Asterionella (cells total) | Bacillariophyta | Bacillariophyceae | | 0 | 0 | 0 | | 0 | 0.041 | 0 | 134 | 0.00E+00 |
| Asterionella (colonies) | Bacillariophyta | Bacillariophyceae | | 0 | 0 | 0 | | 0 | 0.041 | 0 | 806 | 0.00E+00 |
| Aulacoseira | Bacillariophyta | Coscinodiscophyceae | | 0 | 0 | 0 | | 0 | 0.041 | 0 | 610 | 0.00E+00 |
| Cyclotella | Bacillariophyta | Mediophyceae | | 0 | 0 | 0 | | 0 | 0.041 | 0 | 393 | 0.00E+00 |
| Cocconeis | Bacillariophyta | Bacillariophyceae | | 0 | 0 | 0 | | 0 | 0.041 | 0 | 110 | 0.00E+00 |
| Cymbella | Bacillariophyta | Bacillariophyceae | | 0 | 0 | 0 | | 0 | 0.041 | 0 | 59 | 0.00E+00 |
| Diatoma | Bacillariophyta | Bacillariophyceae | | 0 | 0 | 0 | | 0 | 0.041 | 0 | 65 | 0.00E+00 |
| Fragilaria (cells) | Bacillariophyta | Bacillariophyceae | | 48 | 0 | 12 | | 60 | 0.041 | 2923 | 155 | 4.53E+05 |
| Fragilaria (filaments) | Bacillariophyta | Bacillariophyceae | | 4 | 0 | 2 | | 6 | 0.041 | 292 | 1438 | 4.20E+05 |
| Gyrosigma | Bacillariophyta | Bacillariophyceae | | 0 | 0 | 0 | | 0 | 0.041 | 0 | 2676 | 0.00E+00 |
| Navicula | Bacillariophyta | Bacillariophyceae | | 0 | 0 | 0 | | 0 | 0.041 | 0 | 1104 | 0.00E+00 |
| Nitzschia | Bacillariophyta | Bacillariophyceae | | 5 | 0 | 0 | | 5 | 0.041 | 244 | 625 | 1.52E+05 |
| Surirella | Bacillariophyta | Bacillariophyceae | | 0 | 0 | 0 | | 0 | 0.041 | 0 | 227 | 0.00E+00 |
| Synedra | Bacillariophyta | Bacillariophyceae | | 1 | 3 | 6 | | 10 | 0.041 | 487 | 934 | 4.55E+05 |
| Tabellaria | Bacillariophyta | Bacillariophyceae | | 0 | 0 | 0 | | 0 | 0.041 | 0 | 1894 | 0.00E+00 |
| Urosolenia | Bacillariophyta | Bacillariophyceae | | 0 | 0 | 0 | | 0 | 0.041 | 0 | 4502 | 0.00E+00 |
| Cosmarium | Charophyta | Zygnematophyceae | | 0 | 0 | 0 | | 0 | 0.041 | 0 | 681 | 0.00E+00 |
| eukaryotic oval cell non-flagellate* | Chlorophyta | * | Most are likely in Chlorophy | 10 | 2 | 4 | | 16 | 0.041 | 779 | 25 | 1.91E+04 |
| eukaryotic round cell non-flagellate | Chlorophyta | * | Most are likely in Chlorophy | 2 | 3 | 3 | | 8 | 0.041 | 390 | 22 | 8.67E+03 |
| eukaryotic round flagellate | Chlorophyta | * | Most are likely in Chlorophy | 0 | 0 | 0 | | 0 | 0.041 | 0 | 89 | 0.00E+00 |
| Pediastrum | Chlorophyta | Chlorophyceae | | 0 | 0 | 0 | | 0 | 0.041 | 0 | 350770 | 0.00E+00 |
| Scenedesmus (cells) | Chlorophyta | Chlorophyceae | | 4 | 6 | 4 | | 14 | 0.041 | 682 | 25 | 1.67E+04 |
| Scenedesmus (filaments) | Chlorophyta | Chlorophyceae | | 1 | 2 | 1 | | 4 | 0.041 | 195 | 66 | 1.28E+04 |
| Sphaerocystis | Chlorophyta | Chlorophyceae | | 0 | 0 | 0 | | 0 | 0.041 | 0 | 184 | 0.00E+00 |
| Selenastrum | Chlorophyta | Chlorophyceae | | 0 | 0 | 0 | | 0 | 0.041 | 0 | 67 | 0.00E+00 |
| Tetraspora | Chlorophyta | Chlorophyceae | colony | 18 | 13 | 14 | | 45 | 0.041 | 2192 | 357 | 7.83E+05 |
| Cryptomonas-like flagellate | Cryptophyta | Cryptomonas | | 0 | 0 | 1 | | 1 | 0.041 | 49 | 356 | 1.74E+04 |
| Anabaena | Cyanobacteria | Cyanophycea | | 0 | 0 | 0 | | 0 | 0.041 | 0 | 117 | 0.00E+00 |
| Anabaena (filaments) | Cyanobacteria | Cyanophycea | | 0 | 0 | 0 | | 0 | 0.041 | 0 | 117 | 0.00E+00 |
| Anabaena flosaquae morph (oval cells | Cyanobacteria | Cyanophycea | | 0 | 0 | 0 | | 0 | 0.041 | 0 | 117 | 0.00E+00 |
| Aphanizomenon | Cyanobacteria | Cyanophycea | | 0 | 0 | 0 | | 0 | 0.041 | 0 | 196 | 0.00E+00 |
| Calothrix | Cyanobacteria | Cyanophycea | | 2 | 1 | 0 | | 3 | 0.041 | 146 | 85 | 1.24E+04 |
| Chroococcus | Cyanobacteria | Cyanophycea | | 5 | 2 | 4 | | 11 | 0.041 | 536 | 170 | 9.09E+04 |
| Coelosphaerium | Cyanobacteria | Cyanophycea | | 0 | 0 | 0 | | 0 | 0.041 | 0 | 7 | 0.00E+00 |
| Gleocapsa | Cyanobacteria | Cyanophycea | | 0 | 0 | 0 | | 0 | 0.041 | 0 | 7 | 0.00E+00 |
| Merismopedia | Cyanobacteria | Cyanophycea | cells | 0 | 0 | 8 | | 8 | 0.041 | 390 | 6 | 2.32E+03 |
| Microcystis | Cyanobacteria | Microcystaceae | cells | 44 | 350 | 18 | | 412 | 0.041 | 20071 | 3 | 6.82E+04 |
| Oscillatoria | Cyanobacteria | Cyanophycea | filaments | 0 | 0 | 0 | | 0 | 0.041 | 0 | 43 | 0.00E+00 |
| Synechococcus | Cyanobacteria | Cyanophycea | | 16 | 18 | 21 | | 55 | 0.041 | 2679 | 6 | 1.59E+04 |
| Synecocystis | Cyanobacteria | Cyanophycea | | 26 | 0 | 0 | | 26 | 0.041 | 1267 | 32 | 4.03E+04 |
| Euglenoid | Euglenozoa | Euglenophyceae | | 0 | 0 | 0 | | 0 | 0.041 | 0 | 1728 | 0.00E+00 |
| Peridinium | Miozoa | Dinophyceae | | 0 | 0 | 0 | | 0 | 0.041 | 0 | 4211 | 0 |
| Dinobryon | Ochrophyta | Chrysophyceae | | 0 | 0 | 0 | | 0 | 0.041 | 0 | 94 | 0 |
| Mallomonas | Ochrophyta | Synurophyceae | | 0 | 0 | 0 | | 0 | 0.041 | 0 | 759 | 0 |

# Appendix 3C. Detailed taxonomic composition of phytoplankton and biovolume calculations for Owasco Lake Phytoplankton, 2 August 2018

| | | | | | | Cyanob. | Chlorop. | Bacill. | Chyrsop. | Cryptop. | Euglenop. | Dino/Pyrrop. | |
|---|---|---|---|---|---|---|---|---|---|---|---|---|---|
| | | | | density | (#/mL) | 408116 | 4238 | 3946 | 0 | 49 | 0 | 0 | |
| Sample 3 | 2-Aug-18 | | | biovolume | um^3/mL | 5.01E+06 | 8.40E+05 | 1.48E+06 | 0.00E+00 | 1.74E+04 | 0.00E+00 | 0.00E+00 | |
| Site: UFI Owasco Site 2 | | Depth on bottle | none (but should be 0.5m) | | | | | | | | | | |
| UFI ID: OW SITE 2 | site 2 | units are # of cells unless listed as filament | | | | | | | | | | | |
| extremely high amount of Microcystis (MC) in sample; counted the highlighted taxa at higher power - the field was crammed with MC | | | | | counted at higher power; volume | | | # Cells | Volume Cou | Cell Density | Cell biovol | Total biovolume | |
| Genus or Lowest Taxonomic Unit | Phylum/Larger taxonomic group | Class | Additional Information | Field 1 | Field 2 | Field 3 | | | mL sample | #/mL | um^3 | um^3/mL | |
| Asterionella (cells total) | Bacillariophyta | Bacillariophyceae | | 0 | 0 | 0 | | 0 | 0.041 | 0 | 134 | 0.00E+00 | |
| Asterionella (colonies) | Bacillariophyta | Bacillariophyceae | | 0 | 0 | 0 | | 0 | 0.041 | 0 | 806 | 0.00E+00 | |
| Aulacoseira | Bacillariophyta | Coscinodiscophyceae | | 0 | 0 | 0 | | 0 | 0.041 | 0 | 610 | 0.00E+00 | |
| Cyclotella | Bacillariophyta | Mediophyceae | | 0 | 0 | 0 | | 0 | 0.041 | 0 | 393 | 0.00E+00 | |
| Cocconeis | Bacillariophyta | Bacillariophyceae | | 0 | 0 | 0 | | 0 | 0.041 | 0 | 110 | 0.00E+00 | |
| Cymbella | Bacillariophyta | Bacillariophyceae | | 0 | 0 | 0 | | 0 | 0.041 | 0 | 59 | 0.00E+00 | |
| Diatoma | Bacillariophyta | Bacillariophyceae | | 0 | 0 | 0 | | 0 | 0.041 | 0 | 65 | 0.00E+00 | |
| Fragilaria (cells) | Bacillariophyta | Bacillariophyceae | | 48 | 0 | 12 | | 60 | 0.041 | 2923 | 155 | 4.53E+05 | |
| Fragilaria (filaments) | Bacillariophyta | Bacillariophyceae | | 4 | 0 | 2 | | 6 | 0.041 | 292 | 1438 | 4.20E+05 | |
| Gyrosigma | Bacillariophyta | Bacillariophyceae | | 0 | 0 | 0 | | 0 | 0.041 | 0 | 2676 | 0.00E+00 | |
| Navicula | Bacillariophyta | Bacillariophyceae | | 0 | 0 | 0 | | 0 | 0.041 | 0 | 1104 | 0.00E+00 | |
| Nitzschia | Bacillariophyta | Bacillariophyceae | | 5 | 0 | 0 | | 5 | 0.041 | 244 | 625 | 1.52E+05 | |
| Surirella | Bacillariophyta | Bacillariophyceae | | 0 | 0 | 0 | | 0 | 0.041 | 0 | 227 | 0.00E+00 | |
| Synedra | Bacillariophyta | Bacillariophyceae | | 1 | 3 | 6 | | 10 | 0.041 | 487 | 934 | 4.55E+05 | |
| Tabellaria | Bacillariophyta | Bacillariophyceae | | 0 | 0 | 0 | | 0 | 0.041 | 0 | 1894 | 0.00E+00 | |
| Urosolenia | Bacillariophyta | Bacillariophyceae | | 0 | 0 | 0 | | 0 | 0.041 | 0 | 4502 | 0.00E+00 | |
| Cosmarium | Charophyta | Zygnematophyceae | | 0 | 0 | 0 | | 0 | 0.041 | 0 | 681 | 0.00E+00 | |
| eukaryotic oval cell non-flagellate* | Chlorophyta | * | Most are likely in Chlorophy | 10 | 2 | 4 | | 16 | 0.041 | 779 | 25 | 1.91E+04 | |
| eukaryotic round cell non-flagellate | Chlorophyta | * | Most are likely in Chlorophy | 2 | 3 | 3 | | 8 | 0.041 | 390 | 22 | 8.67E+03 | |
| eukaryotic round flagellate | Chlorophyta | * | Most are likely in Chlorophy | 0 | 0 | 0 | | 0 | 0.041 | 0 | 89 | 0.00E+00 | |
| Pediastrum | Chlorophyta | Chlorophyceae | | 0 | 0 | 0 | | 0 | 0.041 | 0 | 350770 | 0.00E+00 | |
| Scenedesmus (cells) | Chlorophyta | Chlorophyceae | | 4 | 6 | 4 | | 14 | 0.041 | 682 | 25 | 1.67E+04 | |
| Scenedesmus (filaments) | Chlorophyta | Chlorophyceae | | 1 | 2 | 1 | | 4 | 0.041 | 195 | 66 | 1.28E+04 | |
| Sphaerocystis | Chlorophyta | Chlorophyceae | | 0 | 0 | 0 | | 0 | 0.041 | 0 | 184 | 0.00E+00 | |
| Selenastrum | Chlorophyta | Chlorophyceae | | 0 | 0 | 0 | | 0 | 0.041 | 0 | 67 | 0.00E+00 | |
| Tetraspora | Chlorophyta | Chlorophyceae | colony | 18 | 13 | 14 | | 45 | 0.041 | 2192 | 357 | 7.83E+05 | |
| Cryptomonas-like flagellate | Cryptophyta | Cryptomonas | | 0 | 0 | 1 | | 1 | 0.041 | 49 | 356 | 1.74E+04 | |
| Anabaena | Cyanobacteria | Cyanophycea | | 0 | 0 | 0 | | 0 | 0.041 | 0 | 117 | 0.00E+00 | |
| Anabaena (filaments) | Cyanobacteria | Cyanophycea | | 0 | 0 | 0 | | 0 | 0.041 | 0 | 117 | 0.00E+00 | |
| Anabaena flosaquae morph (oval cells | Cyanobacteria | Cyanophycea | | 0 | 0 | 0 | | 0 | 0.041 | 0 | 117 | 0.00E+00 | |
| Aphanizomenon | Cyanobacteria | Cyanophycea | filaments | 75 | 71 | 61 | | 207 | 0.041 | 10084 | 196 | 1.98E+06 | |
| Calothrix | Cyanobacteria | Cyanophycea | | 2 | 1 | 0 | | 3 | 0.041 | 146 | 85 | 1.24E+04 | |
| Chroococcus | Cyanobacteria | Cyanophycea | | 5 | 2 | 4 | | 11 | 0.002 | 9118 | 170 | 1.55E+06 | |
| Coelosphaerium | Cyanobacteria | Cyanophycea | | 0 | 0 | 0 | | 0 | 0.041 | 0 | 7 | 0.00E+00 | |
| Gleocapsa | Cyanobacteria | Cyanophycea | | 0 | 0 | 0 | | 0 | 0.041 | 0 | 7 | 0.00E+00 | |
| Merismopedia | Cyanobacteria | Cyanophycea | cells | 0 | 0 | 8 | | 8 | 0.041 | 390 | 6 | 2.32E+03 | 1 colony |
| Microcystis | Cyanobacteria | Microcystaceae | cells | 44 | 350 | 18 | | 412 | 0.002 | 341520 | 3 | 1.16E+06 | rep 2 had s |
| Oscillatoria | Cyanobacteria | Cyanophycea | filaments | 0 | 0 | 0 | | 0 | 0.041 | 0 | 43 | 0.00E+00 | |
| Synechococcus | Cyanobacteria | Cyanophycea | | 16 | 18 | 21 | | 55 | 0.002 | 45591 | 6 | 2.71E+05 | |
| Synecocystis | Cyanobacteria | Cyanophycea | | 26 | 0 | 0 | | 26 | 0.041 | 1267 | 32 | 4.03E+04 | |
| Euglenoid | Euglenozoa | Euglenophyceae | | 0 | 0 | 0 | | 0 | 0.041 | 0 | 1728 | 0.00E+00 | |
| Peridinium | Miozoa | Dinophyceae | | 0 | 0 | 0 | | 0 | 0.041 | 0 | 4211 | 0.00E+00 | |
| Dinobryon | Ochrophyta | Chrysophyceae | | 0 | 0 | 0 | | 0 | 0.041 | 0 | 94 | 0.00E+00 | |
| Mallomonas | Ochrophyta | Synurophyceae | | 0 | 0 | 0 | | 0 | 0.041 | 0 | 759 | 0.00E+00 | |

**Appendix 3 D. Detailed taxonomic composition of phytoplankton and biovolume calculations for Owasco Lake Phytoplankton, 31 August 2018**

| | | | | | | Cyanob. | Chlorop. | Bacill. | Chrysop. | Cryptop. | Euglenop. | Dino/Pyrrop. |
|---|---|---|---|---|---|---|---|---|---|---|---|---|
| Sample 4 | 31-Aug-18 | | | density | (#/mL) | 8477 | 2972 | 1364 | 0 | 0 | 0 | 49 |
| Site: UFI Owasco Site 2 | | | | biovolume | um^3/mL | 1.92E+05 | 2.01E+05 | 1.23E+06 | 0.00E+00 | 0.00E+00 | 0.00E+00 | 2.05E+05 |
| UFI ID: OW SITE 2 | site 2 | Depth on bottle | none (but should be 0.5m) | | | | | | | | | |
| | | units are # of cells unless listed as filament | | | | | | | | | | |
| | | | | | | | | | Volume Cou | Cell Density | Cell biovol | Total biovolume |
| Genus or Lowest Taxonomic Unit | Phylum/Larger taxonomic group | Class | Additional Information | Field 1 | Field 2 | Field 3 | | # Cells | mL sample | #/mL | um^3 | um^3/mL |
| Asterionella (cells total) | Bacillariophyta | Bacillariophyceae | | 0 | 0 | 0 | | 0 | 0.041 | 0 | 134 | 0.00E+00 |
| Asterionella (colonies) | Bacillariophyta | Bacillariophyceae | | 0 | 0 | 0 | | 0 | 0.041 | 0 | 806 | 0.00E+00 |
| Aulacoseira | Bacillariophyta | Coscinodiscophyceae | | 0 | 0 | 0 | | 0 | 0.041 | 0 | 610 | 0.00E+00 |
| Cyclotella | Bacillariophyta | Mediophyceae | | 0 | 0 | 0 | | 0 | 0.041 | 0 | 393 | 0.00E+00 |
| Cocconeis | Bacillariophyta | Bacillariophyceae | | 0 | 0 | 0 | | 0 | 0.041 | 0 | 110 | 0.00E+00 |
| Cymbella | Bacillariophyta | Bacillariophyceae | | 0 | 0 | 0 | | 0 | 0.041 | 0 | 59 | 0.00E+00 |
| Diatoma | Bacillariophyta | Bacillariophyceae | | 0 | 0 | 1 | | 1 | 0.041 | 49 | 65 | 3.19E+03 |
| Fragilaria (cells) | Bacillariophyta | Bacillariophyceae | | 0 | 0 | 0 | | 0 | 0.041 | 0 | 155 | 0.00E+00 |
| Fragilaria (filaments) | Bacillariophyta | Bacillariophyceae | | 0 | 0 | 0 | | 0 | 0.041 | 0 | 1438 | 0.00E+00 |
| Gyrosigma | Bacillariophyta | Bacillariophyceae | | 0 | 0 | 0 | | 0 | 0.041 | 0 | 2676 | 0.00E+00 |
| Navicula | Bacillariophyta | Bacillariophyceae | | 0 | 0 | 0 | | 0 | 0.041 | 0 | 1104 | 0.00E+00 |
| Nitzschia | Bacillariophyta | Bacillariophyceae | | 0 | 0 | 0 | | 0 | 0.041 | 0 | 625 | 0.00E+00 |
| Surirella | Bacillariophyta | Bacillariophyceae | | 0 | 0 | 0 | | 0 | 0.041 | 0 | 227 | 0.00E+00 |
| Synedra | Bacillariophyta | Bacillariophyceae | | 9 | 12 | 6 | | 27 | 0.041 | 1315 | 934 | 1.23E+06 |
| Tabellaria | Bacillariophyta | Bacillariophyceae | | 0 | 0 | 0 | | 0 | 0.041 | 0 | 1894 | 0.00E+00 |
| Urosolenia | Bacillariophyta | Bacillariophyceae | | 0 | 0 | 0 | | 0 | 0.041 | 0 | 4502 | 0.00E+00 |
| Cosmarium | Charophyta | Zygnematophyceae | | 0 | 0 | 0 | | 0 | 0.041 | 0 | 681 | 0.00E+00 |
| eukaryotic oval cell non-flagellate* | Chlorophyta | * | Most are likely in Chloroph | 3 | 2 | 0 | | 5 | 0.041 | 244 | 25 | 5.98E+03 |
| eukaryotic round cell non-flagellate | Chlorophyta | * | Most are likely in Chloroph | 2 | 1 | 6 | | 9 | 0.041 | 438 | 22 | 9.76E+03 |
| eukaryotic round flagellate | Chlorophyta | * | Most are likely in Chloroph | 0 | 0 | 0 | | 0 | 0.041 | 0 | 89 | 0.00E+00 |
| Pediastrum | Chlorophyta | Chlorophyceae | | 0 | 0 | 0 | | 0 | 0.041 | 0 | 350770 | 0.00E+00 |
| Scenedesmus (cells) | Chlorophyta | Chlorophyceae | | 8 | 8 | 16 | | 32 | 0.041 | 1559 | 25 | 3.82E+04 |
| Scenedesmus (filaments) | Chlorophyta | Chlorophyceae | | 2 | 2 | 4 | | 8 | 0.041 | 390 | 66 | 2.56E+04 |
| Sphaerocystis | Chlorophyta | Chlorophyceae | | 0 | 0 | 0 | | 0 | 0.041 | 0 | 184 | 0.00E+00 |
| Selenastrum | Chlorophyta | Chlorophyceae | | 0 | 0 | 0 | | 0 | 0.041 | 0 | 67 | 0.00E+00 |
| Tetraspora | Chlorophyta | Chlorophyceae | colony | 2 | 3 | 2 | | 7 | 0.041 | 341 | 357 | 1.22E+05 |
| Cryptomonas-like flagellate | Cryptophyta | Cryptomonas | | 0 | 0 | 0 | | 0 | 0.041 | 0 | 356 | 0.00E+00 |
| Anabaena | Cyanobacteria | Cyanophycea | | 8 | 0 | 0 | | 8 | 0.041 | 390 | 117 | 4.56E+04 |
| Anabaena (filaments) | Cyanobacteria | Cyanophycea | | 1 | 0 | 0 | | 1 | 0.041 | 49 | 117 | 5.70E+03 |
| Anabaena flosaquae morph (oval cells | Cyanobacteria | Cyanophycea | | 0 | 0 | 0 | | 0 | 0.041 | 0 | 117 | 0.00E+00 |
| Aphanizomenon | Cyanobacteria | Cyanophycea | filaments | 0 | 2 | 1 | | 3 | 0.041 | 146 | 196 | 2.86E+04 |
| Calothrix | Cyanobacteria | Cyanophycea | | 0 | 0 | 0 | | 0 | 0.041 | 0 | 85 | 0.00E+00 |
| Chroococcus | Cyanobacteria | Cyanophycea | | 4 | 2 | 4 | | 10 | 0.041 | 487 | 170 | 8.26E+04 |
| Coelosphaerium | Cyanobacteria | Cyanophycea | | 0 | 0 | 0 | | 0 | 0.041 | 0 | 7 | 0.00E+00 |
| Gleocapsa | Cyanobacteria | Cyanophycea | | 2 | 3 | 0 | | 5 | 0.041 | 244 | 7 | 1.61E+03 |
| Merismopedia | Cyanobacteria | Cyanophycea | cells | 0 | 0 | 0 | | 0 | 0.041 | 0 | 6 | 0.00E+00 |
| Microcystis | Cyanobacteria | Microcystaceae | cells | 41 | 41 | 51 | | 133 | 0.041 | 6479 | 3 | 2.20E+04 |
| Oscillatoria | Cyanobacteria | Cyanophycea | filaments | 0 | 1 | 0 | | 1 | 0.041 | 49 | 43 | 2.09E+03 |
| Synechococcus | Cyanobacteria | Cyanophycea | | 6 | 1 | 6 | | 13 | 0.041 | 633 | 6 | 3.76E+03 |
| Synecocystis | Cyanobacteria | Cyanophycea | | 0 | 0 | 0 | | 0 | 0.041 | 0 | 32 | 0.00E+00 |
| Euglenoid | Euglenozoa | Euglenophyceae | | 0 | 0 | 0 | | 0 | 0.041 | 0 | 1728 | 0.00E+00 |
| Peridinium | Miozoa | Dinophyceae | | 0 | 1 | 0 | | 1 | 0.041 | 49 | 4211 | 2.05E+05 |
| Dinobryon | Ochrophyta | Chrysophyceae | | 0 | 0 | 0 | | 0 | 0.041 | 0 | 94 | 0.00E+00 |
| Mallomonas | Ochrophyta | Synurophyceae | | 0 | 0 | 0 | | 0 | 0.041 | 0 | 759 | 0.00E+00 |

**Appendix 3E.** Detailed taxonomic composition of phytoplankton and biovolume calculations for Owasco Lake Phytoplankton, 12 September 2018

| | | | | | | Cyanob. | Chlorop. | Bacill. | Chyrsop. | Cryptop. | Euglenop. | Dino/Pyrrop. |
|---|---|---|---|---|---|---|---|---|---|---|---|---|
| | | | | density | (#/mL) | 30301 | 3215 | 4287 | 0 | 49 | 0 | 0 |
| Sample 5 | 12-Sep-18 | | | biovolume | um^3/mL | 1.33E+05 | 9.26E+04 | 3.92E+06 | 0.00E+00 | 1.74E+04 | 0.00E+00 | 0.00E+00 |
| Site: UFI Owasco Site 2 | | Depth on bottle | none (but should be 0.5m) | | | | | | | | | |
| UFI ID: OW SITE 2 | site 2 | units are # of cells unless listed as filament | | | | | | | | | | |
| | | | | | | | | | Volume Cou | Cell Density | Cell biovol | Total biovolume |
| Genus or Lowest Taxonomic Unit | Phylum/Larger taxonomic group | Class | Additional Information | Field 1 | Field 2 | Field 3 | | # Cells | mL sample | #/mL | um^3 | um^3/mL |
| Asterionella (cells total) | Bacillariophyta | Bacillariophyceae | | 0 | 0 | 0 | | 0 | 0.041 | 0 | 134 | 0.00E+00 |
| Asterionella (colonies) | Bacillariophyta | Bacillariophyceae | | 0 | 0 | 0 | | 0 | 0.041 | 0 | 806 | 0.00E+00 |
| Aulacoseira | Bacillariophyta | Coscinodiscophyceae | | 0 | 0 | 0 | | 0 | 0.041 | 0 | 610 | 0.00E+00 |
| Cyclotella | Bacillariophyta | Mediophyceae | | 0 | 0 | 0 | | 0 | 0.041 | 0 | 393 | 0.00E+00 |
| Cocconeis | Bacillariophyta | Bacillariophyceae | | 0 | 0 | 0 | | 0 | 0.041 | 0 | 110 | 0.00E+00 |
| Cymbella | Bacillariophyta | Bacillariophyceae | | 0 | 1 | 0 | | 1 | 0.041 | 49 | 59 | 2.87E+03 |
| Diatoma | Bacillariophyta | Bacillariophyceae | | 1 | 0 | 0 | | 1 | 0.041 | 49 | 65 | 3.19E+03 |
| Fragilaria (cells) | Bacillariophyta | Bacillariophyceae | | 0 | 0 | 0 | | 0 | 0.041 | 0 | 155 | 0.00E+00 |
| Fragilaria (filaments) | Bacillariophyta | Bacillariophyceae | | 0 | 0 | 0 | | 0 | 0.041 | 0 | 1438 | 0.00E+00 |
| Gyrosigma | Bacillariophyta | Bacillariophyceae | | 0 | 0 | 0 | | 0 | 0.041 | 0 | 2676 | 0.00E+00 |
| Navicula | Bacillariophyta | Bacillariophyceae | | 0 | 0 | 0 | | 0 | 0.041 | 0 | 1104 | 0.00E+00 |
| Nitzschia | Bacillariophyta | Bacillariophyceae | | 0 | 0 | 0 | | 0 | 0.041 | 0 | 625 | 0.00E+00 |
| Surirella | Bacillariophyta | Bacillariophyceae | | 0 | 0 | 0 | | 0 | 0.041 | 0 | 227 | 0.00E+00 |
| Synedra | Bacillariophyta | Bacillariophyceae | | 27 | 28 | 31 | | 86 | 0.041 | 4190 | 934 | 3.91E+06 |
| Tabellaria | Bacillariophyta | Bacillariophyceae | | 0 | 0 | 0 | | 0 | 0.041 | 0 | 1894 | 0.00E+00 |
| Urosolenia | Bacillariophyta | Bacillariophyceae | | 0 | 0 | 0 | | 0 | 0.041 | 0 | 4502 | 0.00E+00 |
| Cosmarium | Charophyta | Zygnematophyceae | | 0 | 0 | 0 | | 0 | 0.041 | 0 | 681 | 0.00E+00 |
| eukaryotic oval cell non-flagellate* | Chlorophyta | * | Most are likely in Chloroph | 3 | 1 | 3 | | 7 | 0.041 | 341 | 25 | 8.37E+03 |
| eukaryotic round cell non-flagellate | Chlorophyta | * | Most are likely in Chloroph | 9 | 7 | 5 | | 21 | 0.041 | 1023 | 22 | 2.28E+04 |
| eukaryotic round flagellate | Chlorophyta | * | Most are likely in Chloroph | 0 | 0 | 0 | | 0 | 0.041 | 0 | 89 | 0.00E+00 |
| Pediastrum | Chlorophyta | Chlorophyceae | | 0 | 0 | 0 | | 0 | 0.041 | 0 | 350770 | 0.00E+00 |
| Scenedesmus (cells) | Chlorophyta | Chlorophyceae | | 12 | 12 | 6 | | 30 | 0.041 | 1461 | 25 | 3.58E+04 |
| Scenedesmus (filaments) | Chlorophyta | Chlorophyceae | | 3 | 3 | 2 | | 8 | 0.041 | 390 | 66 | 2.56E+04 |
| Sphaerocystis | Chlorophyta | Chlorophyceae | | 0 | 0 | 0 | | 0 | 0.041 | 0 | 184 | 0.00E+00 |
| Selenastrum | Chlorophyta | Chlorophyceae | | 0 | 0 | 0 | | 0 | 0.041 | 0 | 67 | 0.00E+00 |
| Tetraspora | Chlorophyta | Chlorophyceae | colony | 0 | 0 | 0 | | 0 | 0.041 | 0 | 357 | 0.00E+00 |
| Cryptomonas-like flagellate | Cryptophyta | Cryptomonas | | 0 | 1 | 0 | | 1 | 0.041 | 49 | 356 | 1.74E+04 |
| Anabaena | Cyanobacteria | Cyanophycea | | 0 | 0 | 0 | | 0 | 0.041 | 0 | 117 | 0.00E+00 |
| Anabaena (filaments) | Cyanobacteria | Cyanophycea | | 0 | 0 | 0 | | 0 | 0.041 | 0 | 117 | 0.00E+00 |
| Anabaena flosaquae morph (oval cells | Cyanobacteria | Cyanophycea | | 0 | 0 | 0 | | 0 | 0.041 | 0 | 117 | 0.00E+00 |
| Aphanizomenon | Cyanobacteria | Cyanophycea | filaments | 0 | 0 | 0 | | 0 | 0.041 | 0 | 196 | 0.00E+00 |
| Calothrix | Cyanobacteria | Cyanophycea | | 0 | 0 | 0 | | 0 | 0.041 | 0 | 85 | 0.00E+00 |
| Chroococcus | Cyanobacteria | Cyanophycea | | 0 | 2 | 0 | | 2 | 0.041 | 97 | 170 | 1.65E+04 |
| Coelosphaerium | Cyanobacteria | Cyanophycea | | 0 | 0 | 0 | | 0 | 0.041 | 0 | 7 | 0.00E+00 |
| Gleocapsa | Cyanobacteria | Cyanophycea | | 0 | 0 | 0 | | 0 | 0.041 | 0 | 7 | 0.00E+00 |
| Merismopedia | Cyanobacteria | Cyanophycea | cells | 0 | 0 | 0 | | 0 | 0.041 | 0 | 6 | 0.00E+00 |
| Microcystis | Cyanobacteria | Microcystaceae | cells | 17 | 30 | 460 | | 507 | 0.041 | 24699 | 3 | 8.40E+04 |
| Oscillatoria | Cyanobacteria | Cyanophycea | filaments | 0 | 0 | 0 | | 0 | 0.041 | 0 | 43 | 0.00E+00 |
| Synechococcus | Cyanobacteria | Cyanophycea | | 16 | 6 | 91 | | 113 | 0.041 | 5505 | 6 | 3.27E+04 |
| Synecocystis | Cyanobacteria | Cyanophycea | | 0 | 0 | 0 | | 0 | 0.041 | 0 | 32 | 0.00E+00 |
| Euglenoid | Euglenozoa | Euglenophyceae | | 0 | 0 | 0 | | 0 | 0.041 | 0 | 1728 | 0.00E+00 |
| Peridinium | Miozoa | Dinophyceae | | 0 | 0 | 0 | | 0 | 0.041 | 0 | 4211 | 0.00E+00 |
| Dinobryon | Ochrophyta | Chrysophyceae | | 0 | 0 | 0 | | 0 | 0.041 | 0 | 94 | 0.00E+00 |
| Mallomonas | Ochrophyta | Synurophyceae | | 0 | 0 | 0 | | 0 | 0.041 | 0 | 759 | 0.00E+00 |

**Appendix 3F. Detailed taxonomic composition of phytoplankton and biovolume calculations for Owasco Lake Phytoplankton, 27 August 2018**

| | | | | | | Cyanob. | Chlorop. | Bacill. | Chyrsop. | Cryptop. | Euglenop. | Dino/Pyrrop. |
|---|---|---|---|---|---|---|---|---|---|---|---|---|
| | | | | density | (#/mL) | 5213 | 974 | 633 | 1705 | 49 | 0 | 244 |
| Sample 6 | 27-Sep-18 | much less dense sample visually | | biovolume | um^3/mL | 3.51E+04 | 2.79E+04 | 5.49E+05 | 1.60E+05 | 1.74E+04 | 0.00E+00 | 1.03E+06 |
| Site: UFI Owasco Site 2 | | Depth on bottle | none (but should be 0.5m) | | | | | | | | | |
| UFI ID: OW SITE 2 | site 2 | units are # of cells unless listed as filament | | | | | | | | | | |
| | | | | | | | | | Volume Cou | Cell Density | Cell biovol | Total biovolume |
| Genus or Lowest Taxonomic Unit | Phylum/Larger taxonomic group | Class | Additional Information | Field 1 | Field 2 | Field 3 | | # Cells | mL sample | #/mL | um^3 | um^3/mL |
| Asterionella (cells total) | Bacillariophyta | Bacillariophyceae | | 0 | 0 | 0 | | 0 | 0.041 | 0 | 134 | 0.00E+00 |
| Asterionella (colonies) | Bacillariophyta | Bacillariophyceae | | 0 | 0 | 0 | | 0 | 0.041 | 0 | 806 | 0.00E+00 |
| Aulacoseira | Bacillariophyta | Coscinodiscophyceae | | 0 | 0 | 0 | | 0 | 0.041 | 0 | 610 | 0.00E+00 |
| Cyclotella | Bacillariophyta | Mediophyceae | | 0 | 0 | 0 | | 0 | 0.041 | 0 | 393 | 0.00E+00 |
| Cocconeis | Bacillariophyta | Bacillariophyceae | | 0 | 0 | 0 | | 0 | 0.041 | 0 | 110 | 0.00E+00 |
| Cymbella | Bacillariophyta | Bacillariophyceae | | 0 | 0 | 1 | | 1 | 0.041 | 49 | 59 | 2.87E+03 |
| Diatoma | Bacillariophyta | Bacillariophyceae | | 0 | 0 | 0 | | 0 | 0.041 | 0 | 65 | 0.00E+00 |
| Fragilaria (cells) | Bacillariophyta | Bacillariophyceae | | 0 | 0 | 0 | | 0 | 0.041 | 0 | 155 | 0.00E+00 |
| Fragilaria (filaments) | Bacillariophyta | Bacillariophyceae | | 0 | 0 | 0 | | 0 | 0.041 | 0 | 1438 | 0.00E+00 |
| Gyrosigma | Bacillariophyta | Bacillariophyceae | | 0 | 0 | 0 | | 0 | 0.041 | 0 | 2676 | 0.00E+00 |
| Navicula | Bacillariophyta | Bacillariophyceae | | 0 | 0 | 0 | | 0 | 0.041 | 0 | 1104 | 0.00E+00 |
| Nitzschia | Bacillariophyta | Bacillariophyceae | | 0 | 0 | 0 | | 0 | 0.041 | 0 | 625 | 0.00E+00 |
| Surirella | Bacillariophyta | Bacillariophyceae | | 0 | 0 | 0 | | 0 | 0.041 | 0 | 227 | 0.00E+00 |
| Synedra | Bacillariophyta | Bacillariophyceae | | 4 | 2 | 6 | | 12 | 0.041 | 585 | 934 | 5.46E+05 |
| Tabellaria | Bacillariophyta | Bacillariophyceae | | 0 | 0 | 0 | | 0 | 0.041 | 0 | 1894 | 0.00E+00 |
| Urosolenia | Bacillariophyta | Bacillariophyceae | | 0 | 0 | 0 | | 0 | 0.041 | 0 | 4502 | 0.00E+00 |
| Cosmarium | Charophyta | Zygnematophyceae | | 0 | 0 | 0 | | 0 | 0.041 | 0 | 681 | 0.00E+00 |
| eukaryotic oval cell non-flagellate* | Chlorophyta | * | Most are likely in Chlorophy | 9 | 3 | 0 | | 12 | 0.041 | 585 | 25 | 1.43E+04 |
| eukaryotic round cell non-flagellate | Chlorophyta | * | Most are likely in Chlorophy | 0 | 0 | 0 | | 0 | 0.041 | 0 | 22 | 0.00E+00 |
| eukaryotic round flagellate | Chlorophyta | * | Most are likely in Chlorophy | 0 | 0 | 0 | | 0 | 0.041 | 0 | 89 | 0.00E+00 |
| Pediastrum | Chlorophyta | Chlorophyceae | | 0 | 0 | 0 | | 0 | 0.041 | 0 | 350770 | 0.00E+00 |
| Scenedesmus (cells) | Chlorophyta | Chlorophyceae | | 2 | 0 | 4 | | 6 | 0.041 | 292 | 25 | 7.17E+03 |
| Scenedesmus (filaments) | Chlorophyta | Chlorophyceae | | 1 | 0 | 1 | | 2 | 0.041 | 97 | 66 | 6.40E+03 |
| Sphaerocystis | Chlorophyta | Chlorophyceae | | 0 | 0 | 0 | | 0 | 0.041 | 0 | 184 | 0.00E+00 |
| Selenastrum | Chlorophyta | Chlorophyceae | | 0 | 0 | 0 | | 0 | 0.041 | 0 | 67 | 0.00E+00 |
| Tetraspora | Chlorophyta | Chlorophyceae | colony | 0 | 0 | 0 | | 0 | 0.041 | 0 | 357 | 0.00E+00 |
| Cryptomonas-like flagellate | Cryptophyta | Cryptomonas | | 0 | 1 | 0 | | 1 | 0.041 | 49 | 356.3867 | 1.74E+04 |
| Anabaena | Cyanobacteria | Cyanophycea | | 0 | 0 | 0 | | 0 | 0.041 | 0 | 117 | 0.00E+00 |
| Anabaena (filaments) | Cyanobacteria | Cyanophycea | | 0 | 0 | 0 | | 0 | 0.041 | 0 | 117 | 0.00E+00 |
| Anabaena flosaquae morph (oval cells | Cyanobacteria | Cyanophycea | | 0 | 0 | 0 | | 0 | 0.041 | 0 | 117 | 0.00E+00 |
| Aphanizomenon | Cyanobacteria | Cyanophycea | filaments | 0 | 0 | 0 | | 0 | 0.041 | 0 | 196 | 0.00E+00 |
| Calothrix | Cyanobacteria | Cyanophycea | | 0 | 0 | 0 | | 0 | 0.041 | 0 | 85 | 0.00E+00 |
| Chroococcus | Cyanobacteria | Cyanophycea | | 0 | 0 | 1 | | 1 | 0.041 | 49 | 170 | 8.26E+03 |
| Coelosphaerium | Cyanobacteria | Cyanophycea | | 0 | 0 | 0 | | 0 | 0.041 | 0 | 7 | 0.00E+00 |
| Gleocapsa | Cyanobacteria | Cyanophycea | | 0 | 0 | 0 | | 0 | 0.041 | 0 | 7 | 0.00E+00 |
| Merismopedia | Cyanobacteria | Cyanophycea | cells | 0 | 0 | 0 | | 0 | 0.041 | 0 | 6 | 0.00E+00 |
| Microcystis | Cyanobacteria | Microcystaceae | cells | 32 | 28 | 15 | | 75 | 0.041 | 3654 | 3 | 1.24E+04 |
| Oscillatoria | Cyanobacteria | Cyanophycea | filaments | 1 | 0 | 2 | | 3 | 0.041 | 146 | 43 | 6.28E+03 |
| Synechococcus | Cyanobacteria | Cyanophycea | | 10 | 7 | 11 | | 28 | 0.041 | 1364 | 6 | 8.11E+03 |
| Synecocystis | Cyanobacteria | Cyanophycea | | 0 | 0 | 0 | | 0 | 0.041 | 0 | 32 | 0.00E+00 |
| Euglenoid | Euglenozoa | Euglenophyceae | | 0 | 0 | 0 | | 0 | 0.041 | 0 | 1728 | 0.00E+00 |
| Peridinium | Miozoa | Dinophyceae | | 2 | 3 | 0 | | 5 | 0.041 | 244 | 4211 | 1.03E+06 |
| Dinobryon | Ochrophyta | Chrysophyceae | | 20 | 2 | 13 | | 35 | 0.041 | 1705.057548 | 94 | 1.60E+05 |
| Mallomonas | Ochrophyta | Synurophyceae | | 0 | 0 | 0 | | 0 | 0.041 | 0 | 759 | 0.00E+00 |

# Appendix D: Model Drivers

## Appendix D-1 Meteorology

The meteorological drivers have a tremendously important impact on the hydrothermal/transport water quality sub-models. Therefore considerable effort was expended in selecting the best source of these data. The ideal data source would located on or near the lake, provide year-round, hourly (or more frequent) measurements, provide historical data (1999 or early), and be freely available. Two autonomous buoys located near site 10 measured meteorological from 2005-2008 and 2014-present. The early buoy was maintained by UFI and latter was maintained the Finger Lake Institute (FLI). These buoys although ideally located, have several important limitations: (1) large data gap between 2008 and 2014, (2) only available from April-October with occasional seasonal data gaps, and (3) unavailable before 2005. These limitations clearly limit using these data directly as model inputs, however these data can be used to evaluate and possibly improve (i.e., adjust) onshore metrological data. We evaluated other sites (Figure 5-3), we selected the National Weather Service station located at the Syracuse Airport (KSYR) as the primary source of meteorological data. Paired measurements between KSYR, UFI and FLI data are shown in Figures D-1—Figures D-11. We found that Tair, Tdp, and incident light were adequately correlated between the lake buoys and KSYR (Table D-1), while there were considerable differences between wind velocities (Figure 5-4). With exception of wind velocity, these data were merged and used without modification.

The KSYR wind velocity was transformed as described in Section 5.3.1 using the coefficients (A, B, C, D) from Eq. 5-1 and 5-2 shown in the Table D-2.

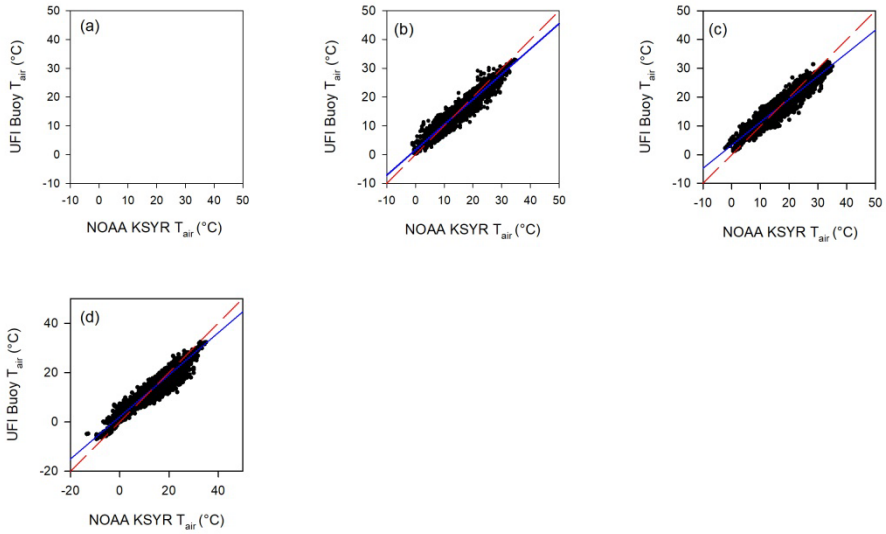


**Figure D-1**. Air temperature (°C) hourly regressions for Owasco Lake UFI buoy met station versus NOAA Hancock Airport (KSYR) for (a) 2005, (b) 2006, (c) 2007, (d) 2008. The regressions are shown as a solid blue line. The dashed red line is a 1:1 relationship for reference. *Note that no temperature was available from the UFI buoy in 2005.

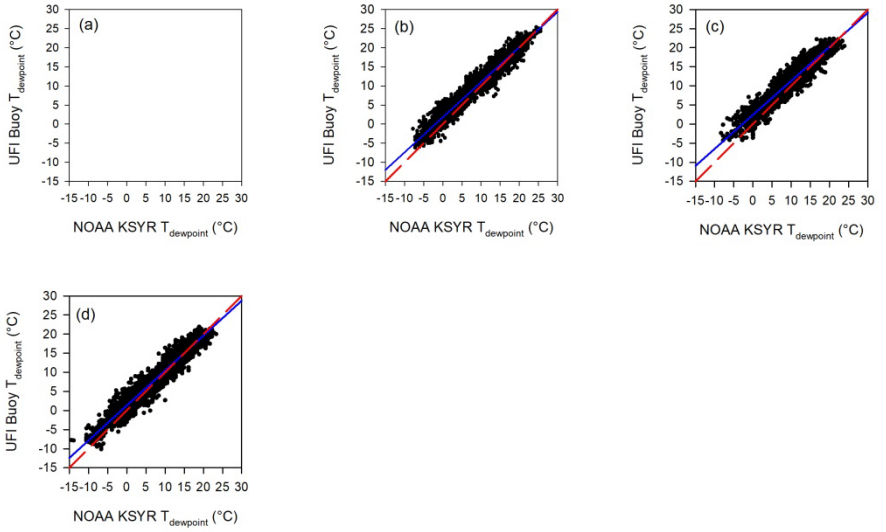


**Figure D-2**. Dew point temperature (°C) hourly regressions for Owasco Lake UFI buoy met station versus NOAA Hancock Airport (KSYR) for (a) 2005, (b) 2006, (c) 2007, (d) 2008. The regressions are shown as a solid blue line The dashed red line is a 1:1 relationship for reference. *Note that due to lack of temperature data for 2005 no dew point could be calculated for the UFI buoy.

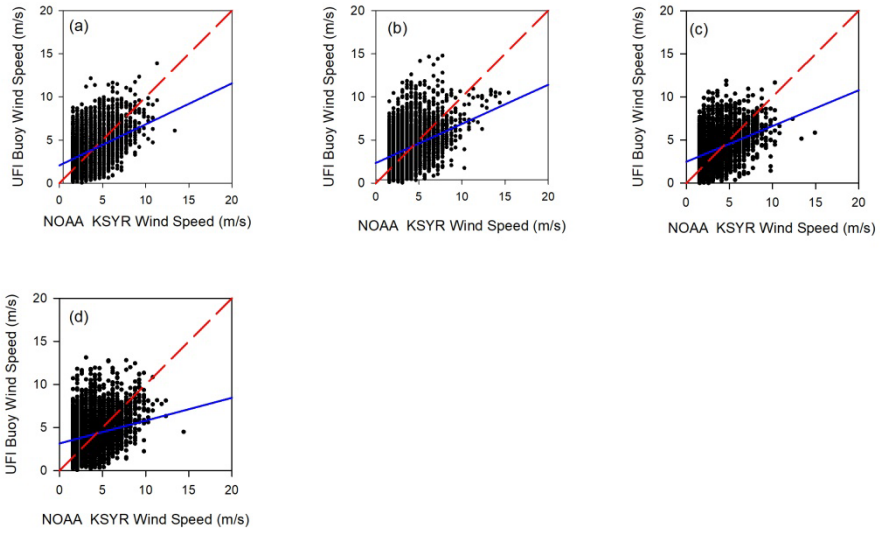


**Figure D-3**. Wind speed (m/s) hourly regressions for Owasco Lake UFI buoy met station versus NOAA Hancock Airport (KSYR) for (a) 2005, (b) 2006, (c) 2007, (d) 2008. The regressions are shown as a solid blue line. The dashed red line is a 1:1 relationship for reference.

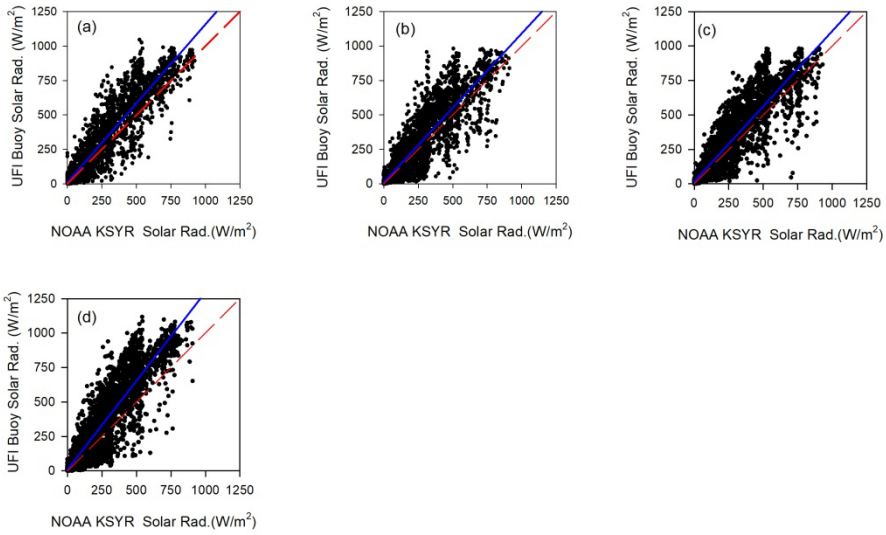


**Figure D-4**. Solar radiation ($W/m^2$) hourly regressions for Owasco Lake UFI buoy met station versus NOAA Hancock Airport (KSYR) for (a) 2005, (b) 2006, (c) 2007, (d) 2008. The regressions are shown as a solid blue line. The dashed red line is a 1:1 relationship for reference.

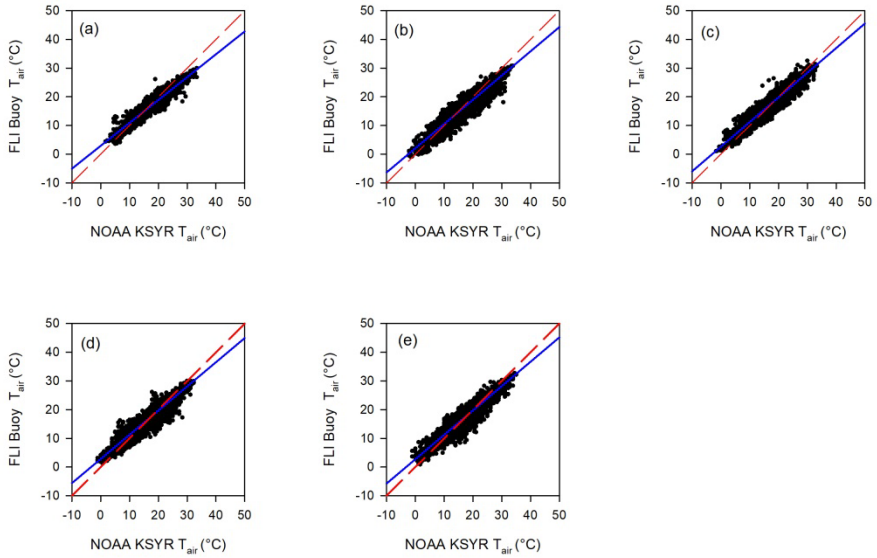


**Figure D-5**. Air temperature (°C) hourly regressions for Owasco Lake FLI buoy met station versus NOAA Hancock Airport (KSYR) for (a) 2014, (b) 2015, (c) 2016, (d) 2017, (e) 2018. The regressions are shown as a solid blue line. The dashed red line is a 1:1 relationship for reference.

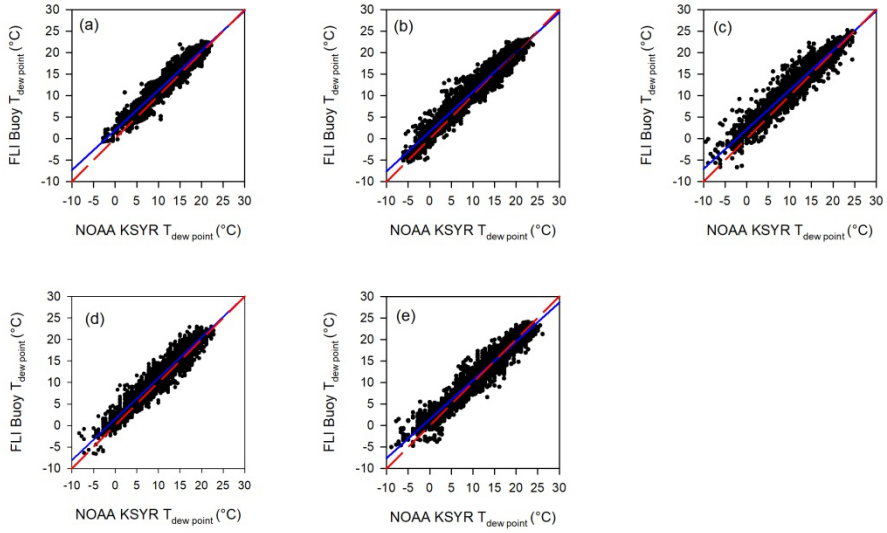


**Figure D-6**. Dew point temperature (°C) hourly regressions for Owasco Lake FLI buoy met station versus NOAA Hancock Airport (KSYR) for (a) 2014, (b) 2015, (c) 2016, (d) 2017, (e) 2018. The regressions are shown as a solid blue line. The dashed red line is a 1:1 relationship for reference.

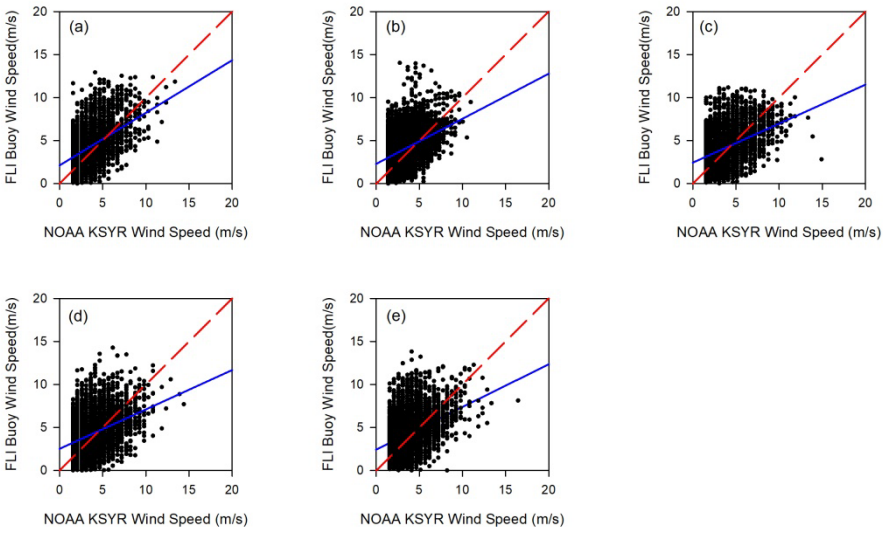


**Figure D-7**. Wind speed (m/s) hourly regressions for Owasco Lake FLI buoy met station versus NOAA Hancock Airport (KSYR) for (a) 2014, (b) 2015, (c) 2016, (d) 2017, (e) 2018. The regressions are shown as a solid blue line. The dashed red line is a 1:1 relationship for reference.

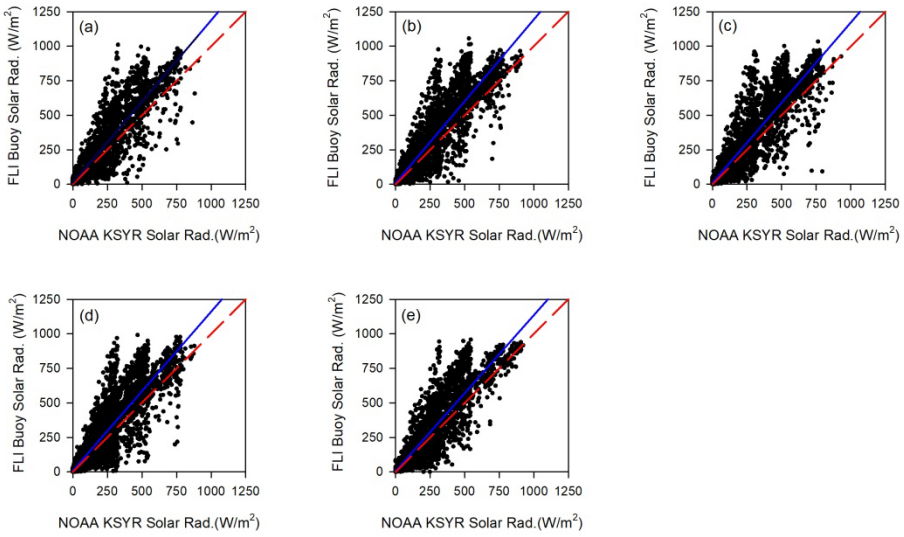


**Figure D-8**. Solar radiation ($W/m^2$) hourly regressions for Owasco Lake FLI buoy met station versus NOAA Hancock Airport (KSYR) for (a) 2014, (b) 2015, (c) 2016, (d) 2017, (e) 2018. The regressions are shown as a solid blue line. The dashed red line is a 1:1 relationship for reference.

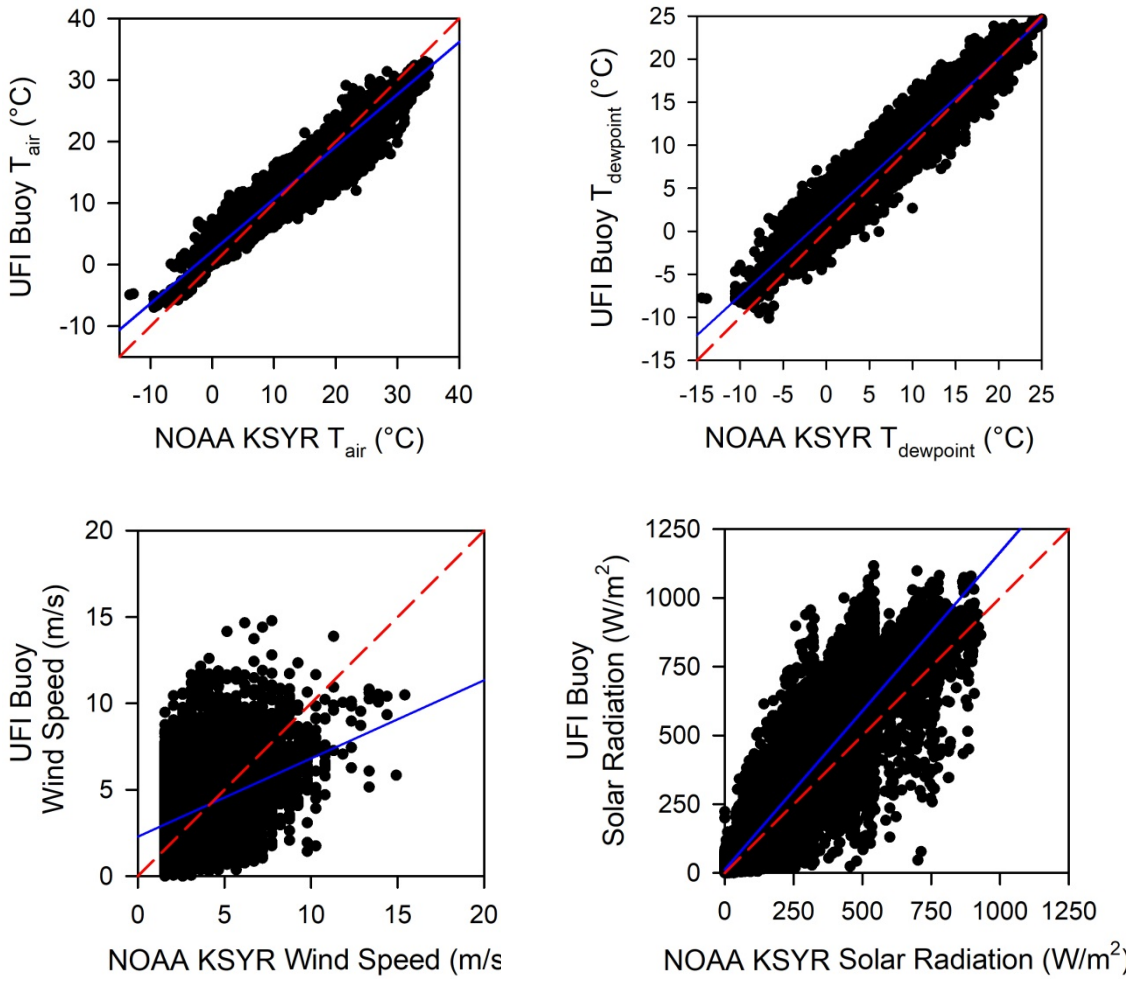


**Figure D-9**. Lumped hourly regressions (2005-2008) for Owasco Lake UFI buoy met station versus NOAA Hancock Airport (KSYR). The regressions are shown as a solid blue line. The dashed red line is a 1:1 relationship for reference. The windspeed regression excludes 2008 data which was determined to be an outlier.

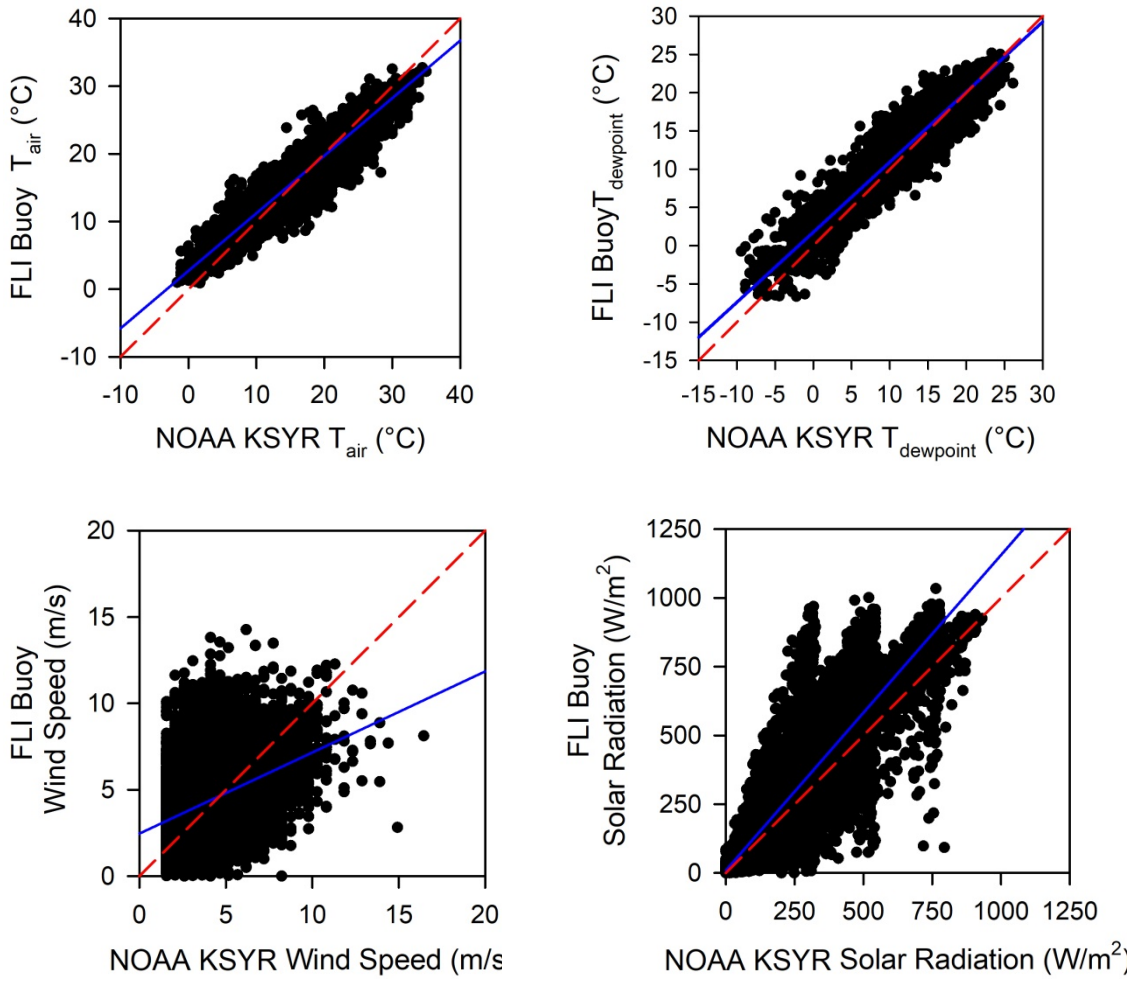


**Figure D-10.** Lumped hourly regressions (2016-2018) for Owasco Lake FLI buoy met station versus NOAA Hancock Airport (KSYR). The regressions are shown as a solid blue line. The dashed red line is a 1:1 relationship for reference. FLI buoy data from 2014-2015 is excluded (not collected under an approved QAPP).

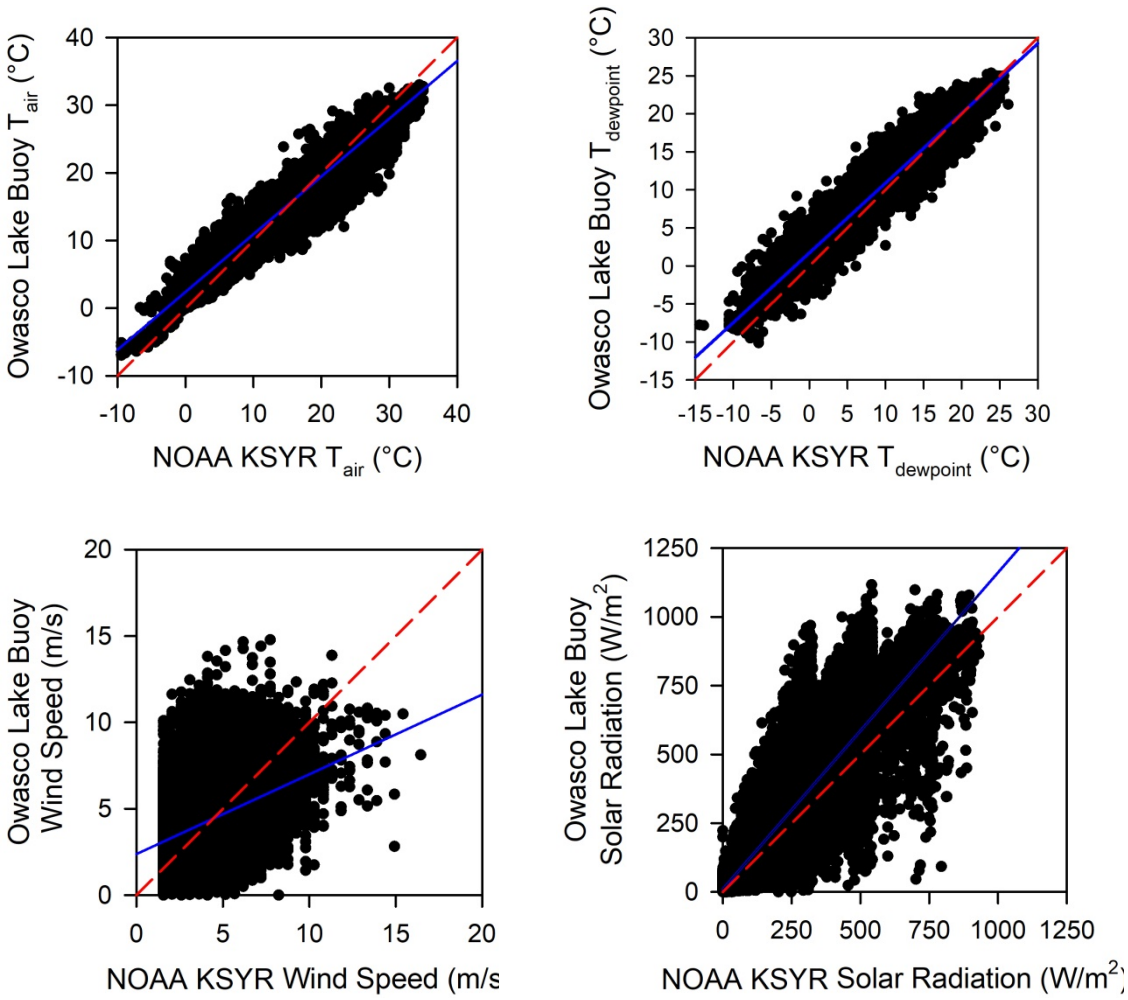


**Figure D-11**. Lumped hourly regressions of all available data (2005-2008 + 2016-2018) for Owasco Lake buoy met stations versus NOAA Hancock Airport (KSYR). The regressions are shown as a solid blue line. The dashed red line is a 1:1 relationship for reference. FLI buoy data from 2014-2015 is excluded (not collected under an approved QAPP), and UFI buoy wind speed data from 2008 is excluded (determined to be an outlier).

**Table D-1**. Regressions statistics for Owasco Lake UFI and FLI buoy MET Hourly Average Data verses KSYR.

| Year | $T_{air}$ (°C) | | | $T_{dew}$ (°C) | | | Solar Radiation (Watts/$m^2$) | | | Wind Speed (m/s) | | |
|---|---|---|---|---|---|---|---|---|---|---|---|---|
| | slope | int. | r2 | slope | int. | r2 | slope | int. | r2 | slope | int. | r2 |
| **UFI Buoy** | | | | | | | | | | | | |
| 2005 | N/A | N/A | N/A | N/A | N/A | N/A | 1.15 | 10.86 | 0.88 | 0.49 | 2.00 | 0.17 |
| 2006 | 0.88 | 1.65 | 0.93 | 0.92 | 1.77 | 0.95 | 1.08 | 10.22 | 0.83 | 0.45 | 2.35 | 0.16 |
| 2007 | 0.80 | 3.30 | 0.92 | 0.89 | 2.42 | 0.92 | 1.09 | 16.75 | 0.85 | 0.42 | 2.49 | 0.13 |
| 2008 | 0.85 | 2.04 | 0.94 | 0.91 | 1.32 | 0.95 | 1.29 | 9.52 | 0.87 | 0.27 | 3.13 | 0.08 |
| **FLI Buoy** | | | | | | | | | | | | |
| 2014 | 0.80 | 2.96 | 0.93 | 0.93 | 1.97 | 0.93 | 1.18 | 8.75 | 0.84 | 0.61 | 2.13 | 0.22 |
| 2015 | 0.85 | 2.10 | 0.91 | 0.92 | 1.65 | 0.94 | 1.18 | 9.78 | 0.85 | 0.52 | 2.30 | 0.16 |
| 2016 | 0.86 | 2.62 | 0.93 | 0.92 | 2.14 | 0.93 | 1.16 | 11.61 | 0.86 | 0.45 | 2.45 | 0.15 |
| 2017 | 0.84 | 2.83 | 0.90 | 0.95 | 1.48 | 0.93 | 1.15 | 9.99 | 0.83 | 0.46 | 2.52 | 0.14 |
| 2018 | 0.85 | 2.76 | 0.92 | 0.90 | 1.45 | 0.94 | 1.13 | 6.43 | 0.87 | 0.50 | 2.43 | 0.16 |
| Overall lumped regression UFI[2] | 0.85 | 2.18 | 0.93 | 0.92 | 1.70 | 0.94 | 1.15 | 12.17 | 0.85 | 0.45 | 2.29 | 0.15 |
| Overall lumped regression FLI[1] | 0.85 | 2.74 | 0.92 | 0.92 | 1.77 | 0.93 | 1.15 | 9.25 | 0.85 | 0.47 | 2.47 | 0.15 |
| ALL DATA[1,2] | 0.85 | 2.41 | 0.93 | 0.92 | 1.73 | 0.94 | 1.15 | 10.79 | 0.85 | 0.46 | 2.39 | 0.15 |

**Table D-2**. KSYR wind velocity transformation coefficients.

| Θ≥ | Θ< | A | B | C | D |
|---|---|---|---|---|---|
| 0 | 45 | 0.485 | -0.205 | -1.31 | 0.765 |
| 45 | 90 | 0.895 | -1.2 | -0.75 | -0.325 |
| 90 | 135 | 0.33 | -0.155 | -1.145 | 1.035 |
| 135 | 180 | 0.825 | 0.05 | -0.285 | 1.38 |
| 180 | 225 | 0.505 | -0.095 | -0.3 | 1.275 |
| 225 | 270 | 0.62 | -0.165 | -0.215 | 1.245 |
| 270 | 315 | 1.01 | 0.99 | -0.135 | 1.22 |
| 315 | 360 | 0.55 | -0.025 | -0.195 | 0.82 |

# Appendix E: Hydrothermal Model

# Appendix E-1 Hydrothermal Model Equations

### 1.1.1 Horizontal momentum

(**Eq. 4-1**). $$\frac{\partial UB}{\partial t}+\frac{\partial UUB}{\partial x}+\frac{\partial WUB}{\partial z}=-\frac{1}{\rho}\frac{\partial BP}{\partial x}+\frac{\partial\left[BA_x\frac{\partial U}{\partial x}\right]}{\partial x}+\frac{\partial B\tau_x}{\partial z}$$

where

U = longitudinal, laterally averaged velocity, m/sec
B = waterbody width, m
t = time, sec
x = longitudinal Cartesian coordinate: x is along the lake centerline at the water surface, positive to the right
z = vertical Cartesian coordinate: z is positive downward
W = vertical, laterally averaged velocity, m/sec
$\rho$ = density, kg/m$^3$
P = pressure, N/m$^2$
$A_x$ = longitudinal momentum dispersion coefficient, m$^2$/sec
$\tau_x$ = shear stress per unit mass resulting from the vertical gradient of the horizontal velocity, U, m$^2$/sec2

The first term represents the time rate of change of horizontal momentum, and the second and third terms are the horizontal and vertical advection of momentum. The first term on the right hand side (RHS) of Eq. 4-5 is the force imposed by the horizontal pressure gradient. The second term on the RHS is the horizontal dispersion of momentum, and the third term is the force due to shear stress.

### 1.1.2 Constituent transport

(**Eq. 4-2**). $$\frac{\partial B\phi}{\partial t}+\frac{\partial UB\phi}{\partial x}+\frac{\partial WB\phi}{\partial z}-\frac{\partial\left[BD_x\frac{\partial\phi}{\partial x}\right]}{\partial x}-\frac{\partial\left[BD_z\frac{\partial\phi}{\partial z}\right]}{\partial z}=q_\phi B+S_\phi B$$

where

$\phi$ = laterally averaged constituent concentration, g/m$^3$
$D_x$ = longitudinal temperature and constituent dispersion coefficient, m$^2$/sec
$D_z$ = vertical temperature and constituent dispersion coefficient, m$^2$/sec
$q_\phi$ = lateral inflow or outflow mass flow rate of constituent per unit volume, g/m$^3$/sec
$S_\phi$=kinetics source/sink term for constituent concentrations, g/m$^3$/sec

Each constituent has a balance as in Eq. 4-6 with specific source and sink terms. The first term in Eq. 4-6 represents the time rate of change of constituent concentrations and the second and third terms are the horizontal and vertical advection of constituents. The fourth and fifth terms are the horizontal and vertical diffusion of constituents. The first term on the RHS is the

lateral inflow/outflow of constituents, and the second term represents kinetic source/sink rates for constituents.

### 1.1.3 Free water surface elevation

(**Eq. 4-3**). $$\frac{\partial B_\eta \eta}{\partial t} = \frac{\partial}{\partial x}\int_\eta^h UBdz - \int_\eta^h qBdz$$

where

$B_\eta$ = time and spatially varying surface width, m
$\eta$ = free water surface location, m
h = total depth, m
q = lateral boundary inflow or outflow, $m^3$/sec

### 1.1.4 Hydrostatic pressure

**(Eq. 4-4)**. $$\frac{\partial P}{\partial z} = \rho g$$

where

g = acceleration due to gravity, $m/sec^2$

### 1.1.5 Continuity

(**Eq. 4-5**). $$\frac{\partial UB}{\partial x} + \frac{\partial WB}{\partial z} = qB$$

### 1.1.6 Equation of state

(**Eq. 4-6**). $$\rho = f(T_{W,}\phi_{TDS}, \phi_{SS})$$

where

$f(T_w, \phi_{TDS}, \phi_{SS})$ = density function dependent upon temperature, total dissolved solids or salinity, and suspended solids.

The six equations result in six unknowns: (1) free water surface elevation, η; (2) pressure, P; (3) horizontal velocity, U; (4) vertical velocity, W; (5) constituent concentration, ϕ; and (6) density, ρ. Lateral averaging eliminates the lateral momentum balance, lateral velocity, and Coriolis acceleration. The solution of the six equations for the six unknowns forms the basic model structure.

# Appendix E-1 Calibration, 2018

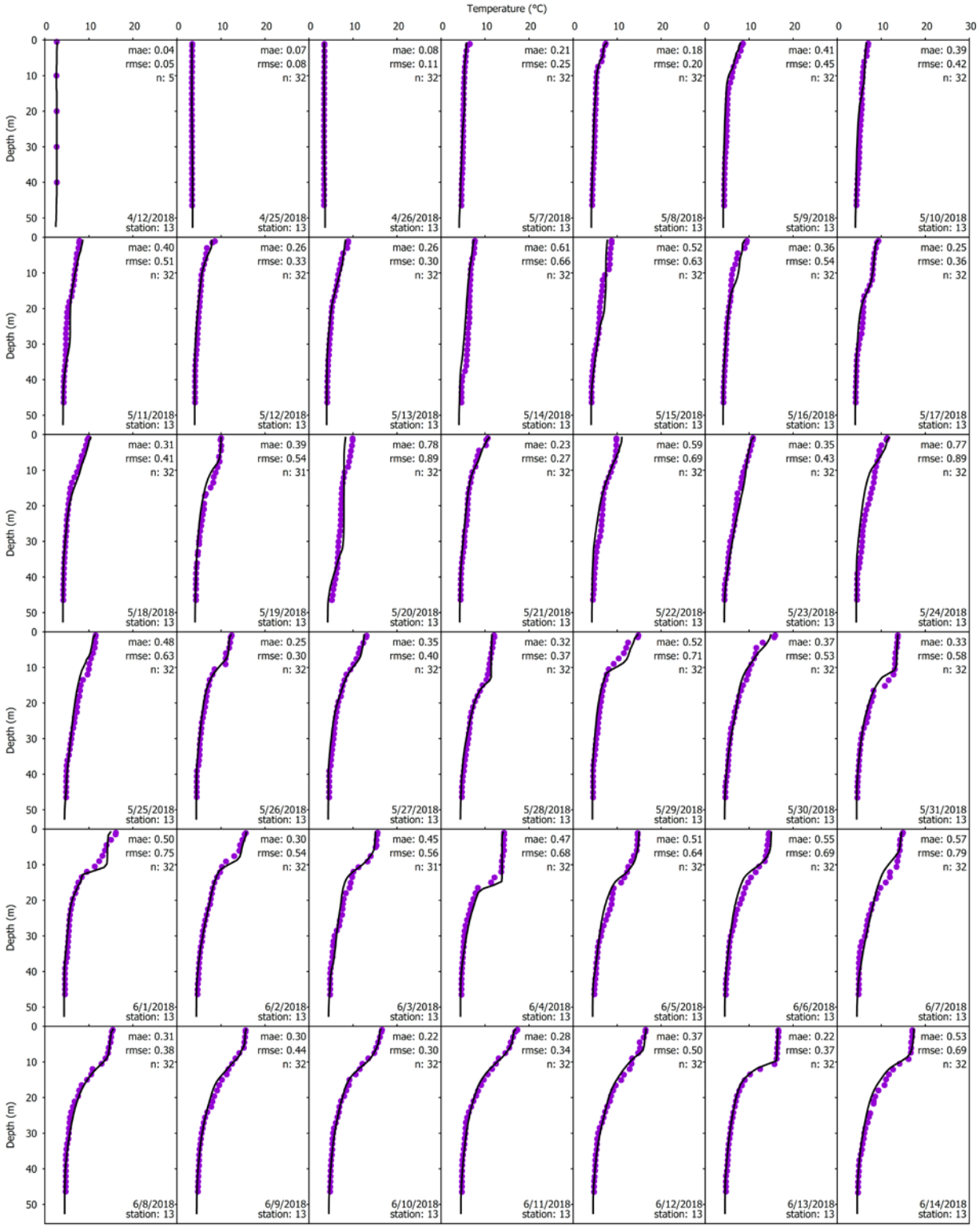


**Figure E-1**. Hydrothermal Model fit to daily buoy profiles at site 13 (Figure 5-14) on Owasco Lake for calibration year, 2018 page 1 of 5.

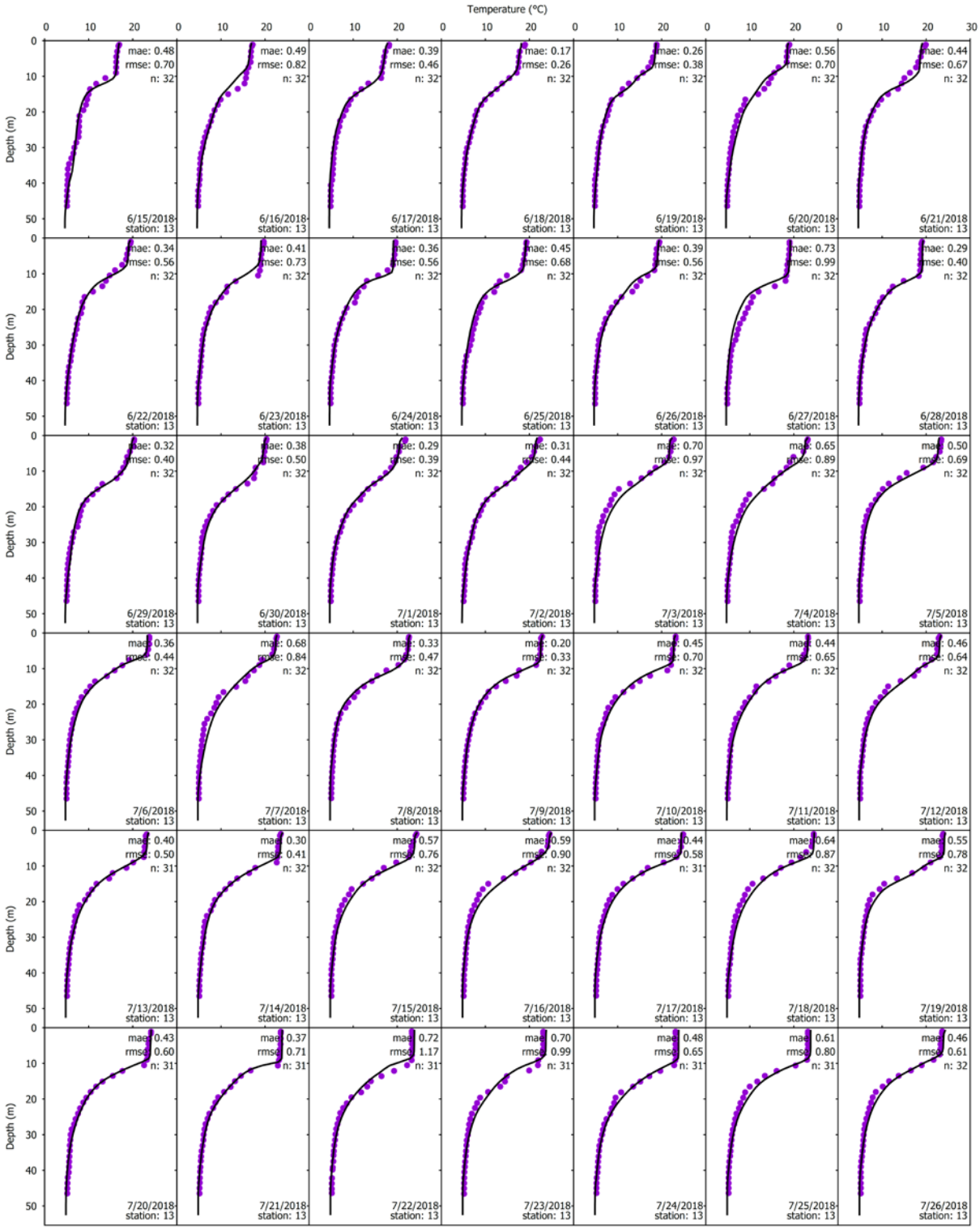


**Figure E-1**. Hydrothermal Model fit to daily buoy profiles at site 13 (Figure 5-14) on Owasco Lake for calibration year, 2018 page 2 of 5.

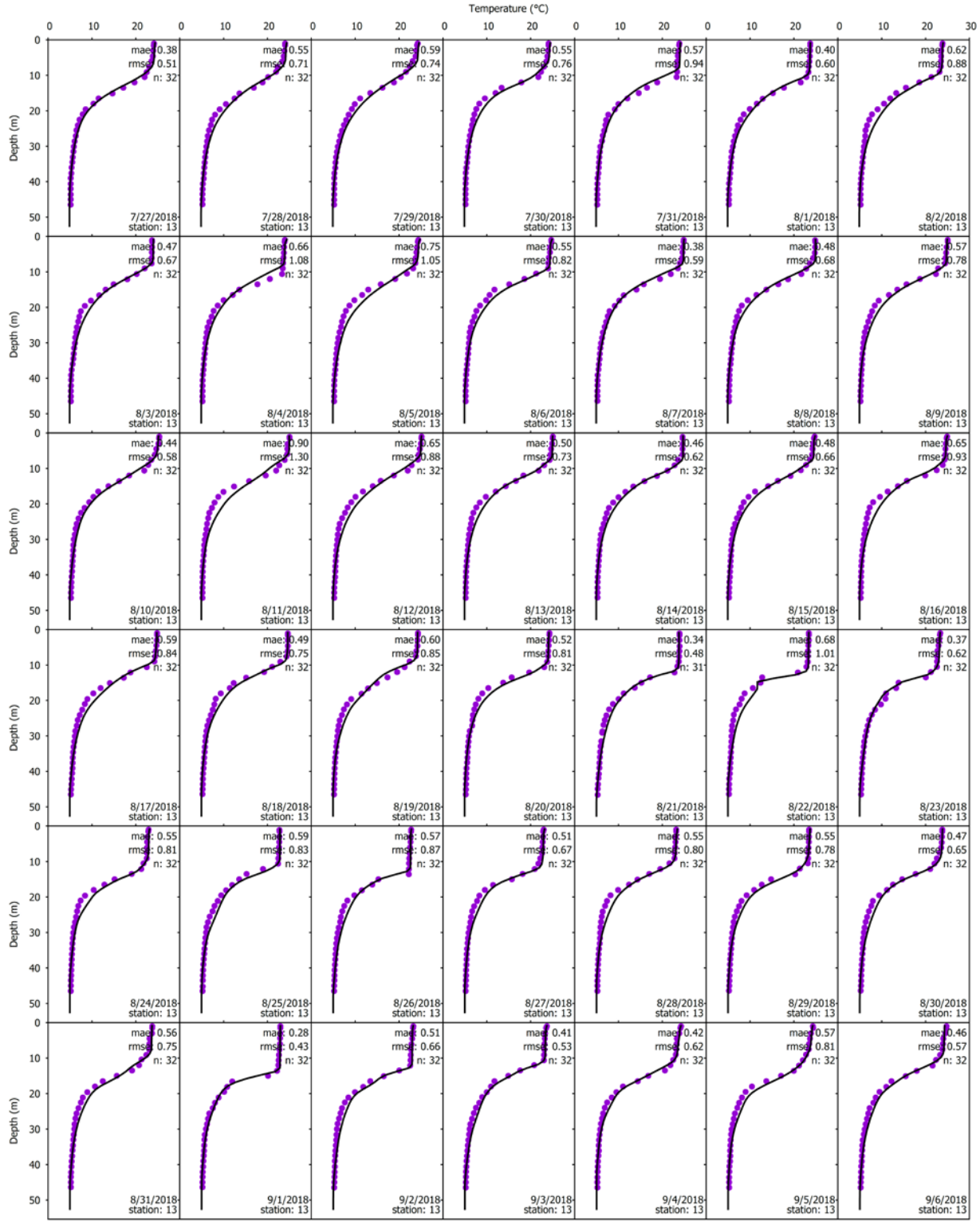


**Figure E-1**. Hydrothermal Model fit to daily buoy profiles at site 13 (Figure 5-14) on Owasco Lake for calibration year, 2018 page 3 of 5.

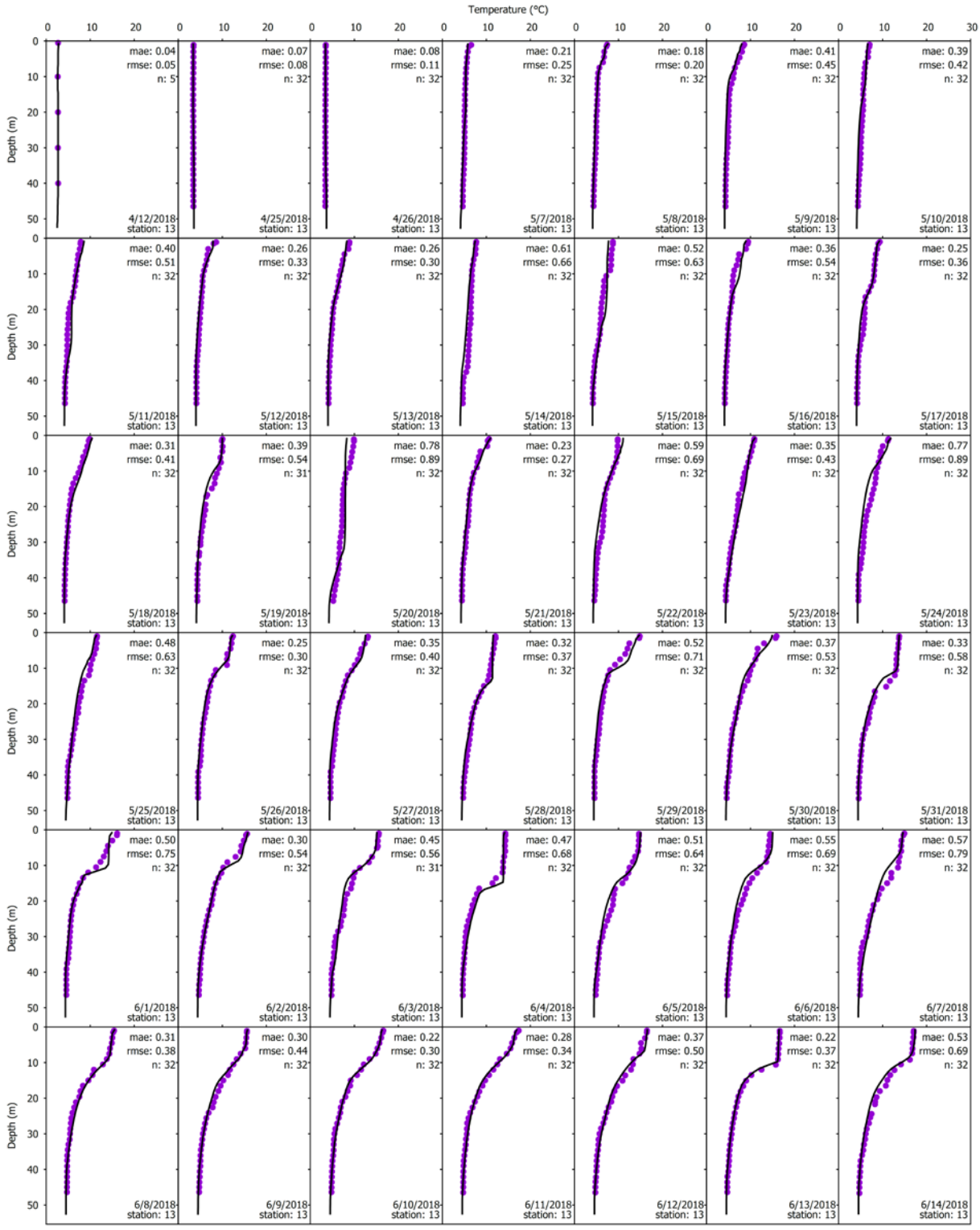


**Figure E-1**. Hydrothermal Model fit to daily buoy profiles at site 13 (Figure 5-14) on Owasco Lake for calibration year, 2018 page 4 of 5.

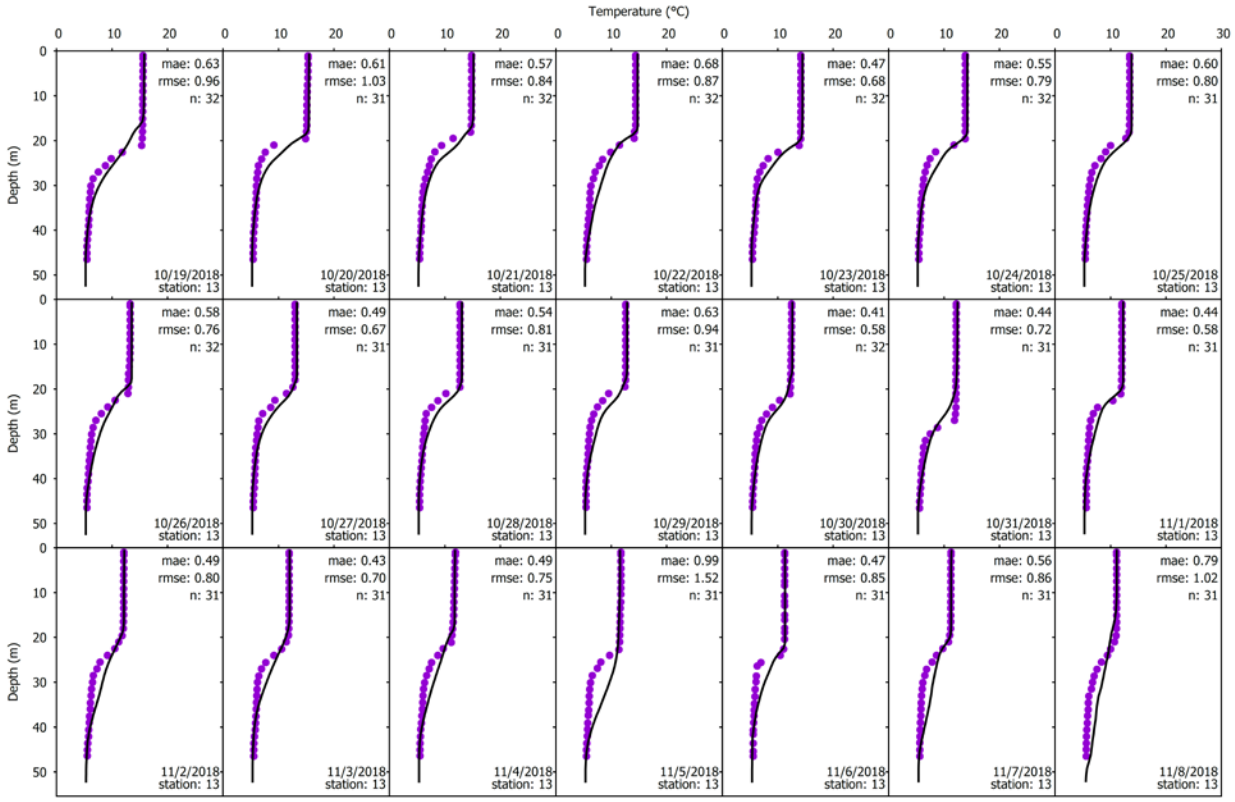


**Figure E-1**. Hydrothermal Model fit to daily buoy profiles at site 13 (Figure 5-14) on Owasco Lake for calibration year, 2018 page 5 of 5.

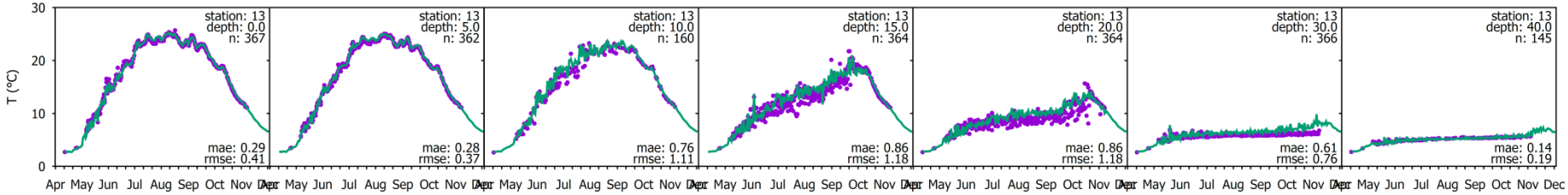


**Figure E-2**. Time series of hydrothermal model fit to daily buoy profiles at site 13 (Figure 5-14) on Owasco Lake for calibration year, 2018 at seven depths, 0, 5, 10, 15, 20, 30, and 40m.

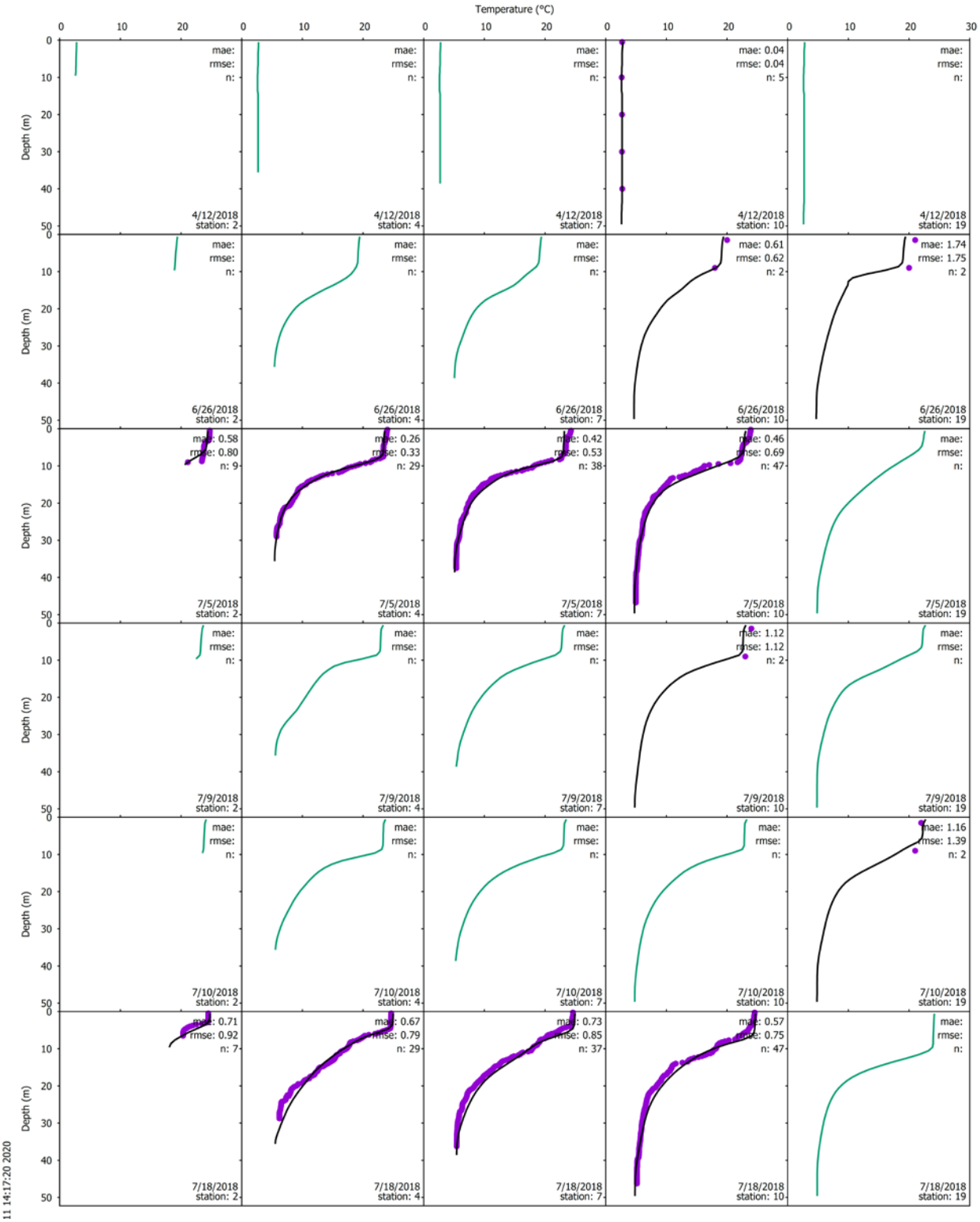


**Figure E-3**. Hydrothermal Model fit to daily UFI SeaBird profiles and CSLAP temperature measurements at multiple sites (Figure 5-14) down the longitudinal axis of Owasco Lake for calibration year, 2018 page 1 of 4

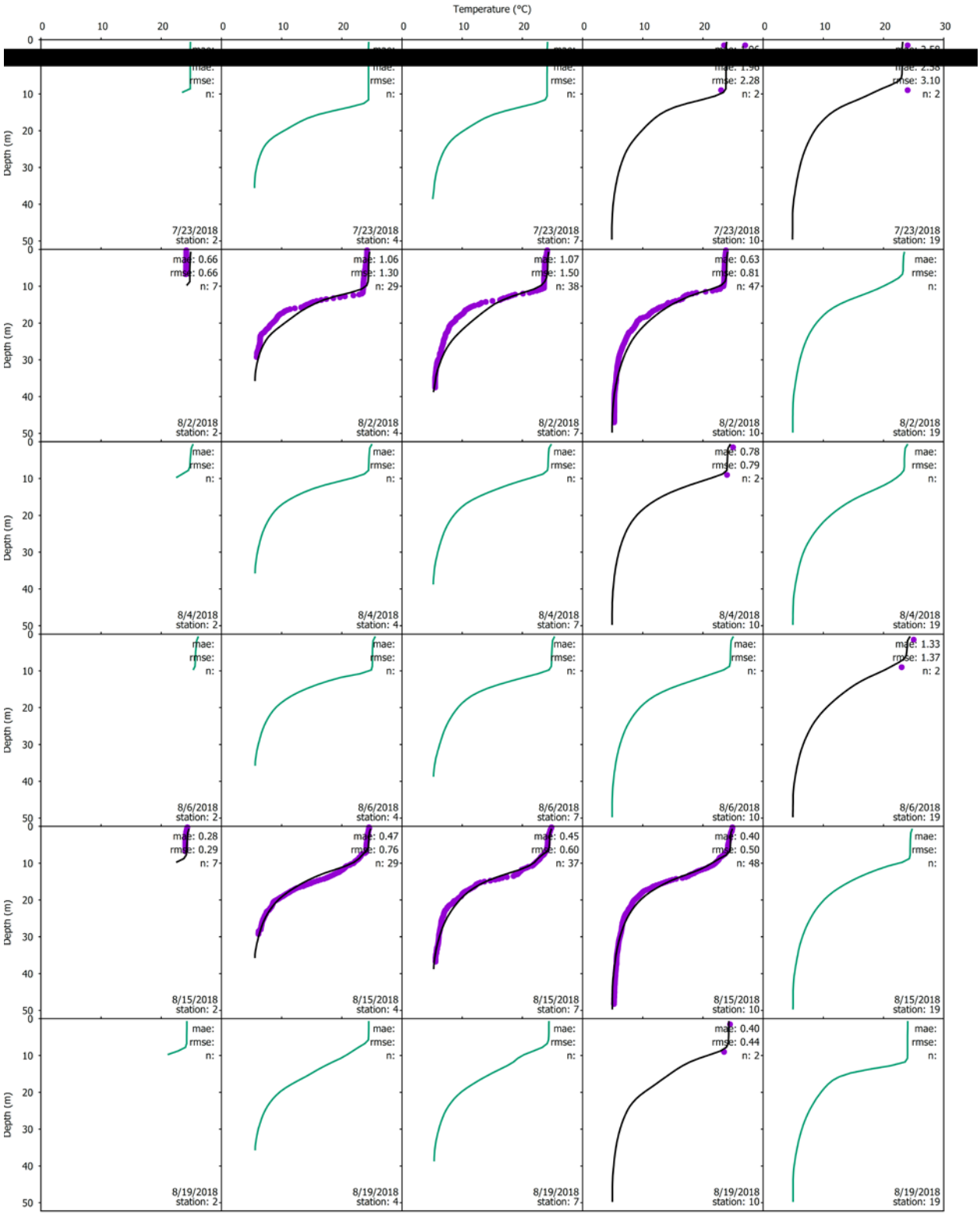


**Figure E-3**. Hydrothermal Model fit to daily UFI SeaBird profiles and CSLAP temperature measurements at multiple sites (Figure 5-14) down the longitudinal axis of Owasco Lake for calibration year, 2018 page 2 of 4

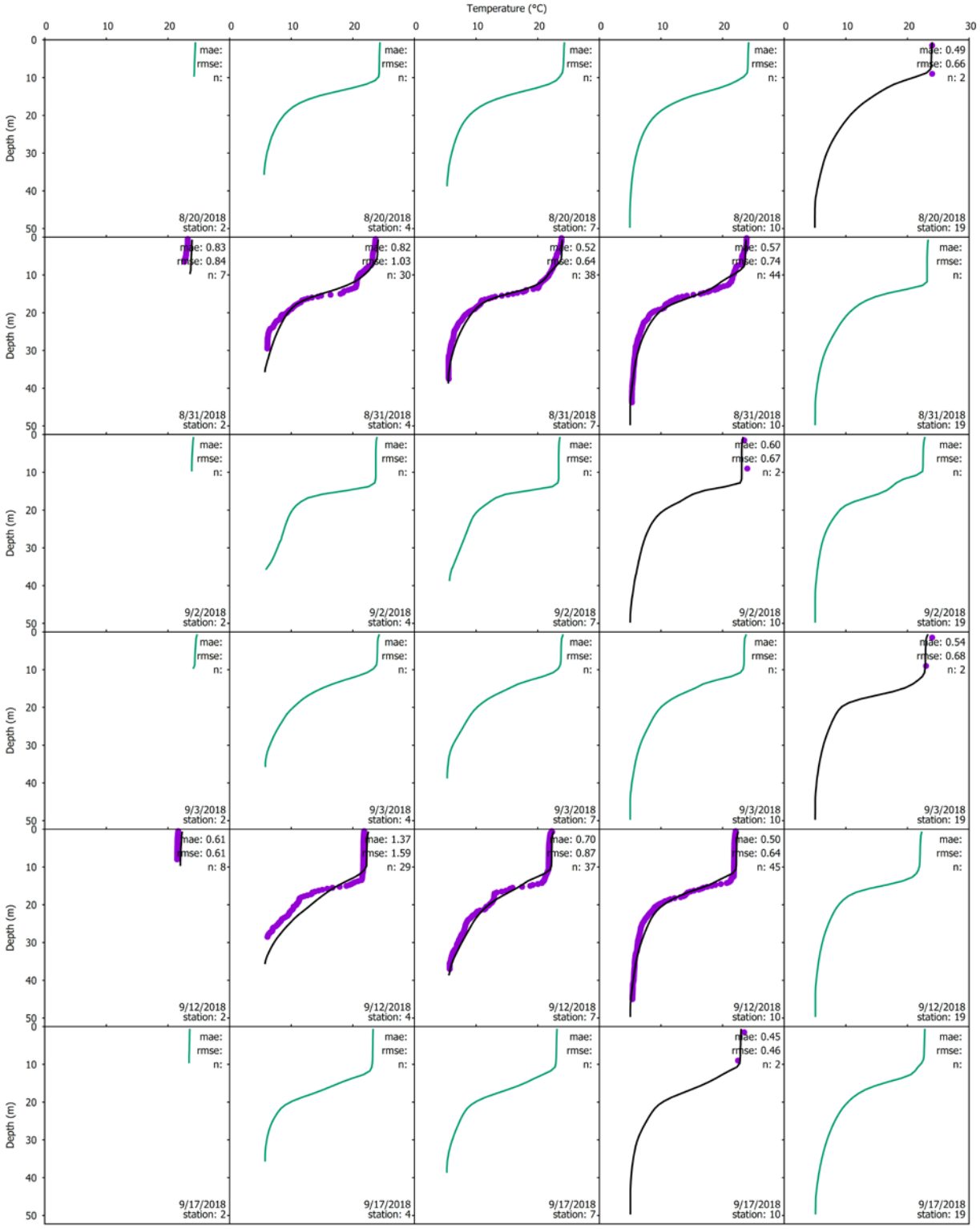


**Figure E-3**. Hydrothermal Model fit to daily UFI SeaBird profiles and CSLAP temperature measurements at multiple sites (Figure 5-14) down the longitudinal axis of Owasco Lake for calibration year, 2018 page 3 of 4

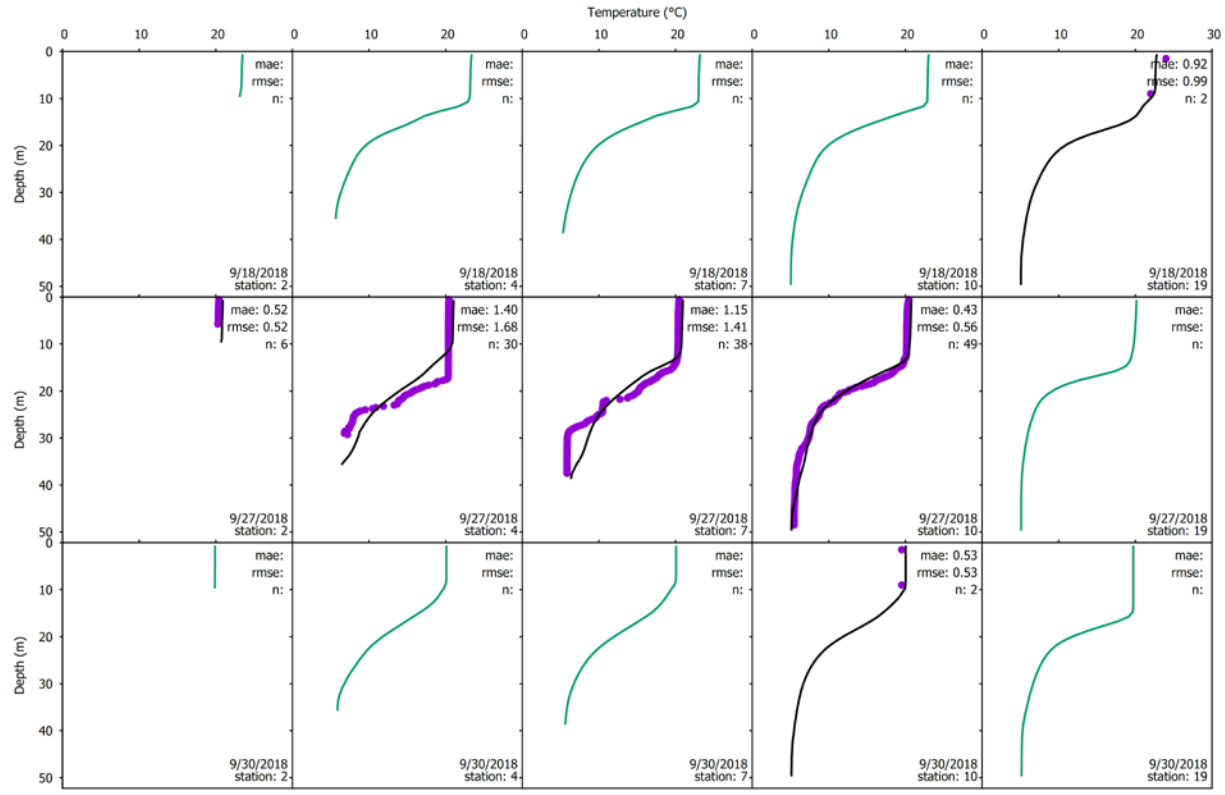


**Figure E-3**. Hydrothermal Model fit to daily UFI SeaBird profiles and CSLAP temperature measurements at multiple sites (Figure 5-14) down the longitudinal axis of Owasco Lake for calibration year, 2018 page 4 of 4

# Appendix E-2 Confirmation, 2017

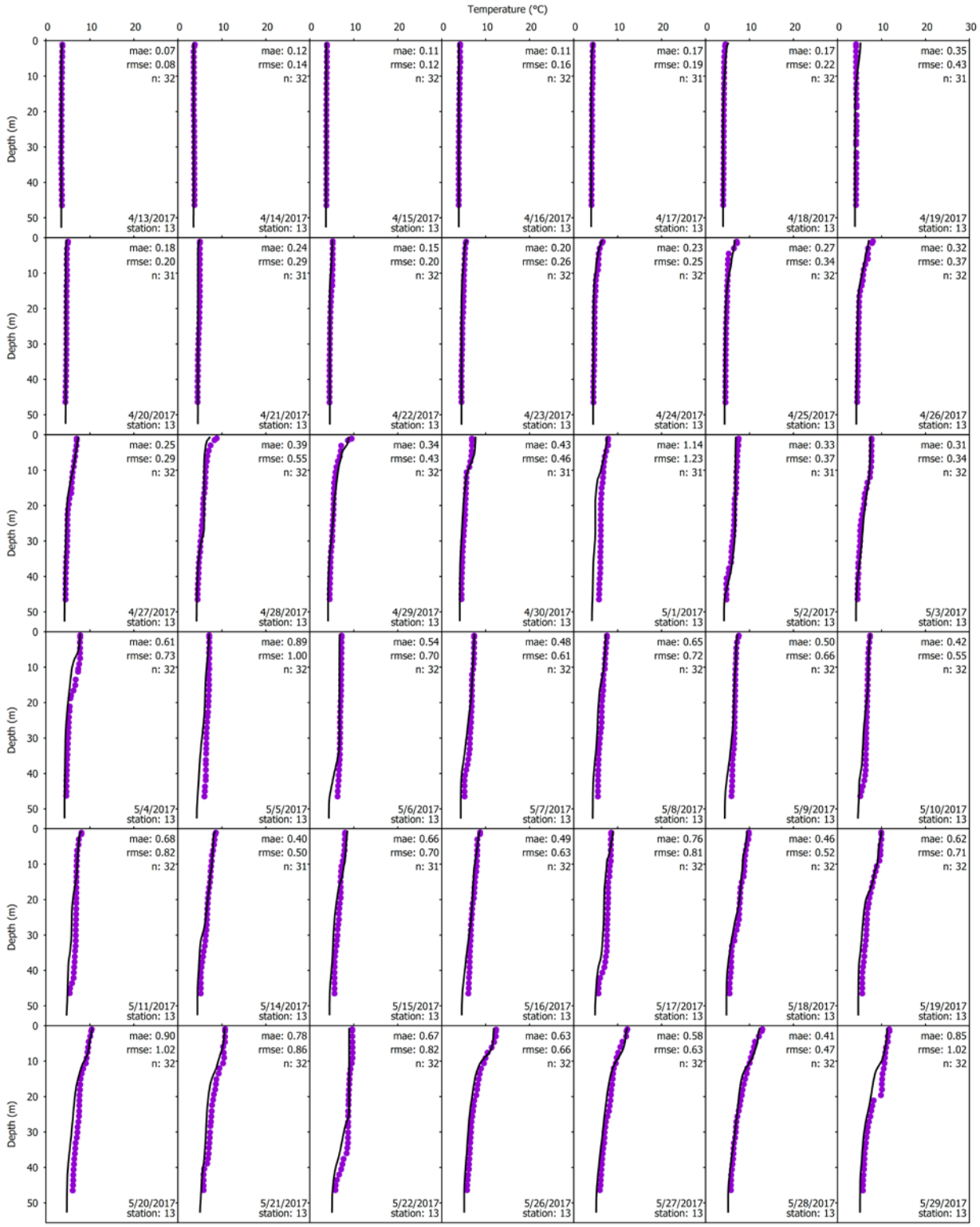


**Figure E-4**. Hydrothermal model fit to daily buoy profiles at site 13 (Figure 5-14) on Owasco Lake for primary confirmation year, 2017 page 1 of 5.

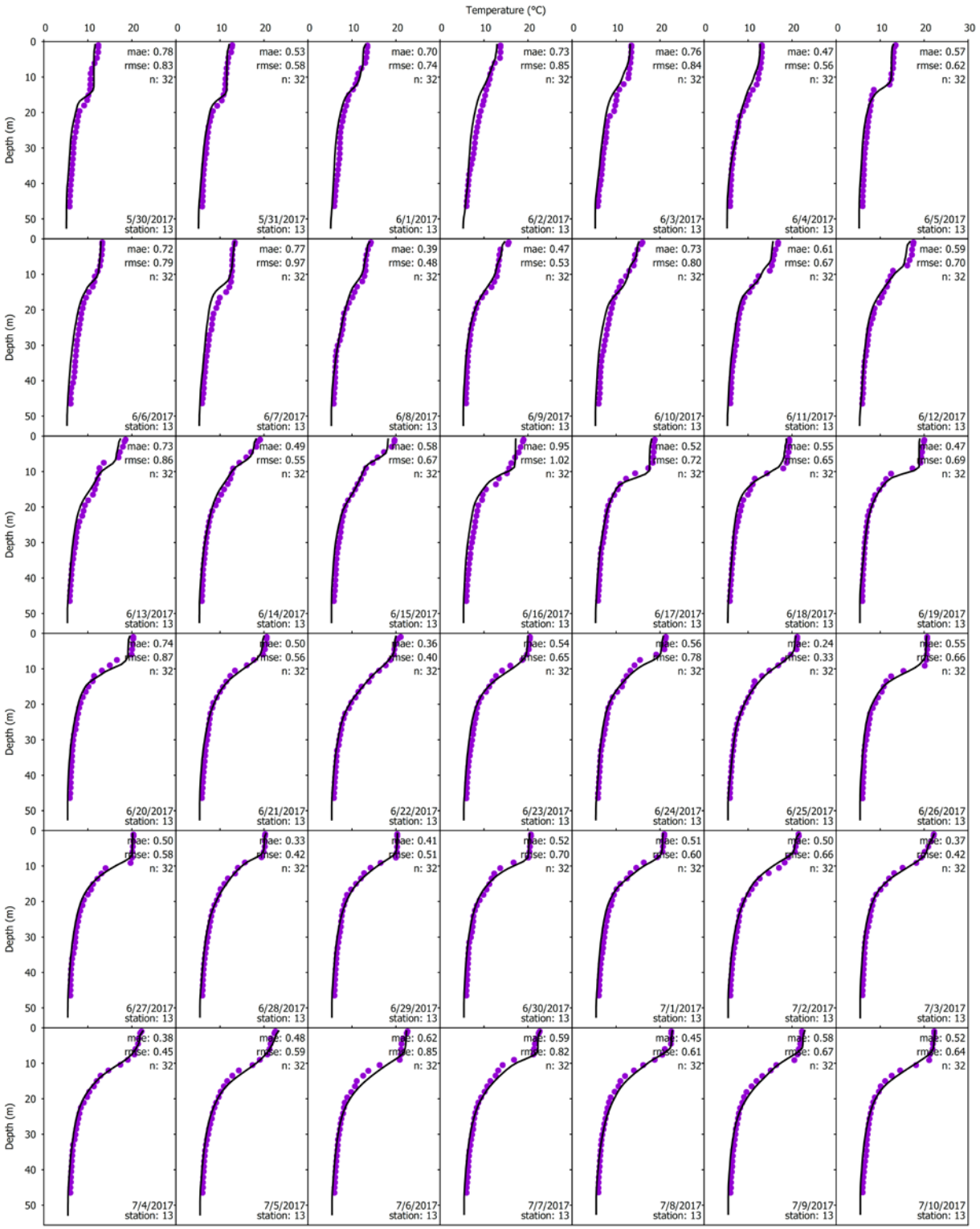


**Figure E-4**. Hydrothermal model fit to daily buoy profiles at site 13 (Figure 5-14) on Owasco Lake for primary confirmation year, 2017 page 2 of 5.

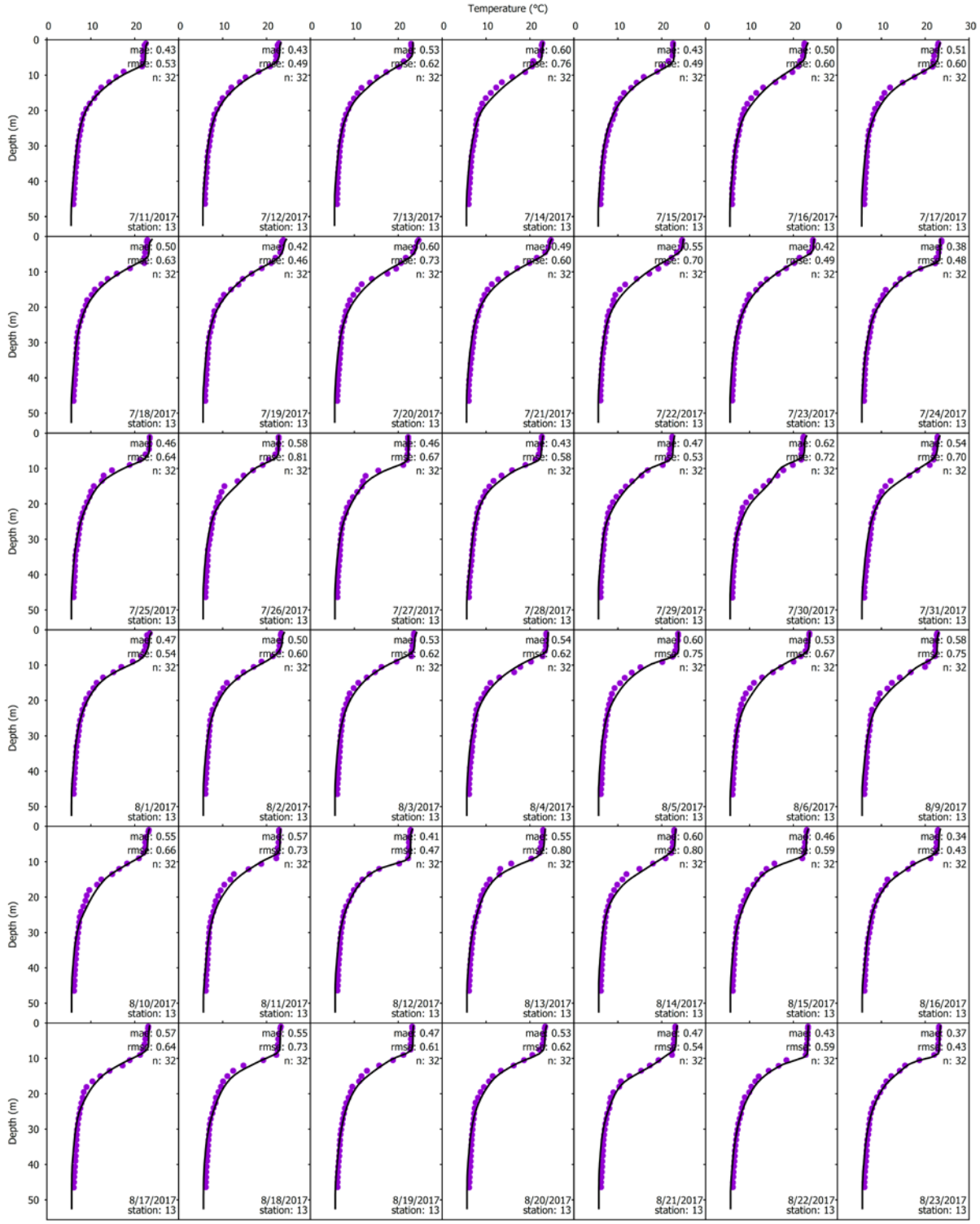


**Figure E-4**. Hydrothermal model fit to daily buoy profiles at site 13 (Figure 5-14) on Owasco Lake for primary confirmation year, 2017 page 3 of 5

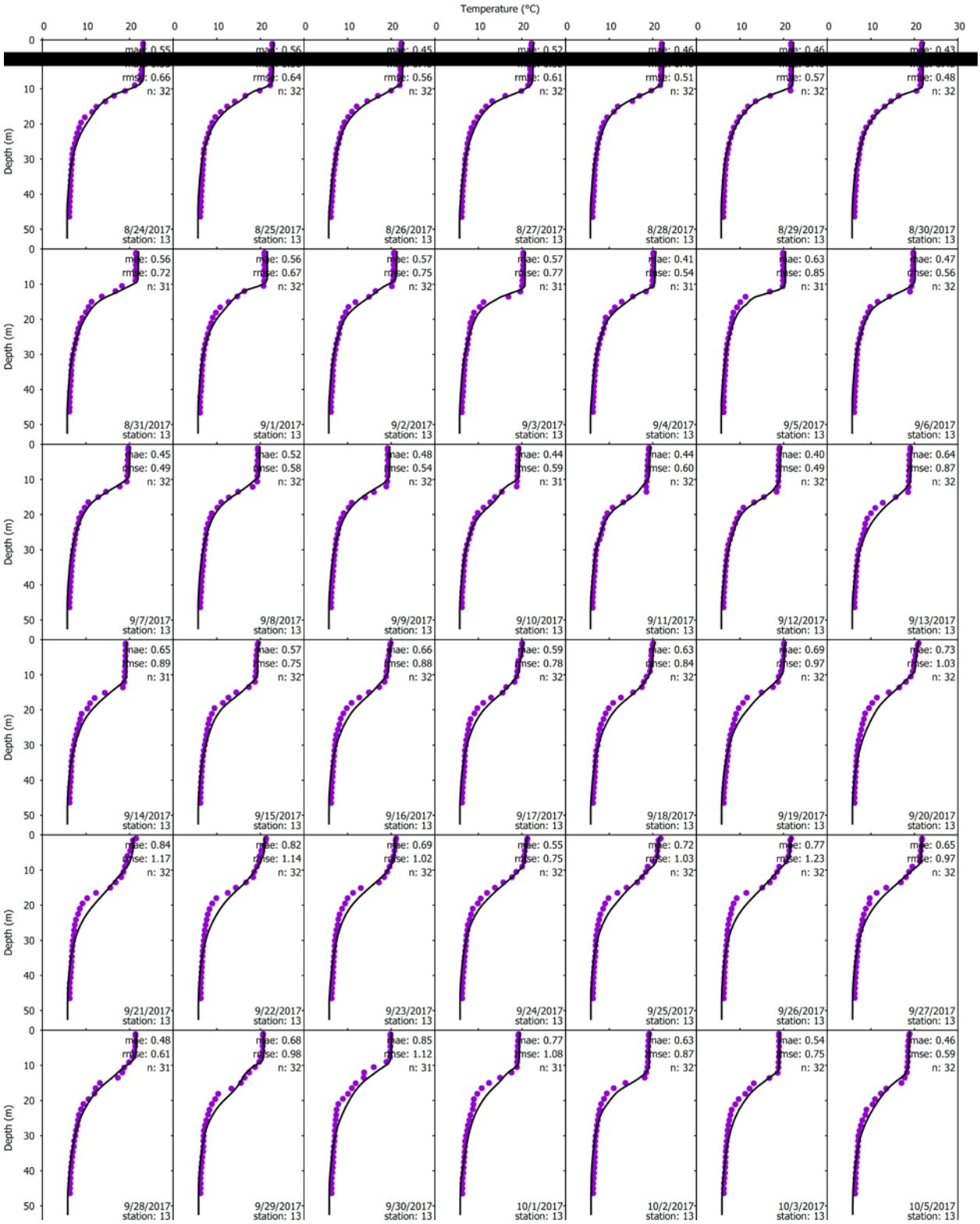


**Figure E-4**. Hydrothermal model fit to daily buoy profiles at site 13 (Figure 5-14) on Owasco Lake for primary confirmation year, 2017 page 4 of 5

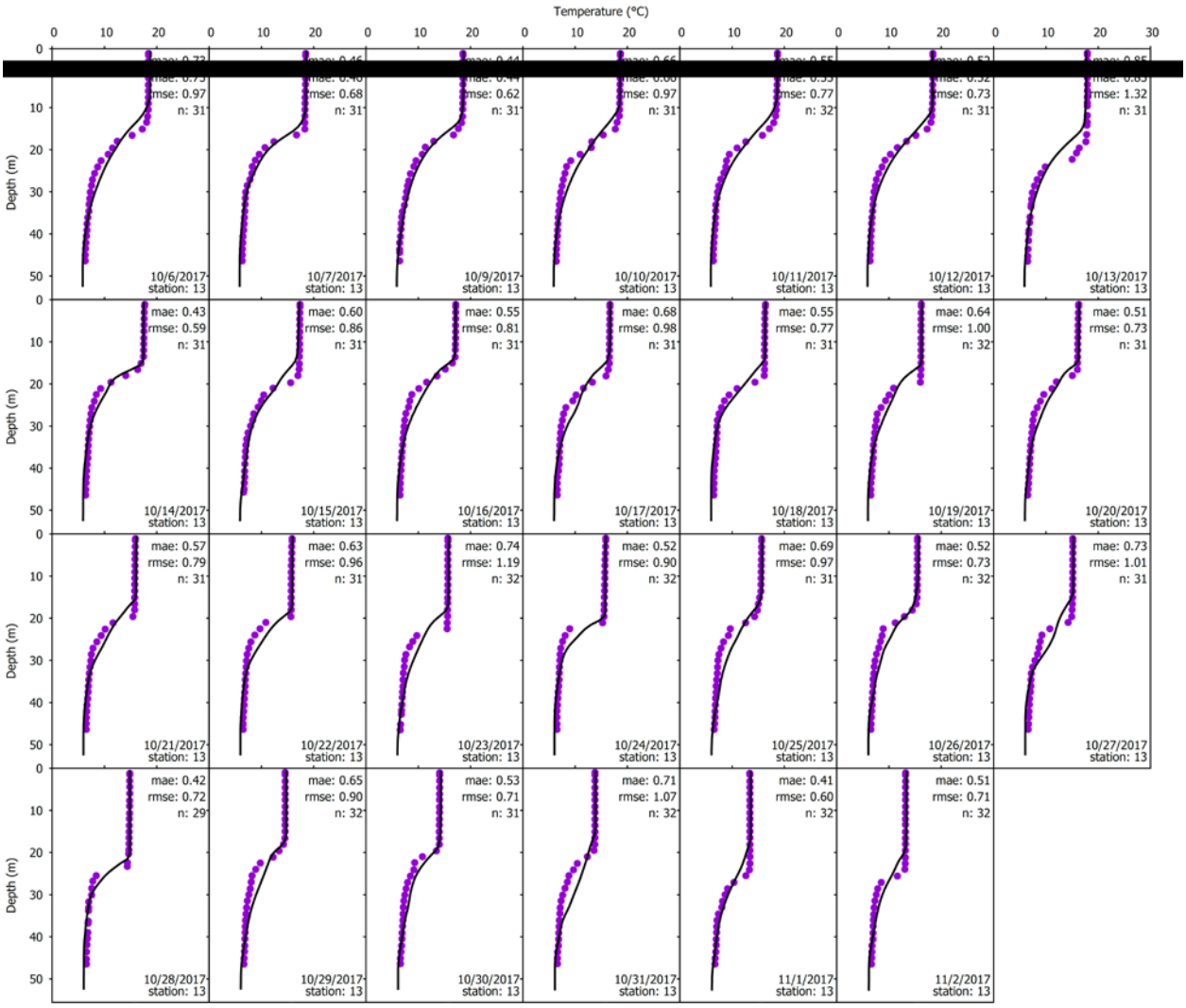


**Figure E-4**. Hydrothermal model fit to daily buoy profiles at site 13 (Figure 5-14) on Owasco Lake for primary confirmation year, 2017 page 5 of 5

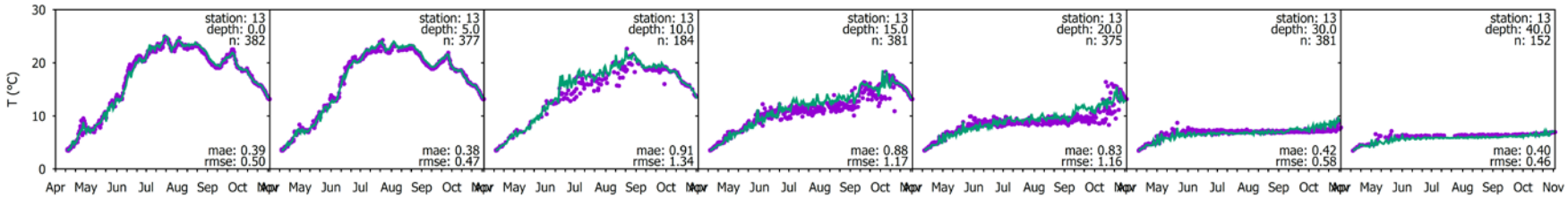


**Figure E-5**. Time series of hydrothermal model fit to daily buoy profiles at site 13 (Figure 5-14) on Owasco Lake for primary confirmation year, 2017 at seven depths, 0, 5, 10, 15, 20, 30, and 40m.

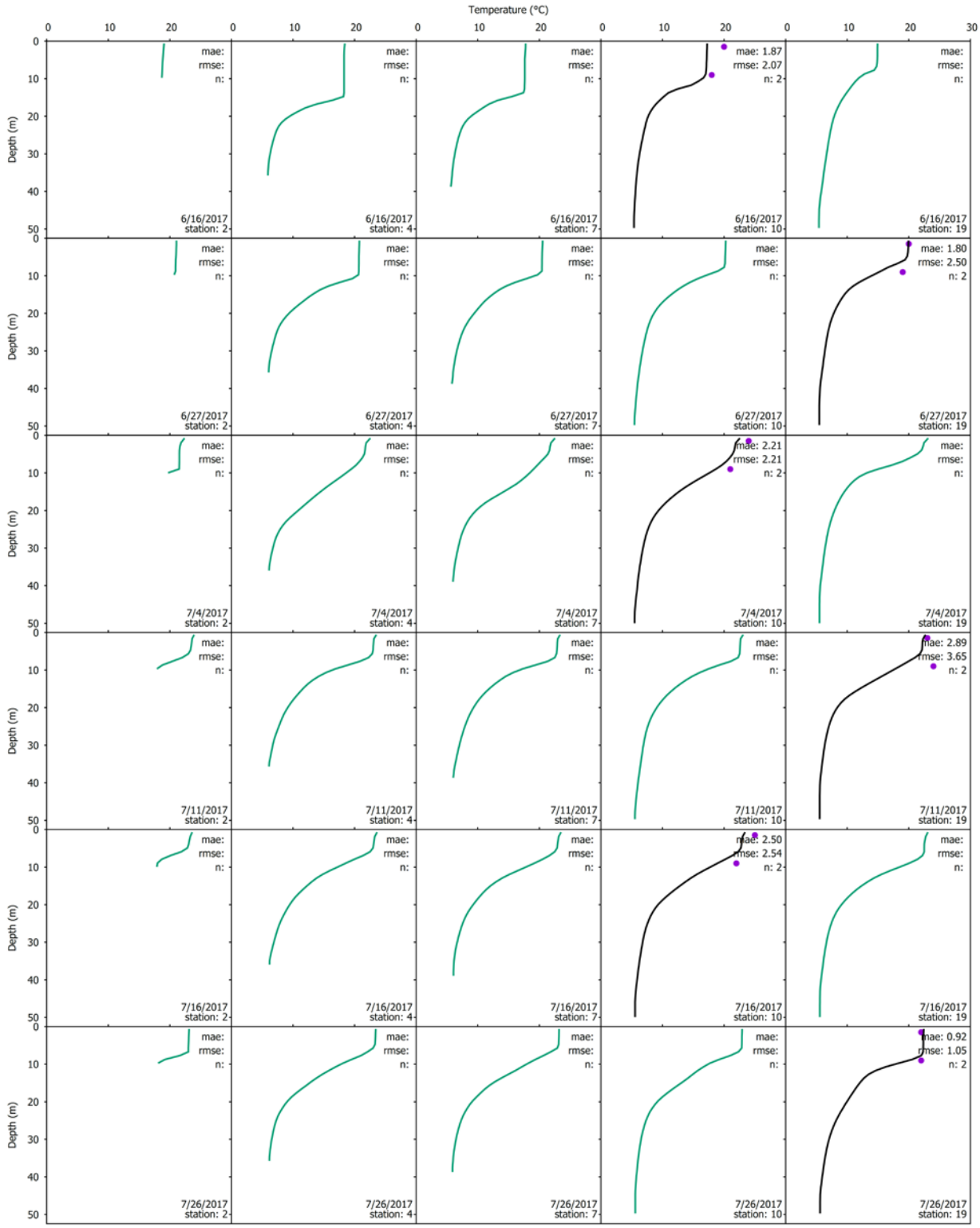


**Figure E-6**. Hydrothermal model fit to daily CSLAP temperature measurements at two sites (Figure 5-14) down the longitudinal axis of Owasco Lake for the primary confirmation year , 2017 page 1 of 3

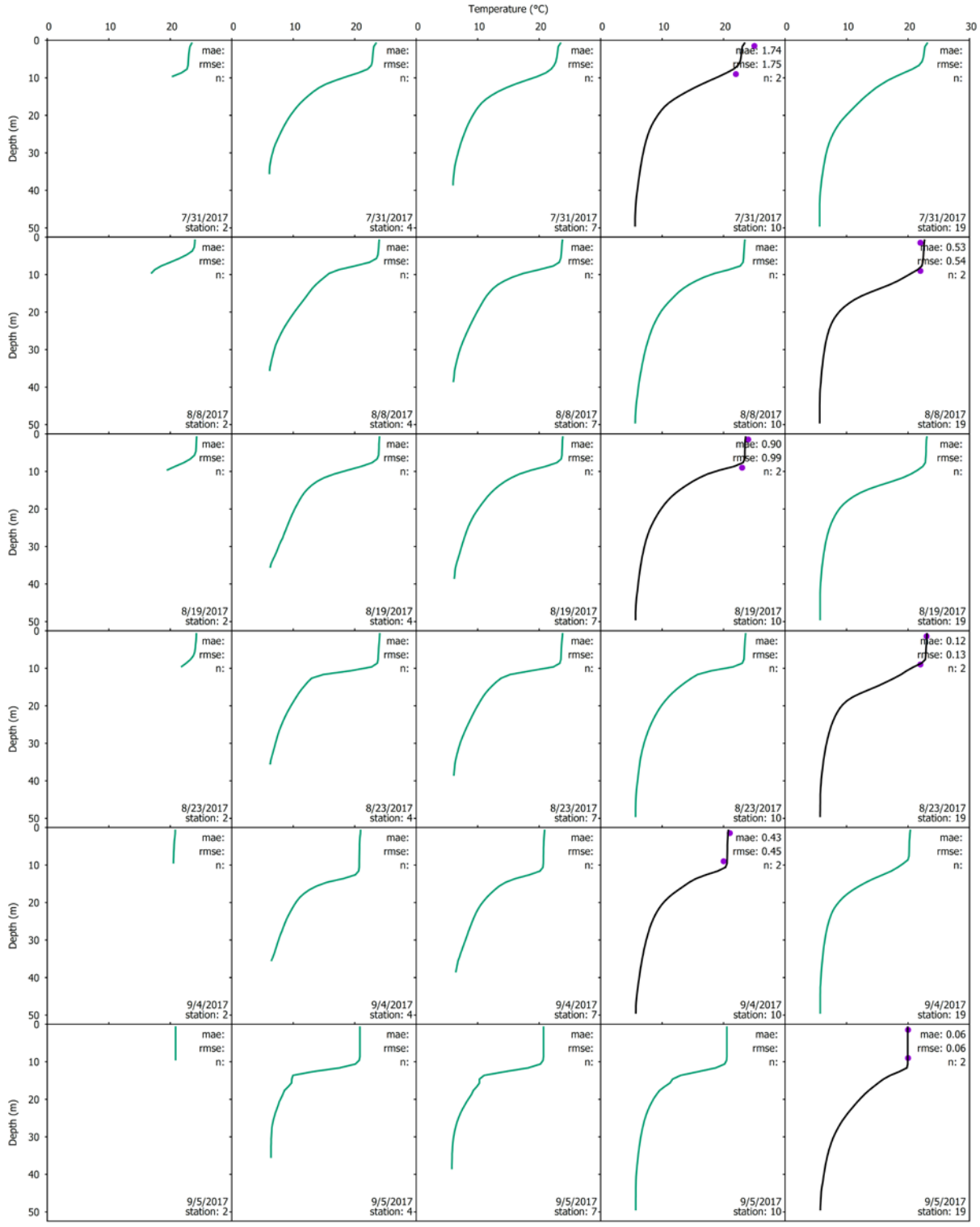


**Figure E-6**. Hydrothermal model fit to daily CSLAP temperature measurements at two sites (Figure 5-14) down the longitudinal axis of Owasco Lake for the primary confirmation year, 2017 page 2 of 3.

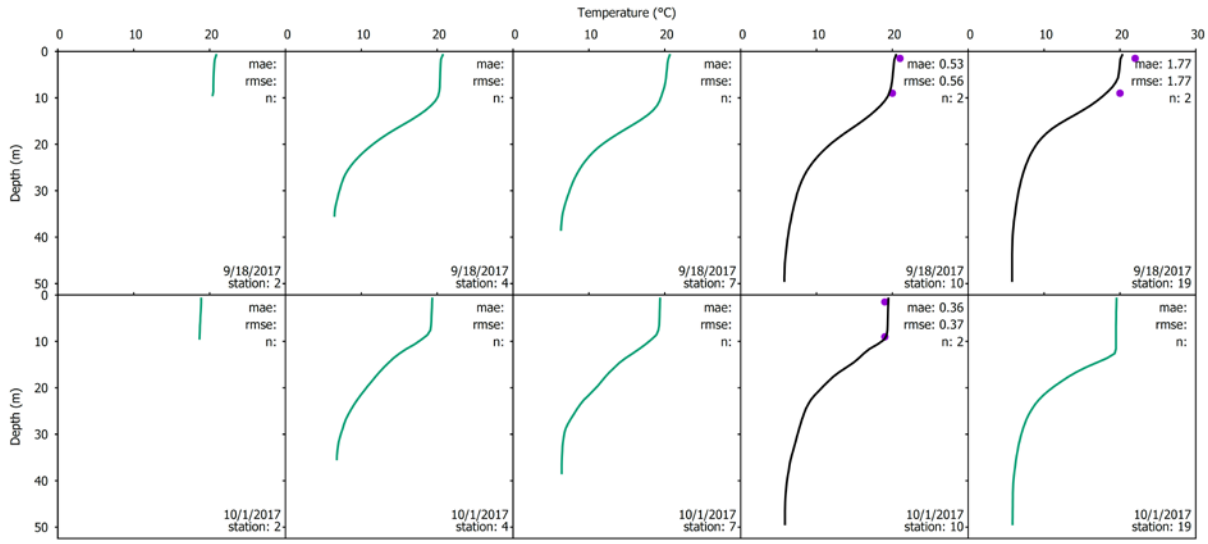


**Figure E-6**. Hydrothermal model fit to daily CSLAP temperature measurements at two sites (Figure 5-14) down the longitudinal axis of Owasco Lake for the primary confirmation year, 2017 page 3 of 3.

# Appendix E-3 Further Confirmation, 2005-2008, 2014-2016

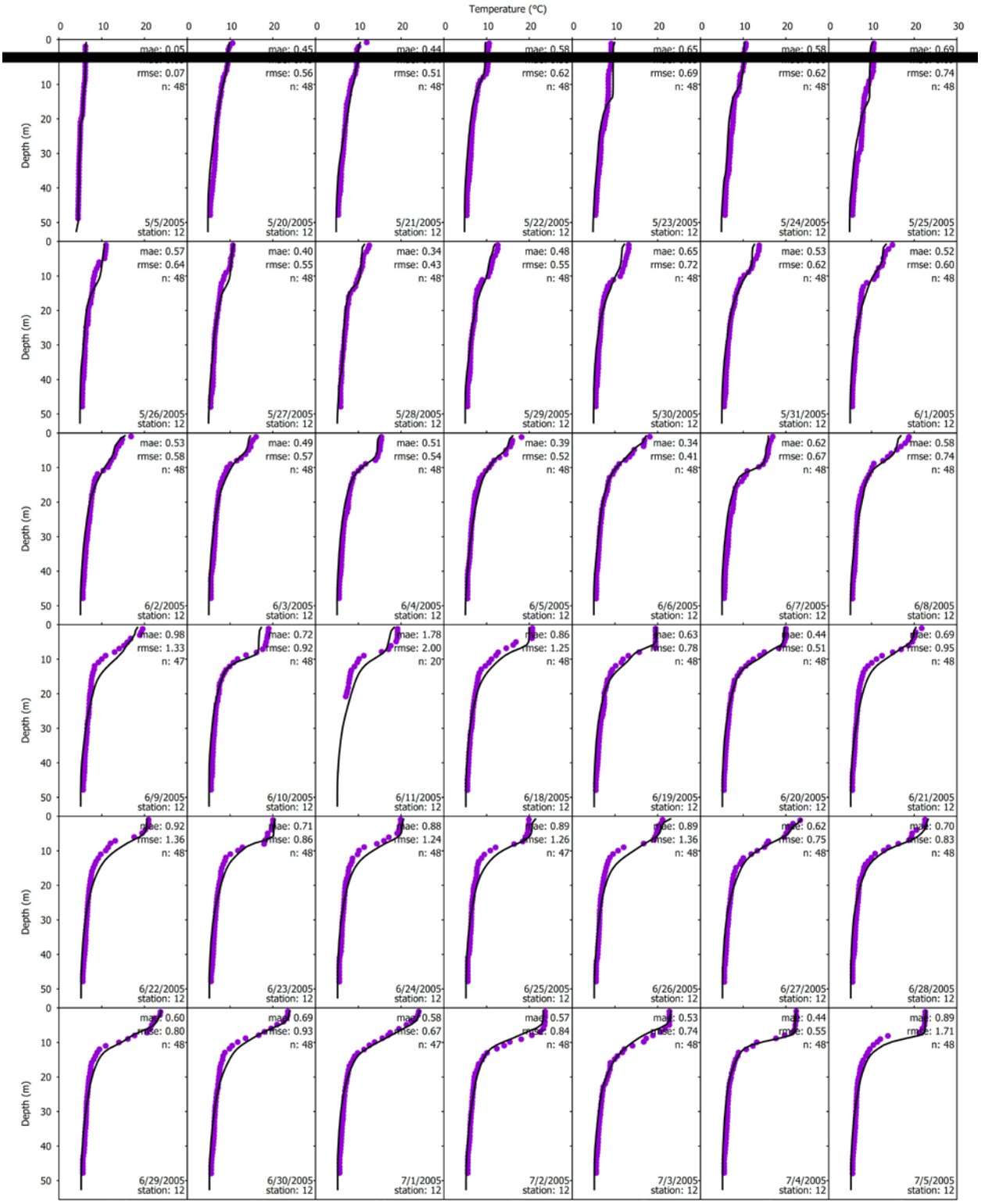


**Figure E-7**. Hydrothermal model fit to daily buoy profiles at site 12 (Figure 5-14) on Owasco Lake for confirmation year, 2005 page 1 of 4

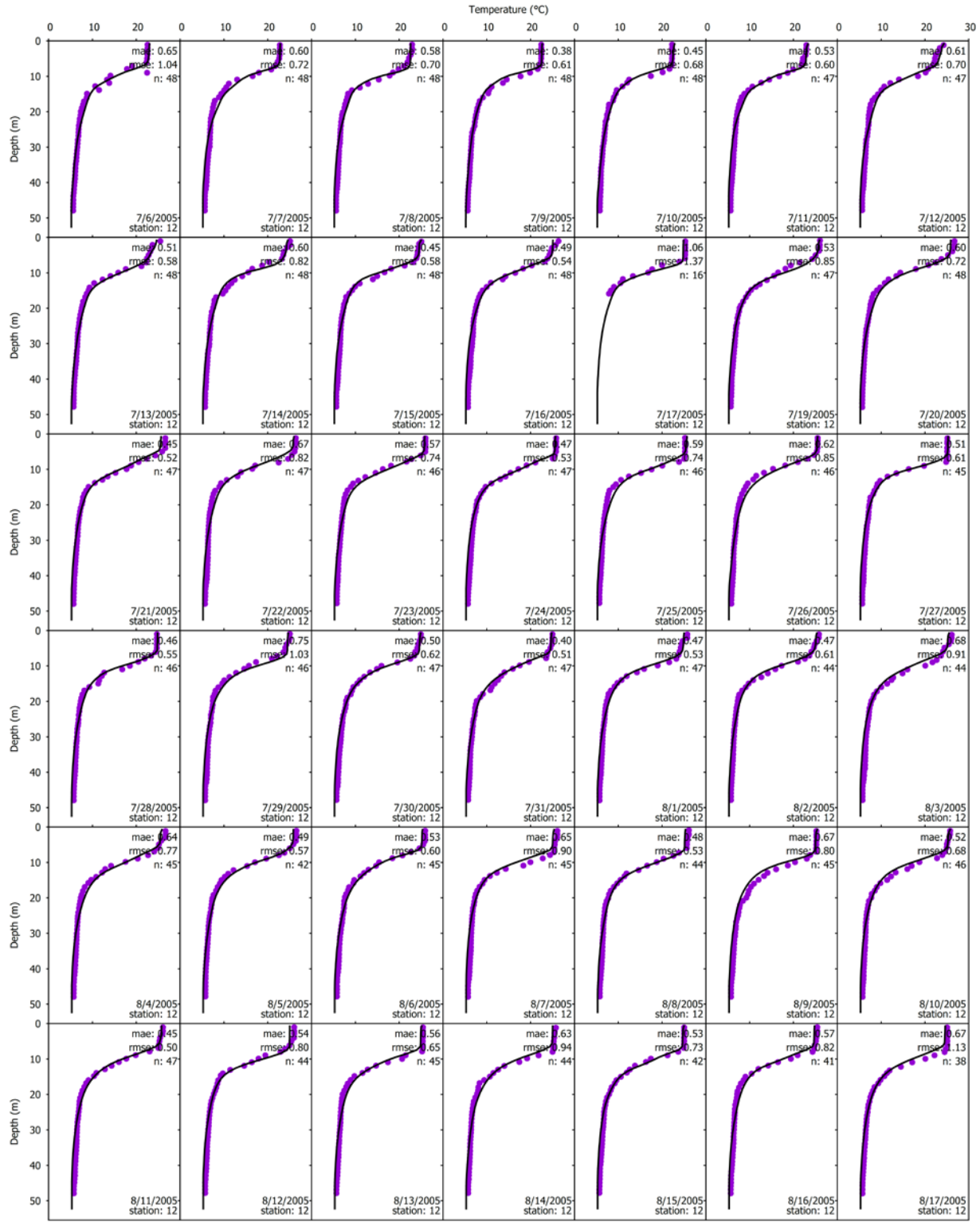


**Figure E-7**. Hydrothermal model fit to daily buoy profiles at site 12 (Figure 5-14) on Owasco Lake for confirmation year, 2005 page 2 of 4

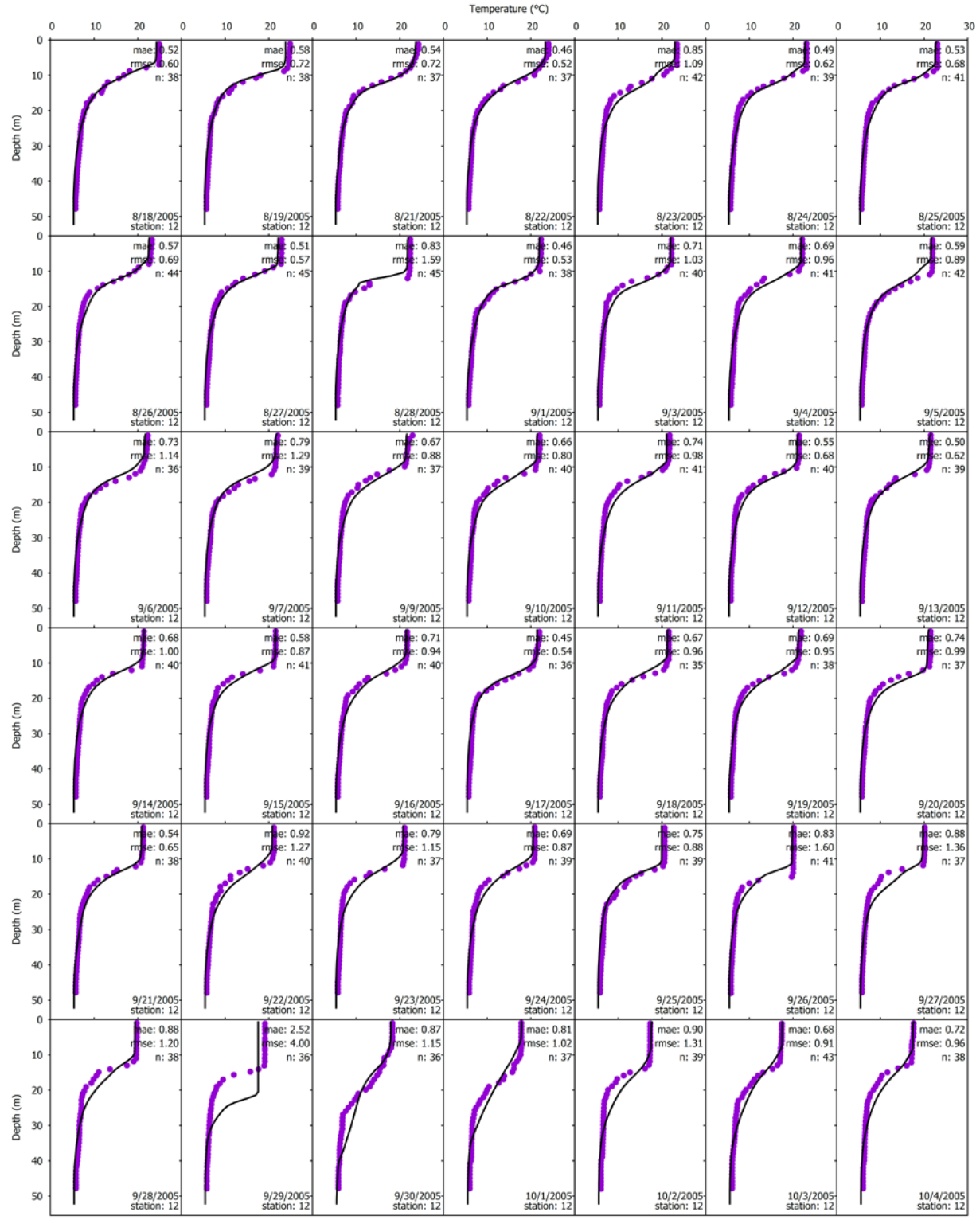


**Figure E-7**. Hydrothermal model fit to daily buoy profiles at site 12 (Figure 5-14) on Owasco Lake for confirmation year, 2005 page 3 of 4


**Figure E-7**. Hydrothermal model fit to daily buoy profiles at site 12 (Figure 5-14) on Owasco Lake for confirmation year, 2005 page 4 of 4

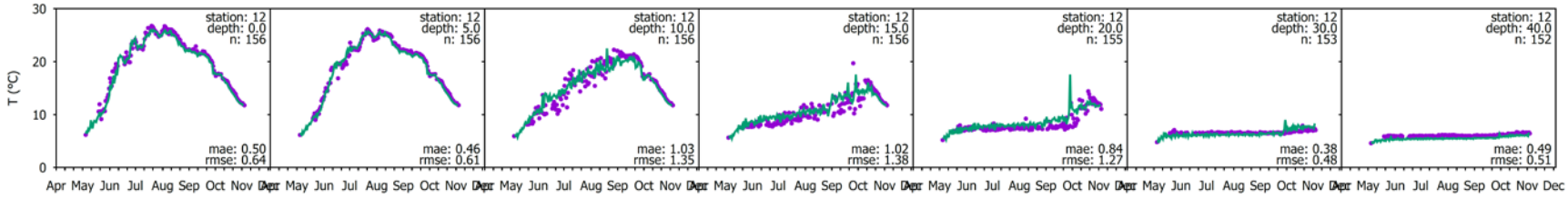


**Figure E-8**. Time series of hydrothermal model fit to daily buoy profiles at site 12 (Figure 5-14) on Owasco Lake for primary confirmation year, 2005 at seven depths, 0, 5, 10, 15, 20, 30, and 40m.

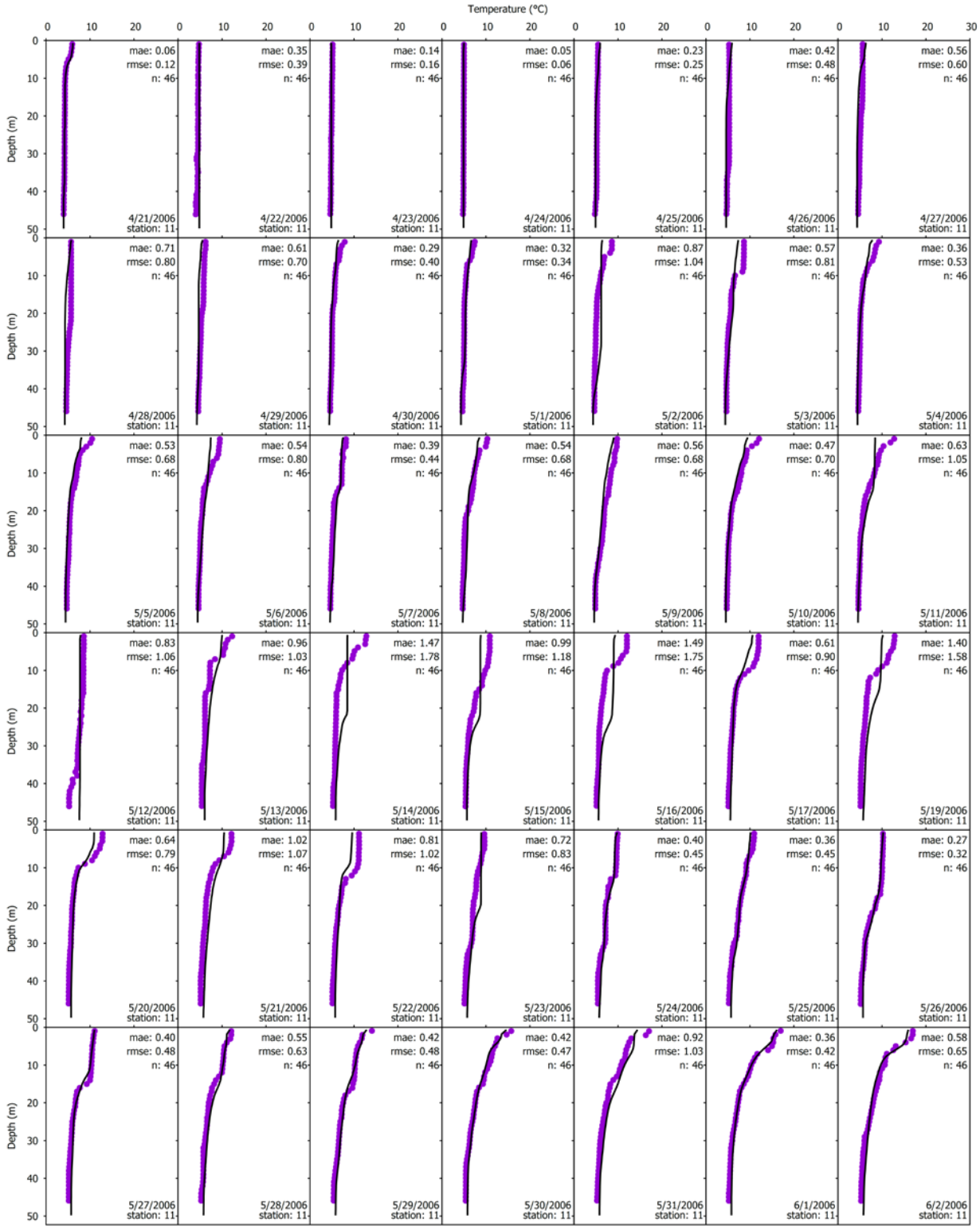


**Figure E-9**. Hydrothermal model fit to daily buoy profiles at site 11 (Figure 5-14) on Owasco Lake for confirmation year, 2006 page 1 of 5.

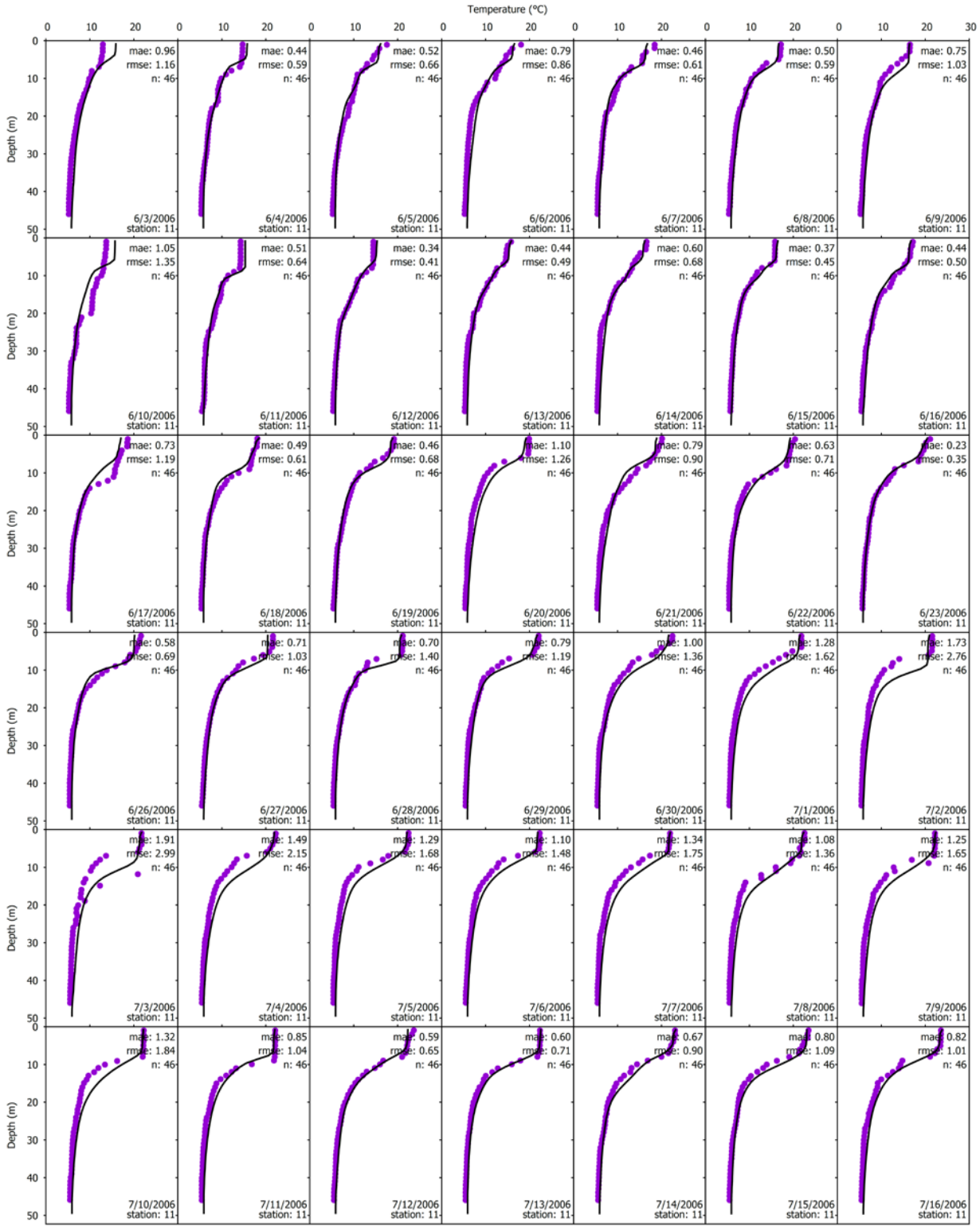


**Figure E-9**. Hydrothermal model fit to daily buoy profiles at site 11 (Figure 5-14) on Owasco Lake for confirmation year, 2006 page 2 of 5.

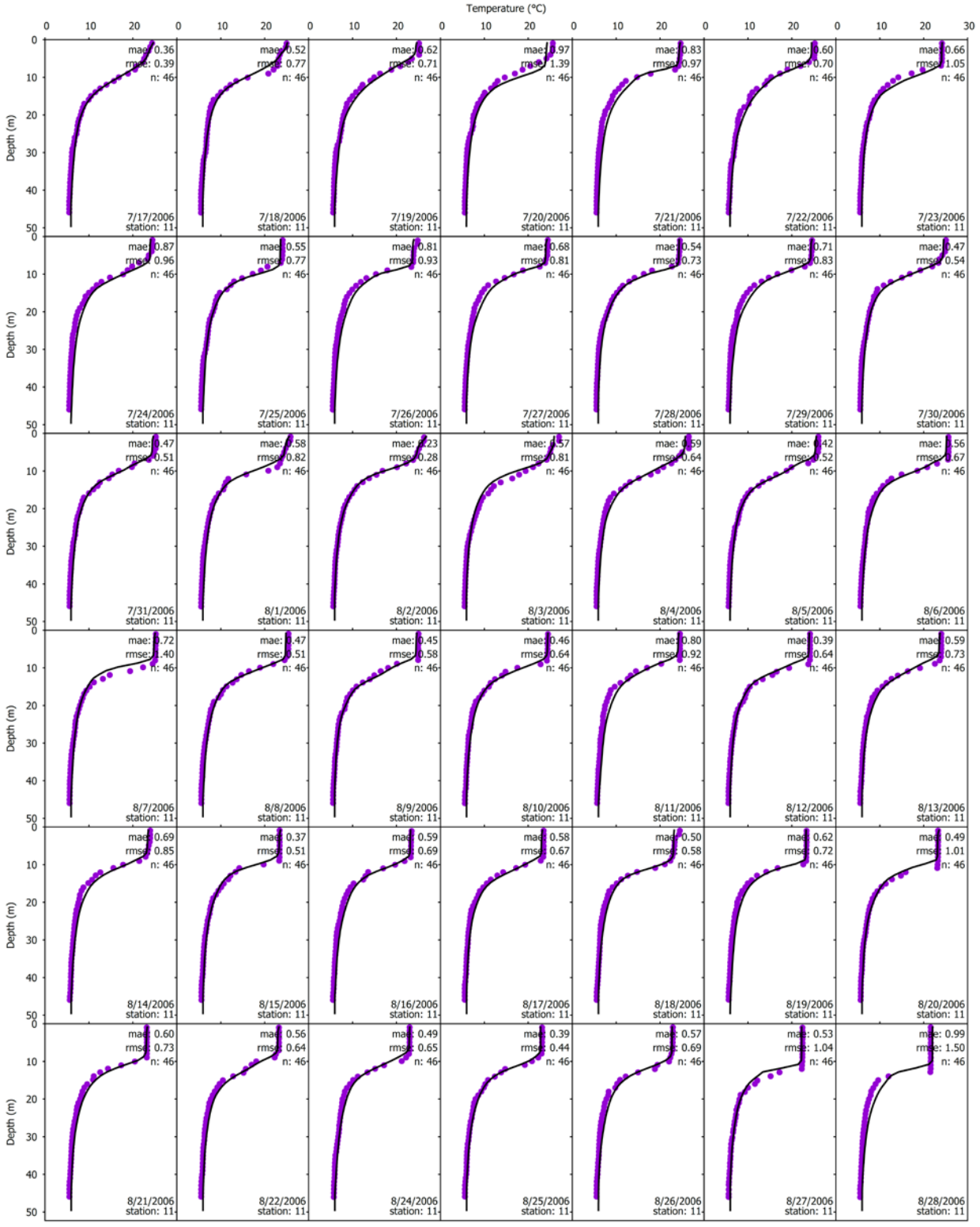


**Figure E-9**. Hydrothermal model fit to daily buoy profiles at site 11 (Figure 5-14) on Owasco Lake for confirmation year, 2006 page 3 of 5.

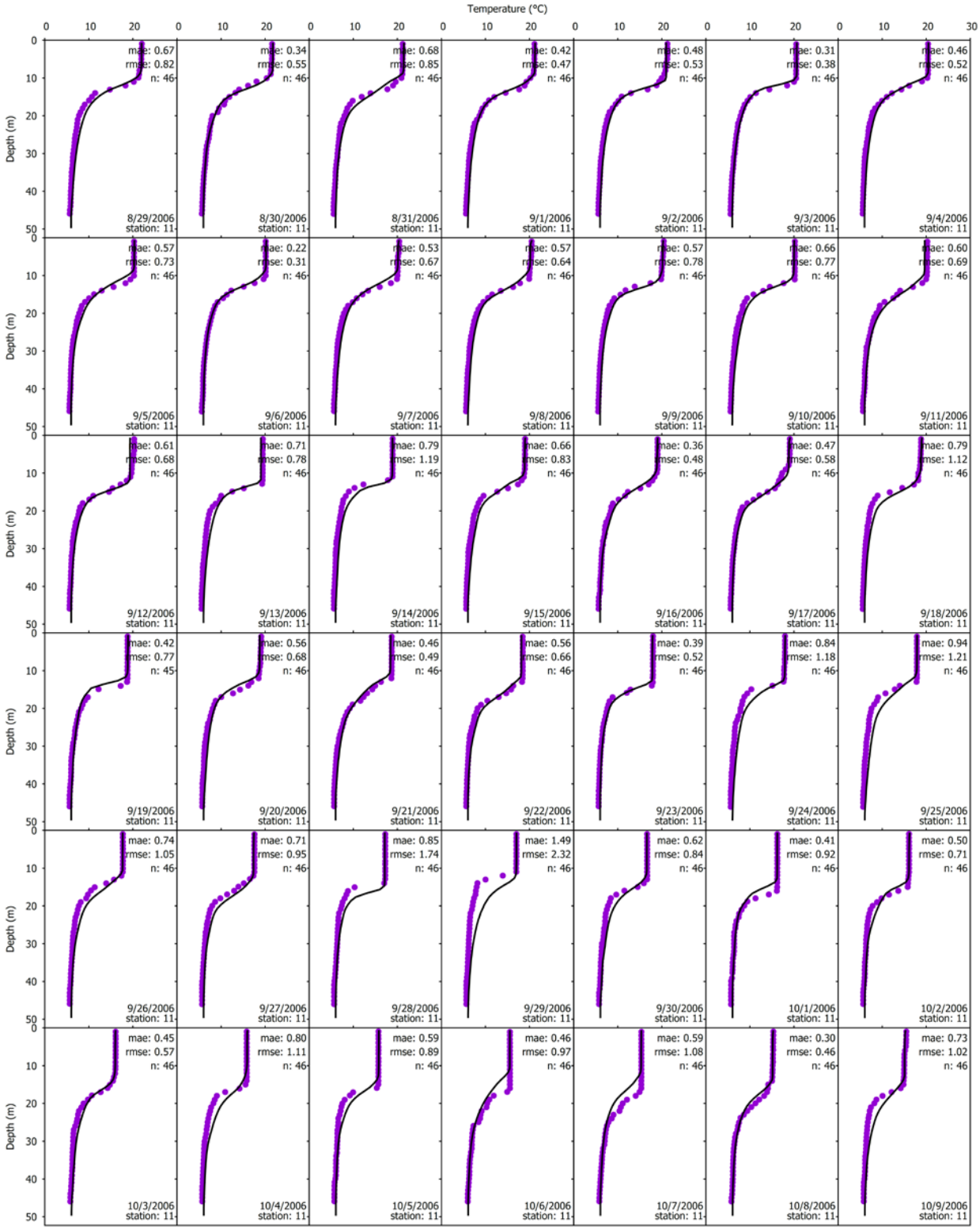


**Figure E-9**. Hydrothermal model fit to daily buoy profiles at site 11 (Figure 5-14) on Owasco Lake for confirmation year, 2006 page 4 of 5.

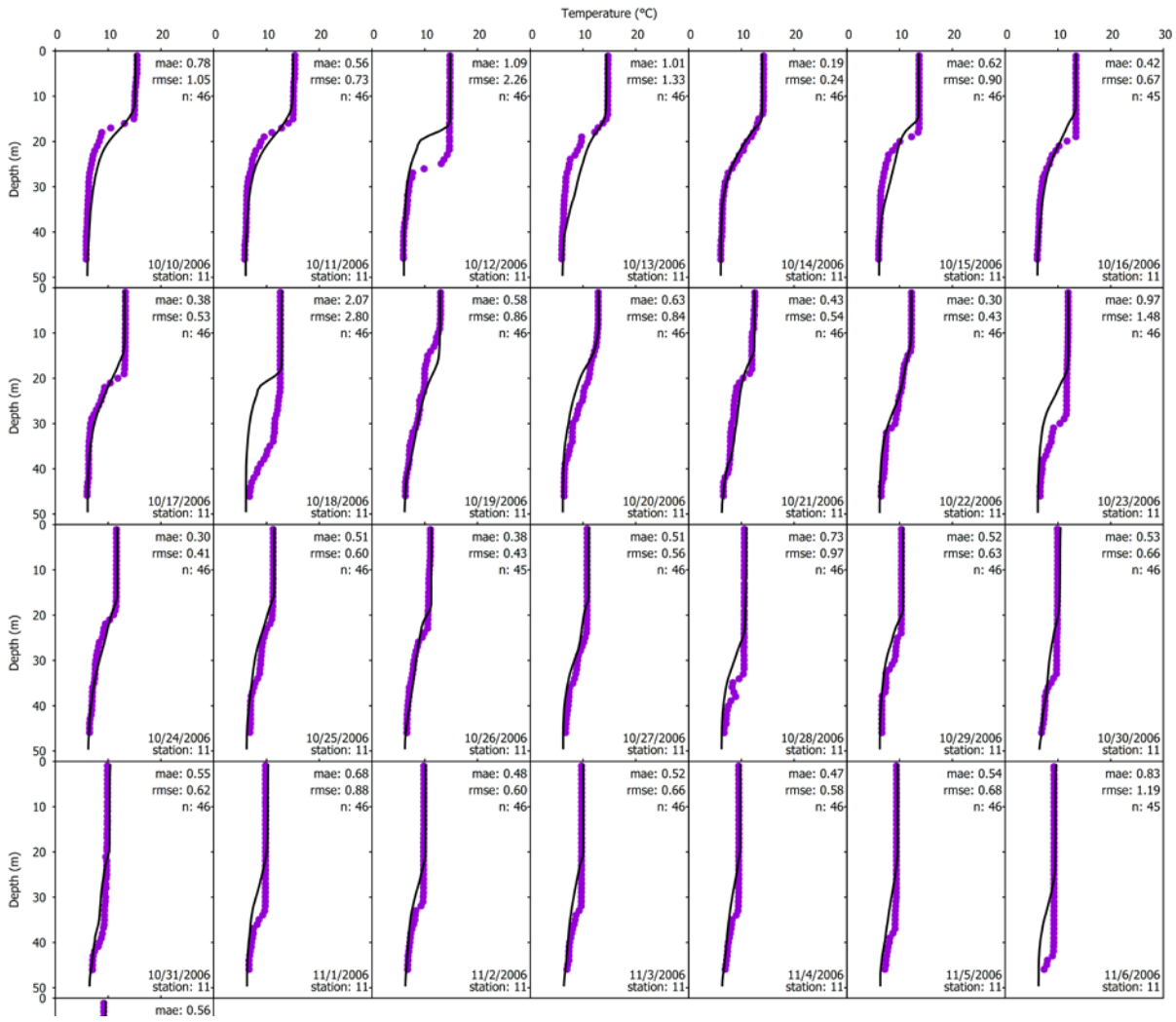


**Figure E-9**. Hydrothermal model fit to daily buoy profiles at site 11 (Figure 5-14) on Owasco Lake for confirmation year, 2006 page 5 of 5.

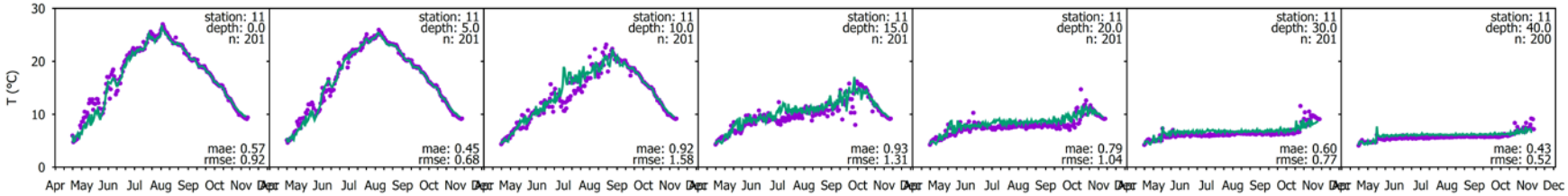


**Figure E-10**. Time series of hydrothermal model fit to daily buoy profiles at site 11 (Figure 5-14) on Owasco Lake for primary confirmation year, 2006 at seven depths, 0, 5, 10, 15, 20, 30, and 40m.

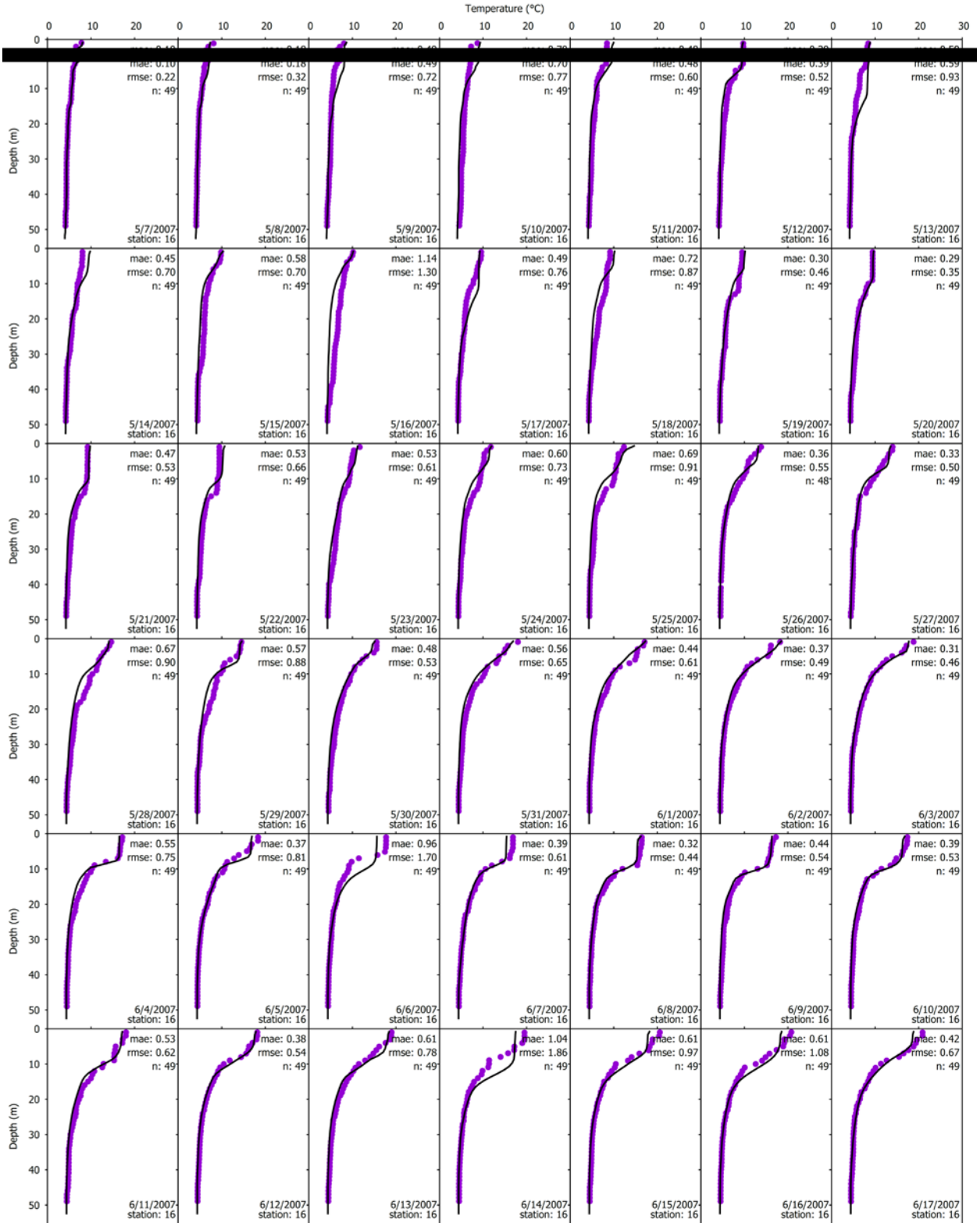


**Figure E-11**. Hydrothermal model fit to daily buoy profiles at site 16 (Figure 5-14) on Owasco Lake for confirmation year, 2007 page 1 of 4.

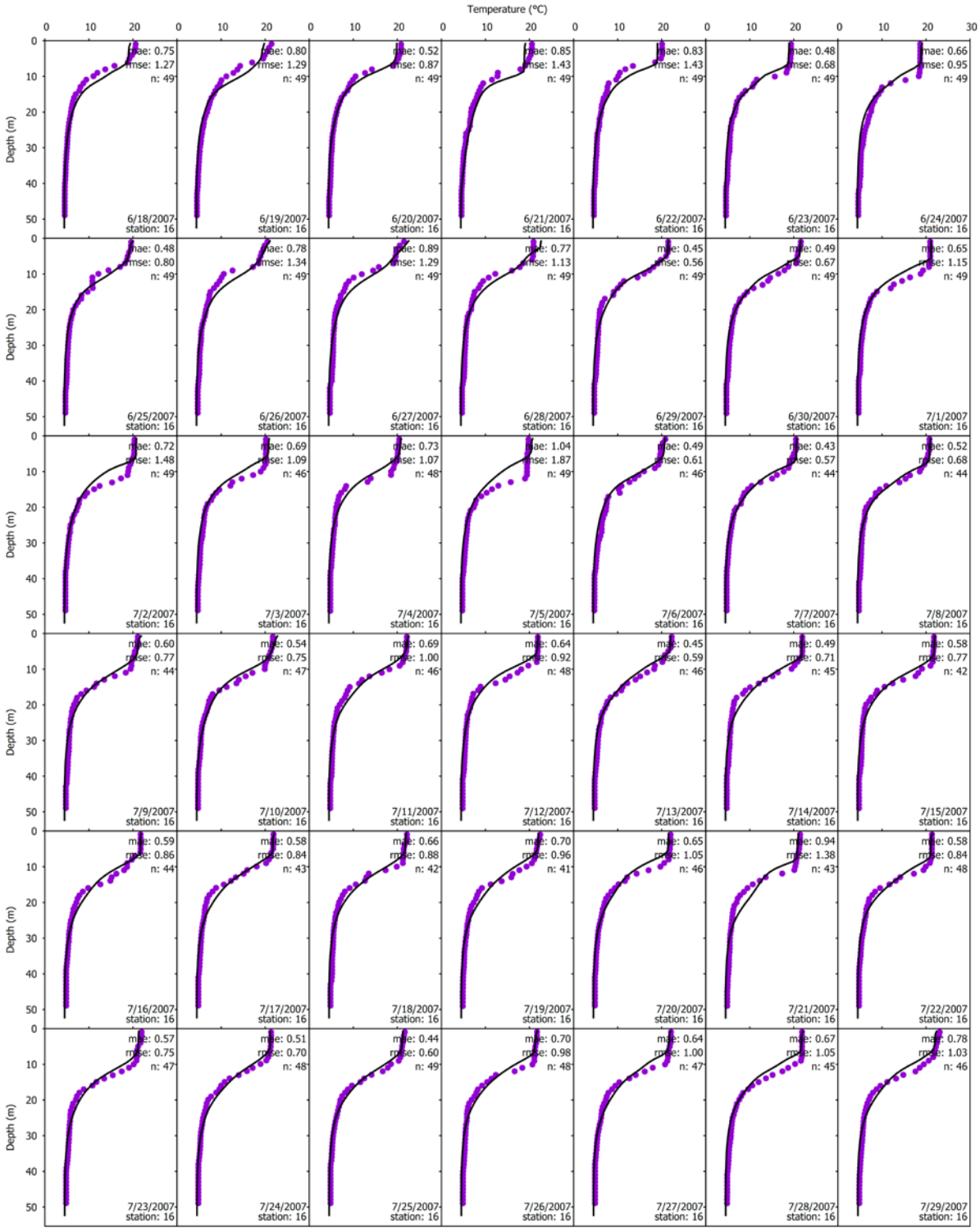


**Figure E-11**. Hydrothermal model fit to daily buoy profiles at site 16 (Figure 5-14) on Owasco Lake for confirmation year, 2007 page 2 of 4.

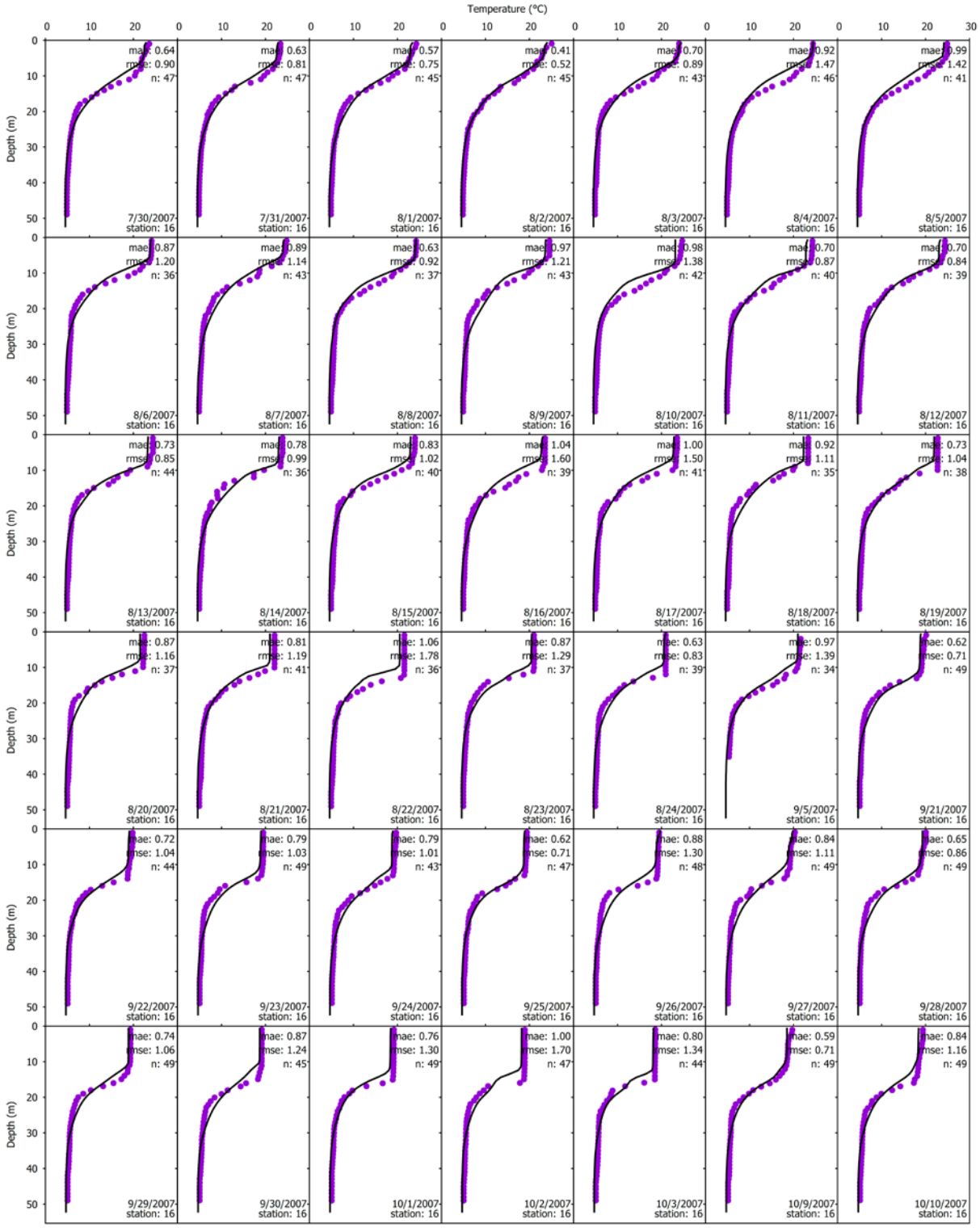


**Figure E-11**. Hydrothermal model fit to daily buoy profiles at site 16 (Figure 5-14) on Owasco Lake for confirmation year, 2007 page 3 of 4.


**Figure E-11**. Hydrothermal model fit to daily buoy profiles at site 16 (Figure 5-14) on Owasco Lake for confirmation year, 2007 page 4 of 4.

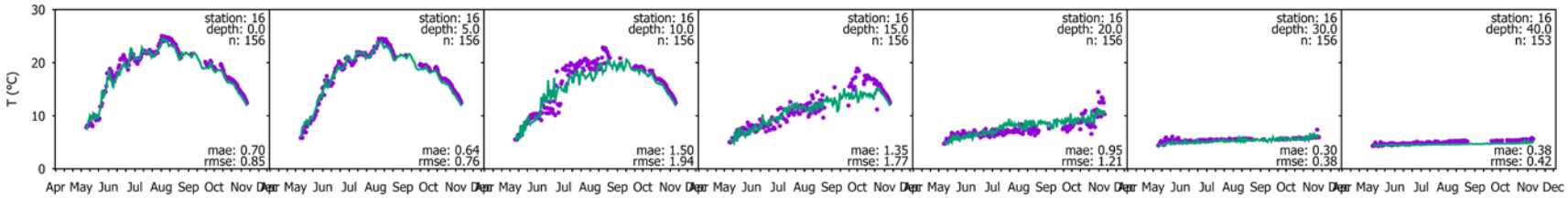


**Figure E-12**. Time series of hydrothermal model fit to daily buoy profiles at site 16 (Figure 5-14) on Owasco Lake for primary confirmation year, 2007 at seven depths, 0, 5, 10, 15, 20, 30, and 40m.

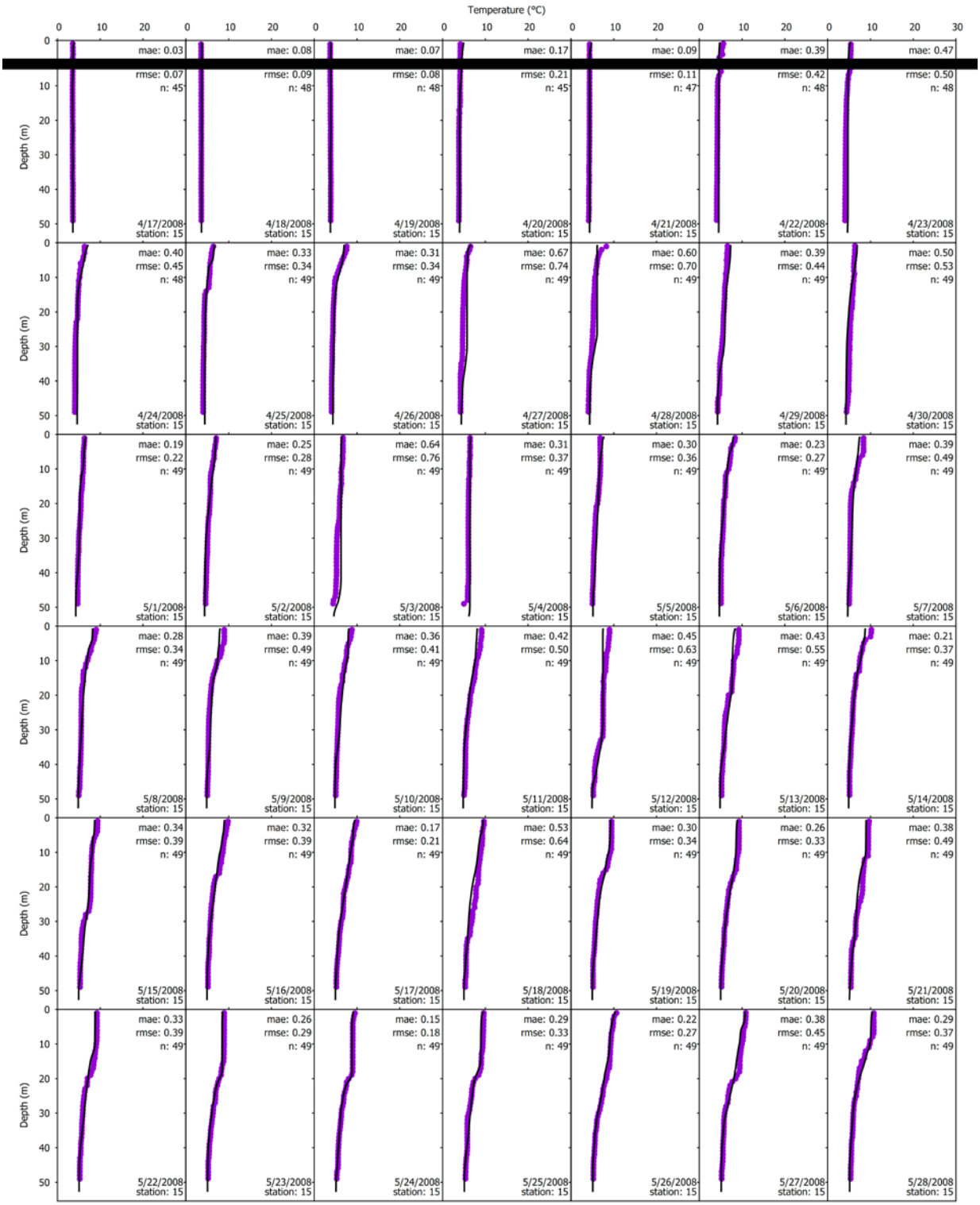


**Figure E-13.** Hydrothermal model fit to daily buoy profiles at site 15 (Figure 5-14) on Owasco Lake for confirmation year, 2008 page 1 of 5.

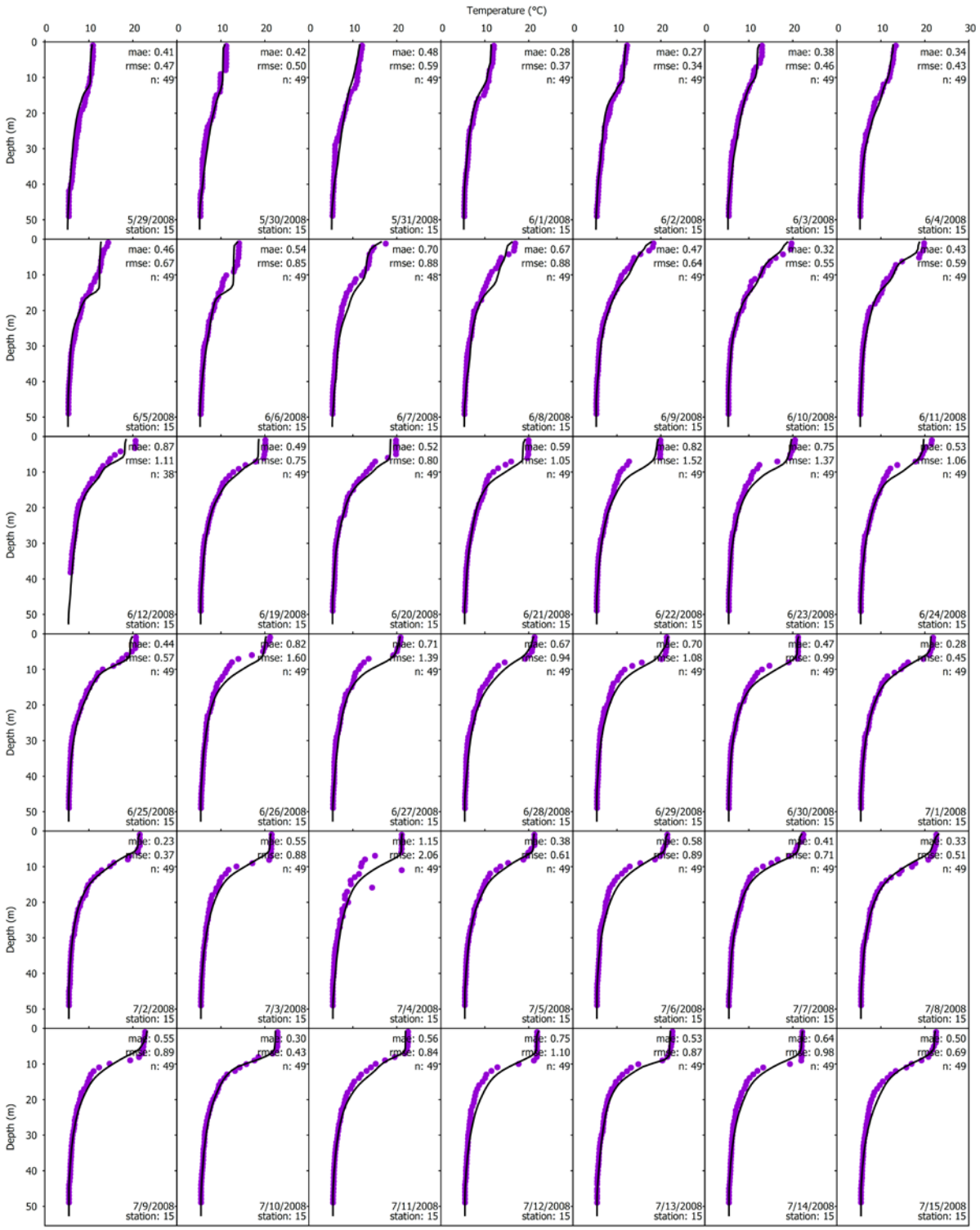


**Figure E-13.** Hydrothermal model fit to daily buoy profiles at site 15 (Figure 5-14) on Owasco Lake for confirmation year, 2008 page 2 of 5.

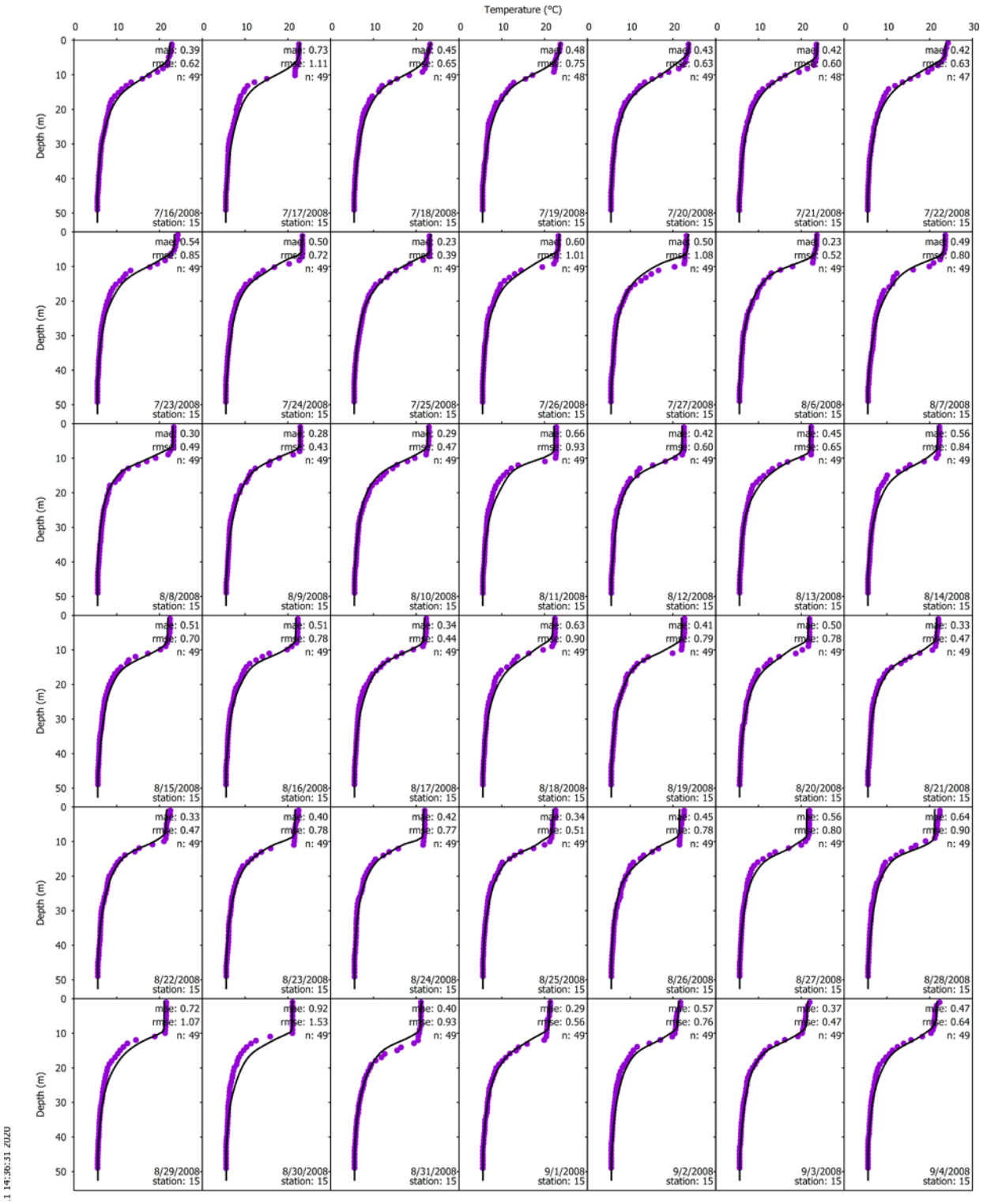


**Figure E-13.** Hydrothermal model fit to daily buoy profiles at site 15 (Figure 5-14) on Owasco Lake for confirmation year, 2008 page 3 of 5.

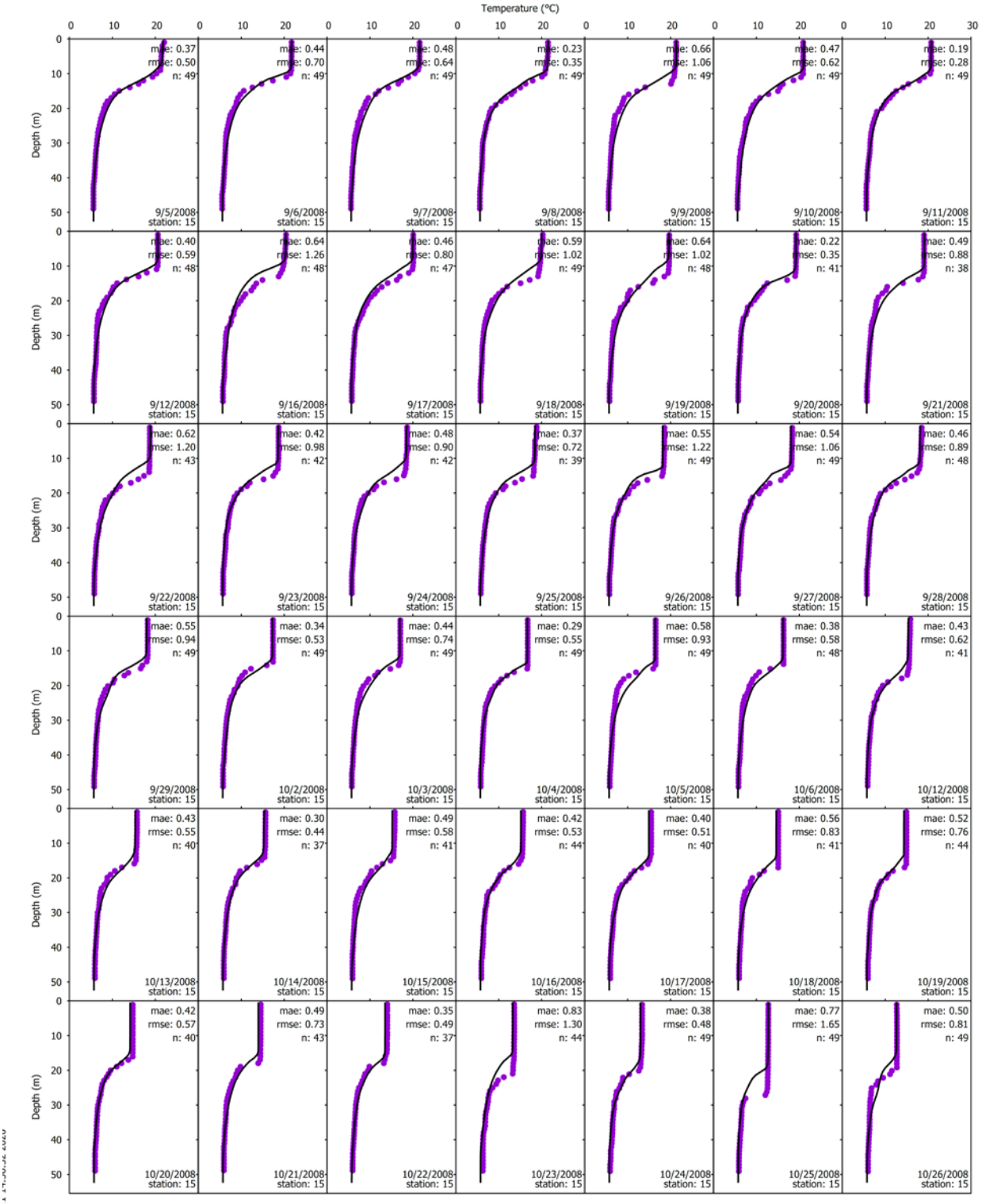


**Figure E-13.** Hydrothermal model fit to daily buoy profiles at site 15 (Figure 5-14) on Owasco Lake for confirmation year, 2008 page 4 of 5.

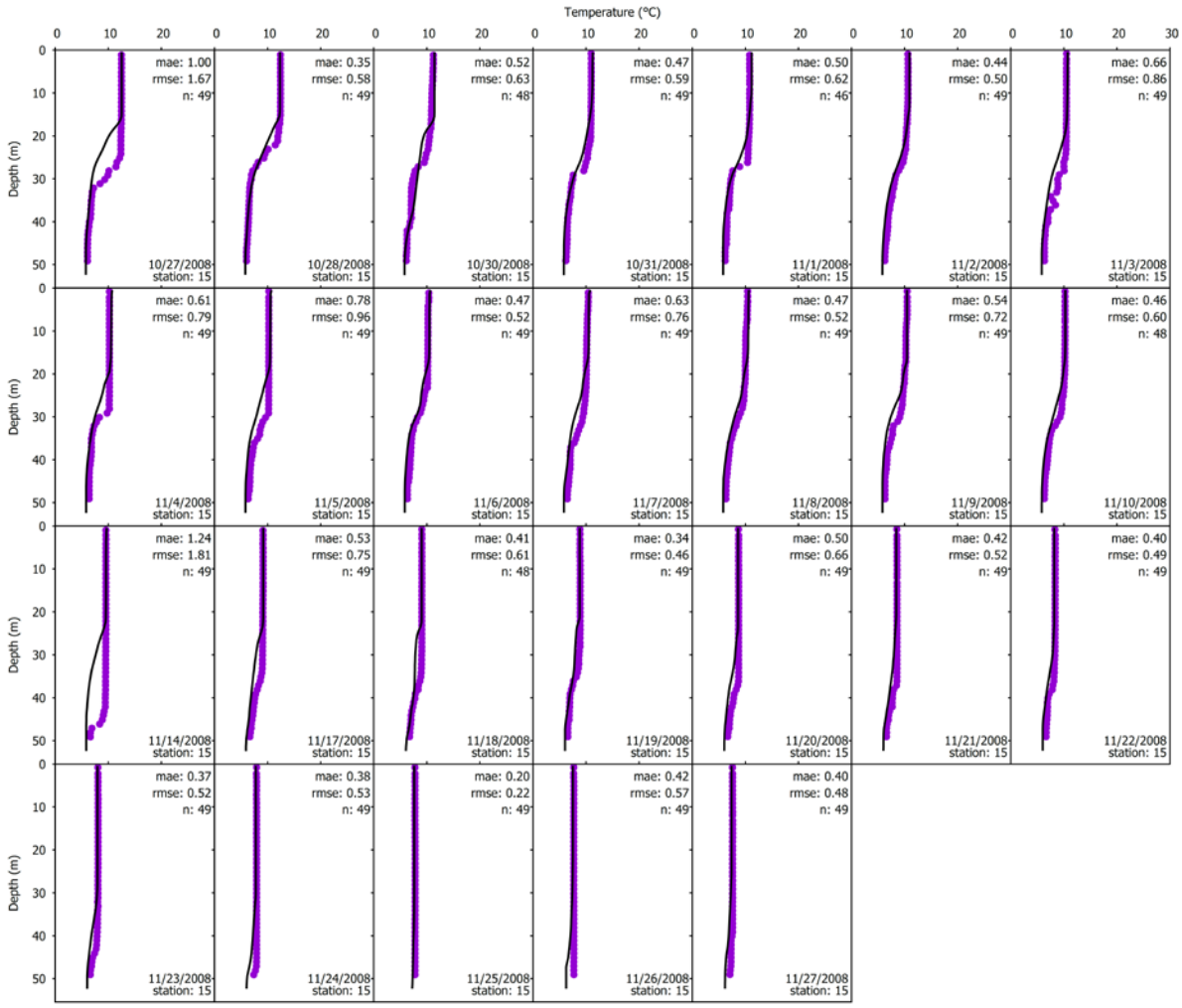


**Figure E-13.** Hydrothermal model fit to daily buoy profiles at site 15 (Figure 5-14) on Owasco Lake for confirmation year, 2008 page 5 of 5.

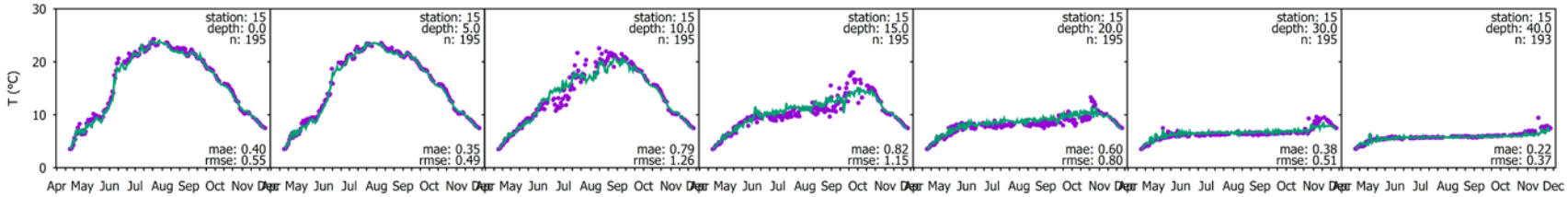


**Figure E-14**. Time series of hydrothermal model fit to daily buoy profiles at site 15 (Figure 5-14) on Owasco Lake for primary confirmation year, 2008 at seven depths, 0, 5, 10, 15, 20, 30, and 40m.

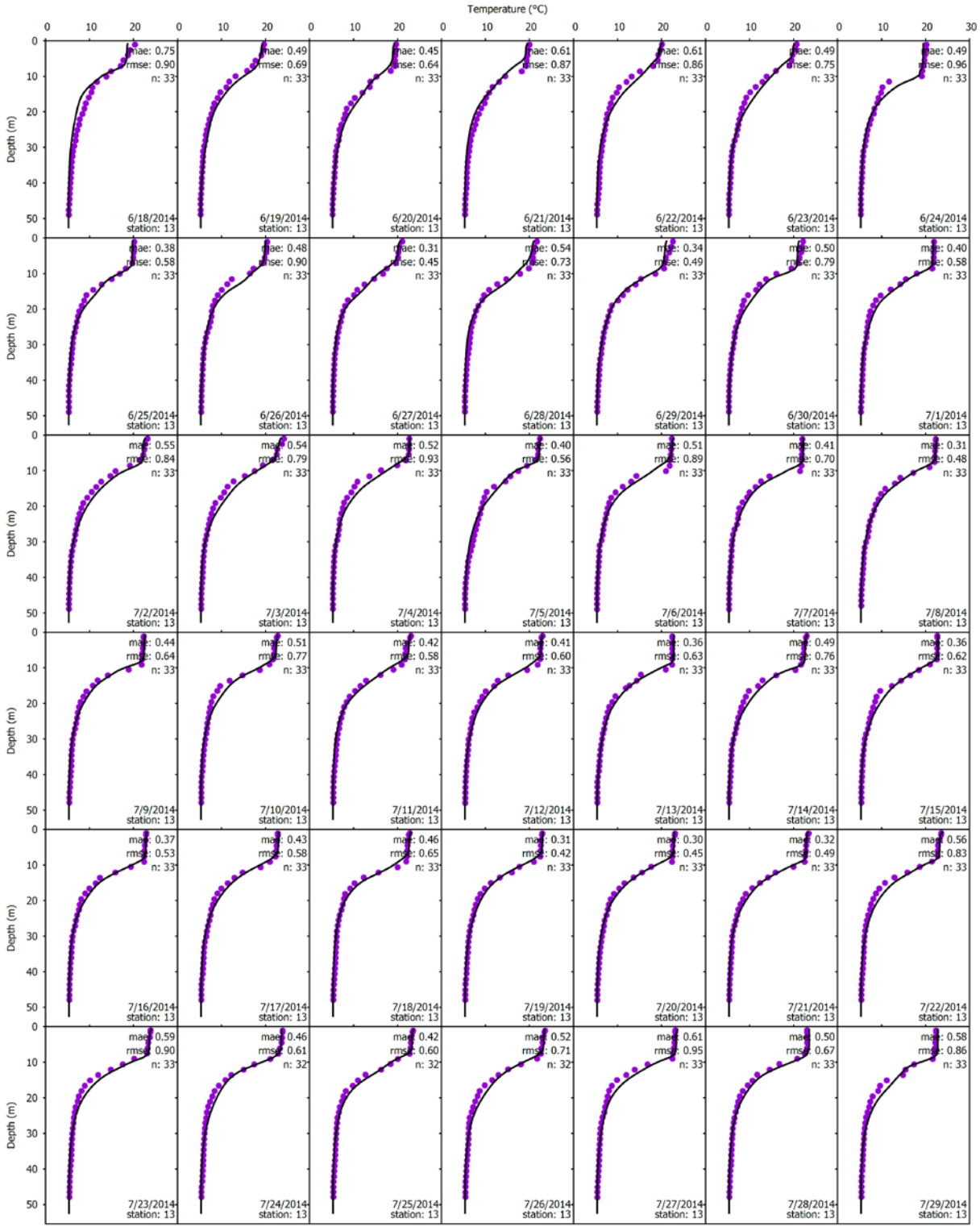


**Figure E-15**. Hydrothermal model fit to daily buoy profiles at site 13 (Figure 5-14) on Owasco Lake for confirmation year, 2014 page 1 of 4.

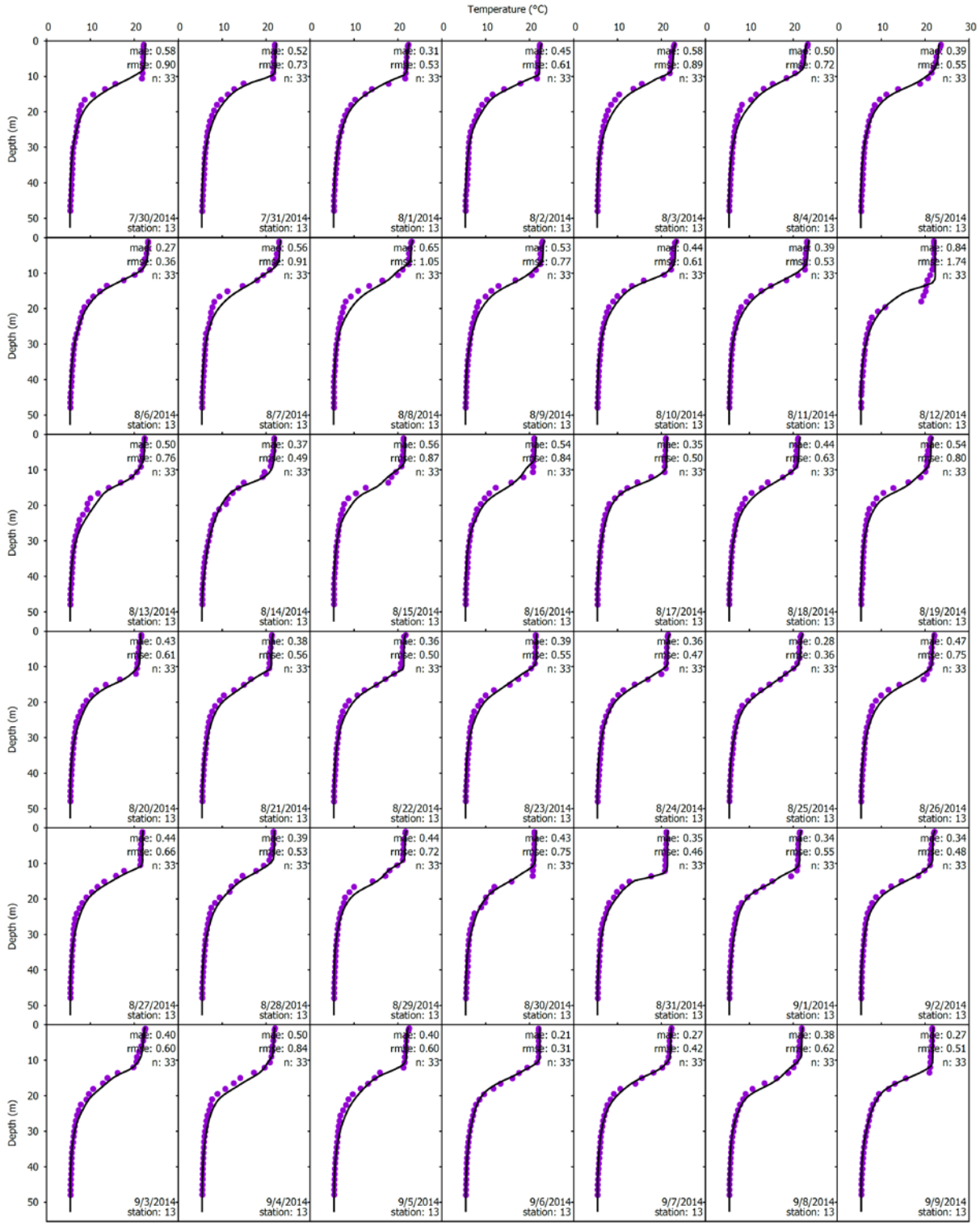


**Figure E-15**. Hydrothermal model fit to daily buoy profiles at site 13 (Figure 5-14) on Owasco Lake for confirmation year, 2014 page 2 of 4.

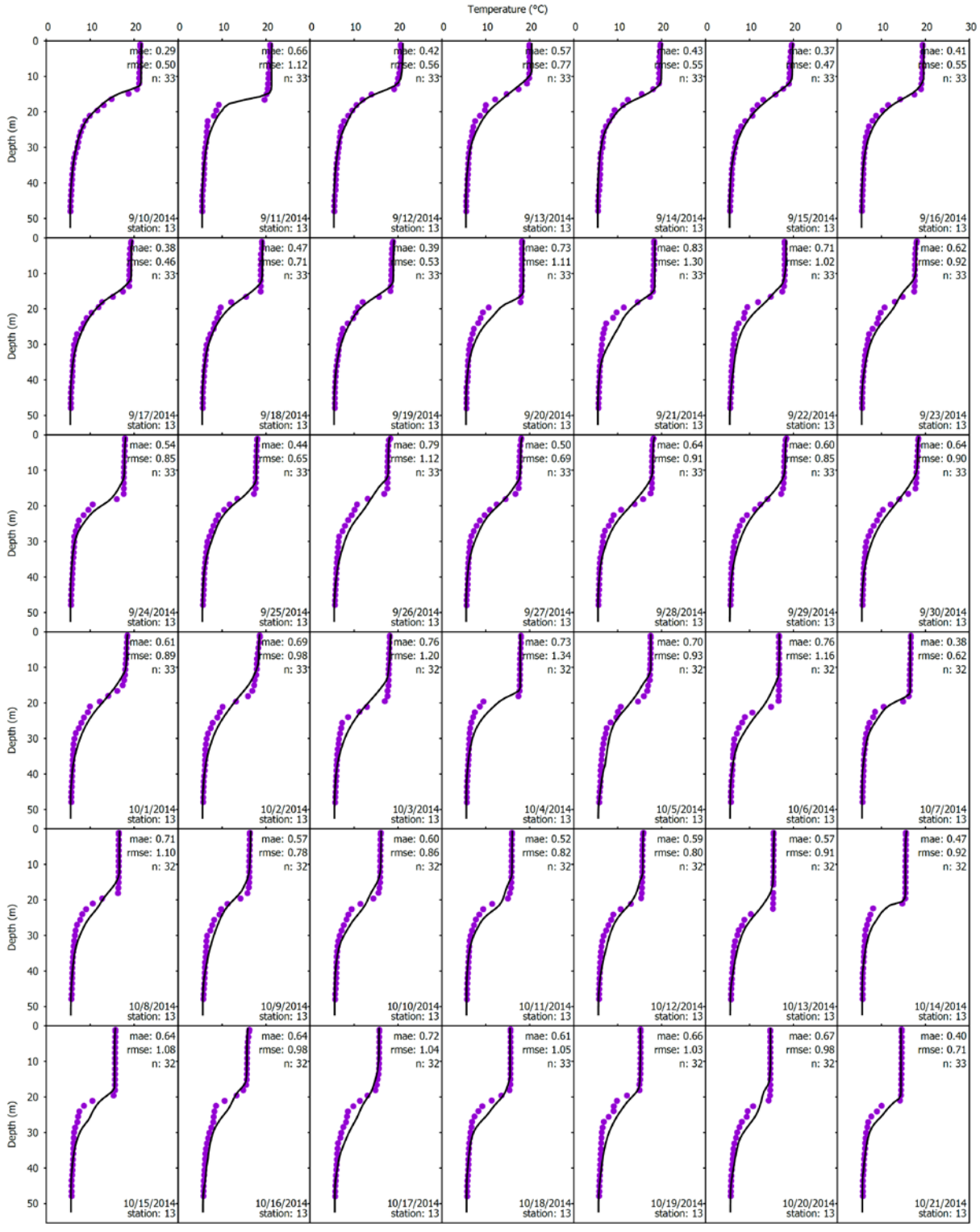


**Figure E-15**. Hydrothermal model fit to daily buoy profiles at site 13 (Figure 5-14) on Owasco Lake for confirmation year, 2014 page 3 of 4.

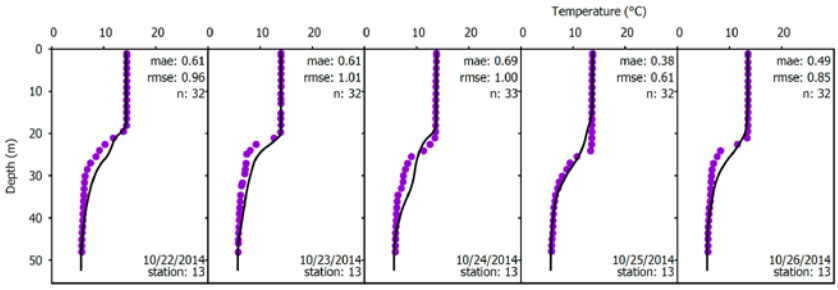


**Figure E-15**. Hydrothermal model fit to daily buoy profiles at site 13 (Figure 5-14) on Owasco Lake for confirmation year, 2014 page 4 of 4.

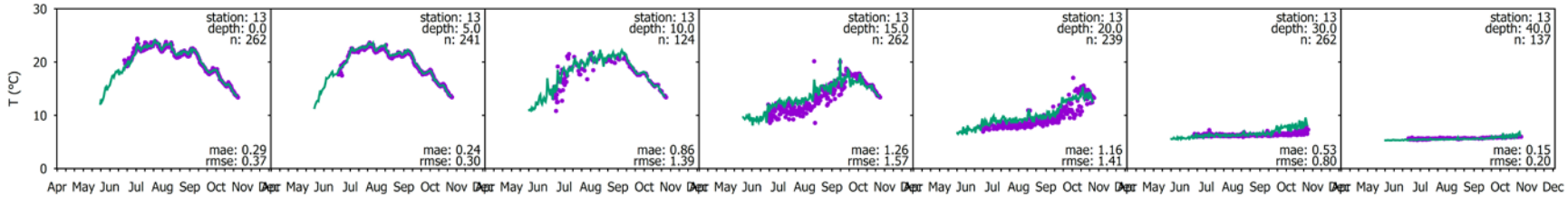


**Figure E-16**. Time series of hydrothermal model fit to daily buoy profiles at site 13 (Figure 5-14) on Owasco Lake for primary confirmation year, 2014 at seven depths, 0, 5, 10, 15, 20, 30, and 40m.

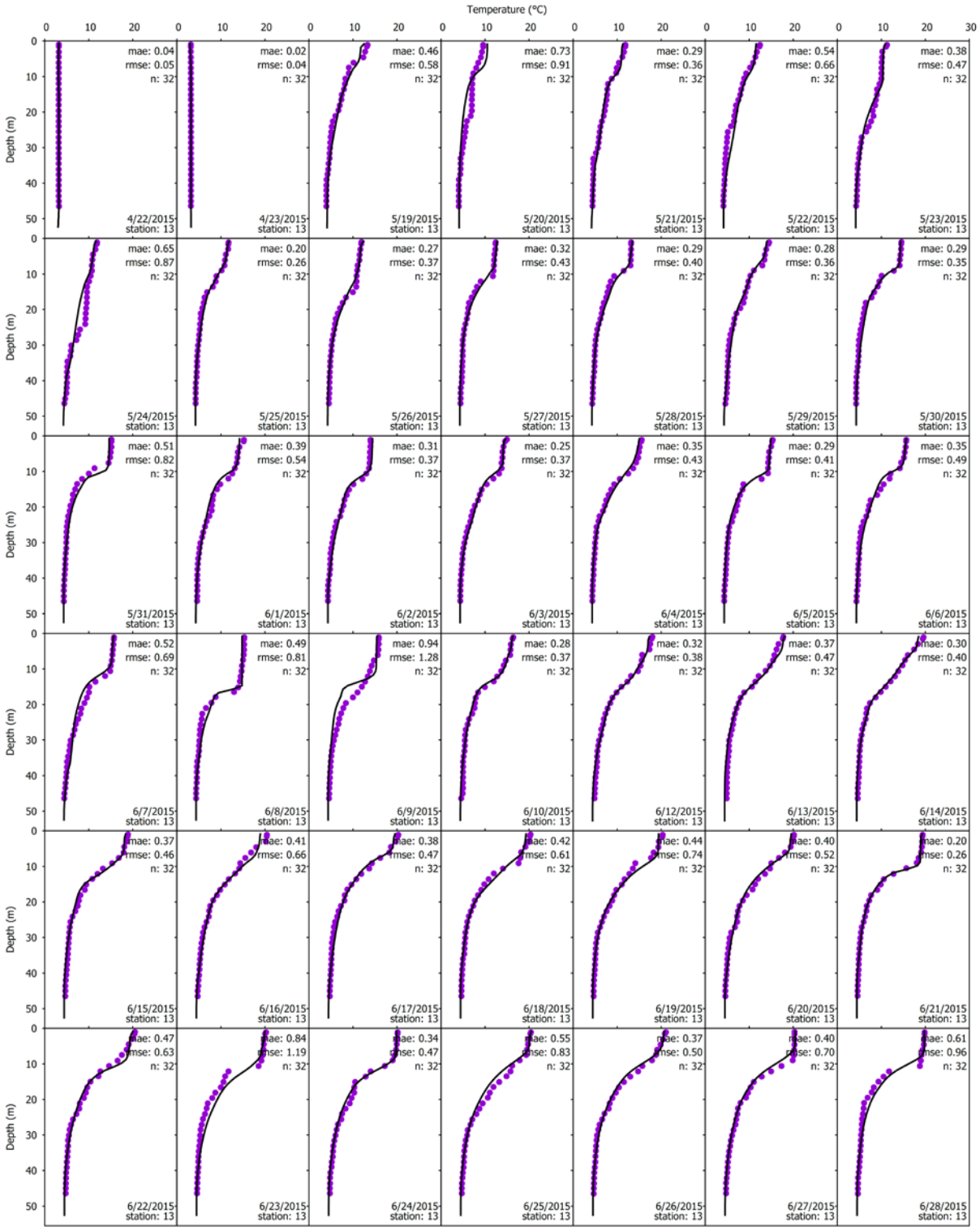


**Figure E-17**. Hydrothermal model fit to daily buoy profiles at site 13 (Figure 5-14) on Owasco Lake for confirmation year, 2015 page 1 of 4.

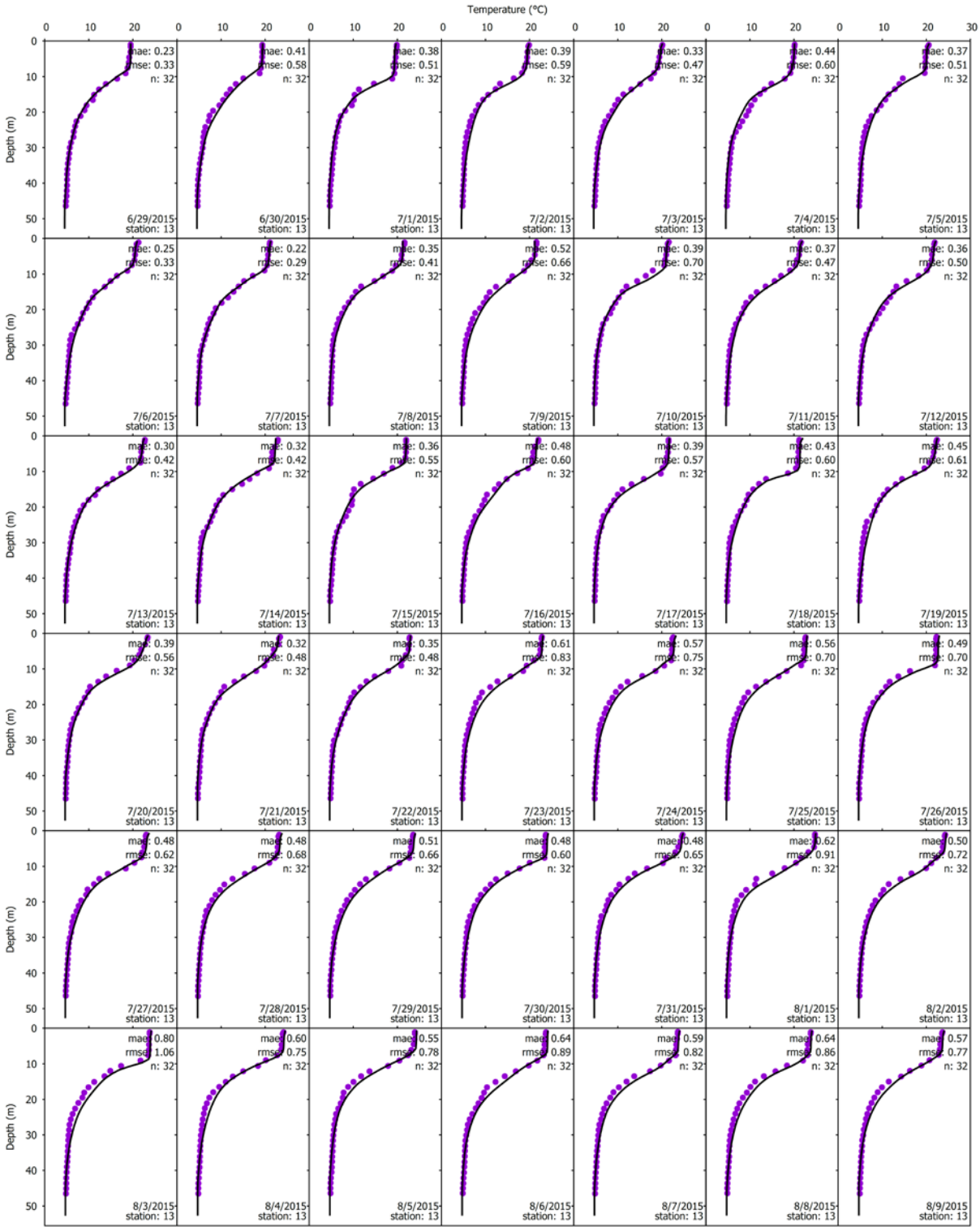


**Figure E-17**. Hydrothermal model fit to daily buoy profiles at site 13 (Figure 5-14) on Owasco Lake for confirmation year, 2015 page 2 of 4.

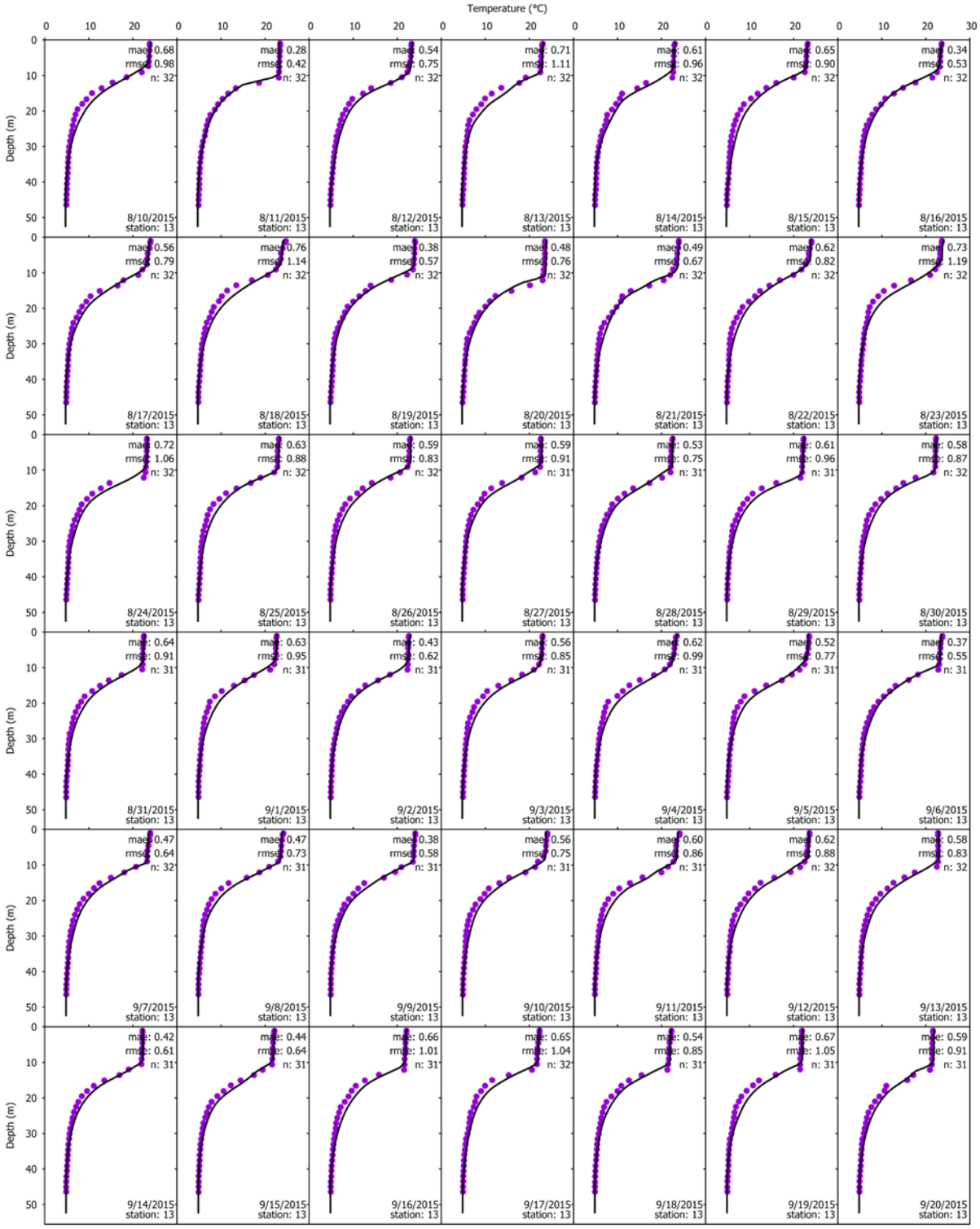


**Figure E-17**. Hydrothermal model fit to daily buoy profiles at site 13 (Figure 5-14) on Owasco Lake for confirmation year, 2015 page 3 of 4.

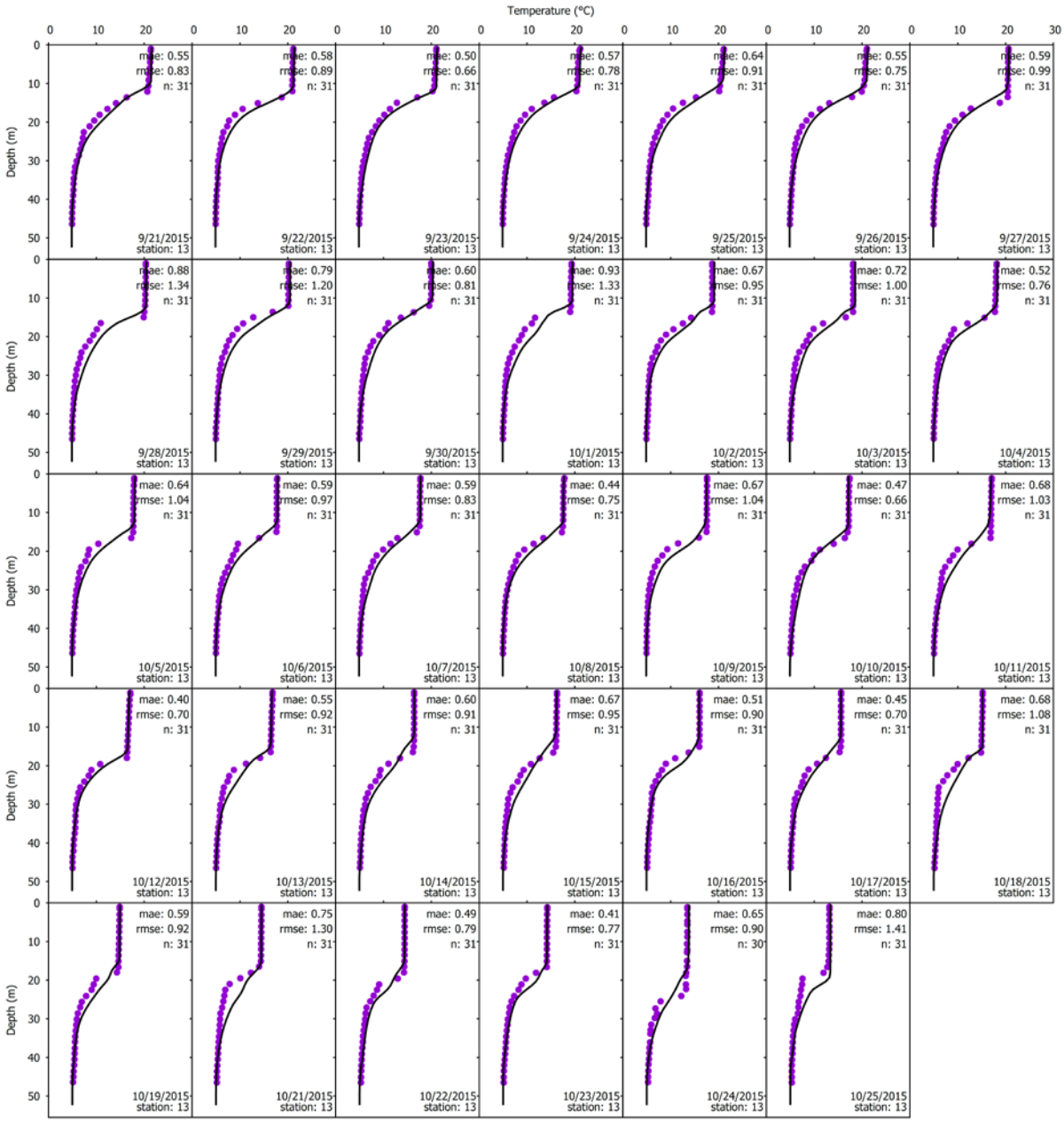


**Figure E-17**. Hydrothermal model fit to daily buoy profiles at site 13 (Figure 5-14) on Owasco Lake for confirmation year, 2015 page 4 of 4.

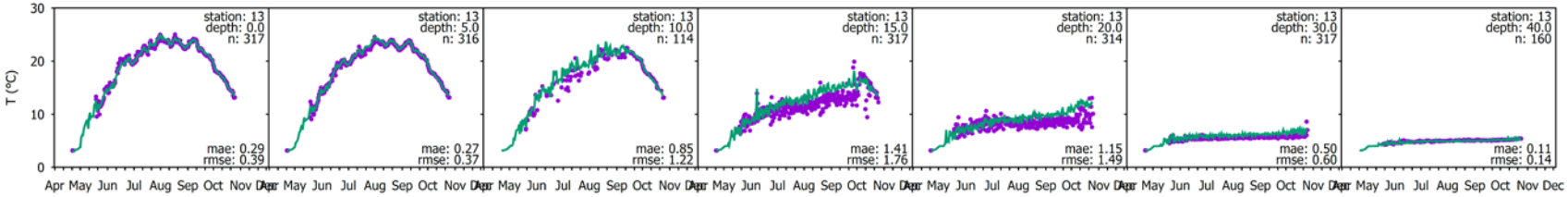


**Figure E-18**. Time series of hydrothermal model fit to daily buoy profiles at site 13 (Figure 5-14) on Owasco Lake for primary confirmation year, 2015 at seven depths, 0, 5, 10, 15, 20, 30, and 40 m.

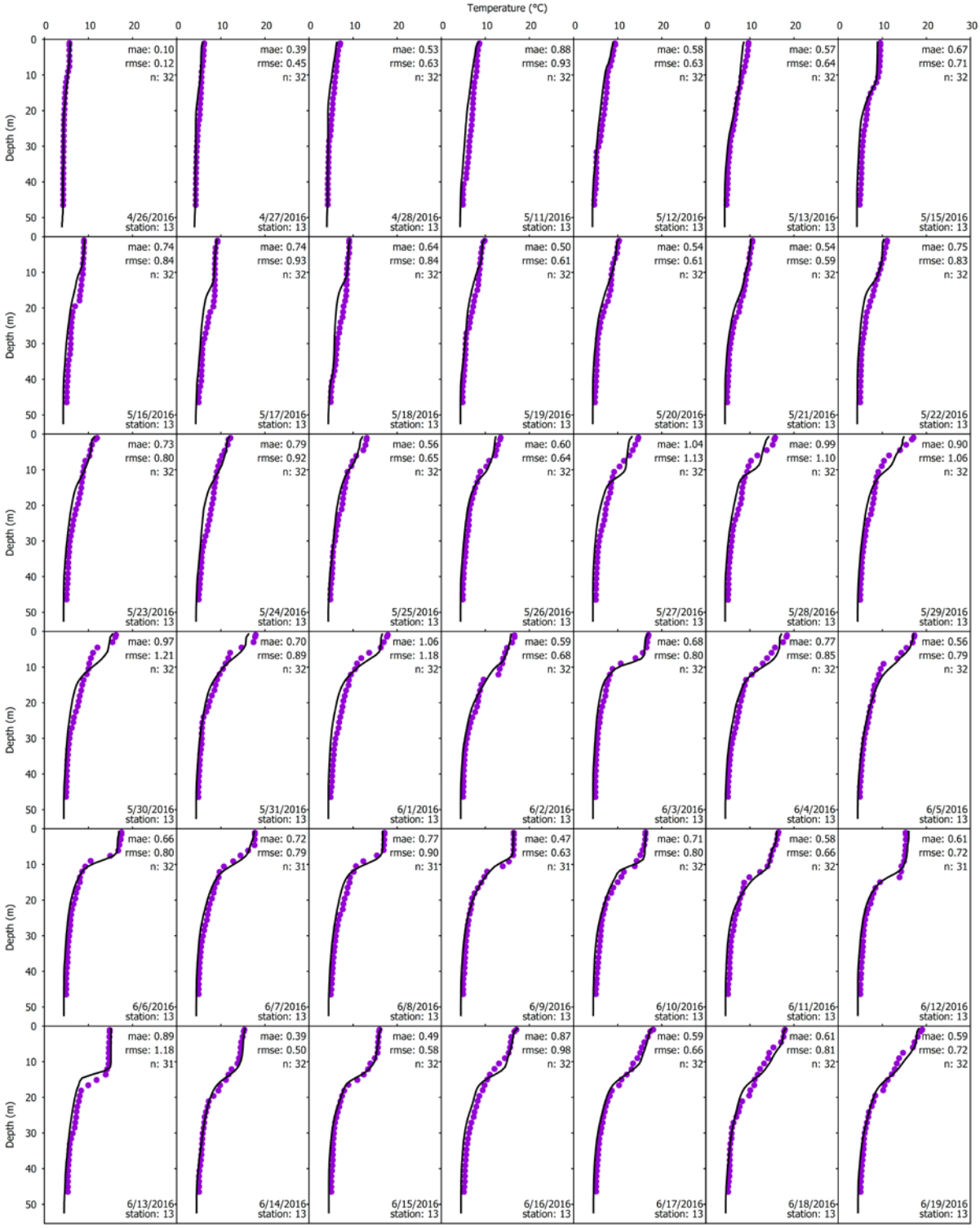


**Figure E-19**. Hydrothermal model fit to daily buoy profiles at site 13 (Figure 5-14) on Owasco Lake for confirmation year, 2016 page 1 of 4.

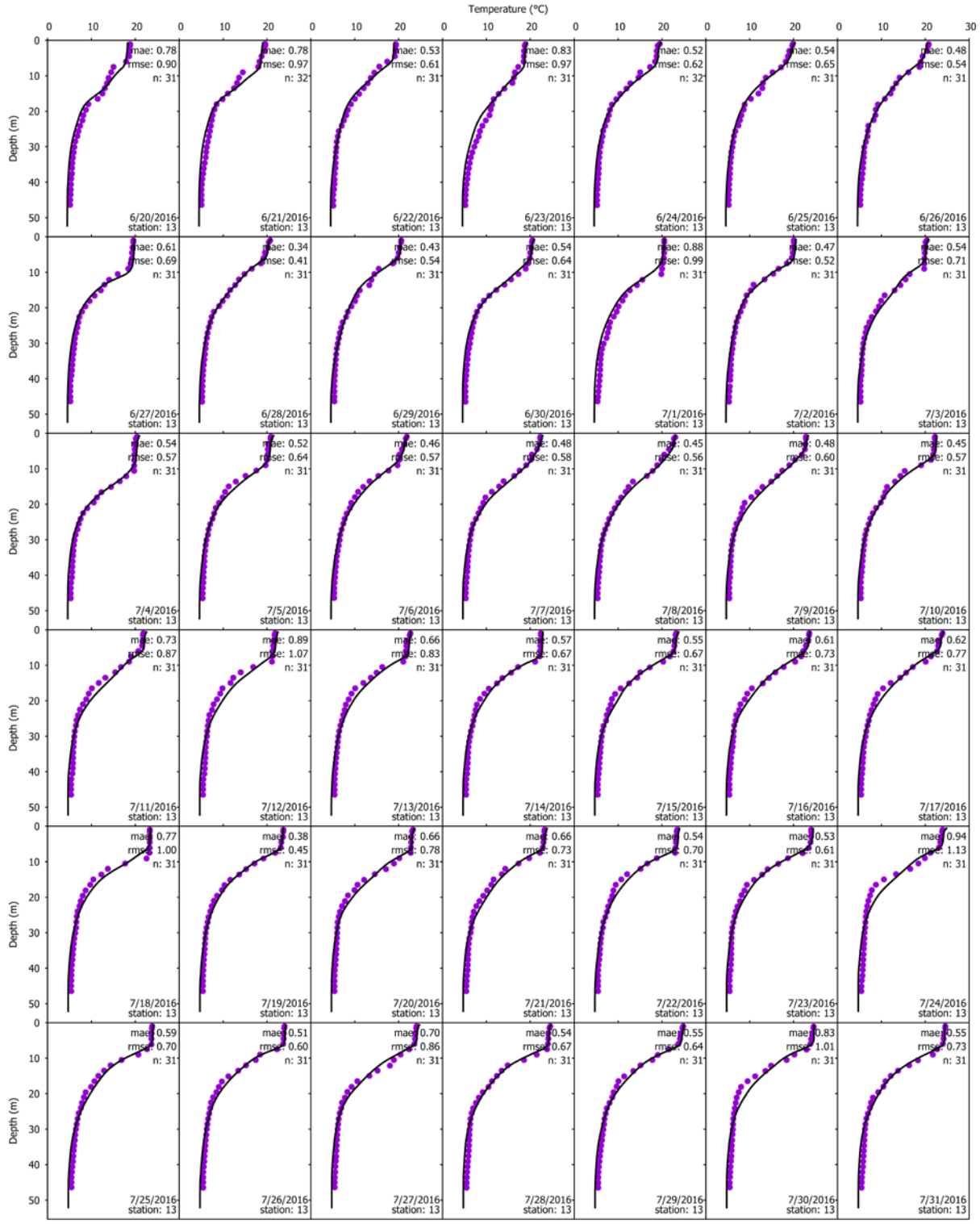


**Figure E-19**. Hydrothermal model fit to daily buoy profiles at site 13 (Figure 5-14) on Owasco Lake for confirmation year, 2016 page 2 of 4.

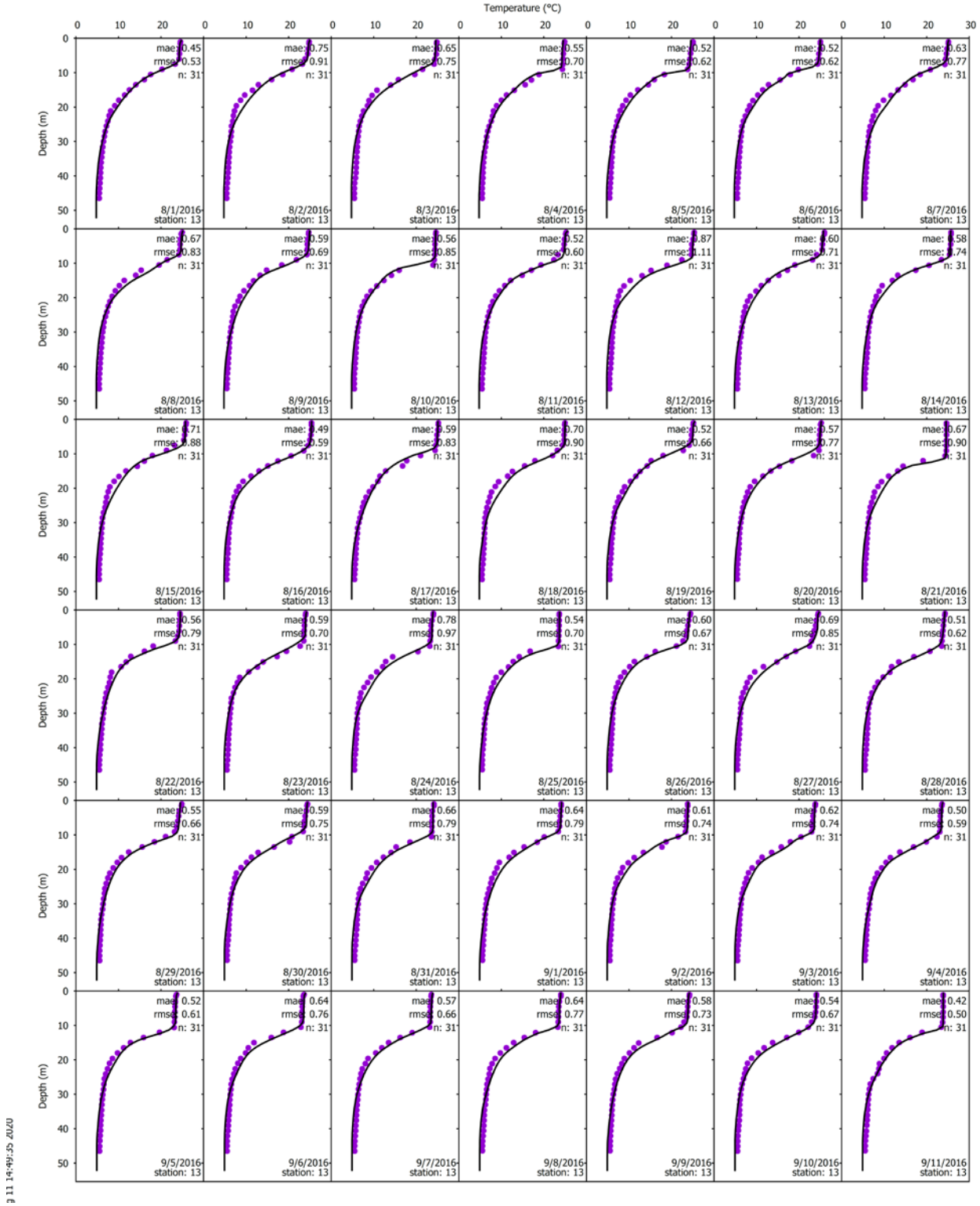


**Figure E-19**. Hydrothermal model fit to daily buoy profiles at site 13 (Figure 5-14) on Owasco Lake for confirmation year, 2016 page 3 of 4.

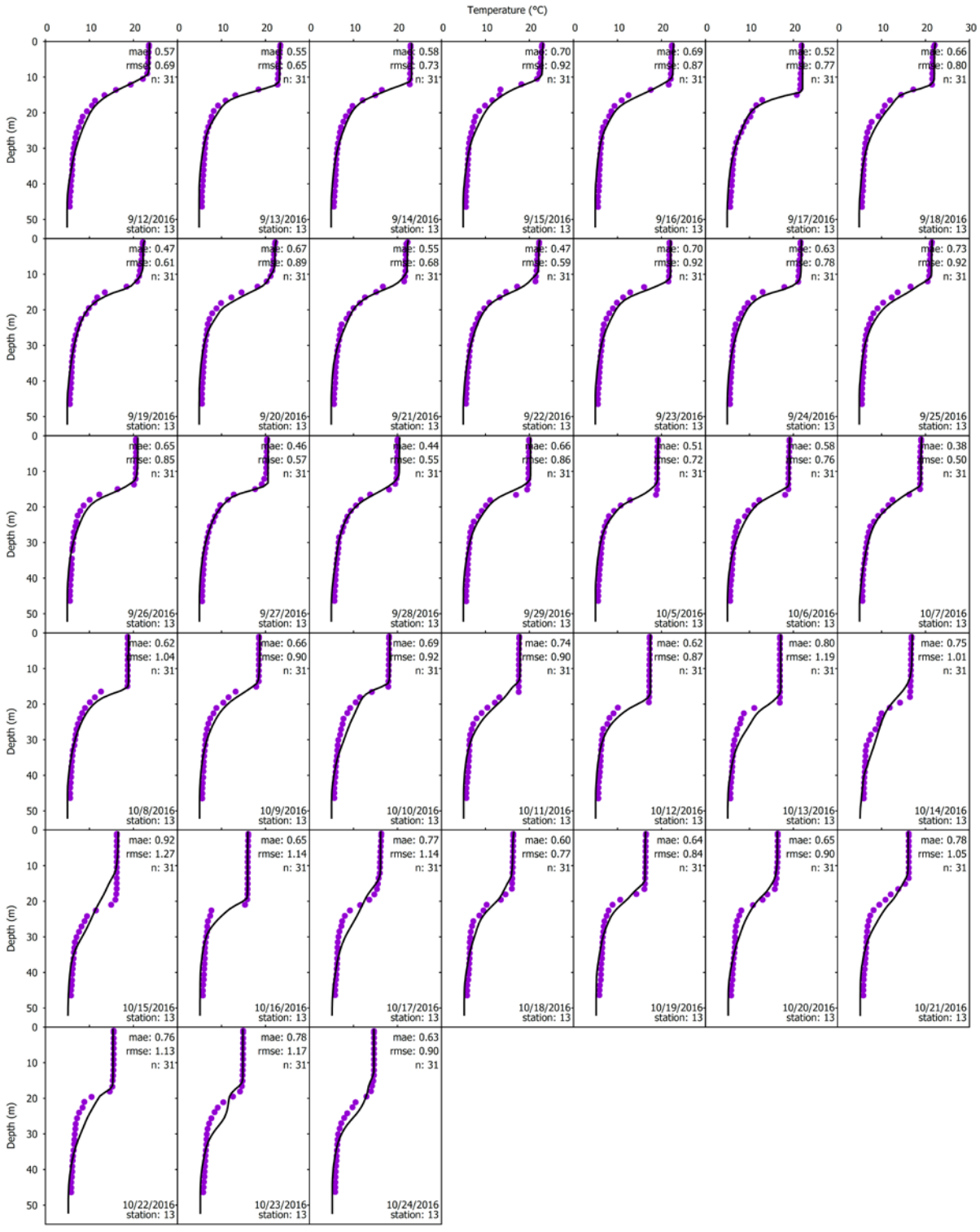


**Figure E-19**. Hydrothermal model fit to daily buoy profiles at site 13 (Figure 5-14) on Owasco Lake for confirmation year, 2016 page 4 of 4.

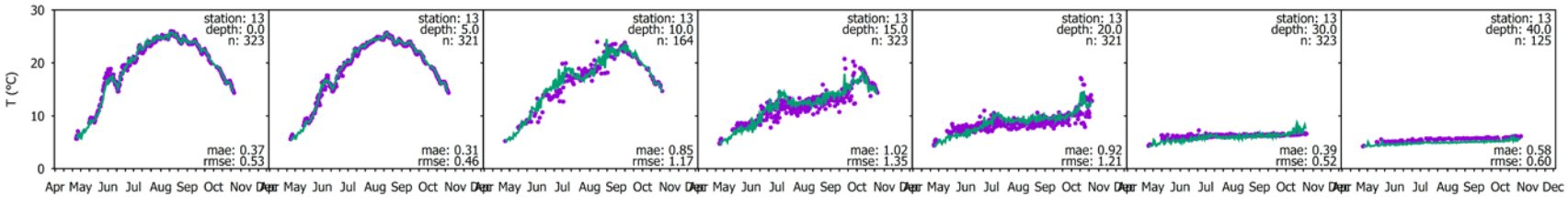


**Figure E-20**. Time series of hydrothermal model fit to daily buoy profiles at site 13 (Figure 5-14) on Owasco Lake for primary confirmation year, 2016 at seven depths, 0, 5, 10, 15, 20, 30, and 40m.

# Appendix F: Water Quality

## Appendix F-1 Model Coefficients

**Table F-1**. Algal kinetics for calibration/confirmation of the Owasco Lake water quality sub-model (A1 is diatoms, A2 is others (not diatoms or cyanobacteria), A3 is cyanobacteria).

| Coefficient | unit | Abbreviation | W2 default | Calibration | | |
|---|---|---|---|---|---|---|
| | | | | Algal group | | |
| | | | | A1 | A2 | A3 |
| maximum algal growth rate | 1/d | AG | 2.0 | 2.5 | 2.75 | 1.75 |
| maximum algal respiration rate | 1/d | AR | 0.04 | 0.04 | .04 | 0.04 |
| maximum algal excretion rate | 1/d | AE | 0.04 | 0.02 | 0.02 | 0.02 |
| maximum algal mortality rate | 1/d | AM | 0.1 | 0.08 | 0.8 | 0.08 |
| algal settling rate | m/d | AS | 0.1 | 0.20 | 0.10 | -0.50 |
| algal half-saturation for phosphorus limited growth | mg/L | AHSP | 0.003 | 0.003 | 0.003 | 0.003 |
| algal half-saturation for nitrogen limited growth | mg/L | AHSN | 0.014 | 0.04 | 0.04 | 0.04 |
| algal half-saturation for silica limited growth | mg/L | AHSSI | 0.0 | 0.30 | 0 | 0 |
| light saturation intensity at maximum photosynthetic rate | W/m2 | ASAT | 100 | 40 | 120 | 100 |
| lower temperature for algal rates (AG, AR, AE, AM) | °C | AT1 | 5 | 4 | 10 | 18 |
| lower temperature for maximum algal rates (AG, AR, AE, AM) | °C | AT2 | 25 | 12 | 16 | 26 |
| upper temperature for maximum algal rates (AG, AR, AE, AM) | °C | AT3 | 35 | 16 | 28 | 30 |
| upper temperature for algal rates (AG, AR, AE, AM) | °C | AT4 | 40 | 30 | 35 | 40 |
| fraction of algal rates at AT1 | unitless | AK1 | 0.1 | 0.1 | 0.1 | 0.1 |
| fraction of maximum algal rate at AT2 | unitless | AK2 | 0.99 | 0.99 | 0.99 | 0.99 |
| fraction of maximum algal rate at AT3 | unitless | AK3 | 0.99 | 0.99 | 0.99 | 0.99 |
| fraction of algal rate at AT4 | unitless | AK4 | 0.1 | 0.1 | 0.1 | 0.1 |
| stoichiometric equivalent between algal phosphorus and algal biomass | mg P/mg algal biomass | ALGP | 0.005 | 0.005 | 0.005 | 0.005 |
| stoichiometric equivalent between algal nitrogen and algal biomass | mg N/mg algal biomass | ALGN | 0.08 | 0.15 | 0.15 | 0.15 |
| stoichiometric equivalent between algal carbon and algal biomass | mg C/mg algal biomass | ALGC | 0.45 | 0.45 | 0.45 | 0.45 |
| stoichiometric equivalent between algal silica and algal biomass | mg Si/mg algal biomass | ALGSI | 0.18 | 0.26 | 0 | 0 |
| ratio between algal biomass and chlorophyll-*a* | mg algal biomass/µg Chl-a | ACHLA | 0.05 | 0.10 | 0.10 | 0.10 |
| fraction of algal biomass that is converted to particulate organic matter when algae die | unitless | ALPOM | 0.8 | 0.8 | 0.8 | 0.8 |
| equation number for algal ammonium preference (1 = simple, 2 = complex) | unitless | ANEQN | 2 | 2 | 2 | 2 |
| half saturation constant for ammonium preference | mgN/L | ANPR | 0.001 | 0.02 | 0.02 | 0.02 |

**Table F**-2. Zooplankton kinetics for calibration/confirmation of the Owasco Lake water quality sub-model (one zooplankton group - herbivores).

| Coefficient | Unit | Abbreviation | W2 default | Calibration |
|---|---|---|---|---|
| | | | | Zooplankton group |
| | | | | Z1 |
| maximum zooplankton growth rate or ingestion rate | 1/d | ZG | 1 | 0.7 |
| maximum zooplankton respiration rate | 1/d | ZR | 0.1 | 0.15 |
| maximum zooplankton mortality (non-predatory) rate | 1/d | ZM | 0.1 | 0.15 |
| zooplankton assimilation efficiency or proportion of food assimilated to food consumed | unitless | ZEFF | 0.5 | 0.5 |
| preference factor of zooplankton for detritus or lPOM | unitless | PREFP | 0.5 | 0.5 |
| threshold food concentration at which zooplankton feeding begins | mg alg bio/L | ZOOMIN | 0.01 | 0.02 |
| zooplankton half saturation constant for food (includes LPOM, algae and zoops. ) | mg alg bio/L | ZS2P | 0.3 | 0.30 |
| preference factor of zooplankton for algae | unitless | PREFA | 0.5 | 1, 1, 0.1 |
| preference factor of zooplankton for zooplankton | unitless | PREFZ | 0.0 | 0 |
| lower temperature for zooplankton rates (ZG, ZR, ZM) | °C | ZT1 | 5 | 4 |
| lower temperature for maximum zooplankton rates (ZG, ZR, ZM) | °C | ZT2 | 25 | 16 |
| upper temperature for maximum zooplankton rates (ZG, ZR, ZM) | °C | ZT3 | 35 | 26 |
| upper temperature for zooplankton rates (ZG, ZR, ZM) | °C | ZT4 | 40 | 35 |
| fraction of zooplankton rates (ZG, ZR, ZM) at ZT1 | unitless | ZK1 | 0.1 | 0.1 |
| fraction of zooplankton rates (ZG, ZR, ZM) at ZT2 | unitless | ZK2 | 0.99 | 0.99 |
| fraction of zooplankton rates (ZG, ZR, ZM) at ZT3 | unitless | ZK3 | 0.99 | 0.99 |
| fraction of zooplankton rates (ZG, ZR, ZM) at ZT4 | unitless | ZK4 | 0.1 | 0.1 |
| stoichiometric equivalent between zooplankton phosphorus and zooplankton biomass | gP/g Zoo biomass | ZP | 0.005 | 0.005 |
| stoichiometric equivalent between zooplankton nitrogen and zooplankton biomass | gN/g Zoo biomass | ZN | 0.08 | 0.08 |
| stoichiometric equivalent between zooplankton carbon and zooplankton biomass | µgC/µg zoo biomass | ZC | 0.45 | 0.45 |

**Table F-3**. Organic matter coefficients.

| Coefficient | unit | Abbreviation | W2 default | Calibration/ Confirmation |
|---|---|---|---|---|
| labile DOM decay rate | 1/d | LDOMDK | 0.1 | 0.07 |
| refractory DOM decay rate | 1/d | RDOMDK | 0.001 | 0.001 |
| labile to refractory DOM decay rate | 1/d | LRDDK | 0.01 | 0.005 |
| labile POM decay rate | 1/d | LPOMDK | 0.08 | 0.1 |
| refractory POM decay rate | 1/d | RPOMDK | 0.001 | 0.001 |
| labile to refractory POM decay rate | 1/d | LRPDK | 0.01 | 0.005 |
| POM settling rate | m/d | POMS | 0.1 | 0.1 |
| stoichiometric equivalent between phosphorus and organic matter | µgP/µg OM | ORGP | 0.005 | 0.005 |
| stoichiometric equivalent between nitrogen and organic matter | µgN/µg OM | ORGN | 0.08 | 0.08 |
| stoichiometric equivalent between carbon and organic matter | µgC/µg OM | ORGC | 0.45 | 0.45 |
| stoichiometric equivalent between silica and organic matter | µgSi/µg OM | ORGSI | 0.18 | 0.18 |
| lower temperature for organic matter decay | °C | OMT1 | 4 | 5 |
| upper temperature for organic matter decay | °C | OMT2 | 25 | 25 |
| fraction of organic matter decay rate at OMT1 | unitless | OMK1 | 0.1 | 0.1 |
| fraction of organic matter decay rate at OMT2 | unitless | OMK2 | 0.99 | 0.99 |

**Table F-4**. Phosphorus, nitrogen and silica coefficients.

| Coefficient | unit | Abbreviation | W2 default | Calibration/ confirmation |
|---|---|---|---|---|
| sediment release rate of phosphorus, fraction of SOD | unitless | PO4R | 0.001 | 0 |
| phosphorus partitioning coefficient for suspended solids | unitless | PARTP | 0 | 0 |
| sediment release of ammonium fraction of SOD | unitless | NH4R | 0.001 | 0.001 |
| ammonium decay (nitrification - requires DO) | 1/d | NH4DK | 0.12 | 0.08 |
| lower temperature for ammonia decay | °C | NH4T1 | 5 | 5 |
| upper temperature for ammonia decay | °C | NH4T2 | 25 | 24.5 |
| fraction of nitrification rate at NH4K1 | unitless | NH4K1 | 0.1 | 0.1 |
| fraction of nitrification rate at NH4K2 | unitless | NH4K2 | 0.99 | 0.99 |
| water column denitrification rate or nitrate decay rate (requires DO to be gone) | 1/d | NO3DK | 0.03 | 0.03 |
| denitrification rate from sediments | m/d | NO3S | 0.001 | 0.006 |
| fraction of the $NO_X$ that diffused into the sediments that become part of ON in sediments (rest denitrified) | unitless | FNO3SED | 0 | 1 |
| lower temperature for nitrate decay | °C | NO3T1 | 5 | 5 |
| upper temperature for nitrate decay | °C | NO3T2 | 25 | 24 |
| fraction of denitrification rate at NO3T1 | unitless | NO3K1 | 0.1 | 0.1 |
| fraction of denitrification rate at NO3T2 | unitless | NO3K2 | 0.99 | 0.99 |
| dissolved silica sediment release rate, fraction of SOD | unitless | DSIR | 0.1 | 0.1 |
| particulate biogenic silica settling rate | m/d | PSIS | 1 | 1.0 |
| particulate biogenic silica decay rate | 1/d | PSIDK | 0.3 | 0.3 |
| dissolved silica partitioning coefficient | unitless | PARTSI | 0 | 0 |

**Table F-5**. Dissolved oxygen coefficients.

| Coefficient | unit | Abbreviation | W2 default | Calibration/ confirmation |
|---|---|---|---|---|
| sediment carbon dioxide release rate, fraction of sediment oxygen demand (p C-215) | gC/gO2 | CO2Rel | 0.358 | 0.358 |
| oxygen stoichiometry for nitrification (ammonia decay) | mg $O_2$/mg $N_2$ | O2NH4 | 4.57 | 4.57 |
| oxygen stoichiometry for organic matter decay | mg $O_2$/mg organic matter | O2OM | 1.4 | 1.4 |
| oxygen stoichiometry for algal respiration | mgO2/mg algal biomass | O2AR | 1.1 | 1.1 |
| oxygen stoichiometry for algal primary production | mg O2/mg algal biomass | O2AG | 1.4 | 1.8 |
| oxygen stoichiometry for zooplankton respiration | g O2/g dry wt zoo biomass | O2ZR | 1.1 | 1.1 |
| half saturation constant $K_{do}$ in manual O2lIM in control file (concentration at which aerobic processes are at 50%) | mg/L or g/m3 | O2LIM (KDO) | 0.1 | 0.4 |
| fraction of zero order SOD rate used | fSOD | | 1 | 1 |
| lower temperature for zero order SOD | °C | SODT1 | 4 | 4 |
| upper temperature for zero order SOD | °C | SODT2 | 25 | 25 |
| T correction rising limb; fraction of SOD at SODT1 | unitless | SODK1 | 0.1 | 0.1 |
| fraction of SOD at SODT2 | unitless | SODK2 | 0.99 | 0.99 |
| Sediment oxygen demand by segment | g/m2/d | SOD | 0.2 | 2-8, 14-22 =0<br>9-13 0.8 |
| Waterbody type | unitless | REARC | 2 | 2 |
| reaeration equation # see page C-227 or 595 | unitless | EQN# | 6 | 9 |

**Table F-6**. Dreissenid mussel coefficients.

| Coefficient | unit | Abbreviation | Calibration/ confirmation |
|---|---|---|---|
| Turn on mussels | unitless | MUSSELC | ON |
| phosphorus excretion rate | umol/gDW/hr | PEXCR | 0.18 |
| nitrogen excretion rate | umol/gDW/hr | NEXCR | 2.70 |
| oxygen respiration rate | umol/gDW/hr | O2con | 54.0 |
| zebra mussel filtering rate | ml/mg DW/hr | FILTER | 5.0 |
| temperature correction rate for all zebra mussel reactions(Pex,Nex,O2) | unitless | | 1.08 |
| mussel conversion of lPOM to lDOM | unitless | frMUSLD | 0.45 |
| fraction of algal biomass that is converted to lDOM from mussels filtering of algea | unitless | frMUSPF | 0.45 |
| preference for mussel filtering of Alg1 | unitless | perfa | 1.0 |
| preference for mussel filtering of Alg2 | unitless | perfa | 1.0 |
| preference for mussel filtering of Alg3 | unitless | perfa | 0.2 |

**Table F-7**. Other revisions to CE-QUAL-W2.

| Coefficient | unit | Abbreviation | Calibration/ confirmation |
|---|---|---|---|
| Algae minima set for Alg1 used in long-term runs | unitless | minAlg1 | 0.001 |
| Algae minima set for Alg2 used in long-term runs | unitless | minAlg2 | 0.001 |
| Algae minima set for Alg3 used in long-term runs | unitless | minAlg2 | 0.001 |
| SRP loss rate (hypolimnion) | mgP/L/d | SRPrate | 0.001 |
| half saturation on loss | µgP/L | 1/2Sat | 0.002 |
| Fraction of SRP to labile particulate (remainder to refractory) | unitless | frPO4LP | 0.5 |

## Appendix F-2 Calibration of the Water Quality Sub-model, 2018

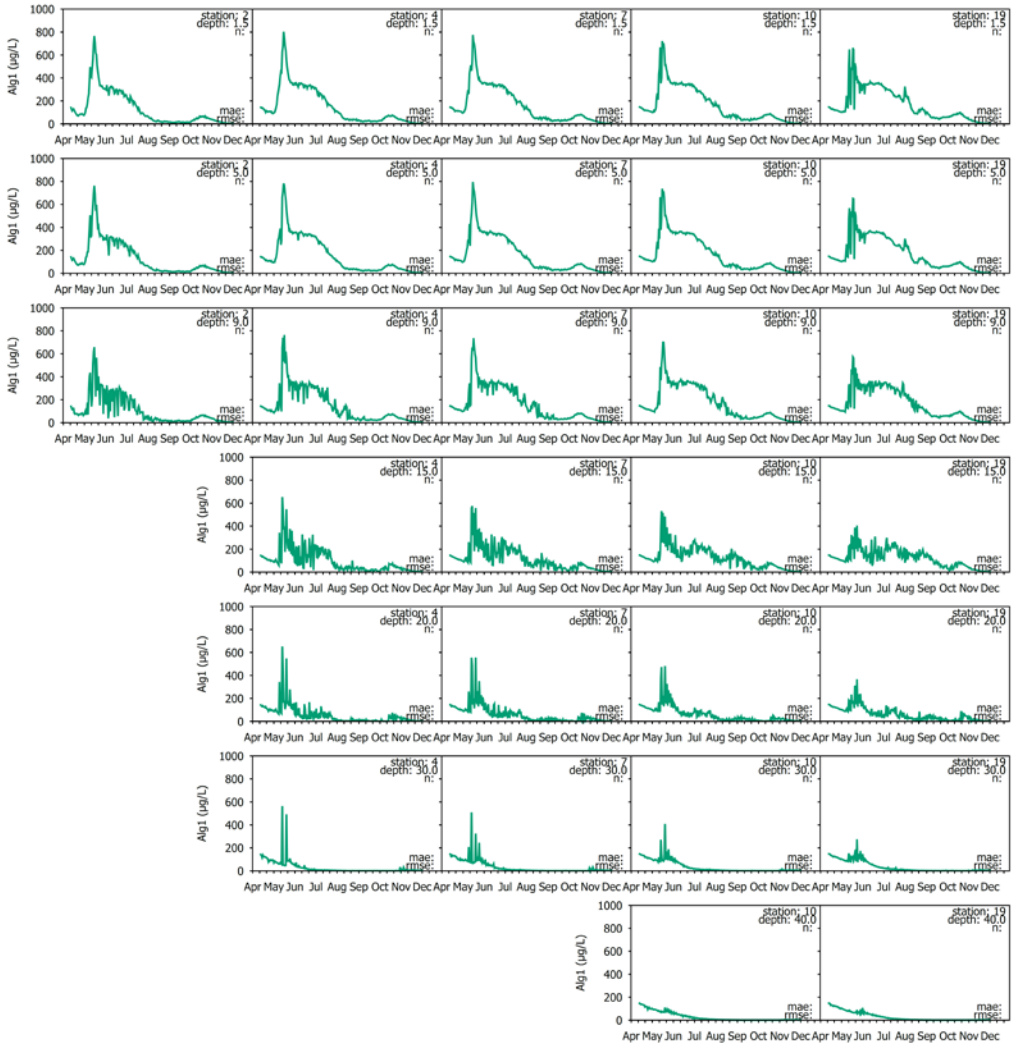


**Figure F-1**. Time series of 2018 model predictions and observations when available at multiple sites (2, 4, 7, 10 and 19 and at multiple depths (1, 5, 9, 15, 20, 30 and 40 m) for Alg1.

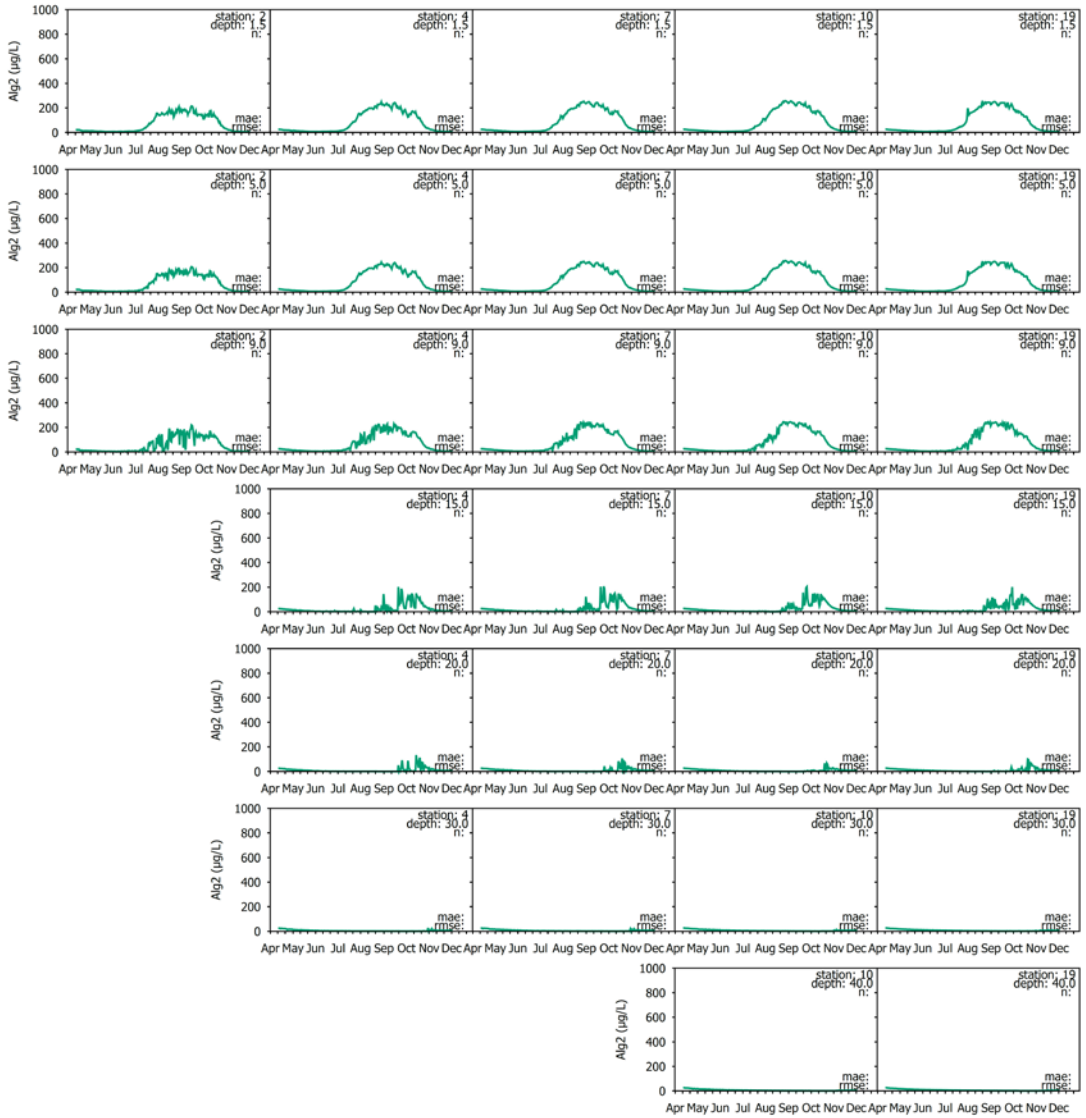


**Figure F-2**. Time series of 2018 model predictions and observations when available at multiple sites (2, 4, 7, 10 and 19 and at multiple depths (1, 5, 9, 15, 20, 30 and 40 m) for Alg2.

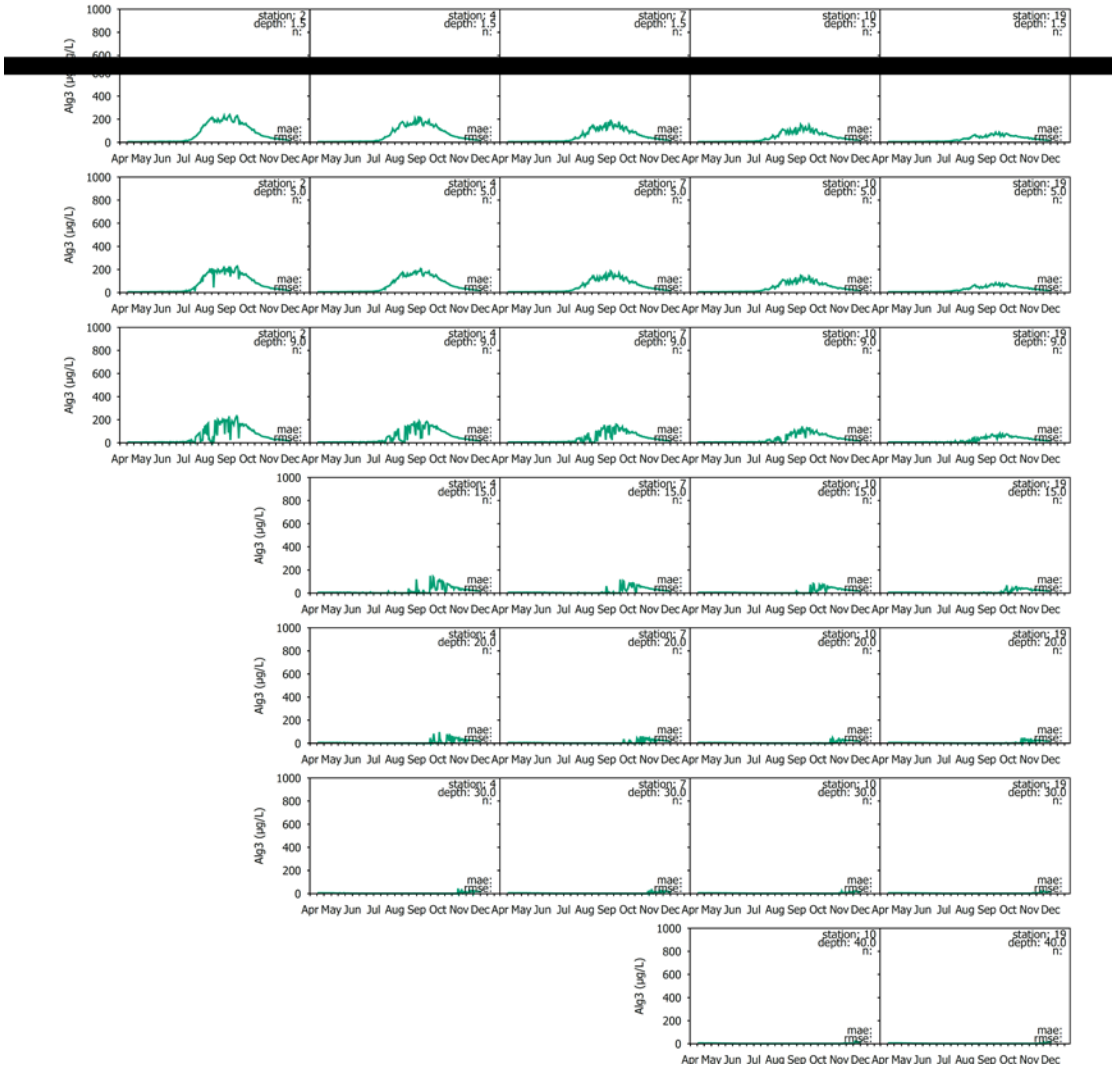


**Figure F-3**. Time series of 2018 model predictions and observations when available at multiple sites (2, 4, 7, 10 and 19 and at multiple depths (1, 5, 9, 15, 20, 30 and 40 m) for Alg3.

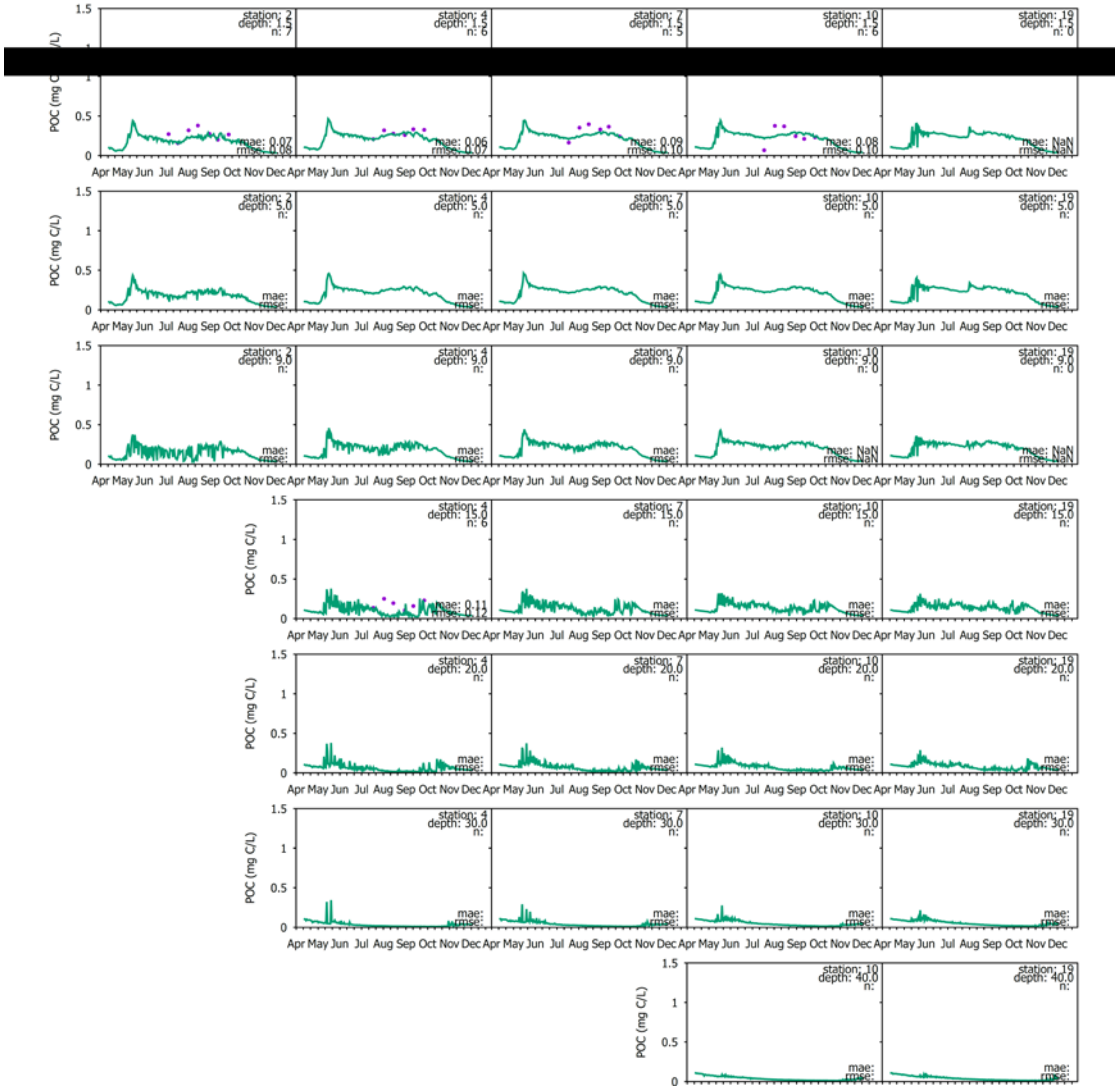


**Figure F-4**. Time series of 2018 model predictions and observations when available at multiple sites (2, 4, 7, 10 and 19 and at multiple depths (1, 5, 9, 15, 20, 30 and 40 m) for POC.

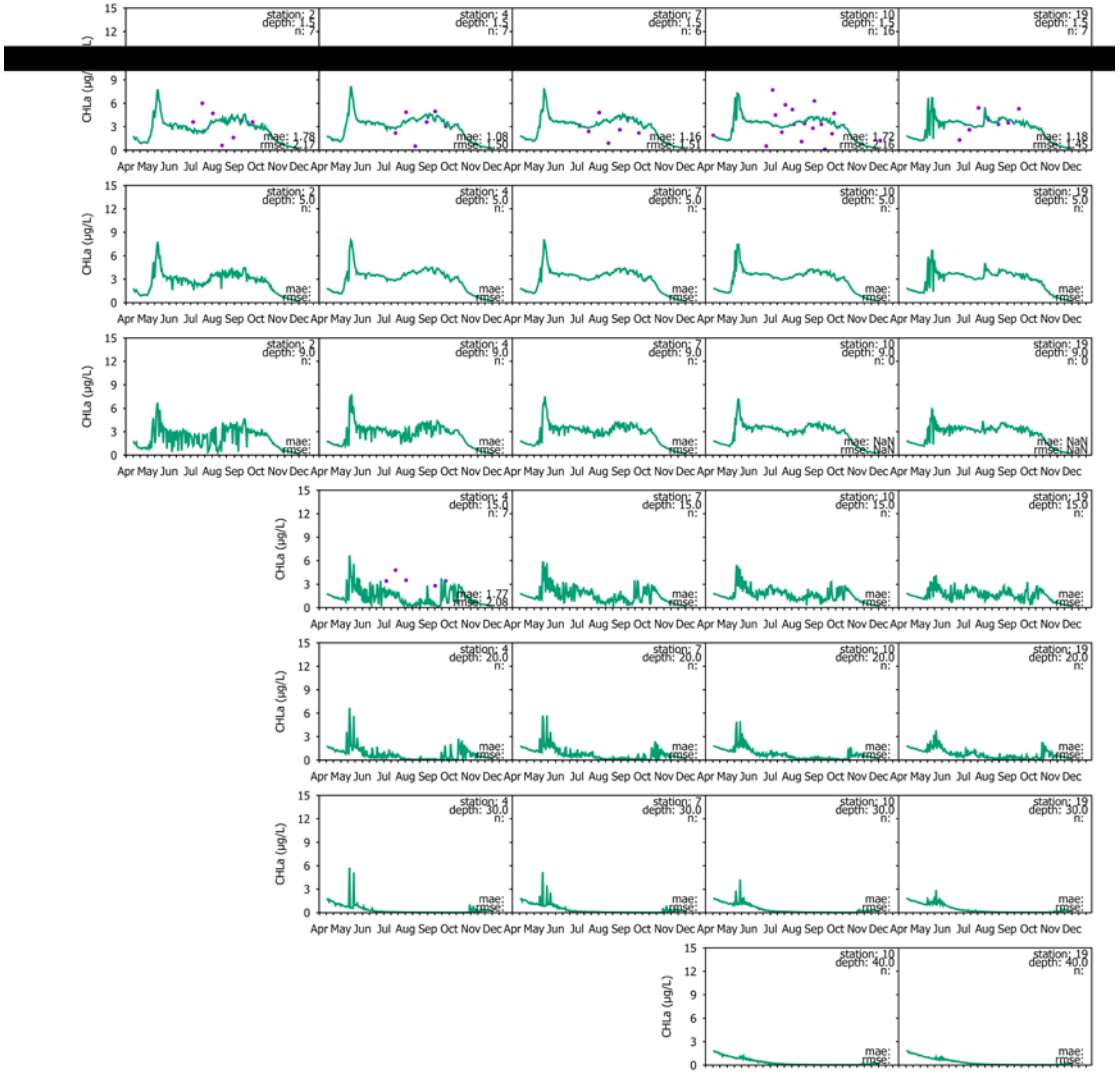


**Figure F-5**. Time series of 2018 model predictions and observations when available at multiple sites (2, 4, 7, 10 and 19 and at multiple depths (1, 5, 9, 15, 20, 30 and 40 m) for Chl-*a*.

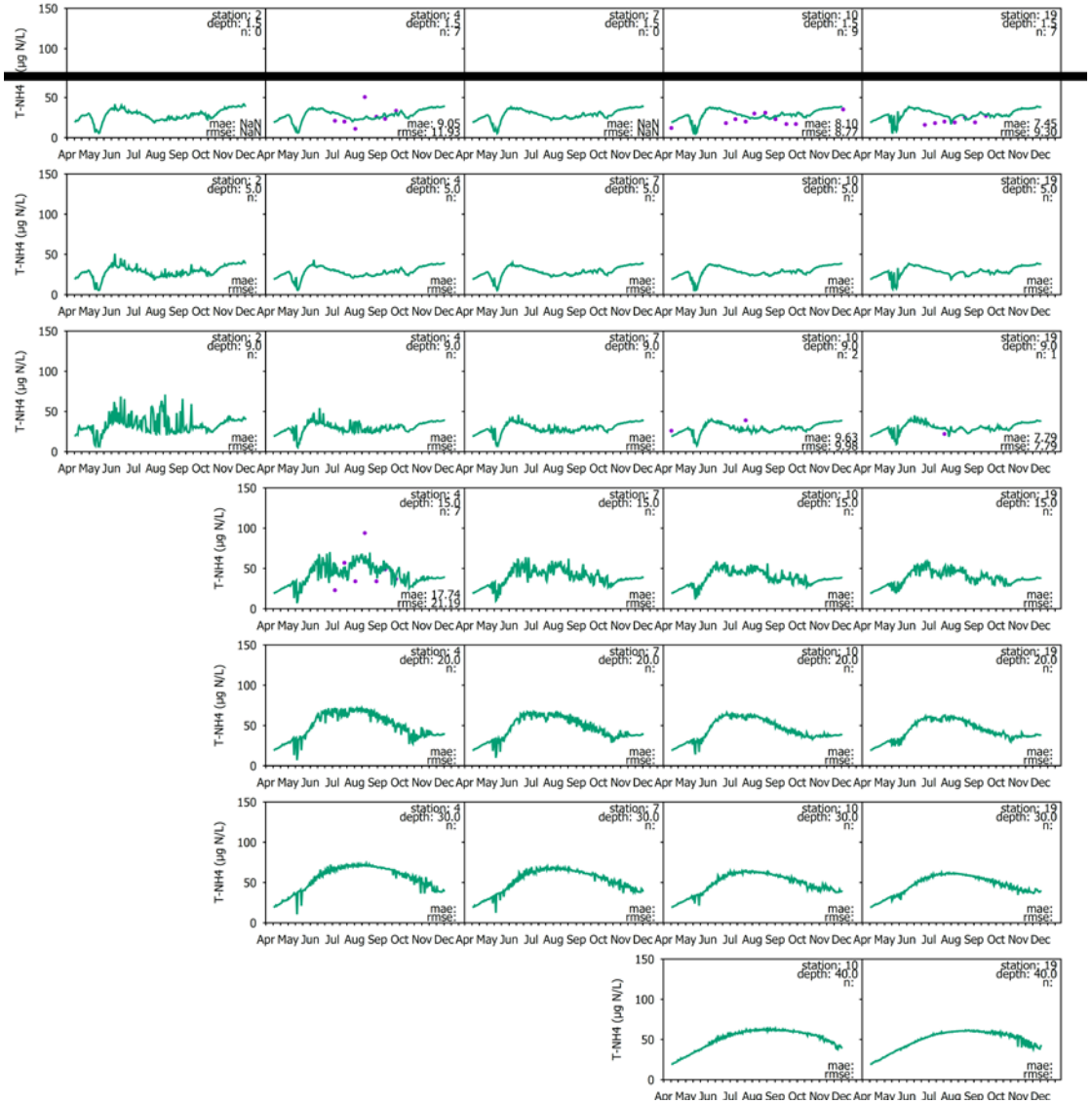


**Figure F-6**. Time series of 2018 model predictions and observations when available at multiple sites (2, 4, 7, 10 and 19 and at multiple depths (1, 5, 9, 15, 20, 30 and 40 m) for $tNH_3$.

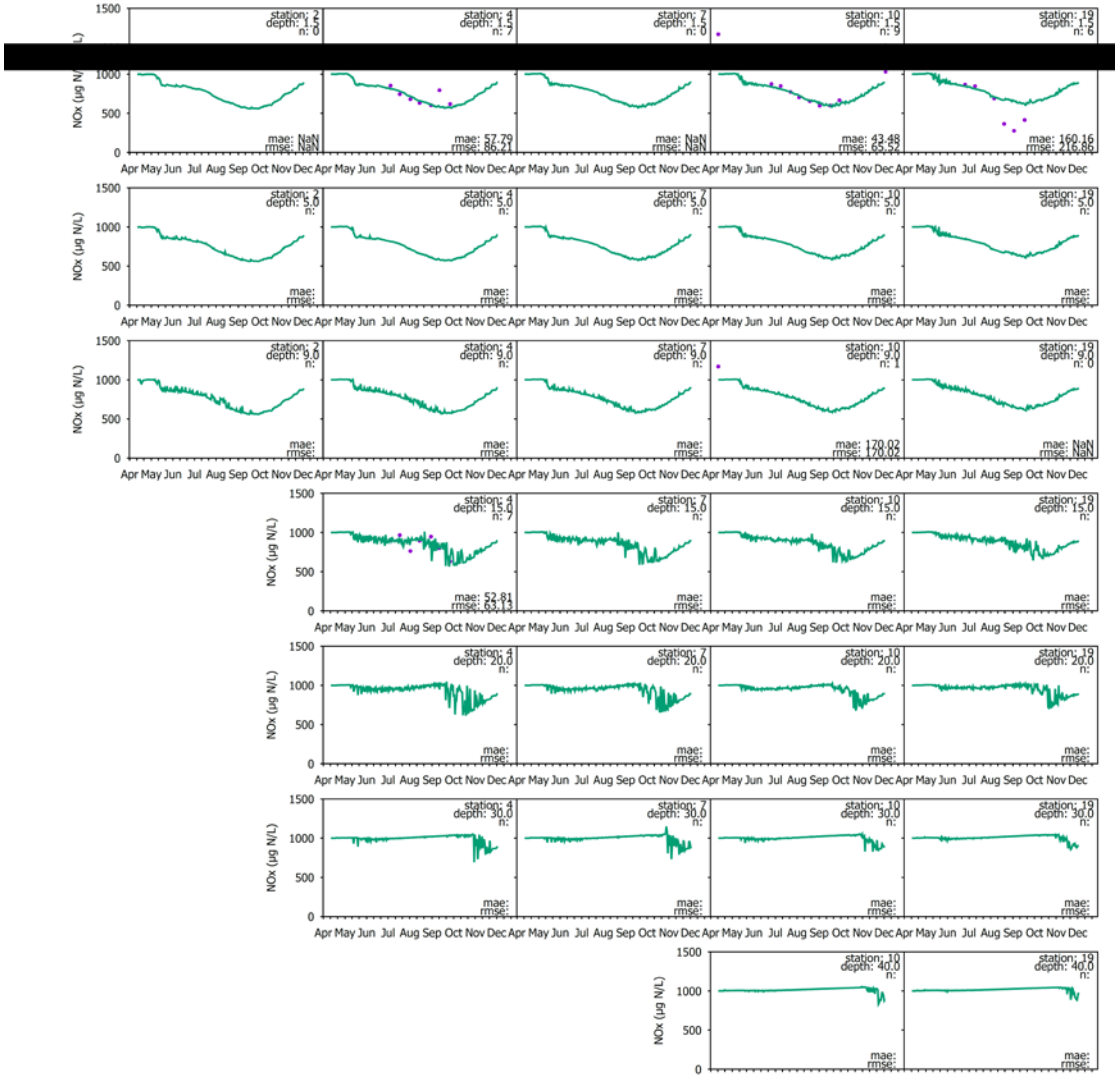


**Figure F-7**. Time series of 2018 model predictions and observations when available at multiple sites (2, 4, 7, 10 and 19 and at multiple depths (1, 5, 9, 15, 20, 30 and 40 m) for $NO_X$.

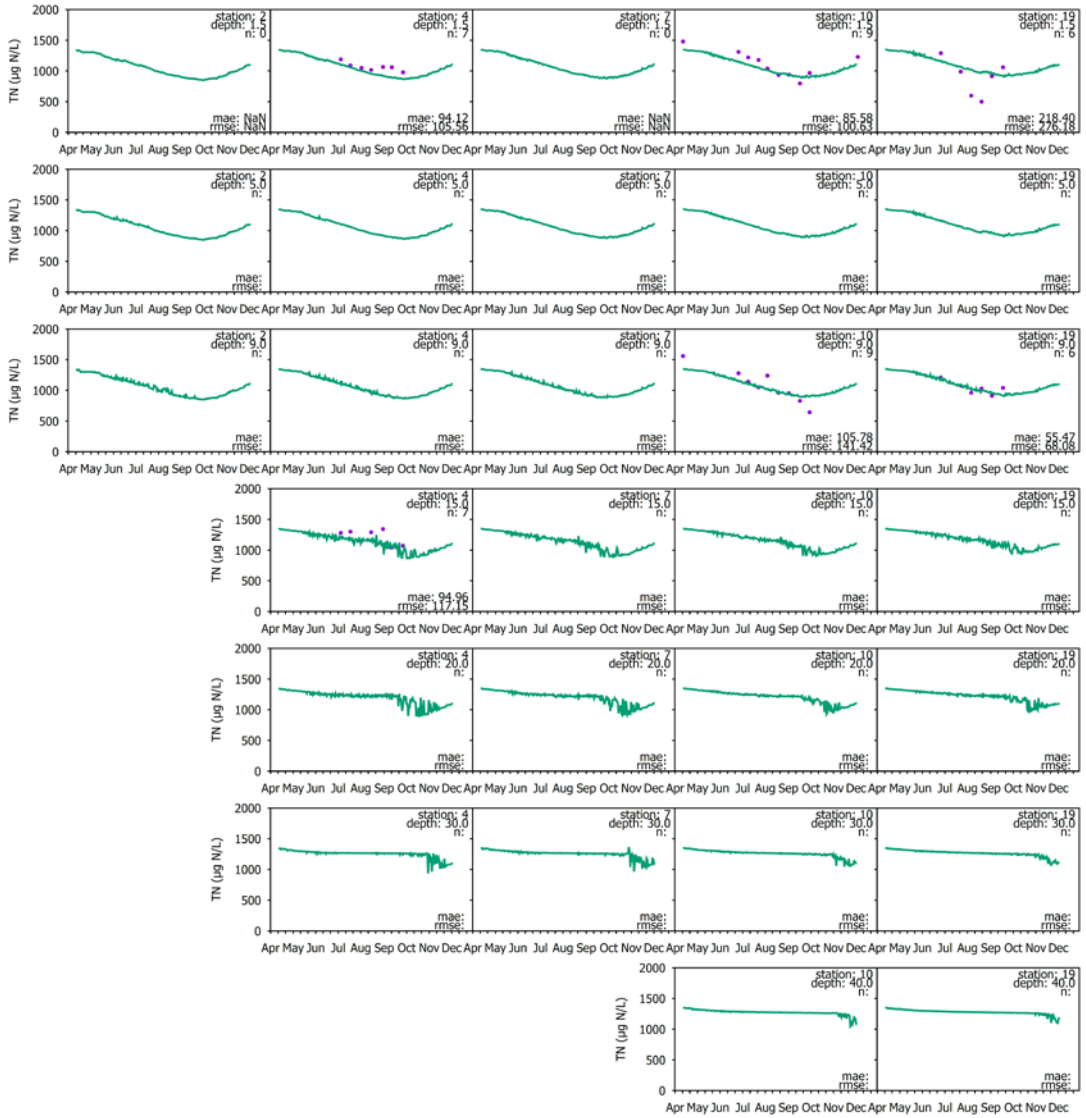


**Figure F-8**. Time series of 2018 model predictions and observations when available at multiple sites (2, 4, 7, 10 and 19 and at multiple depths (1, 5, 9, 15, 20, 30 and 40 m) for TN.

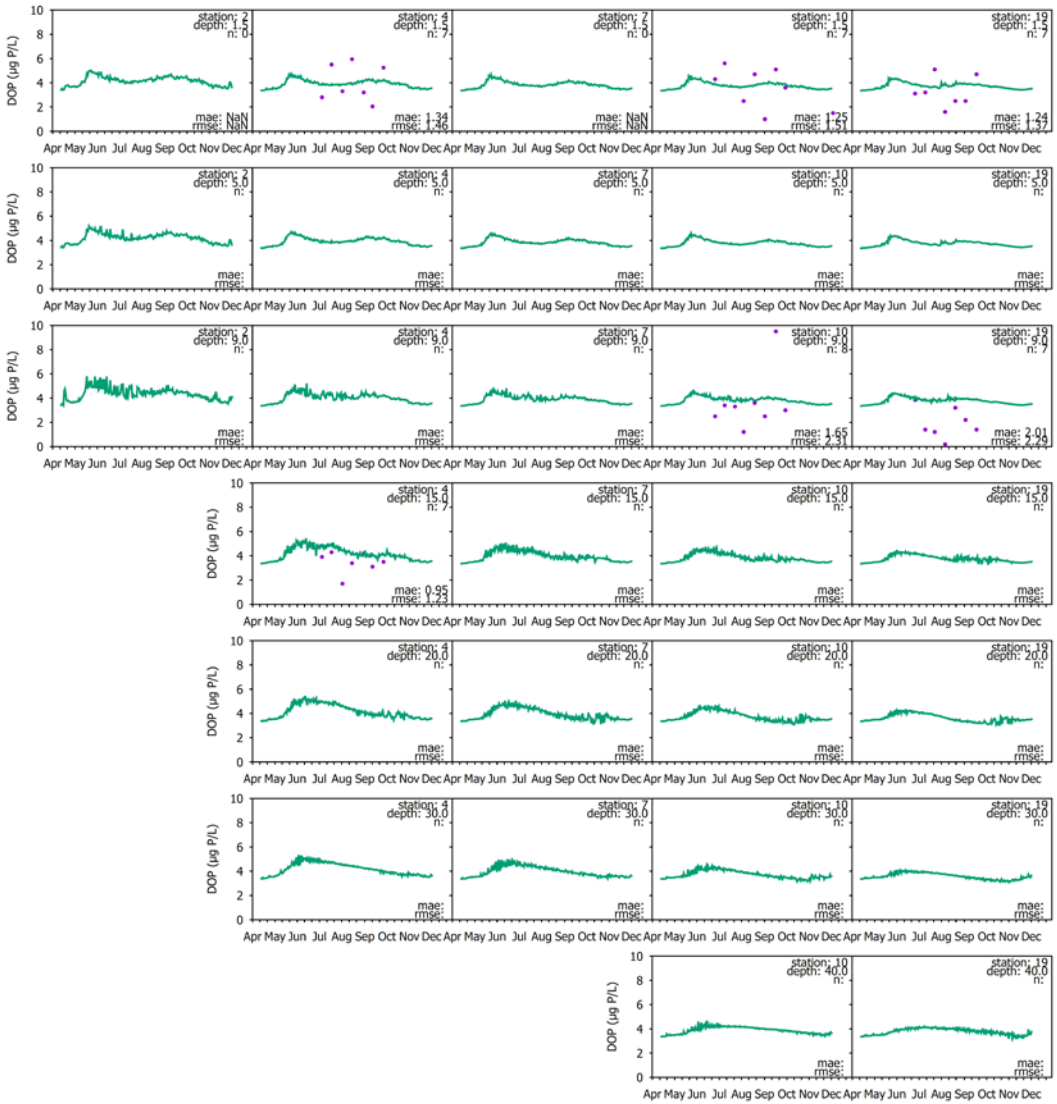


**Figure F-9**. Time series of 2018 model predictions and observations when available at multiple sites (2, 4, 7, 10 and 19 and at multiple depths (1, 5, 9, 15, 20, 30 and 40 m) for DOP.

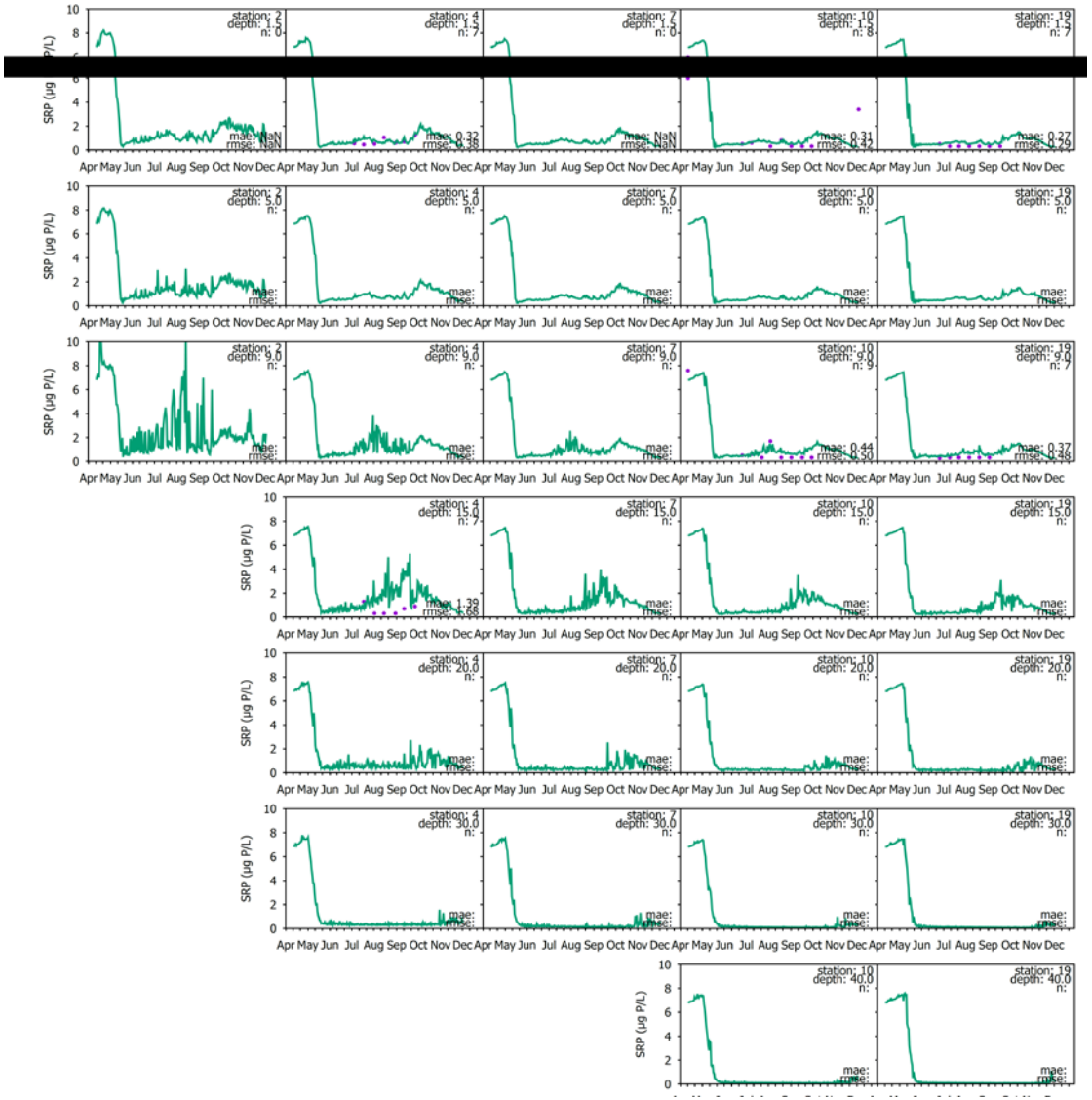


**Figure F-10**. Time series of 2018 model predictions and observations when available at multiple sites (2, 4, 7, 10 and 19 and at multiple depths (1, 5, 9, 15, 20, 30 and 40 m) for SRP.

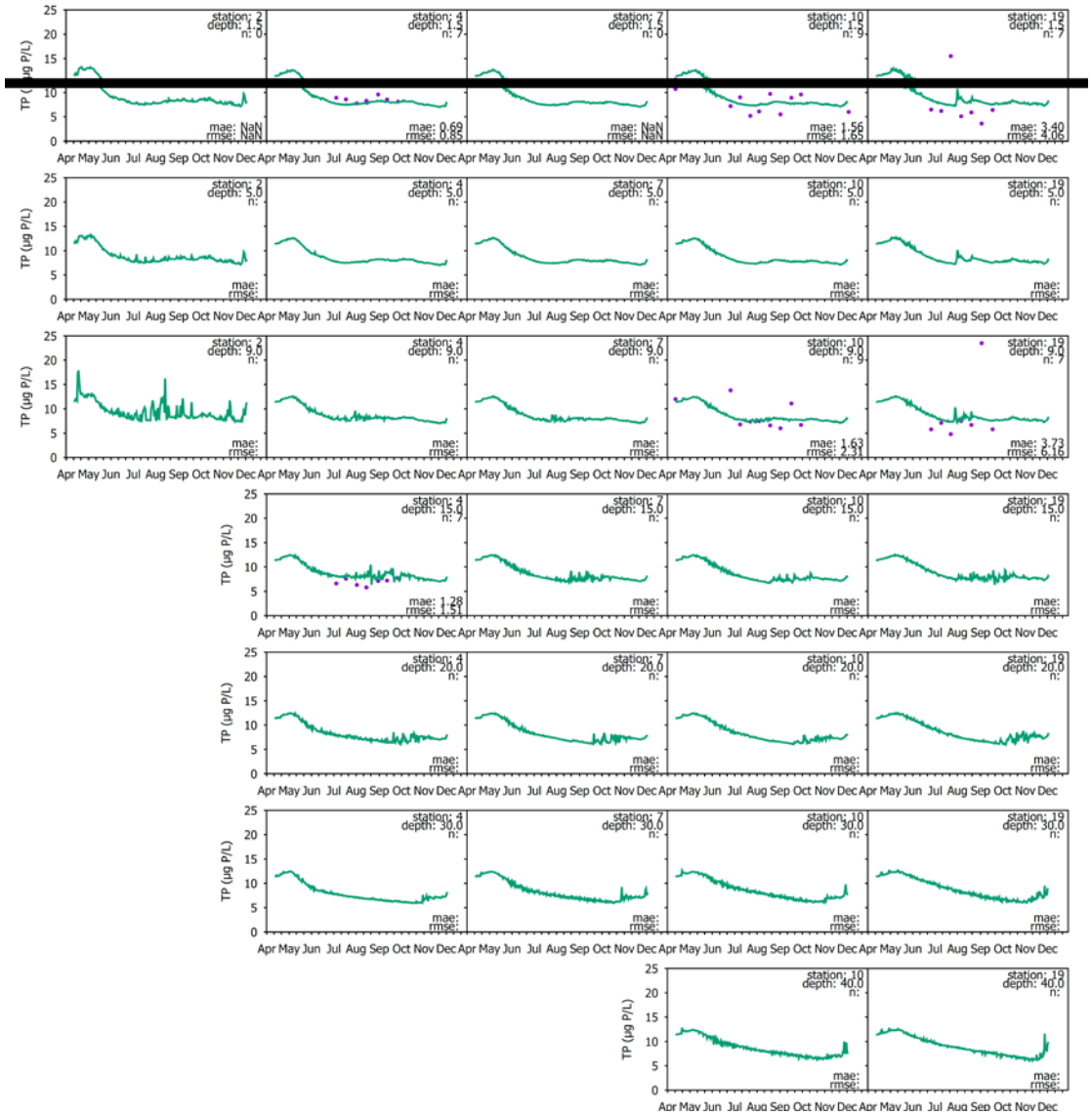


**Figure F-11**. Time series of 2018 model predictions and observations when available at multiple sites (2, 4, 7, 10 and 19 and at multiple depths (1, 5, 9, 15, 20, 30 and 40 m) for TP.

## Appendix F-2 Confirmation of the Water Quality Sub-model, 2017


**Figure F-12**. Time series of 2017 model predictions and observations when available at multiple sites (2, 4, 7, 10 and 19 and at multiple depths (1, 5, 9, 15, 20, 30 and 40 m) for Alg1.

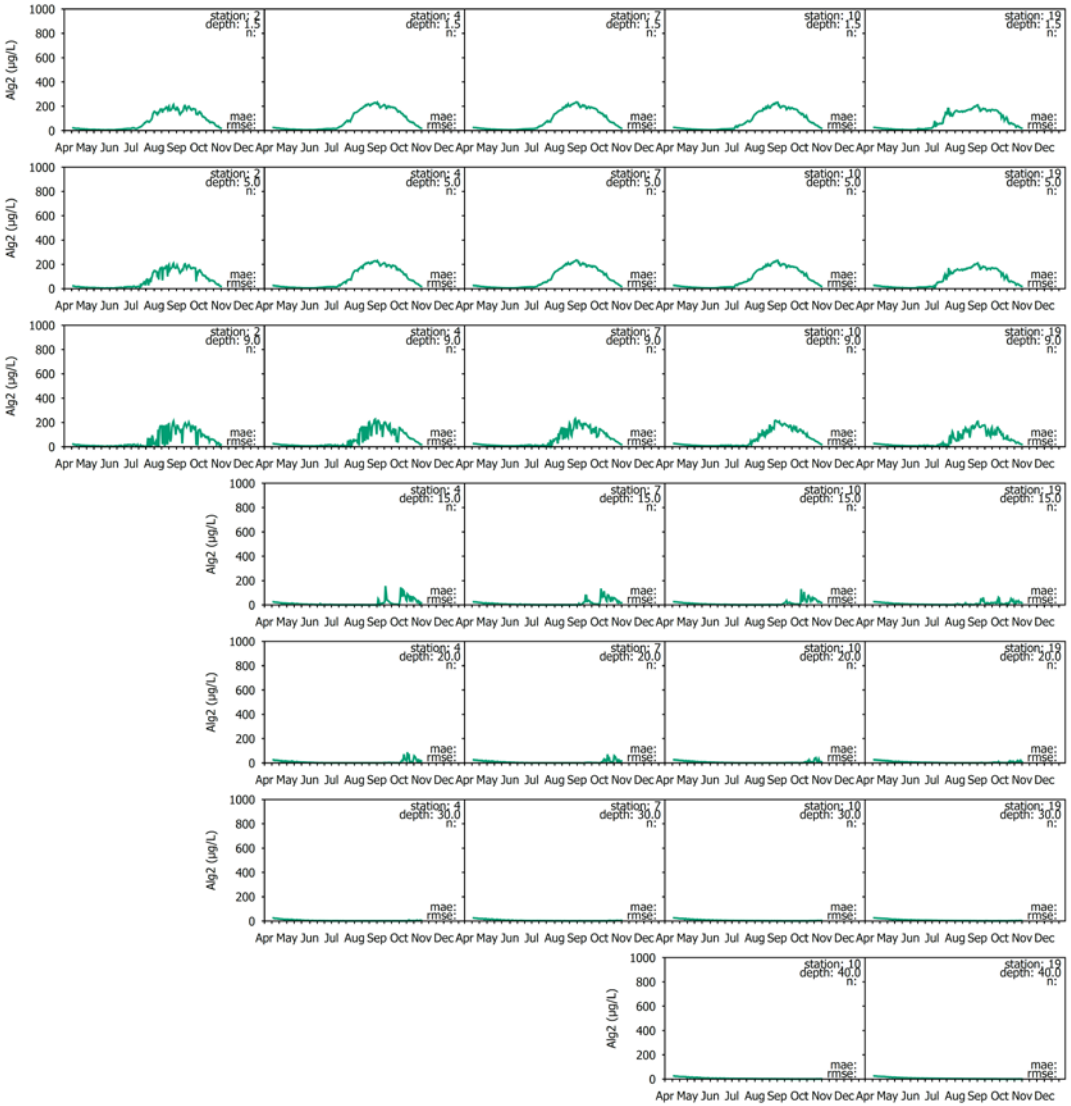


**Figure F-13**. Time series of 2017 model predictions and observations when available at multiple sites (2, 4, 7, 10 and 19 and at multiple depths (1, 5, 9, 15, 20, 30 and 40 m) for Alg2.

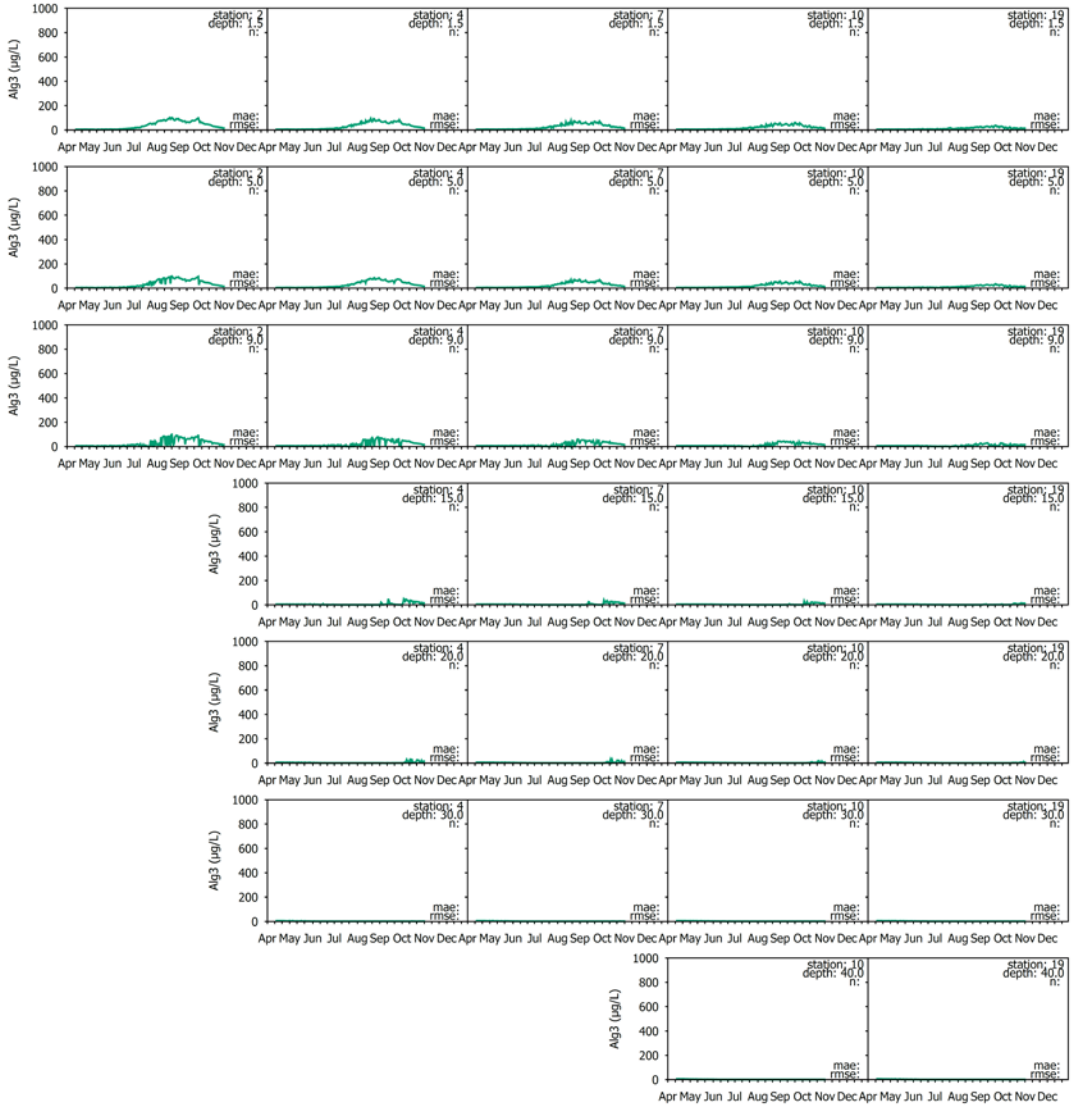


**Figure F-14**. Time series of 2017 model predictions and observations when available at multiple sites (2, 4, 7, 10 and 19 and at multiple depths (1, 5, 9, 15, 20, 30 and 40 m) for Alg3.

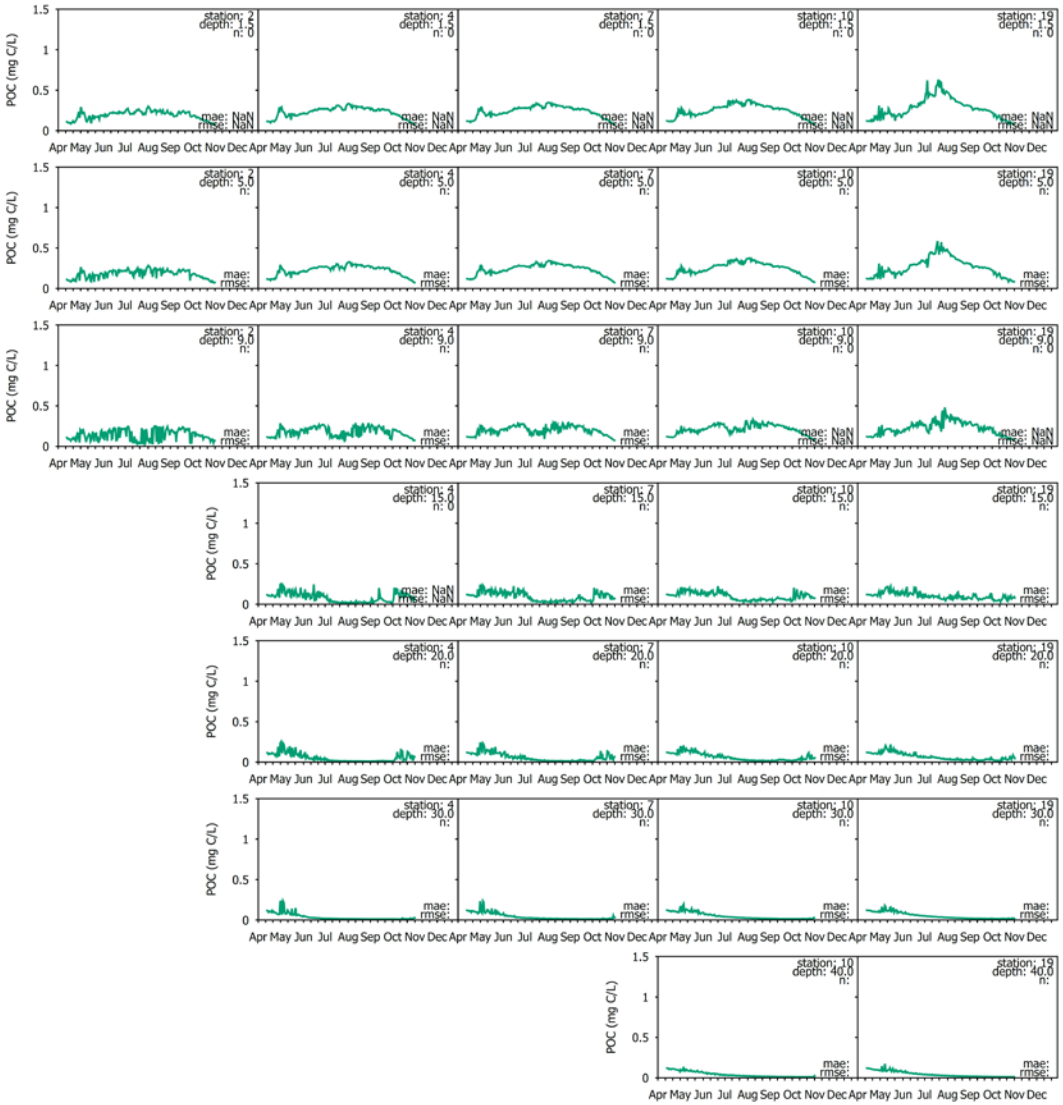


**Figure F-15**. Time series of 2017 model predictions and observations when available at multiple sites (2, 4, 7, 10 and 19 and at multiple depths (1, 5, 9, 15, 20, 30 and 40 m) for POC.

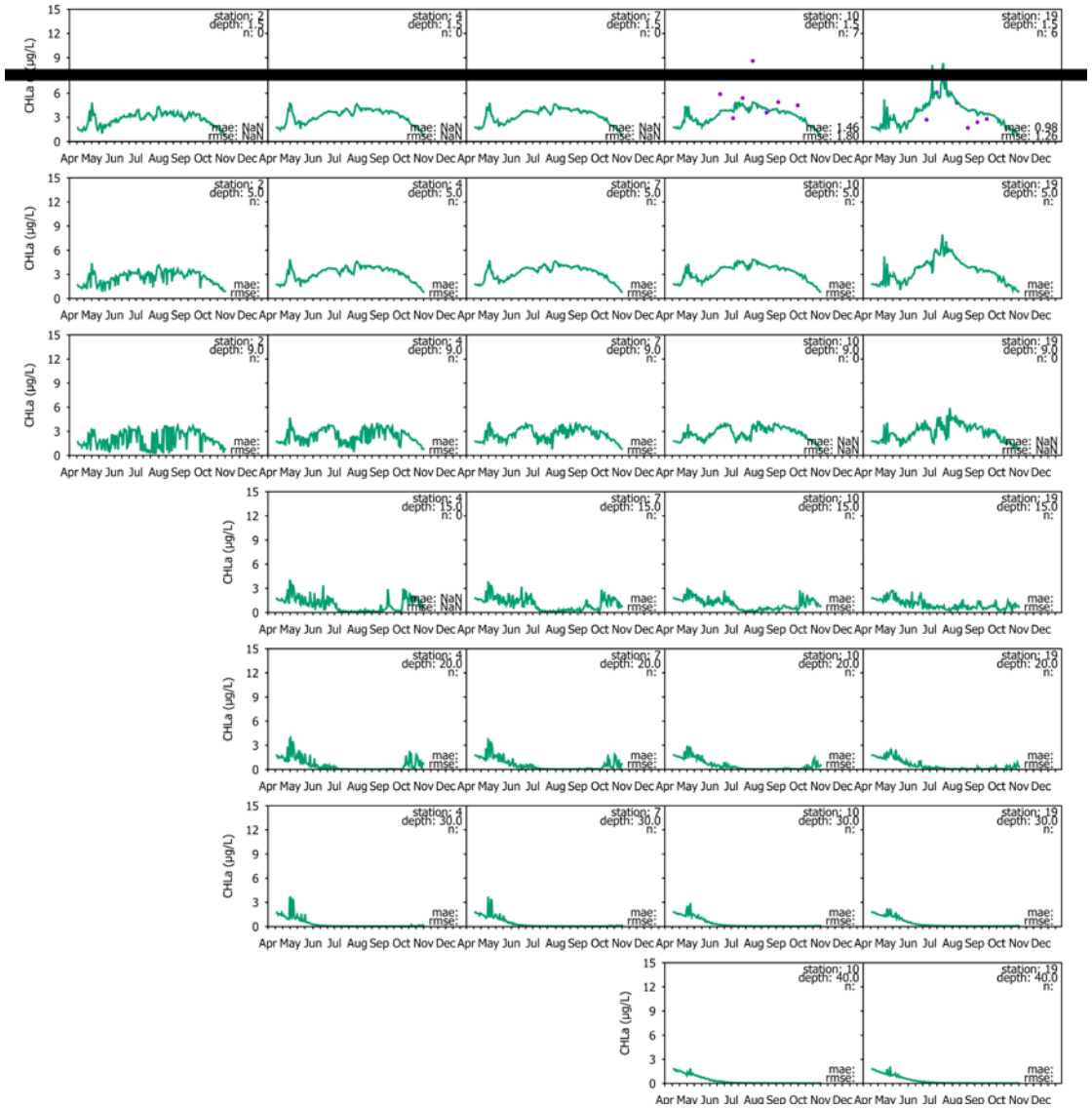


**Figure F-16**. Time series of 2017 model predictions and observations when available at multiple sites (2, 4, 7, 10 and 19 and at multiple depths (1, 5, 9, 15, 20, 30 and 40 m) for Chl-*a*.

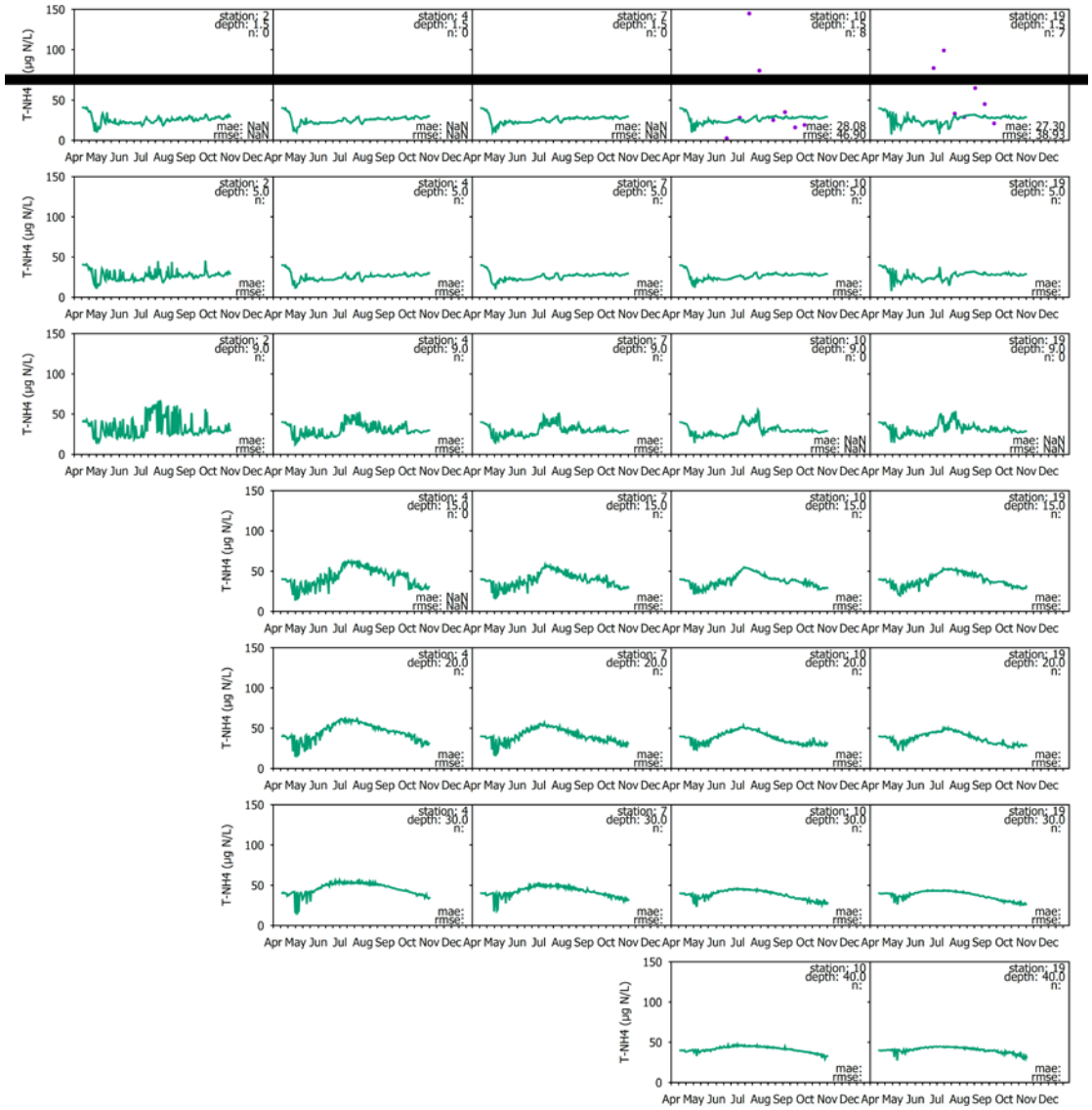


**Figure F-17**. Time series of 2017 model predictions and observations when available at multiple sites (2, 4, 7, 10 and 19 and at multiple depths (1, 5, 9, 15, 20, 30 and 40 m) for $tNH_3$.

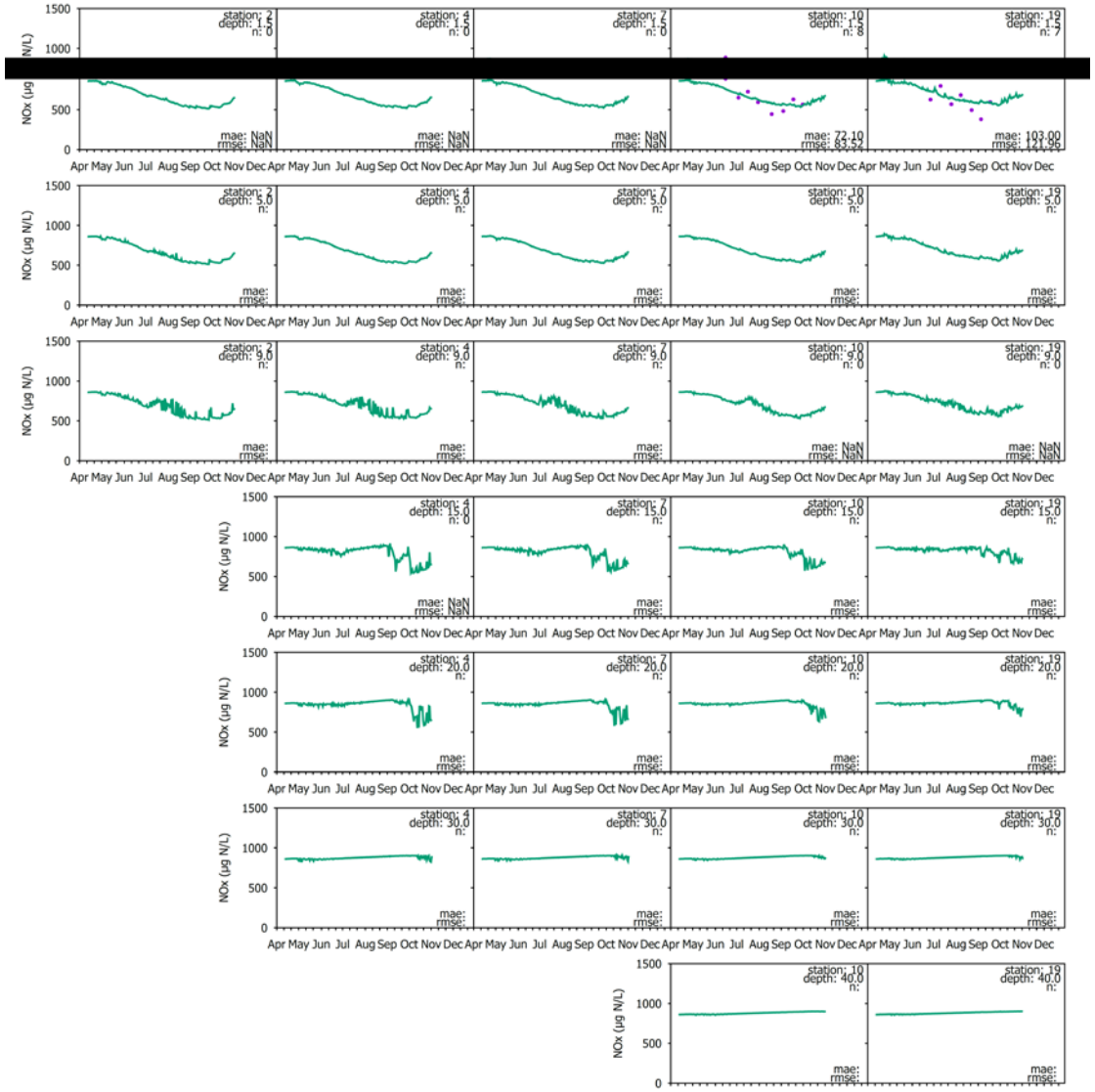


**Figure F-`18**. Time series of 2017 model predictions and observations when available at multiple sites (2, 4, 7, 10 and 19 and at multiple depths (1, 5, 9, 15, 20, 30 and 40 m) for $NO_X$.

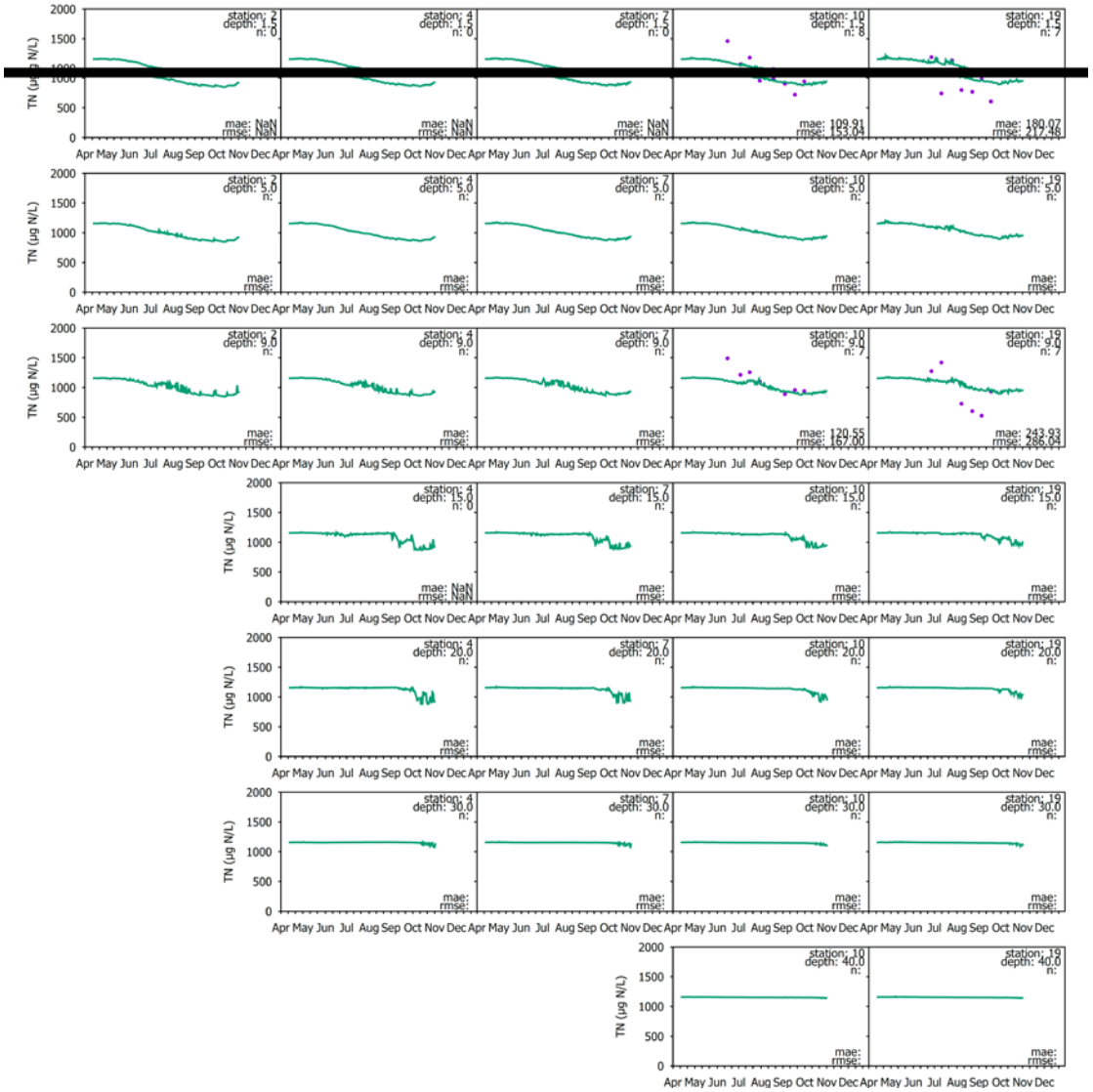


**Figure F-19**. Time series of 2018 model predictions and observations when available at multiple sites (2, 4, 7, 10 and 19 and at multiple depths (1, 5, 9, 15, 20, 30 and 40 m) for TN.

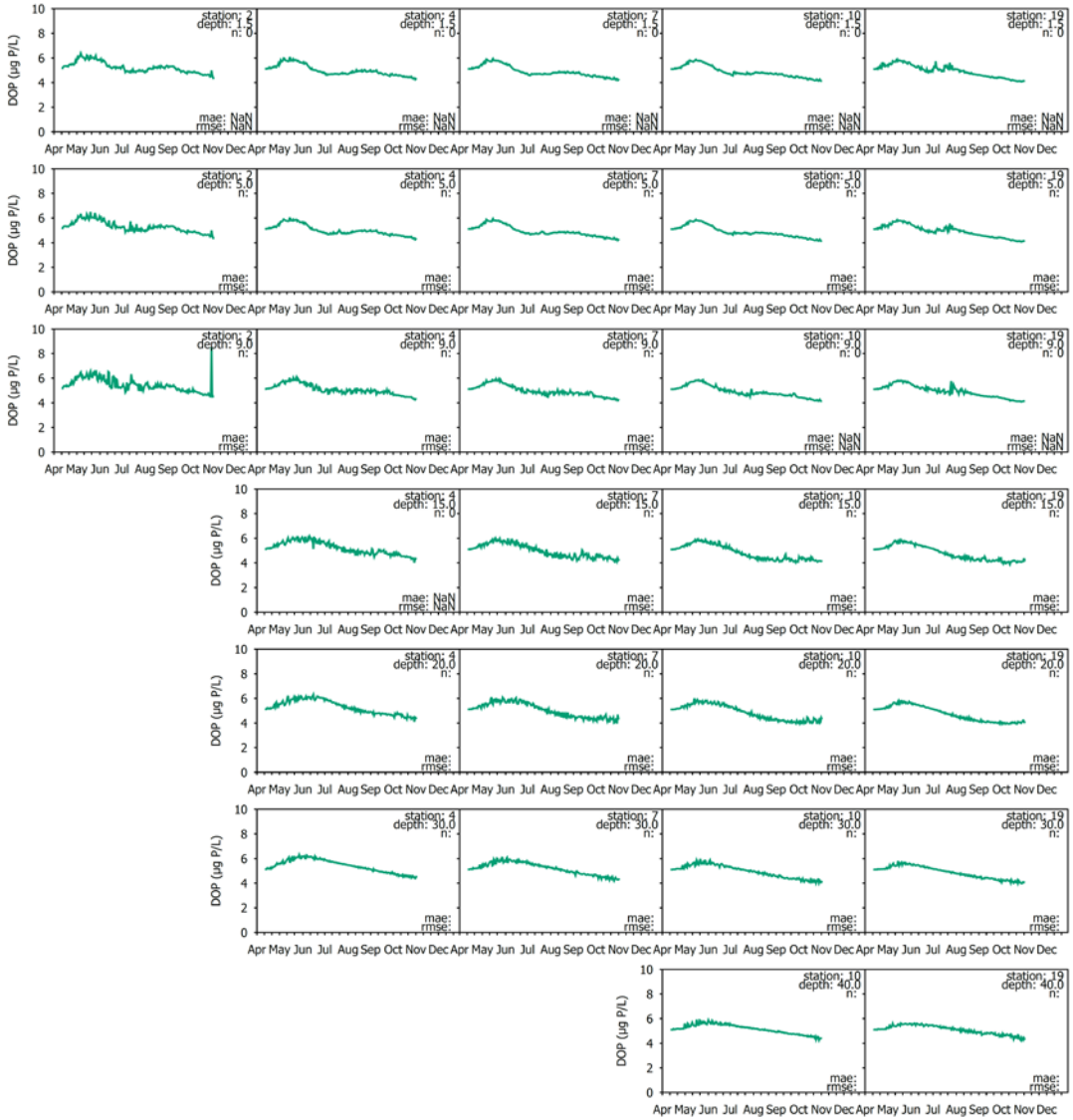


**Figure F-20**. Time series of 2017 model predictions and observations when available at multiple sites (2, 4, 7, 10 and 19 and at multiple depths (1, 5, 9, 15, 20, 30 and 40 m) for DOP.

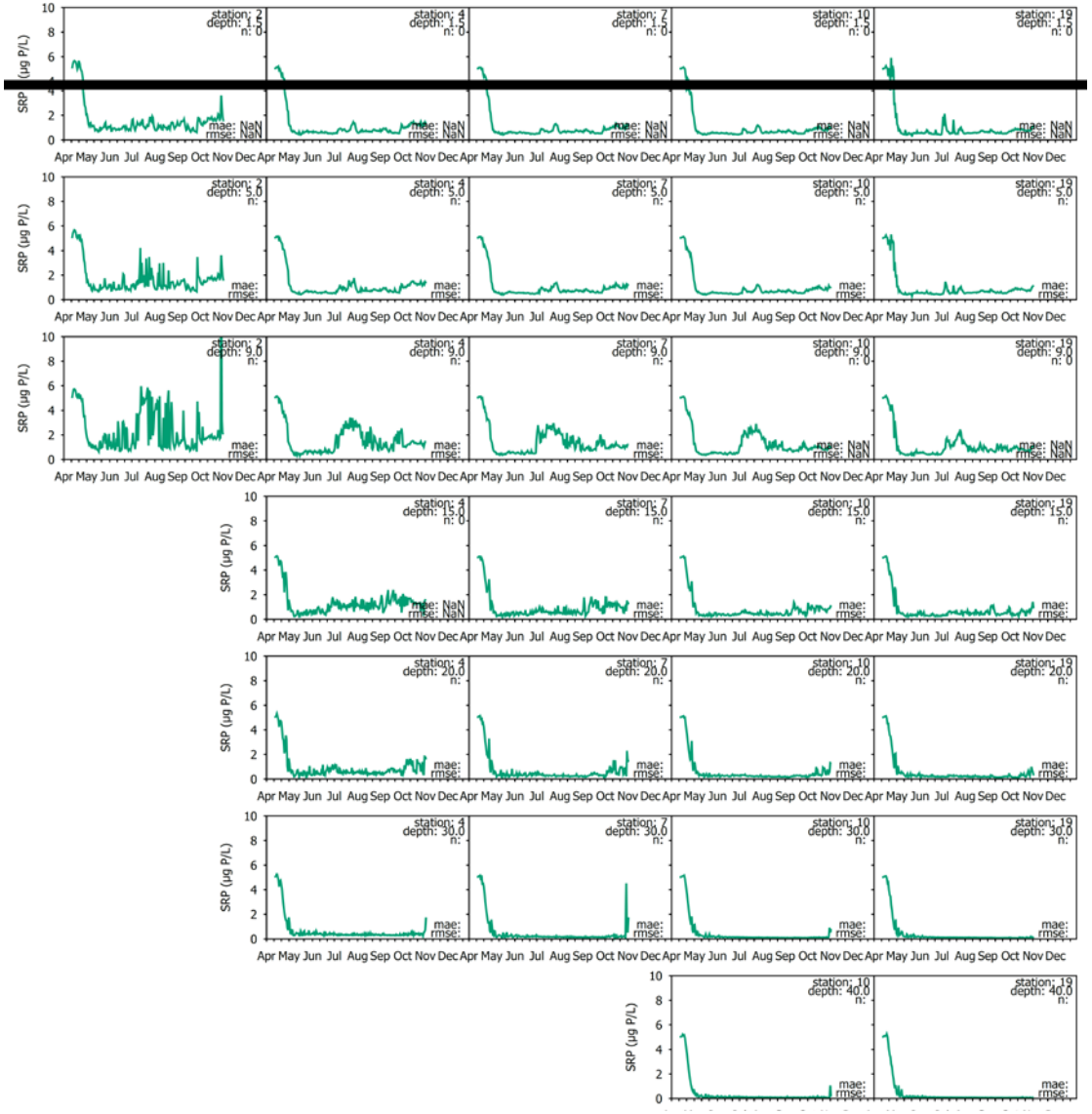


**Figure F-21**. Time series of 2017 model predictions and observations when available at multiple sites (2, 4, 7, 10 and 19 and at multiple depths (1, 5, 9, 15, 20, 30 and 40 m) for SRP.

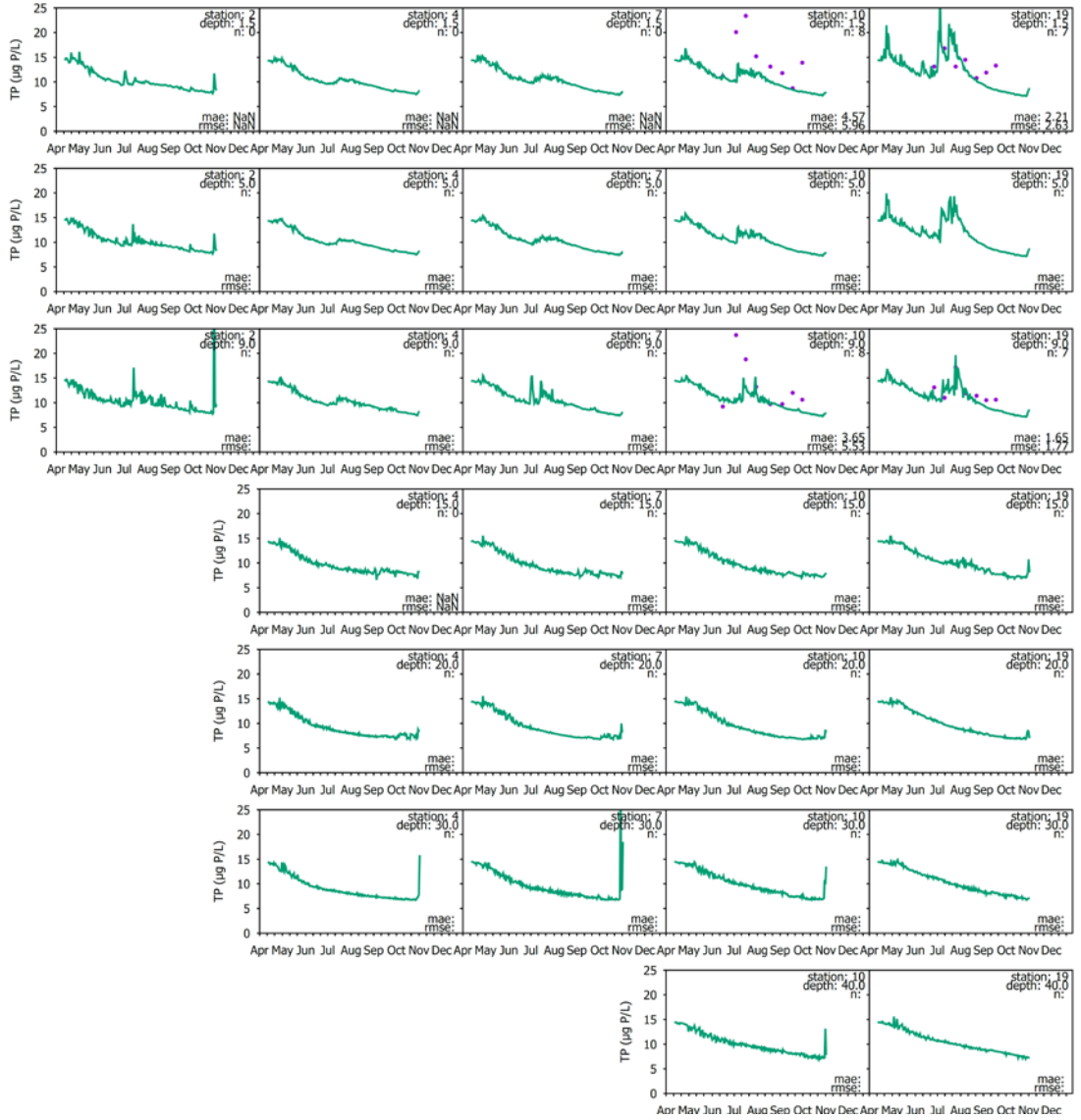


**Figure F-22**. Time series of 2017 model predictions and observations when available at multiple sites (2, 4, 7, 10 and 19 and at multiple depths (1, 5, 9, 15, 20, 30 and 40 m) for TP.